

University of Massachusetts Boston

## ScholarWorks at UMass Boston

---

Graduate Doctoral Dissertations

Doctoral Dissertations and Masters Theses

---

5-31-2018

# Design And Assessment of Small Molecules as Free Radical Scavengers and Potential Multi-Target Therapeutic Agents against Alzheimer's Disease, Diabetes and Cancer

William Horton

*University of Massachusetts Boston*

Follow this and additional works at: [https://scholarworks.umb.edu/doctoral\\_dissertations](https://scholarworks.umb.edu/doctoral_dissertations)

 Part of the [Biochemistry Commons](#), and the [Chemistry Commons](#)

---

### Recommended Citation

Horton, William, "Design And Assessment of Small Molecules as Free Radical Scavengers and Potential Multi-Target Therapeutic Agents against Alzheimer's Disease, Diabetes and Cancer" (2018). *Graduate Doctoral Dissertations*. 403.

[https://scholarworks.umb.edu/doctoral\\_dissertations/403](https://scholarworks.umb.edu/doctoral_dissertations/403)

This Open Access Dissertation is brought to you for free and open access by the Doctoral Dissertations and Masters Theses at ScholarWorks at UMass Boston. It has been accepted for inclusion in Graduate Doctoral Dissertations by an authorized administrator of ScholarWorks at UMass Boston. For more information, please contact [scholarworks@umb.edu](mailto:scholarworks@umb.edu).

DESIGN AND ASSESSMENT OF SMALL MOLECULES AS FREE RADICAL  
SCAVENGERS AND POTENTIAL MULTI-TARGET THERAPEUTIC AGENTS  
AGAINST ALZHEIMER'S DISEASE, DIABETES AND CANCER

A Dissertation Presented

by

WILLIAM HORTON

Submitted to the Office of Graduate Studies,  
University of Massachusetts Boston,  
in partial fulfillment of the requirements for the degree of

DOCTOR OF PHILOSOPHY

May 2018

Chemistry Ph.D. Program

© 2018 by William Horton  
All rights reserved

DESIGN AND ASSESSMENT OF SMALL MOLECULES AS FREE RADICAL  
SCAVENGERS AND POTENTIAL MULTI-TARGET THERAPEUTIC AGENTS  
AGAINST ALZHEIMER'S DISEASE, DIABETES AND CANCER

A Dissertation Presented

by

WILLIAM HORTON

Approved as to style and content by:

---

Marianna Török, Associate Professor  
Chairperson of Committee

---

Bela Török, Professor  
Member

---

Daniel Dowling, Assistant Professor  
Member

---

Gregory Beck, Associate Professor  
Member

---

Hannah Sevia, Professor  
Chemistry Graduate Program Director

---

Robert Carter, Chairperson  
Chemistry Department

## ABSTRACT

# DESIGN AND ASSESSMENT OF SMALL MOLECULES AS FREE RADICAL SCAVENGERS AND POTENTIAL MULTI-TARGET THERAPEUTIC AGENTS AGAINST ALZHEIMER'S DISEASE, DIABETES AND CANCER

May 2018

William Horton, B.S., University of Massachusetts Boston  
Ph.D., University of Massachusetts Boston

Directed by Professors Marianna and Bela Török

Complex diseases such as Alzheimer's disease (AD), diabetes and cancer are difficult to manage with single target treatment approaches and unfortunately, they are wide-spread. For example, over 16 million people are expected to have AD in the US by 2050, thus new therapeutic approaches have to be developed. Multi-functional drug candidates have gained increasing popularity in treating complex diseases. The impact of oxidative stress in almost every disease progression makes them essential components in therapies for complex diseases. Endogenous systems typically maintain redox homeostasis within the cell, but in the diseased state these systems fail to alleviate oxidative stress. Supplementation with exogenous antioxidants can boost the endogenous systems and maintain redox homeostasis. Therefore, the development of multi-functional drug candidates should also include investigations of the radical scavenging activity of the compounds screened.

The radical scavenging activity and multi-target profiles of 61 small molecules were assessed by three different radical scavenging activity assays. These compounds were selected or designed by taking into account the presence of structural motifs common to currently used therapeutic compounds. The drug candidates were screened for amyloid  $\beta$  ( $A\beta$ ) oligomer and fibril formation as well as cholinesterase inhibition. In addition, this work aims to address the structure-activity relationship (SAR) between experimental radical scavenging effect and the structural characteristics of the compounds studied. In a continuation of this idea, phenol and aniline model compounds were investigated to identify important physicochemical properties such as the bond dissociation energy (BDE) and ionization potential (IP).

The work completed here highlights several compounds with multi-functional activity for further development. The SAR studies have identified important structural motifs responsible and necessary for therapeutic function. These results can be applied to future compound design and further support the multi-functional drug development process.

## DEDICATION

I would like to dedicate this to my loving wife and my advisors.

## ACKNOWLEDGMENTS

First and foremost, I would like to thank my PI, Marianna Török, for her help and guidance for these past 5 years. This dissertation would have not been possible without her support.

I would also like to thank Bela Török for his help with many of the projects I have worked on. The encouragement to constantly challenge and reassess the material I was working on was invaluable to the completion of my dissertation.

I would like to thank Marianna Török, Bela Török, Daniel Dowling and Greg Beck for serving on my dissertation committee. They encouraged me to embrace the material I was working with and apply it to new bodies of work. They were there to inspire me to investigate the unexplained and apply new approaches to difficult problems.

I would like to thank the writers of my letters of recommendation Marianna Török, Bela Török and Mridula Satyamurti for their swift responses to letter requests. Their guidance and support have made me who I am today.

I would like to thank Swarada for her timely evaluations for the various structure-activity relationship studies I conducted and Sumeyra and Elfa as well as the Foster group for help with the lysozyme and insulin fibril AFM image processing. I would also like to thank all of the members of the Bela Török lab for synthesizing the compounds used in this work. All of their work was invaluable to completing my research.

I would also like to thank Mridula Satyamurti, who I have had the pleasure to work with since I was an undergraduate student at UMB. Working with her to run the general chemistry labs at the University of Massachusetts Boston has been an excellent



experience that I will keep with me for the rest of my life. Her desire and passion to teach students chemistry has been moving.

I wish to express my deepest appreciation for my family. Samantha, my loving wife, has been by my side since I was an undergraduate student and supported everything I do. My loving parents have supported me in every way since I was a kid and I would not be where I am today without them.

I would also like to thank my friends, Nick, Ben, James and many others for everything. You guys have been some of the best people I have known, and we will always be friends.

Lastly, I want to thank the University of Massachusetts Boston. In the time I have been there I have been afforded so many opportunities. They have provided an excellent space to work in with ample funding to conduct the research I was interested in. The people here are some of the smartest and nicest people I have ever had the pleasure of meeting.

## TABLE OF CONTENTS

DEDICATION.....	vi
ACKNOWLEDGEMENTS.....	vii
TABLE OF CONTENTS.....	ix
LIST OF TABLES.....	xiii
LIST OF FIGURES.....	xiv
LIST OF SCHEMES AND EQUATIONS.....	xvii
LIST OF ABBREVIATIONS.....	xviii

CHAPTER	Page
1. INTRODUCTION AND RESEARCH GOALS .....	1
1.1 Introduction.....	1
1.2 Research goals .....	3
1.2.1 $\beta$ -carboline as multi-functional drug candidates for Alzheimer's disease .....	3
1.2.2 Hydrazone and nipectic acid derivatives as multi-functional drug candidates.....	3
1.2.3 SAR study of hydrazones as radical scavenging compounds.....	4
1.2.4 SAR study on radical scavenging activity of phenol and aniline model compounds .....	5
1.2.5 Hydrazones as multi-functional drug candidates.....	5
1.2.6 Method development of amyloid fibril formation for lysozyme and Insulin .....	5
2. LITERATURE OVERVIEW AND BACKGROUND .....	7
2.1 Definition and role of reactive oxygen and nitrogen species.....	7
2.1.1 Oxidative species and their functions in the body .....	9
2.1.2 Damage to the body resulting from excessive amounts of oxidative Species .....	10
2.1.3 Endogenous defenses against oxidative stress.....	10
2.1.4 Exogenous defenses against oxidative stress.....	12
2.2 Multi-functional drug development .....	15
2.3 Protein misfolding and its connection to various diseases .....	16
2.3.1 Processes of proper protein folding .....	16
2.3.2 Alzheimer's disease .....	17
2.3.2.1 A $\beta$ Self-assembly inhibition .....	19
2.3.2.2 Disassembly of A $\beta$ oligomer and fibril species .....	20
2.3.2.3 Cholinesterase inhibitors.....	21
2.3.2.4 The role of reactive oxygen species in Alzheimer's disease .....	21
2.3.2.5 Multi-target approaches to the treatment of Alzheimer's disease .....	22
2.3.3 Diabetes mellitus.....	22
2.3.3.1 Diabetes mellitus type 1 and 2 .....	23
2.3.3.2 Diabetes and its possible connections to Alzheimer's disease .....	24
2.4 Cancer .....	25
2.4.1 Reactive oxygen species and cancer development .....	26

CHAPTER	Page
2.4.2 Casein kinase II.....	27
3. TECHNIQUES AND METHODOLOGIES.....	31
3.1 Cholinesterase inhibition assay using Ellman’s method.....	31
3.2 Determination of radical scavenging activity of small molecule antioxidants .....	32
3.2.1 DPPH radical scavenging assay.....	35
3.2.2 ABTS radical scavenging assay.....	37
3.2.3 ORAC radical scavenging assay.....	39
3.3 In vitro protein fibril aggregation .....	41
3.4 Monitoring amyloid fibril formation by Thioflavin T fluorescence spectroscopy.....	42
3.5 Atomic force microscopy of amyloid fibril formations.....	44
3.6 Synthesis of the library of small molecules .....	45
4. MATERIALS AND EXPERIMENTAL METHODS .....	46
4.1 Chemicals and enzymes.....	46
4.2 Amyloid fibril inhibition and disassembly procedures .....	46
4.2.1 Lysozyme amyloid fibril formation .....	46
4.2.2 Insulin amyloid fibril formation .....	47
4.2.3 Thioflavin T binding assay .....	48
4.2.4 Atomic force microscopy.....	49
4.3 Ellman’s method for enzyme inhibition .....	49
4.3.1 Acetylcholinesterase inhibition assay preparation.....	50
4.3.2 Butyrylcholinesterase inhibition assay preparation .....	53
4.4 Free radical scavenging assays .....	55
4.4.1 DPPH radical scavenging assay.....	55
4.4.2 ABTS radical scavenging assay.....	58
4.4.3 ORAC radical scavenging assay.....	60
4.5 Calculation of physical descriptors of synthetic antioxidants and model compounds by Gaussian 09 for structure activity relationship studies.....	62
5. $\beta$ -CARBOLINES AS POTENTIAL MULTI-FUNCTIONAL ALZHEIMER’S DISEASE THERAPUTIC AGENTS.....	63
5.1 Introduction.....	63
5.2 Synthesis .....	66
5.3 Results.....	67
5.3.1 Inhibition of A $\beta$ fibril formation.....	69
5.3.2 Inhibition of A $\beta$ oligomer formation .....	71
5.3.3 Inhibition of cholinesterase activity (AChE, BuChE) .....	72
5.3.4 Free radical scavenging activity (ABTS, DPPH, ORAC) .....	74
5.4 Discussion.....	76

CHAPTER	Page
6. COMPUTER AIDED DRUG DESIGN OF MULTI-FUNCTIONAL HYDRAZIDE AND NIPECOTIC ACID DERIVATIVES .....	83
6.1 Introduction.....	83
6.2 Synthesis .....	85
6.3 Results.....	87
6.3.1 Cholinesterase (AChE, BuChE) docking studies using AutoDock Tools .....	88
6.3.2 Inhibition of cholinesterase activity (AChE, BuChE) .....	89
6.3.3 Free radical scavenging activity (ABTS, DPPH, ORAC) .....	91
6.4 Discussion .....	93
7. STRUCTURE ACTIVITY RELATIONSHIP OF HYDRAZONES AS RADICAL SCAVENGERS.....	95
7.1 Introduction.....	95
7.2 Synthesis .....	98
7.3 Results.....	98
7.3.1 Free radical scavenging activity (ABTS, DPPH, ORAC) .....	101
7.3.2 Physicochemical parameter determination using the Gaussian09 program suite .....	104
7.4 Discussion .....	105
8. EFFECT OF STRUCTURAL PARAMETERS OF PHENOL AND ANILINE MODEL COMPOUNDS ON THEIR RADICAL SCAVENGING ACTIVITY.....	121
8.1 Introduction.....	121
8.2 Results.....	122
8.2.1 Free radical scavenging activity of the model compounds (ABTS, DPPH, ORAC).....	125
8.2.2 Determination of physicochemical parameters using the Gaussian09 program suite .....	130
8.3 Discussion.....	132
9. HYDRAZONES AS MULTI-FUNCTIONAL CK2 ENZYME INHIBITORS .....	152
9.1 Introduction.....	152
9.2 Synthesis .....	153
9.3 Results.....	154
9.3.1 Free radical scavenging activity (ABTS, DPPH, ORAC) .....	156
9.3.2 CK2 enzyme inhibition .....	159
9.4 Discussion .....	160

CHAPTER	Page
10. METHOD DEVELOPMENT OF AMYLOID FIBRIL FORMATION FOR EDUCATION AND RESEARCH.....	162
10.1 Introduction.....	162
10.2 Results.....	164
10.2.1 Lysozyme.....	164
10.2.2 Insulin.....	169
10.3 Discussion.....	172
11 CONCLUSIONS.....	174
11.1 $\beta$ -carboline as multi-functional drug candidates.....	174
11.2 Hydrazide and nipecotic acid derivatives as multi-functional drug candidates.....	174
11.3 SAR study of hydrazones as radical scavenging compounds.....	175
11.4 SAR study on radical scavenging activity of phenol and aniline model compounds.....	176
11.5 Hydrazones as multi-functional drug candidates.....	177
11.6 Optimization of the conditions for the formation of amyloid fibrils.....	178
PUBLICATIONS.....	179
APPENDIX.....	181
A. SELECTED THIOFLAVIN T EMISSION SPECTRA FOR INSULIN FIBRIL FORMATION.....	181
B. PLOT OF BDE ENERGY VS. RADICAL SCAVENGING ACTIVITY FOR SAR OF HYDRAZONES.....	185
ENDNOTES.....	186
BIBLIOGRAPHY.....	215

## LIST OF TABLES

Table		Page
1.	The ROS and RNS family include both free radicals and non-radical species .....	8
2.	Inhibition of A $\beta$ fibril formation by $\beta$ -carbolines <b>1-16</b> .....	70
3.	Inhibition of A $\beta$ oligomer formation by $\beta$ -carboline derivatives ( <b>1-16</b> ) .....	71
4.	Inhibition of AChE and BuChE by $\beta$ -carbolines and IC <sub>50</sub> for BuChE activity is shown below.....	73
5.	Free radical scavenging activity of the $\beta$ -carboline derivatives against the DPPH <sup>a</sup> , ABTS <sup>b</sup> and peroxy radicals <sup>c</sup> .....	75
6.	The inhibition of AChE and BuChE activity by the hydrazide and nipecotic acid derivatives.....	90
7.	Free radical scavenging activity of the hydrazide derivatives against the DPPH <sup>a</sup> , ABTS <sup>b</sup> and peroxy radicals <sup>c</sup> .....	92
8.	Free radical scavenging activity of the hydrazone derivatives 31 – 45 against the DPPH <sup>a</sup> , ABTS <sup>b</sup> and peroxy radicals <sup>c</sup> .....	102
9.	Theoretical parameters of the hydrazones investigated.....	105
10.	Electronic energy (E) are given in hartree while the relative stabilization energies ( $\Delta E_{Rel}$ ) are in parenthesis in kcal/mol units.....	112
11.	Free radical scavenging activity of the phenol model compounds <b>46 – 61</b> against the DPPH <sup>a</sup> , ABTS <sup>b</sup> and peroxy radicals <sup>c</sup> .....	127
12.	Free radical scavenging activity of the phenol and aniline model compounds <b>62 - 77</b> against the DPPH <sup>a</sup> , ABTS <sup>b</sup> and peroxy radicals <sup>c</sup> .....	128
13.	Theoretical parameters of the substituted phenols and anilines investigated .....	131
14.	Major properties of phenols that the show considerable fit with the experimental ABTS radical scavenging data .....	149
15.	Major properties of anilines that the show considerable fit with the experimental ABTS radical scavenging data.....	149
16.	Free radical scavenging activity of the phase 2 hydrazone derivatives against the DPPH <sup>a</sup> , ABTS <sup>b</sup> and peroxy radicals <sup>c</sup> .....	158
17.	ThT intensity and AFM dimension values of lysozyme fibrils grown in concentrated ethanol solutions after 7 days .....	165
18.	ThT intensity and AFM dimension values of lysozyme fibrils grown in concentrated ethanol solutions after 14 days .....	165
19.	ThT intensity values of insulin fibrils grown in various conditions. The ThT values were followed for at most 4 days.....	169

## LIST OF FIGURES

Figure	Page
1. Endogenous radical scavengers .....	11
2. Examples of vitamin radical scavengers.....	12
3. Examples of commonly identified polyphenolic antioxidant species.....	13
4. Examples of non-polyphenolic antioxidant species.....	14
5. Examples of A $\beta$ self-assembly inhibitors .....	19
6. Flavanone derivative CK2 inhibitors .....	28
7. Examples of CK2 holoenzyme inhibitors .....	30
8. Hydrolysis of acetyl and butyrylthiocholine by cholinesterases .....	31
9. DTNB reaction with thiocholine produced by the cholinesterases .....	32
10. Three common mechanisms for radical scavenging in solution by antioxidant species.....	33
11. Structures of known antioxidants used as control compounds for the radical scavenging assays (DPPH, ABTS and ORAC). All compounds were applied at 10 $\mu$ M concentration for each assay .....	35
12. The net chemical reaction of the DPPH radical scavenging assay .....	36
13. The chemical reaction of the ABTS radical scavenging assay .....	38
14. Preparation of the radical and its quenching by the antioxidant in the oxygen radical absorbance capacity (ORAC) radical scavenging assay.....	39
15. Fluorescein is the fluorescent probe currently used to detect the AAPH radical in the ORAC assay .....	41
16. Simplified amyloid fibril formation process.....	42
17. (A) ThT and its interaction (B) with the $\beta$ -sheet rich domains of amyloid fibrils.....	43
18. Control compounds for the AChE and BuChE inhibition .....	50
19. 96-well plate set up for AChE inhibition screening.....	52
20. 96-well plate set up for BuChE inhibition screening.....	54
21. 96-well plate set up for DPPH radical scavenging activity screening.....	57
22. 96-well plate set up for ABTS radical scavenging activity screening.....	59
23. 96-well plate set up for ORAC radical scavenging activity screening.....	61
24. $\beta$ -carboline core structure .....	63
25. Examples of $\beta$ -carboline derivatives with different activities as drug candidates .....	65
26. Compounds <b>1-9</b> are simple $\beta$ -carbolines with an aromatic extension .....	67
27. Compounds <b>10</b> and <b>11</b> are $\beta$ -carbolines with a more prominent aromatic extension to ideally provide increased compound surface for interaction in the active site of cholinesterases.....	68
28. Compounds <b>12-16</b> are $\beta$ -carboline derivatives where the aromatic extension has been linked via a carbonyl group .....	68
29. Electrospray ionization (ESI) mass spectrum of the A $\beta$ <sub>1-40</sub> -peptide- <b>10</b> mixture (30 $\mu$ M to 150 $\mu$ M).....	77

Figure	Page
30. Superimposition of compound <b>10</b> (blue) with donepezil (red) and galantamine (dark green) in the active site of huBuChE (PDB ID: 1P0I). (hydrogens are concealed for clarity) .....	79
31. Superimposition of molecule <b>16</b> (blue) with donepezil (red) and galantamine (dark green) in the active site of huBuChE (PDB ID: 1P0I). (hydrogens are concealed for clarity) .....	79
32. Superimposition of molecule <b>15</b> (purple) with donepezil (red) and galantamine (dark green) in the active site of huAChE (PDB ID-4EY7) (hydrogens are concealed for clarity) .....	81
33. Examples of hydrazide derivatives with different activities as drug candidates .....	84
34. Examples of nipecotic acid and derivatives with different activities as drug candidate anticonvulsants .....	85
35. Structures of the synthesized hydrazones <b>17 – 27</b> .....	87
36. Structures of the synthesized nipecotic acid derivatives <b>28 – 30</b> .....	88
37. Examples of biologically active hydrazones.....	96
38. Additional examples of biologically active hydrazones .....	97
39. Compounds <b>31 - 42</b> are hydrazones derivatized to have halogen and other electron withdrawing substituents .....	99
40. Compound <b>43</b> is a hydrazone that has cyclized through reaction of the hydrazone center with one of the substituents .....	100
41. B3LYP/6-31G(d,p) optimized geometries of hydrazone Form I and azo Form II of benzylidene-phenyl hydrazine .....	107
42. The structure of the transition state of between the two diarylhydrazone tautomers (A) and the intrinsic reaction coordinate diagram for the tautomerization (B) .....	108
43. Hydrazone Form I and azo Form II of benzylidene-phenyl hydrazine at isovalue 0.0004 .....	109
44. Calculated <sup>1</sup> H NMR chemical shifts of the hydrazone form I and azo form II of benzylidene-phenyl hydrazine in DMSO.....	110
45. Selected radical scavenging activity vs. BDE plots to illustrate the effect of the BDE on the activity of the hydrazones.....	116
46. Selected radical scavenging activity vs. IP and logP plots to illustrate the effect of the parameters on the radical scavenging activity of the hydrazones .....	117
47. The structures of phenol model compounds ( <b>46 - 62</b> ) investigated.....	123
48. The structures of aniline model compounds ( <b>63 - 73</b> ) investigated.....	124
49. The structures of phenol model compounds with an -NH group ( <b>74 - 77</b> ) investigated .....	125
50. (A) Effect of the HOMO energies of phenols on the radical scavenging activity of the compounds.....	134



Figure	Page
51. Free radical scavenging activity vs band gap functions of (A) compounds <b>48 - 53, 76</b> and <b>77</b> and (B) compounds <b>47, 56 - 58, 60, 61</b> and <b>74</b> .....	137
52. Effect of bond dissociation energy (BDE) of the phenols <b>46 - 48, 50 - 55, 74</b> and <b>75</b> on their corresponding radical scavenging activity .....	139
53. The structure and ABTS activity data of compounds <b>46, 49, 52</b> and <b>56 - 60</b> .....	141
54. Effect of dipole moment on the ABTS scavenging activity of anilines <b>67 - 72</b> .....	143
55. The effect of HOMO energies of the anilines ( <b>63 - 73</b> and <b>77</b> ) on their scavenging activity .....	144
56. Effect of band gap energy of the anilines on their radical scavenging activity with compounds <b>63 - 65</b> and <b>70</b> removed.....	145
57. Radical scavenging of anilines as a function of their bond dissociation energy (BDE) with compounds <b>67</b> and <b>76</b> removed.....	146
58. Effect of ionization potential (IP) of the anilines on their experimental radical scavenging activity with the compounds <b>70</b> and <b>76</b> removed .....	147
59. Effect of proton affinity (PA) of anilines on the ABTS radical scavenging activity with the compound <b>76</b> removed.....	148
60. Radical scavenging of anilines as a function of their Hammett constants ( <i>para</i> ) with compound <b>76</b> removed .....	149
61. Phase 1 compounds <b>31 - 42</b> are hydrazones identified with those from the SAR study on radical scavenging activity from Chapter 7 .....	155
62. Phase 1 compounds <b>43 - 45</b> are hydrazones identified with those from the SAR study on radical scavenging activity from Chapter 7 .....	156
63. Representative AFM images of prepared lysozyme samples after 7 days of incubation.....	166
64. Representative AFM images of prepared lysozyme samples after 14 days of incubation .....	167
65. Representative AFM images of denatured lysozyme samples (A: 256 x 256 pixel resolution, C: 512 x 512 pixel resolution) compared to the 80% ethanol sample after 14 days of incubation (B: 256 x 256 pixel resolution, D: 512 x 512 pixel resolution).....	168
66. Representative AFM image of prepared insulin fibrils after 3 days of incubation at PBS and 37 °C with shaking at 700 rpm and the addition of a 1/8 in. diameter Teflon bead.....	170
67. Representative AFM image of prepared insulin fibrils after 4 days of incubation under acidic conditions and 70 °C with shaking at 300 rpm .....	171

## LIST OF SCHEMES AND EQUATIONS

	Page
1. Percent radical scavenging (ABTS and DPPH) calculation [Eq. 1] .....	36
2. Net area under the curve calculation [Eq. 2].....	40
3. Percent radical scavenging (ORAC) calculation [Eq. 3] .....	40
4. Synthesis of $\beta$ -carboline derivatives .....	66
5. General synthesis of hydrazide derivatives.....	86
6. General synthesis of nipecotic acid derivatives .....	86
7. Synthesis of the applied hydrazone derivatives .....	98
8. Tautomers and the potential delocalized form of diarylhydrazones .....	106
9. Hydrazone HAT mechanism for radical scavenging [Eq. 4].....	117
10. Hydrazone SET mechanism for radical scavenging [Eq. 5] .....	119
11. Synthesis of the fluorinated hydrazone derivatives .....	154

## LIST OF ABBREVIATIONS

<b><math>\beta</math>-PE:</b>	$\beta$ -Phycoerythrin
<b><math>\mu</math>:</b>	Dipole moment
<b><math>\sigma</math>:</b>	Hammett constant
<b>AAPH:</b>	2,2'-Azobis(2-methylpropionamide) dihydrochloride
<b>A<math>\beta</math>:</b>	Amyloid $\beta$
<b>Abs:</b>	Absorbance
<b>ABTS:</b>	2,2'-Azino-bis (3-ethylbenzothiazoline-6-sulfonic acid)
<b>ACh:</b>	Acetylcholine
<b>AChE:</b>	Acetylcholinesterase
<b>AD:</b>	Alzheimer's disease
<b>AFM:</b>	Atomic force microscopy
<b>AGEs:</b>	Advanced glycation end products
<b>AMPA:</b>	$\alpha$ -Amino-3-hydroxy-5-methyl-4-isoxazolepropionic acid
<b>APP:</b>	Amyloid precursor protein
<b>AUC:</b>	Area under the curve
<b>BBB:</b>	Blood brain barrier
<b>BDE:</b>	Bond dissociation energy
<b>BITC:</b>	Benzyl isothiocyanate
<b>BuCh:</b>	Butyrylcholine
<b>BuChE:</b>	Butyrylcholinesterase
<b>CK2:</b>	Casein kinase II
<b>CRISPR:</b>	Clustered regularly interspaced short palindromic repeats

<b>DFT:</b>	Density functional theory
<b>DI:</b>	De-ionized
<b>DMCM:</b>	Methyl-6,7-dimethoxy-4-ethyl- $\beta$ -carboline-3-carboxylate
<b>DMSO:</b>	Dimethyl sulfoxide
<b>DPP-4:</b>	Dipeptidyl peptidase 4
<b>DPPH:</b>	2,2-Diphenyl-1-picrylhydrazyl
<b>DTNB:</b>	5,5'-Dithio-bis-[2-nitrobenzoic acid]
<b>EGCG:</b>	Epigallocate-3-gallate
<b>EM:</b>	Electron microscopy
<b>ESI:</b>	Electrospray ionization
<b>FBPase:</b>	Fructose 1,6-bisphosphatase
<b>FDA:</b>	Food and drug administration
<b>GC-MS:</b>	Gas chromatography–mass spectrometry
<b>GIAO:</b>	Gauge-independent atomic orbital
<b>GLP-1:</b>	Glucagon-like peptide-1
<b>GluR2:</b>	Glutamate ionotropic receptor AMPA type subunit 2
<b>HAT:</b>	Hydrogen atom transfer
<b>HEPES:</b>	4-(2-Hydroxyethyl)-1-piperazineethanesulfonic acid
<b>HEWL:</b>	Hen egg white lysozyme
<b>HOMO:</b>	Highest occupied molecular orbital
<b>HPLC:</b>	High-performance liquid chromatography
<b>IDE:</b>	Insulin degrading enzyme
<b>IL1<math>\beta</math>:</b>	Interleukin 1 beta

<b>IP:</b>	Ionization potential
<b>LUMO:</b>	Lowest unoccupied molecular orbital
<b>mRNA:</b>	Messenger RNA
<b>MS:</b>	Multiple sclerosis
<b>NADH:</b>	Nicotinamide adenine dinucleotide
<b>NADPH:</b>	Nicotinamide adenine dinucleotide phosphate
<b>Nf-<math>\kappa</math>B:</b>	Nuclear factor kappa-light-chain-enhancer of activated B cells
<b>NMDA:</b>	N-Methyl-D-aspartate
<b>NMEs:</b>	New molecular entities
<b>NMR:</b>	Nuclear magnetic resonance
<b>NOS:</b>	Nitric oxide synthase
<b>ORAC:</b>	Oxygen radical absorbance capacity
<b>PA:</b>	Proton affinity
<b>PBS:</b>	Phosphate buffered saline
<b>PCM:</b>	Polarizable continuum model
<b>PTPs:</b>	Protein tyrosine phosphatases
<b>ROS:</b>	Reactive oxygen species
<b>RNS:</b>	Reactive nitrogen species
<b>SAR:</b>	Structure-activity relationship
<b>SCRf:</b>	Self-consistent reaction field
<b>SET:</b>	Single electron transfer
<b>SPLET:</b>	Sequential proton loss / electron transfer
<b>TAC:</b>	Total antioxidant capacity

**TEAC:** Trolox equivalence antioxidant capacity

**ThT:** Thioflavin T

**TNB:** 5-Thio 2-nitrobenzoic acid

## CHAPTER 1

### INTRODUCTION AND RESEARCH GOALS

#### 1.1 Introduction

Complex diseases are becoming a burden on our healthcare system. As the World's population lives longer, the percentage of people living with currently incurable diseases such as Alzheimer's disease (AD), diabetes mellitus, or cancer is only increasing. In just the United States, over 16 million people are expected to have AD by 2020<sup>1</sup>, 1.5 million people are expected to develop either type 1 or type 2 diabetes every year<sup>2</sup> and more than 1.7 million new cancer cases are expected this year with more than half a million cancer deaths projected to occur<sup>3</sup>. More research needs to be done to provide new, more effective therapeutic approaches and/or disease management for these devastating diseases.

Alzheimer's disease is characterized by amyloid plaques and neurofibrillary tangles in the brain coinciding with neuronal cell death and loss of cholinergic transmission in the brain<sup>4</sup>. The complex characterization of AD gives rise to a growing sentiment that the development of multi-target treatment options could be the right approach. There have been extensive research efforts devoted to cholinesterase inhibitors to retain and even improve the synaptic transmission in the brain<sup>5-7</sup>, as well as the inhibition of amyloid fibril and oligomer formation<sup>8,9</sup>. Many symptomatic treatments are designed to provide a multi-target approach to AD, utilizing several compounds in a pharmaceutical cocktail<sup>10-12</sup>. What if instead of a cocktail of drugs, one compound could inhibit A $\beta$  fibril deposition and boost the lifetime of acetylcholine in the brain?

Cancer has also become a major focus in drug development. Commonly, many labs focus on single areas of interest and treatment rather than the disease as a whole. With the rise in gene editing techniques (such as clustered regularly interspaced short palindromic repeats (CRISPR)) much of the research has moved into understanding the genetic components of cancer, with the goal of early identification and targeted drug delivery systems to cancer cells with specific identifiers<sup>13-16</sup>. There are also extensive research aims to understand the processes leading up to the transition of a normal cell to a cancer cell. Much of the highlight is on the cellular stress as a trigger for mutation and abnormal cellular function. Multi-functional drugs must be an integral part of drug discovery going forward<sup>17</sup>. They could allow for less drug interactions and may reduce the overall side effects that drugs cause during treatments. My work aims to characterize the multi-target ability of several classes of compounds ( $\beta$ -carboline, hydrazones and hydrazides) to provide new insights into their potential therapeutic possibilities. In this work, I also aim to develop multi-target drug candidates for managing the underlying pathologies of AD or inhibiting the casein kinase II (CK2) holoenzyme controlling cellular proliferation, but also focusing on repairing and preventing further damage to the cellular structure with antioxidant compounds.

While oxidative stress is implicated in the pathology of many different diseases, the structure-activity relationship (SAR) of antioxidants is not well understood. Efforts are mostly focused on natural antioxidants; however, their pharmacokinetic properties are less than ideal due to their poor in vivo activity. Thus, free radical scavenging activity of the compounds studied was further investigated through SAR in order to identify essential structural motifs to provide better radical scavenging activity with improved



absorption, distribution, metabolism, and excretion (ADME) properties to these drug candidates.

## **1.2 Research goals**

### **1.2.1 $\beta$ -carbolines as multi-functional drug candidates for Alzheimer's disease**

As a complex disease, AD needs multi-target treatment options. The amyloid plaque and neurofibrillary tangles forming in the brain coincide with neuronal cell death and loss of cholinergic transmission. The basic  $\beta$ -carboline skeleton has a relatively extended structure that can span the active center of the cholinesterases with a variety of hydrophobic units that can interact at the active site. Earlier findings reported by the Török group<sup>18</sup> led to the development of a set of  $\beta$ -carbolines with an additional aromatic ring, either linked directly or via a carbonyl linker, to test the role of molecular flexibility on the efficacy of anti-cholinesterase activity. My work aimed to investigate  $\beta$ -carboline derivatives as new drug candidates for potential use as cholinesterase and A $\beta$  fibril formation inhibitors as well as radical scavengers.

### **1.2.2 Hydrazide and nipecotic acid derivatives as multi-functional drug candidates**

Computer aided drug discovery is a growing field<sup>19,20</sup>. The aim of my collaborative project is to develop drugs based on the molecular interactions expected to occur at the active site of an enzyme, so that the drug will bind efficiently. Along the same lines as the  $\beta$ -carboline project, this work aimed to look into potential new classes of cholinesterase inhibitors guided by molecular docking studies. Docking studies were conducted with AutoDock Tools (Version 1.5.6) to identify new drug candidates for acetylcholinesterase (AChE) inhibition and AD drug discovery. Fourteen compounds were identified and developed based on the docking studies, mimicking the electrostatic

interactions of donepezil. In this work, the cholinesterase inhibition studies and radical scavenging activities of these compounds were investigated.

### **1.2.3 SAR study of hydrazones as radical scavenging compounds**

One of the underlying components to many neurological diseases, cardiovascular diseases and cancers is the cellular damage caused by excessive amounts free radical species. While this may not be the most potent factor in the progression of these diseases, it is worth noting that radical species do influence disease progression<sup>21,22</sup>. Antioxidants are an effective way to prevent/repair the damage done by free radical species in the body. The human body already has endogenous systems in place to maintain redox homeostasis, but we can supplement this system through the consumption of exogenous antioxidants in our diet. Many natural antioxidant structures are complex due to their high substituent content and dispersed electron conjugation over various ring systems. In this work, I aim to assess the relationship between the physicochemical and structural parameters of hydrazone derivatives and their radical scavenging activities. The results of this study will provide insights into substituent effects on radical scavenging and help further the multi-functional drug development process.

#### **1.2.4 SAR study on radical scavenging activity of phenol and aniline model compounds**

To date, no study has yet linked radical scavenging activity to specific substituents of natural antioxidants, other than the presence of the -OH groups<sup>23</sup>. In an effort to elucidate the importance of the substituents on the radical scavenging activity, phenol and aniline model compounds were screened through a SAR study. Driven by my earlier hydrazone SAR study where the complicated geometries made it difficult to directly correlate activity with substituents<sup>24</sup>, this study focuses on single ring aromatic systems with simpler geometries. Using less complex phenol and aniline models, I aim to investigate the effects of substituents on the radical scavenging activity of these compounds.

#### **1.2.5 Hydrazones as multi-functional drug candidates**

The hydrazone structure has already been reported as a suitable backbone for the development of multi-functional drugs in a wide variety of areas, from AD to antibacterial agents<sup>25-27</sup>. Cancer research is an extremely important and highly active area of biochemical, medical and pharmaceutical developments<sup>13-15</sup>. In an effort to further identify the multi-functional capabilities of the hydrazone structure; this work looks at the radical scavenging activity through a SAR study to identify important characteristics of hydrazones as antioxidants. Inhibition of an enzyme, CK2, showing increased expression levels in all cancer types will be assessed in order to identify a new class of potential therapeutic agents.

#### **1.2.6 Method development of amyloid fibril formation from lysozyme and insulin**

The formation of amyloid fibrils is a hallmark and often a cause of several diseases. In order to develop drugs that target fibril formation against these diseases, we need to

develop appropriate assays to assess amyloid fibril formation inhibition. There are many different procedures for generating various types of amyloid fibrils in vitro<sup>28</sup>. However, the most common methods to generate fibrils use acidic media (pH of 1.5) and often extreme temperatures (70 °C) for the protein to form fibrillar aggregates<sup>18,29</sup>. These methods work well to produce large amounts of amyloid fibrils quickly, but the growth conditions required to form these fibrils are often not physiologically relevant. My goal was to investigate new methods of amyloid fibril formation using thioflavin T (ThT) fluorescence and atomic force microscopy (AFM) imaging to identify reproducible physiologically relevant assay conditions.

## CHAPTER 2

### LITERATURE OVERVIEW AND BACKGROUND

#### **2.1 Definition and role of reactive oxygen and nitrogen species**

Reactive oxygen species (ROS), such as superoxide and the hydroxyl radical, are often produced during cellular respiration and in response to cellular stress. The ROS in vivo are generated from enzymatic and non-enzymatic metabolic redox reactions; for example, superoxide or hydrogen peroxide can be produced from molecular oxygen by xanthine oxidase or catalase for example<sup>22</sup>. Interaction of oxygen with transition metal ions, such as  $\text{Cu}^{2+}$ ,  $\text{Co}^{2+}$ ,  $\text{Ni}^{2+}$  or  $\text{Fe}^{2+}$ , can also generate ROS<sup>21,22</sup>. The ROS generated can further react to produce secondary ROS, such as lipid peroxides, which are much longer lived in the cell. Reactive nitrogen species (RNS) are generated in response to cellular stress (such as oxidative stress or bacterial infection). They are typically derived from an initial  $\text{NO}^{\bullet}$  radical synthesized from arginine by nitrogen oxide synthases (NOSs)<sup>22</sup>. Table 1 includes examples of reactive oxygen and nitrogen species, and their structures.

Table 1: The ROS and RNS family include both free radicals and non-radical species.

The most common examples are depicted here<sup>22,30-32</sup>.

<u>Name</u>	<u>Structure</u>
Ozone	$\overset{-}{\text{O}}=\overset{+}{\text{O}}=\overset{-}{\text{O}}$
Singlet Oxygen	$\text{O}=\text{O} \quad {}^1\Delta\text{O}_2$
Superoxide	$\text{O}^{\cdot-}\text{O}^-$
Hydroxyl radical	$\text{H}-\text{O}^{\cdot}$
Hydrogen peroxide	$\text{HO}-\text{OH}$
Hydroperoxyl radical	$\text{HO}-\text{O}^{\cdot}$
Hypochlorous acid	$\text{HO}-\text{Cl}$
Nitrogen oxide	$\text{N}^{\cdot}=\text{O}$
Peroxynitrite ion	$\text{O}=\text{N}^{\cdot}-\text{O}-\text{O}^-$

These oxidative species are both crucial for cell survival and reactive enough to cause cell death, thus the body needs to maintain balanced levels of oxidized and reduced forms of electron carriers in a redox homeostasis<sup>33</sup>. Over-production of ROS and RNS species contributes to the progression of many ailments, such as Alzheimer's disease, Parkinson's disease, diabetes, aging, cancer and multiple sclerosis (MS)<sup>22,32,34-40</sup>. Free radical species may not be the defining factor of these diseases, but the underlying effect radicals have on the progression of diseases is something that cannot be ignored. This

section aims to address the fundamentals of redox homeostasis in the human body and what is required to maintain that balance.

### **2.1.1 Oxidative species and their functions in the body**

Free radicals, at their physiologically relevant concentrations in the body, perform functions such as cell signaling and in the immune response, which are essential for survival<sup>31,32,41-43</sup>. The ROS and RNS are typically synthesized by nitric oxide synthase (NOS) and nicotinamide adenine dinucleotide or nicotinamide adenine dinucleotide phosphate (NAD(P)H) oxidase isoforms<sup>22</sup>. Hydrogen peroxide is a common oxidative species found in cellular systems, with many uses in the cell and its regulation is tightly controlled. One of the ways  $H_2O_2$  acts is through a transient oxidative inactivation of protein tyrosine phosphatases (PTPs)<sup>44</sup>. As long as the PTPs have a catalytic cysteine residue,  $H_2O_2$  converts cysteine to sulfinic acid, which can be reversed in the presence of a reducing agent such as glutathione<sup>45</sup>. This action of  $H_2O_2$  has been noted with the platelet-derived growth and epidermal growth factors to inhibit the activity of the corresponding PTPs<sup>45,46</sup>. It has also been shown that  $H_2O_2$  activates transcription factors in the  $Nf-\kappa B$  family<sup>46</sup>, which lead to the activation of pro-inflammatory genes and cell proliferation<sup>22,47</sup>. It also acts as a signaling molecule for inflammation through phospho-activation of the p38 mitogen activated protein kinase<sup>48</sup> (hyperphosphorylated in brain tissue of Alzheimer's disease patients<sup>44</sup>) which decreases global phosphatase activity in the cell. The p38 mitogen activated protein kinase controls expression of interleukin-1 $\beta$  (IL-1  $\beta$ ), an inflammatory cytokine and regulates expression of COX-II and iNOS<sup>22,43</sup>. Inflammation has a key role in a multitude of diseases as well as in the body's immune response to foreign material. The ROS signaling is part of the pathway for many of these

reactions. Control of these ROS and ROS-induced secondary messengers are important to prevent an overreaction by the immune system. When the redox homeostasis is not balanced properly, reactive species react freely with proteins, lipids and nucleic acids and may modify their biological function<sup>22,32</sup>.

### **2.1.2 Damage to the body resulting from excessive amounts of oxidative species**

Excessive concentrations of ROS/RNS typically arise from metabolic issues where the body cannot maintain the redox homeostasis and begins to produce excessive amounts of these species. Age, lifestyle and environmental factors all contribute to oxidative stress<sup>20,49-52</sup>. One of the recent examples of environmental conditions resulting in oxidative species damage has been reported in China. There has been a significant increase in lung and breast cancer cases that are closely associated with the rapid industrialization and changing lifestyle due to smoking, poor diet and obesity<sup>52</sup>. In such conditions, cells are under excessive oxidative stress, which is usually a signal to the cell to begin apoptosis to preserve the integrity of the host organism<sup>22</sup>. Damage from reactive species oxidizes lipid membranes, proteins, and nucleic acids<sup>53</sup>. However, in the progression of cancer, the oxidative damage to the DNA may be so great that the cell never triggers apoptosis and enters a continuous cell replication state with unchecked cellular division<sup>54</sup>.

### **2.1.3 Endogenous defenses against oxidative stress**

To maintain redox homeostasis, the concentration of ROS/RNS in the body is controlled by endogenous antioxidant systems. Protective enzymes (e.g. superoxide dismutase, catalase, glutathione peroxidase), non-enzymatic peptides/proteins (e.g. glutathione,



ferritin, transferrin, ceruloplasmin, albumin), enzyme cofactors and several metabolites (Fig. 1) all constitute the endogenous antioxidant defense system in our body<sup>32,53,55-58</sup>.

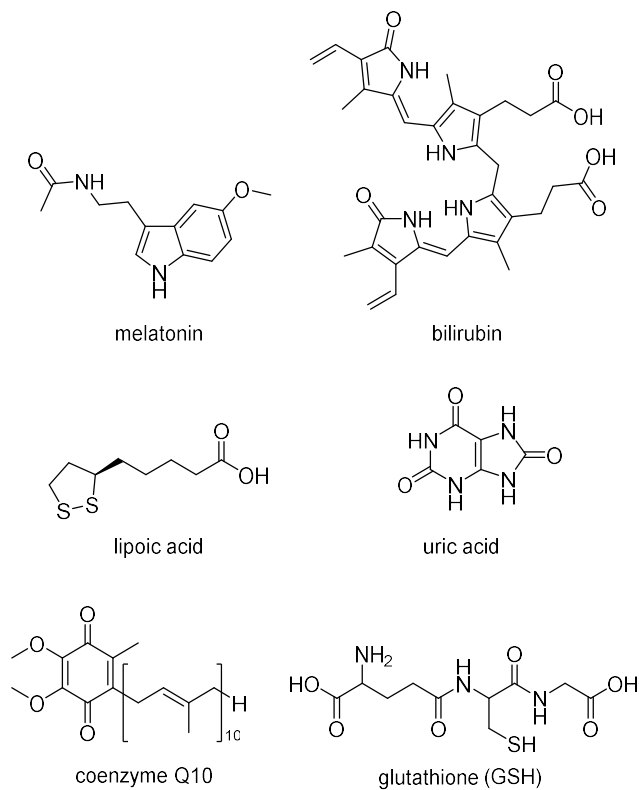


Fig. 1: Examples of endogenous radical scavengers.

The modes of action these systems use to maintain the redox homeostasis can vary greatly, from controlling the expression of ROS/RNS at the genetic level to repairing damage caused by radical species. However, when these systems fail, oxidative stress on the cell can lead to drastic changes in cellular form and function, potentially causing an even greater production of oxidative species.

### 2.1.4 Exogenous defenses against oxidative stress

When endogenous antioxidant systems are not effective enough, the body can rely on exogenous antioxidants. The exogenous antioxidants act as support systems to boost the endogenous defenses. These species have garnered extensive attention as potential candidates for preventing and/or treating many diseases<sup>58</sup>. Exogenous antioxidants are usually supplemented by the diet, these include vitamin C, vitamin E, or polyphenols for example (Figs. 2 and 3)<sup>53,56-59</sup>. Polyphenols are the most common class of exogenous antioxidants discussed in the literature<sup>59-67</sup> due to their high activity, ease of extraction from natural sources and high degree of structural variability<sup>65-70</sup>. Polyphenols (Fig. 3) often show excellent in vitro activity; however, their poor bioavailability has limited their practical applications for in vivo systems<sup>32,40,58,71-75</sup>.

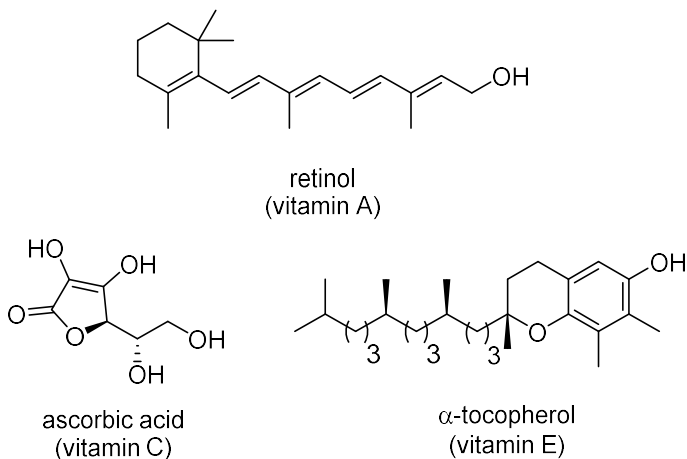


Fig. 2: Examples of vitamin radical scavengers.

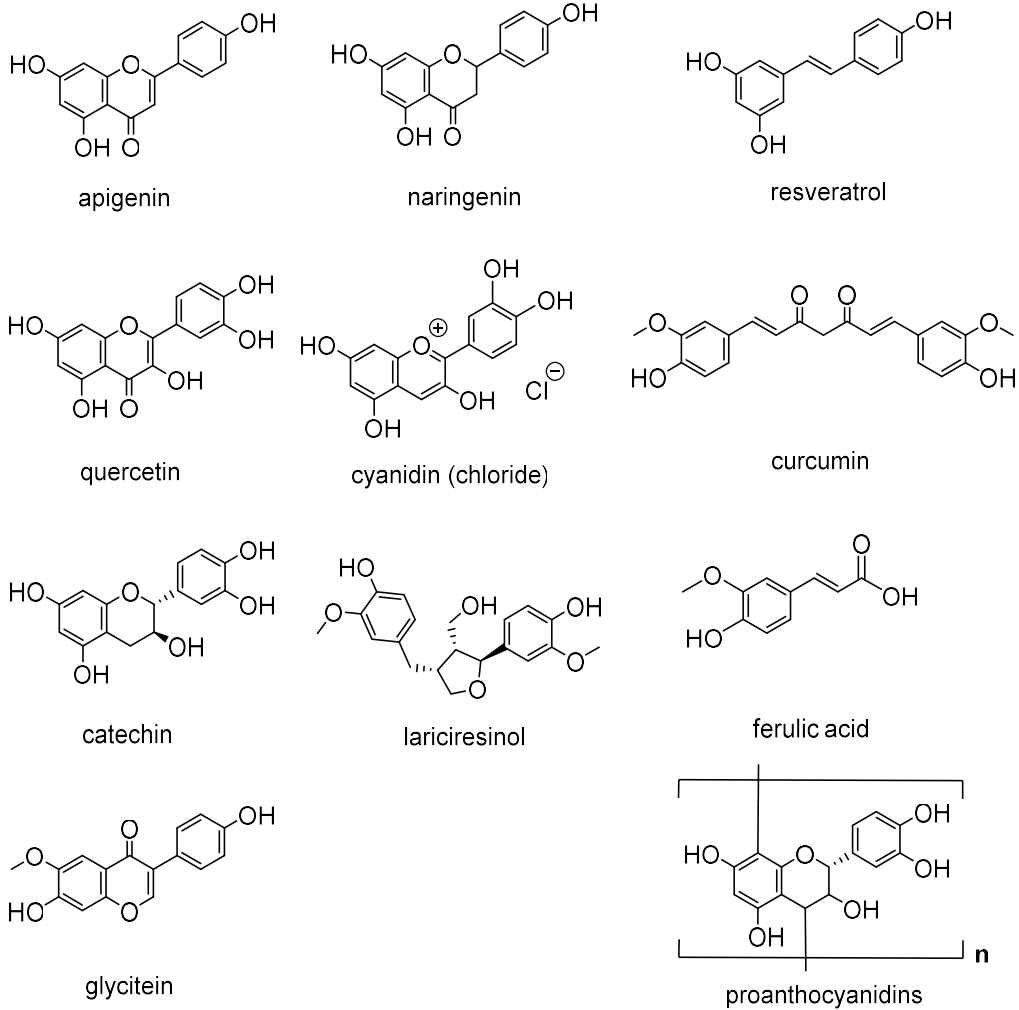


Fig. 3: Examples of commonly identified polyphenolic antioxidant species.

Polyphenols are not the only class of supplementary antioxidants. There are other compounds such as betalains (nitrogen containing), beta-carotene, or, lycopene among others (Fig. 4)<sup>68,73,76</sup>.

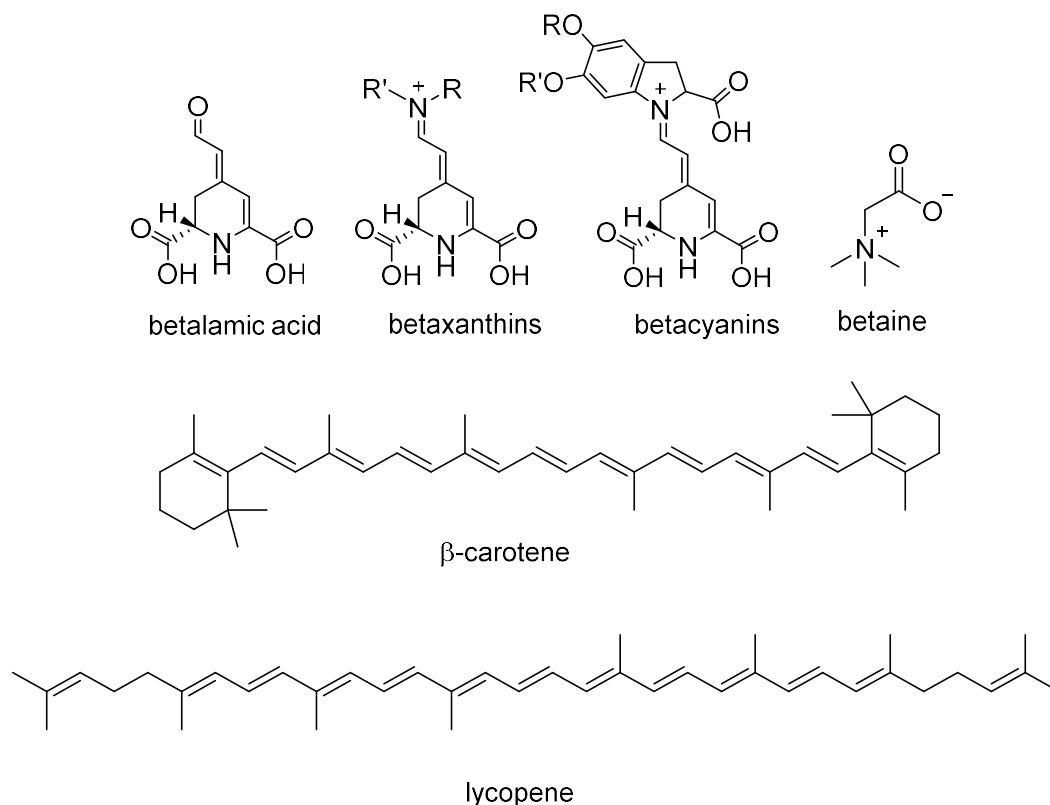


Fig. 4: Examples of non-polyphenolic antioxidant species.

Other properties of antioxidants such as bioavailability, gastric stability and the metabolic degradation are just as important as antioxidant activity when developing new exogenous antioxidants<sup>73-78</sup>. A recent report on exogenous antioxidants has attempted to refine the pharmacophores identified in these compounds to improve the drug-like properties of natural antioxidants through chemical modification<sup>57</sup>. It is important to note that while exogenous antioxidant supplements may help boost the body's defense against free radical species, they can also be harmful. Several studies reported an increase in lung and prostate cancer rates with patients taking  $\beta$ -carotene supplements<sup>17,79,80</sup>. While these systems may help us treat diseases, moderation and mechanistic understanding is key in

using exogenous antioxidants to restore the balance of redox processes. This work aims to provide insight into possible new multi-functional therapeutic candidates with radical scavenging properties to combat a variety of pathological symptoms in diabetes and AD.

## **2.2 Multi-functional drug development**

Treatment of complicated diseases, such as Alzheimer's disease, Parkinson's disease and cancer, have traditionally been met with the same approach to any other disease; one drug, one treatment<sup>81</sup>. However, evidence is mounting that multi-functional drugs may prove advantageous in the treatment of these multi-faceted diseases<sup>82,83</sup>. The pharmaceutical community has avoided multi-functional drugs due to the increased risk of side effects due to non-specific interactions<sup>84</sup>. Multi-target drugs have become increasingly popular since the early 2000s when evidence for their ability to manage these complicated diseases began to increase<sup>85-87</sup>. Twenty-one percent of all approved new molecular entities (NMEs) from 2015 to 2017 by the US Food and Drug Administration (FDA) were multi-target drugs<sup>88</sup>. Specifically speaking for many neurological diseases, treatment is not necessarily curing the disease, but rather managing the symptoms. Tolerance to these drugs may develop over prolonged use of the single target medication leading to increased dosage, with the largely unavoidable risk of increased side effects. Another option is treating the disease with a drug that does not target the same effector<sup>85,89,90,91</sup>. The same issues have also been identified in the treatment of many cancers, where single target drugs that aim to kill cancer cells lead to an adaptation of the cells via by-passing the targeted pathway, rendering the treatment ineffective<sup>91</sup>. However, multi-target compounds have the ability to act on several different effectors, managing the disease from more than one therapeutic avenue<sup>92,93</sup>. This

reduces the overall risk of side effects due to increased dosage and may also reduce the chance of resistance to the drug. Several new multi-target drugs were developed in 2017 that treat schizophrenia and major depressive disorders<sup>94, 95,96</sup>. Designing multi-target drug compounds is a fast-growing field with many compounds no longer being identified serendipitously, but through utilizing structural features of different compounds and combining them into a single structure<sup>96,97</sup>. These hybrid drugs are validated through numerous models such as QSAR studies<sup>98,99</sup>, virtual screening for common pharmacophores among known ligands<sup>96</sup>, molecular docking using the 3D structure of a protein<sup>100,101</sup> and computational methods aiming to look at the physicochemical properties of compounds before any in vivo testing. Investigating the multi-target capabilities of potential drug candidates is an invaluable tool in the race to develop new and effective treatments.

## **2.3 Protein misfolding and its connection to various diseases**

There are a large number of protein misfolding diseases that affect the human body, such as Alzheimer's, Parkinson's, Creutzfeldt–Jakob, and Huntington's diseases<sup>102-104</sup>. This work focuses on two diseases associated with protein misfolding and oxidative stress: Alzheimer's disease and diabetes mellitus.

### **2.3.1 Processes of proper protein folding**

Protein folding can be a complicated process in a cellular environment. As proteins are synthesized by the ribosome from mRNA transcripts, there are a few parameters that help define protein structure. For many proteins a chaperone molecule is present to help ensure that the protein folds into a specific conformation<sup>105,106</sup>. Hydrogen bonding holds together the secondary structure of the protein followed by the tertiary protein structure,

which is held together by interactions between the alpha and beta sheets in the secondary structures. Features like disulfide bonds, hydrophobic and hydrophilic interactions, as well as other intramolecular forces help maintain the folded structure of a protein<sup>106,108</sup>. Finally, the quaternary structure of a protein, which is comprised of multiple subunits, to generate a complete, active state of the protein structure.

Protein folding is a dynamic process with many different structural end points. A protein in solution will arrange so that it has the lowest energy conformation available to it, even if that folded state is only slightly more stable than the unfolded state<sup>106,107,108</sup>. If the process of forming a favorable conformation requires too much energy, specific cellular conditions, or chaperone proteins assist in the folding process, and if those factors are not present the protein will likely fold into a different low energy conformation. Many of these other conformations will not retain the structures necessary for proper protein function and will necessitate that the protein be degraded or re-folded by other proteins. It is also possible for proteins that are correctly folded to become misfolded due to oxidative damage, changes in the cellular environment, or exposure to other misfolded proteins<sup>109</sup>.

### **2.3.2 Alzheimer's disease**

Alzheimer's disease (AD) affects approximately 5.5 million Americans, with that number expected to increase to 16 million by 2050<sup>1</sup>. The cost associated with AD healthcare in 2017 was \$259 billion, which is likely going to increase as more patients develop AD<sup>1</sup>. As the 6<sup>th</sup> leading cause of death in the United states and the 5<sup>th</sup> leading cause of death for people 65 and older, there is a desperate need for practical progress in the field<sup>1,4</sup>. Studies show AD is characterized by three primary signs: extracellular plaques (A $\beta$ ), intracellular

neurofibrillary tangles (tau) and neuronal cell death. The route by which AD leads to death can be different depending on the individual and the symptoms such as loss of neuronal synapses, oxidative stress, mitochondrial abnormalities, hormonal changes and cell cycle anomalies<sup>4</sup>. As a multi-faceted disease caused by genetic and environmental factors, many therapies that are designed for managing AD combat different contributing factors in an effort to slow its progression<sup>110-116</sup>. The most common approaches are based on the cholinergic<sup>117</sup> and amyloid cascade<sup>118</sup> hypotheses<sup>4</sup>. The following section aims to explore a few factors influencing the development of AD and the literature describing their current treatment strategies. For the purpose of this work, I will focus on the cholinergic and amyloid cascade hypotheses, specifically on the A $\beta$  peptide.

The A $\beta$  protein is synthesized by processing of the amyloid precursor protein (APP) at the membrane of the cell. Cleavage by  $\alpha$ -,  $\beta$ - and  $\gamma$  secretases can result in different fragments mainly consisting of 40 or 42 amino acid residues (A $\beta$ <sub>1-40</sub>; A $\beta$ <sub>1-42</sub>)<sup>119</sup>. Though APP has been identified in cells and its structure is resolved, there is still much unknown about its function, with evidence that it may help to induce neuronal growth, synaptogenesis, traffic proteins along the axon, transmembrane signal transduction, cellular adhesion and calcium metabolism<sup>119</sup>. Much of this is not fully replicated in vivo, and need to be verified. APP is known to be highly prone to linking with sugars and advanced glycation end products (AGEs) and derivatized forms can prevent protein degradation by blocking chymotrypsin and trypsinogen<sup>120</sup>.



### 2.3.2.1 A $\beta$ self-assembly inhibition

Self-assembly inhibitors aim to prevent the formation of neurotoxic oligomeric and fibrillar A $\beta$  species in the extracellular space to prevent inflammation and damage to neuronal cells. Due to its importance, an extensive amount of reports are available in the literature about A $\beta$  self-assembly inhibitors<sup>120</sup>. Many different classes of compounds have been investigated as potential A $\beta$  fibril and/or oligomer formation inhibitors<sup>121-135</sup>.

A few examples can be seen in Fig. 5.

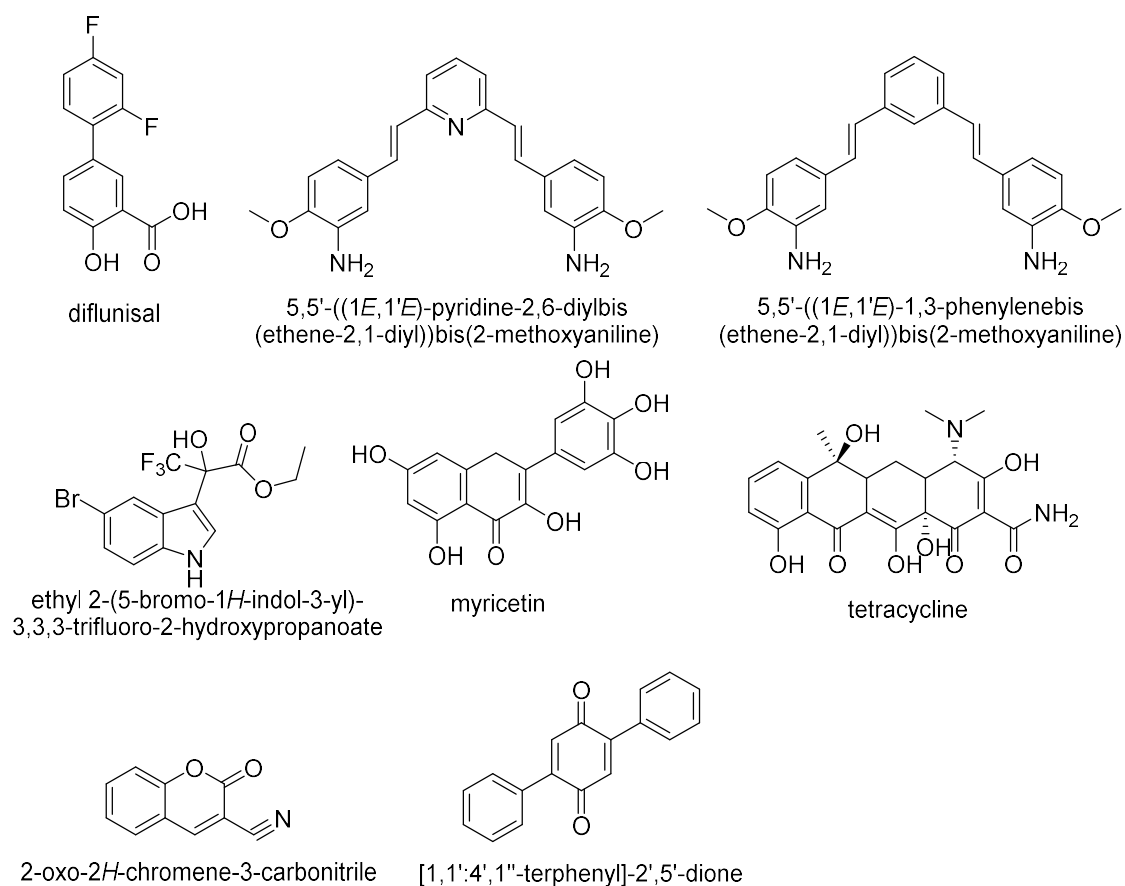


Fig. 5: Examples of A $\beta$  self-assembly inhibitors.

Unlike enzyme inhibitors, A $\beta$  self-assembly inhibitor interactions with A $\beta$  are not completely understood<sup>120</sup>, even the mechanism of A $\beta$  fibrillogenesis is not yet fully uncovered<sup>136-138</sup>. Recent work by Shankar, G.M. *et al.* has proposed a model of A $\beta$  fibrillogenesis where a ring-like structure is the main oligomer that then self-associates to form the various fibril morphologies seen in the literature<sup>138</sup>. However, more research is needed to corroborate this model. These compounds interact with the amyloid monomers preventing their aggregation into oligomers or tightly packed fibrils.

### **2.3.2.2 Disassembly of A $\beta$ oligomer and fibril species**

There is widespread agreement in the literature that both the oligomers and fibrils of A $\beta$  are neurotoxic<sup>139-143</sup>. Many reports also suggest that the oligomers are more toxic than the fibrillar end products<sup>142</sup>. The A $\beta$  oligomers target glutamate ionotropic receptor AMPA type subunit 2 (GluR2)-containing synapses disturbing the  $\alpha$ -amino-3-hydroxy-5-methyl-4-isoxazolepropionic acid (AMPA) receptors, leading to Ca<sup>2+</sup> leakage and synaptic loss<sup>144</sup>. In an effort to focus on clearance of already formed A $\beta$ , several disassembly agents have been developed<sup>8,9</sup> that aim to clear the A $\beta$  oligomers and fibrils in an effort to minimize the effect of the protein's misfolded form on the brain. Several projects have been completed to assess the disassembly of pre-formed A $\beta$  fibrils with small organofluorine compounds<sup>145</sup>, chalcones<sup>18</sup> and coumarins<sup>18</sup>. One therapeutic treatment investigated has been to drive the soluble oligomer species to form fibrils in an effort to prevent further neuronal damage and then focus on clearance of the fibrils with limited success<sup>146</sup>.

### **2.3.2.3 Cholinesterase inhibitors**

Acetylcholine is a neurotransmitter of particular importance to the peripheral and central nervous systems and is involved in processes such as learning, memory, sleep and stress<sup>146</sup>. Acetyl and butyrylcholinesterase inhibitors have been investigated as potential therapeutic avenues for AD. AD patients have an impaired capability to synthesize and transfer acetylcholine (ACh) and butyrylcholine (BuCh)<sup>147</sup>. Acetylcholinesterase (AChE) and butyrylcholinesterase (BuChE) are involved in terminating the neurotransmitter signals of ACh and BuCh in the synaptic cleft. The enzymes bind tightly to their substrates (ACh and BuCh respectively). Inhibitors such as galantamine and donepezil work to reduce the inflammation in the brain and maintain the ACh or BuCh concentration in the synaptic cleft to relay the neuronal signals<sup>5-7</sup>. Dosage of these inhibitors must be very well controlled as concentrations that are too high can lead to disruption of nerve signals and cause constant stimulation of muscle and nerve cells.

### **2.3.2.4 The role of reactive oxygen species in Alzheimer's disease**

It has been shown that ROS and RNS significantly impact the progression of AD, through direct oxidative damage, increase in inflammation from cytokine release, further A $\beta$  fibril development (such as from accumulation of AGEs) and cell death by apoptosis<sup>4,148</sup>. A $\beta$  peptides are also able to generate ROS<sup>149</sup>. With a high fatty acid content, oxygen requirement and iron content, the brain is very susceptible to ROS and RNS<sup>149,150</sup>. Metal ions (e.g. Cu<sup>2+</sup> and Zn<sup>2+</sup>) have also been shown to impact the progression of AD in the brain due to increased ROS production<sup>151</sup>.

### **2.3.2.5 Multi-target approaches to the treatment of Alzheimer's disease**

Alzheimer's disease is a multi-faceted disease characterized by amyloid plaques, neurofibrillary tangles, decreases in synaptic function and decline in memory. It is important when treating AD to look for approaches which help to combat the broad variety of potential drug targets<sup>152</sup>. There is a growing sentiment in the literature that the more targets the drug interacts with the better the outcome of the treatment will be. Drugs like memantine<sup>153</sup>, metformin, sulfonylureas, thiazolidinediones, glucagon-like peptide-1 (GLP-1) agonist and dipeptidyl peptidase 4 (DPP-4) inhibitors<sup>152</sup> work through different pathways to help combat AD through treatment of severe symptoms and targeting underlying conditions to reduce the progression of AD<sup>154</sup>.

### **2.2.3 Diabetes mellitus**

Diabetes affected 30.3 million Americans in 2015, costing the healthcare industry billions of dollars a year, e.g. nearly \$250 billion in 2012. These numbers are expected to rise as around 1.5 million Americans are newly diagnosed with diabetes every year<sup>2</sup>. These costs are not towards curing the disease, but rather for managing it. In an effort to describe the treatment regimens, diabetes has been split into two different types depending on insulin resistance (type 1: insulin responsive and type 2: insulin resistant)<sup>4,155</sup>. Glucose control is essential for improved short and long-term outcomes with either type<sup>156</sup>. There are two common conditions that develop as a result of poorly treated diabetes: hyperglycemia and diabetic ketoacidosis, both of which are fatal.

### 2.2.3.1 Diabetes mellitus type 1 and 2

Type 1 diabetes is associated with the body's inability to produce insulin through impairment of pancreatic  $\beta$ -cell function. This disease is most often genetic, with several different genetic mutations currently noted for patients with type 1 diabetes<sup>155</sup>. Due to the nature of type 1 diabetes, it is not relevant to my work and will not be further discussed.

Type 2 diabetes is non-insulin dependent (or typically termed insulin – resistant) and makes up approximately 90% of the diabetes cases<sup>157</sup>. For patients with type 2 diabetes, managing their disease is much more complicated. It is not as simple as injecting insulin, but also requires managing the different factors contributing to their disease progression. Obesity, poor diet and poor exercise are all contributing factors to the development of type 2 diabetes. As rates of obesity increase across the World, type 2 diabetes rates have also increased<sup>158</sup>. Damage caused through poor management of type 2 diabetes can damage from the pancreatic  $\beta$  cells and the patient can develop type 1 diabetes.

For many type 2 diabetes patients, the current treatment is the same as for type 1 patients: insulin. High doses of insulin help control blood glucose levels preventing hyperglycemia but can increase the body weight of patients and put them at risk for heart failure<sup>159</sup>.

Gluconeogenesis is a common cause of hyperglycemia in patients and inhibiting FBPase prevents endogenous glucose production<sup>160</sup>. The enzyme FBPase catalyzes the hydrolysis of fructose 1,6- bisphosphate to fructose 6-phosphate and is the rate limiting step of gluconeogenesis<sup>161</sup>. There are three main classes of inhibitors for FBPase: substrate site, subunit interface and AMP site binding inhibitors. Indole, benzimidazole, pyrrole and triarylpyrazoles derivatives have been investigated as allosteric inhibitors acting at the AMP binding site of the enzyme<sup>162-164</sup>. These compounds are all designed to mimic AMP

in the binding site of the enzyme, to provide better inhibition profiles with FBPase and reduce the presence of phosphate groups in these compounds to reduce the possibility of non-specific inhibition of other AMP binding enzymes. Glucagon like peptide-1 (GLP-1) receptor agonists (which boost signal to produce more insulin) or dipeptidyl peptidase 4 (DPP-4) inhibitors which block the degradation of normal GLP-1 have also been used to treat type 2 diabetes<sup>165</sup>. As an alternative method, sodium–glucose co-transporter 2 inhibitors have also been used to prevent hyperglycemia by blocking the reabsorption of glucose by the kidneys<sup>165</sup>. There have been other efforts to look at antioxidants as therapeutics for type 2 diabetes as there is evidence that the increase of ROS species (such as H<sub>2</sub>O<sub>2</sub>) in the mitochondria can lead to insulin resistance<sup>159</sup>. Antioxidant supplementation has been shown to increase glucose tolerance and insulin sensitivity<sup>159</sup>.

### **2.2.3.2 Diabetes and its possible connections to Alzheimer’s disease**

Recent evidence suggests that there may be a connection between type 2 diabetes and AD<sup>4,166-168</sup>. Gut and muscle tissue insulin is routinely investigated in the literature, but it is also present in the brain (transported from the pancreatic  $\beta$ -cells and may even be synthesized in the brain<sup>4,169-172</sup>. With the increased insulin production in type 2 diabetes patients, they have an elevated insulin level in the brain. Increases in insulin levels alter the metabolism of amyloid beta and tau, causing increases in the levels of extracellular A $\beta$ <sub>1-40</sub> and A $\beta$ <sub>1-42</sub> as well as APP $\alpha$  in cultures of rat cortical neurons and mouse neuroblastoma cells overexpressing wild-type APP<sup>173,174</sup>. Insulin degrading enzyme (IDE) clears out extracellular A $\beta$  in healthy patients, but due to the high binding affinity for insulin it becomes inactive in patients with type 2 diabetes<sup>175</sup>. Aggregation of A $\beta$  and

tau leads to inflammation in the neuronal cells and changes in the cellular structure that further drive amyloid aggregation in the brain<sup>151</sup>. Insulin fibril formation has also been shown to promote A $\beta$  fibril formation as well as tau phosphorylation in neuronal cells<sup>176,177</sup>. Combined with the effects on increased insulin concentrations in the brain, this will lead to further AD progression.

A third aspect of the effect of diabetes on the development of AD is the increased production of ROS and RNS. Insulin resistance decreases the number of GLUT4 transporters in the plasma membrane, decreasing the amount of glucose available to the neuronal cells, leading to hyperglycemia<sup>4</sup>. The lack of glucose will lead to mitochondrial overload, from processing fatty acids and proteins<sup>156</sup>, increasing the oxidative stress in the cell.

## **2.4 Cancer**

Cancer is a multi-faceted disease with genetic components, environmental factors and physiological contributions that lead to the initialization and progression of cancer in a patient. There has been a significant amount of work published on understanding the genetic components to different types of cancer<sup>13-16</sup>, but there are many underlying physiological problems which also contribute to the development of cancer in an individual.

### 2.4.1 Reactive oxygen species and cancer development

As cancer cells develop, their metabolism shifts from the complex oxidation of glucose to CO<sub>2</sub> toward lactic acid production even under aerobic conditions in a process known as the Warburg effect<sup>178-181</sup>. The ROS and RNS species play a huge role in cancer development. Increased levels of ROS and RNS are central to the progression of most, if not all cancers. Improper redox homeostasis and overall metabolic irregularities, among other things, create excessive amounts of ROS and RNS in the cell<sup>182,183</sup>. As discussed in section 2.4.1, ROS and RNS have dramatic effects within the cell. Constant exposure to the elevated levels of oxidative stress and cellular inflammation lead to irreparable damage to the cell and can push the cell to become cancerous<sup>182,184,185</sup>. Antioxidants have been shown to help combat this progression towards cancer at early stages<sup>182</sup>. However, ROS are involved in pathways promote cell survival or induce apoptosis<sup>183,184</sup>. Redox homeostasis in cancer cells is elevated compared to that of normal cells, but it appears there is still a balance to the increased ROS production, where increasing the ROS concentration further leads to cellular death. Cancer cells are able to produce slowly dividing cells that survive processes such as chemotherapy<sup>185</sup>. They have elevated antioxidant systems that allow the cells to lower the ROS concentrations in the cell and keep them in a stable state. Reduction of ROS levels, through antioxidant supplementation, in cancer cells results in a loss of adhesion of molecules on the surface of the cell and can turn a cancer malignant<sup>182</sup>. Treatment of cancer cells with antioxidants may in fact advance the cancer development resulting in metastasis.

While antioxidants may help protect patients from cancer in some cases, they have also been shown to promote cancer growth<sup>80</sup>. A common treatment of cancer is to increase the



ROS concentrations in the cells to such a high level that it triggers apoptosis. A pancreatic cancer treatment is a combination of gemcitabine with trichostatin A, epigallocate-3-gallate (EGCG), capsaicin and benzyl isothiocyanate (BITC)<sup>184,186-189</sup> which work to increase the ROS concentrations in cells and trigger apoptosis. Chemotherapy is used to induce mutations in the mitochondrial DNA to induce higher ROS formation rates leading to cellular apoptosis<sup>182,190</sup>. Targeting ROS production in cancer cells provides new mechanisms into combating the generation or continued proliferation of cancer in the body. Understanding ROS involvement in cancer cell development and progression, as well as its usefulness in therapeutic approaches, is important for the development of future treatments.

#### **2.4.2 Casein kinase II**

Casein kinase II (CK2) is a ubiquitous serine/threonine kinase, which has been shown to influence cell survival, growth and death<sup>191-193</sup>. It is a holoenzyme (130–150 kDa) consisting of 4 subunits one CK2 $\alpha$  (42 kDa), one CK2 $\alpha'$  (38 kDa) and two CK2 $\beta$  (26 kDa) subunits that can maintain different configurations of subunits forming a  $\alpha 2\beta 2$ ,  $\alpha\alpha'\beta 2$ , or  $\alpha' 2\beta 2$  complexes<sup>191,194</sup>. The CK2 $\alpha$  subunit is 90% similar to CK2 $\alpha'$  at its catalytic site but they are derived from different genes. Interestingly, only CK2 $\alpha$  and CK2 $\beta$  have been shown to be essential for cell survival<sup>192</sup>. More importantly, CK2 can suppress apoptosis, leading to cell survival<sup>192,193,195</sup>. It is no surprise that CK2 deregulation, resulting in elevated CK2 expression, has been identified in many cancer phenotypes<sup>192,195-201</sup>. Due to the different chemical composition of cell types and the ubiquitous presence of CK2, it only makes sense that CK2 potentially has a large variety of substrates<sup>202</sup> and different modes of action, such as inhibiting apoptosis through

phosphorylation of proteins<sup>193, 195, 203-208</sup> or suppressed expression of the NF- $\kappa$ B complex<sup>191</sup>. There has been a significant amount of research published on potential inhibitors of the CK2 holoenzyme. For example, flavanone-based inhibitors have been investigated due to their ease of extraction from natural sources and their potential activity as free radical scavengers, which makes them possible multi-functional drug candidates (Fig. 6)<sup>209-211</sup>. The most potent flavanones have at least two hydroxyl groups located at positions 7 and 4'<sup>209</sup>.

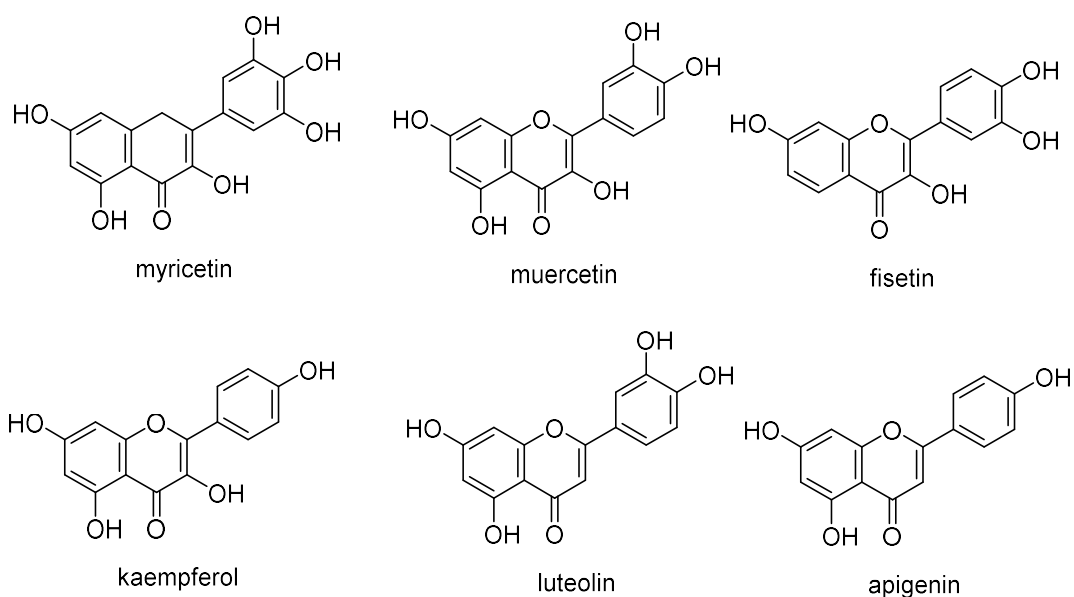
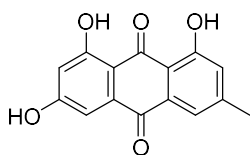


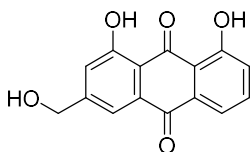
Fig. 6: Flavanone derivative CK2 inhibitors.

Multi-functional drugs are useful in the field of drug development; however, it is important that the active compounds identified are selective inhibitors of only the enzymes targeted. For this reason, other protein kinases are screened to ensure selectivity of the inhibitor. One of the most common types of inhibitors for CK2 identified acts at

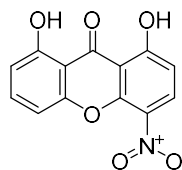
the small ATP binding pocket of the enzyme, such as emodin<sup>212</sup>, emodina<sup>213</sup>, 4,5,6,7-tetrabromo-1H-1,2,3-benzotriazole<sup>214</sup>, 4,5,6,7-tetrabromo-2-(dimethylamino)benzimidazole<sup>215</sup> and 5-oxo-5,6-dihydro-indolo(1,2-a)quinazolin-7-yl]acetic acid<sup>210</sup>. There are other inhibitors such as 1,3-dichloro-6-[(E)-(4-methoxyphenyl)imino)methyl]dibenzo(b,d)furan-2,7-diol, 1,8-dihydroxy-4-nitroxanthene-9-one, 8-hydroxy-4-methyl-9-nitrobenzo[g]chromen-2-one and 3,8-dibromo-7-hydroxy-4-methylchromen-2-one which have potent and selective inhibition activity against CK2 with IC<sub>50</sub> values in the nM to μM range (Fig. 7)<sup>206,216</sup>. Several anthraquinones, xanthenones and coumarins have been shown to be potent inhibitors of CK2. A defining factor of many of these inhibitors is the presence of hydroxyl, nitro, amino, or halogen substituents, which may interact with the enzyme at the ATP binding site, or act via other possible modes of inhibition<sup>216</sup>.



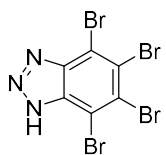
emodin



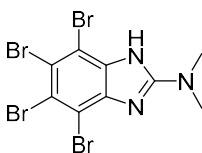
emodina



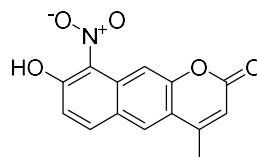
1,8-dihydroxy-4-nitroxanthren-9-one



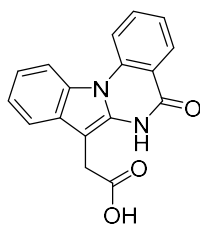
4,5,6,7-tetrabromo-1H-1,2,3-benzotriazole



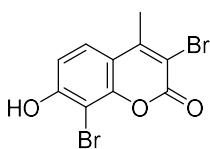
4,5,6,7-tetrabromo-2-(dimethylamino)benzimidazole



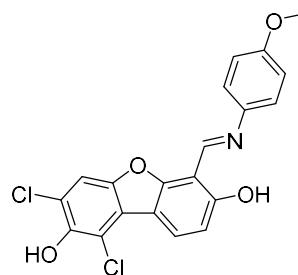
8-hydroxy-4-methyl-9-nitrobenzo[g]chromen-2-one



5-oxo-5,6-dihydro-indolo(1,2-a)quinazolin-7-yl]acetic acid



3,8-dibromo-7-hydroxy-4-methylchromen-2-one



1,3-dichloro-6-[(E)-((4-methoxyphenyl)imino)methyl]dibenzo(b,d)furan-2,7-diol

Fig. 7: Examples of CK2 holoenzyme inhibitors.

## CHAPTER 3

### TECHNIQUES AND METHODOLOGIES

#### 3.1 Cholinesterase inhibition assay using Ellman's method

Originally described by Ellman *et al.*,<sup>217</sup> the Ellman's method monitors the activity of cholinesterase enzymes through the use of an indicator (5,5'-dithio-bis-[2-nitrobenzoic acid] or DTNB) and UV-Vis spectroscopy. The Ellman's method for cholinesterase inhibition works with both acetyl and butyrylcholinesterase enzymes, monitoring the overall activity of the enzyme as it works to hydrolyze the respective substrates (acetylthiocholine and butyrylthiocholine) to acetic acid or butyric acid (depending on the substrate and enzyme) and thiocholine (Fig. 8).

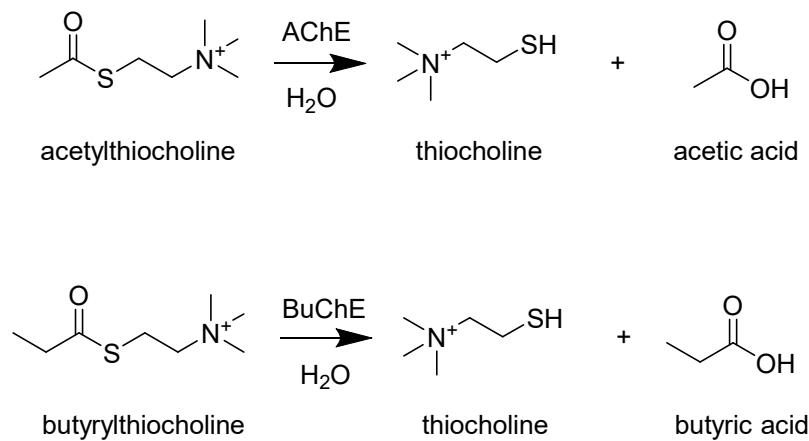


Fig. 8: Hydrolysis of acetyl and butyrylthiocholine by cholinesterases.

The indicator, DTNB, reacts with the free sulfhydryl groups of thiocholine, forming a yellow product which is monitored with UV-vis spectroscopy at 415 nm (Fig.9). During the assay, the kinetics of the absorbance increase is periodically measured for 15 min.

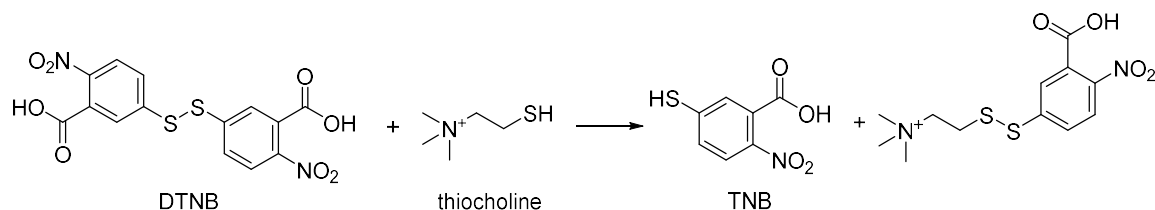


Fig. 9: DTNB reaction with thiocholine produced by the cholinesterases.

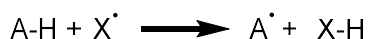
This method allows a comparison of rates of enzymatic reactions observed when carried out in conjunction with an uninhibited control group and a control group with known inhibitors (such as galantamine and donepezil). The ratios of DTNB to substrate must be tightly controlled, since DTNB concentrations higher than ACh has been shown to inhibit cholinesterase activity and is likely related to inhibition of the enzyme<sup>218</sup>. The DTNB is also sensitive to sunlight and must be protected from light prior to performing the assay<sup>219</sup>. The Ellman method provides a rapid and efficient profile of the inhibition of test compounds against cholinesterase enzymes.

### 3.2 Determination of radical scavenging activity of small molecule antioxidants

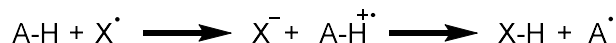
There is a broad assortment of currently used radical scavenging and antioxidant capacity assays in the literature<sup>21,220</sup>. With so many different assays and experimental conditions used, it is often difficult to accurately compare the literature data from different laboratories. High in vitro activity of samples does not necessarily correlate to the same

level of in vivo antioxidant activity<sup>21</sup>. This issue is further complicated by the varying routes that antioxidants go through to scavenge radical species in solution. Three common mechanisms of radical scavenging are illustrated in Fig. 10.

Hydrogen Atom Transfer (HAT)



Single Electron Transfer (SET)



Sequential Proton Loss/Electron Transfer (SPLET)

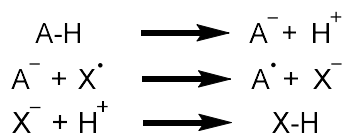


Fig. 10: Three common mechanisms for radical scavenging in solution by antioxidant species.

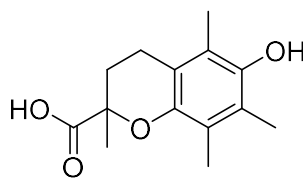
The HAT mechanism is based on a hydrogen atom transfer from the scavenger to the radical species in solution, forming a more stable radical from the antioxidant and quenching the radical species in solution<sup>220,221</sup>. This transfer is an adiabatic process involving the transfer of the hydrogen atom (proton and an electron) in the same step.

The SET mechanism is somewhat more complicated. The end result of SET is similar to that of the HAT mechanism<sup>220</sup>. However, electron transfer is the first step here, followed by the transfer of the proton. The rate limiting step of this reaction is the electron transfer and this mechanism is often mistaken for the HAT mechanism if the proton transfer is rapid.

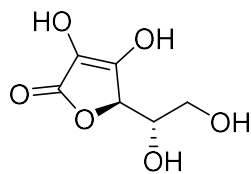
The third common mechanism discussed here is the SPLET mechanism. This mechanism is significantly different than the previous two mechanisms. Here, the antioxidant first loses a proton to the solvent in solution. Next, the radical scavenger donates an electron to the radical species followed by the radical abstracting a hydrogen from an adjacent source<sup>220</sup>. The rate limiting step of this reaction is the electron transfer, which relies on the stability of the antioxidant after this step of the reaction.

The different scavenging mechanisms, kinetic activities and various solvents may have effects on the measured radical scavenging activity of the compounds studied. As such, different radical scavenging assays are used to provide a more comprehensive idea of how the compounds investigated act as free radical scavengers<sup>21,220</sup>. Control antioxidant compounds Trolox (a water-soluble analog of vitamin E), resveratrol (a natural antioxidant found in plants such as grapes or blueberries) and ascorbic acid (also known as vitamin C) were used for comparison and to ensure the radical scavenging assays were carried out properly (Fig. 11).

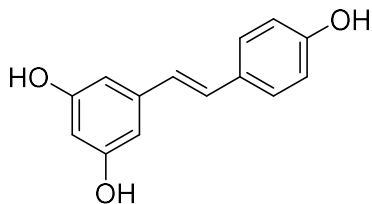




6-hydroxy-2,5,7,8-tetra  
methylchroman-2-  
carboxylic acid  
(Trolox)



ascorbic acid  
(vitamin C)



(*E*)-5-(4-hydroxystyryl)benzene-1,3-diol  
(resveratrol)

Fig. 11: Structures of known antioxidants used as control compounds for the radical scavenging assays (DPPH, ABTS and ORAC). All compounds were applied at 10  $\mu$ M concentration for each assay.

Here, three standard free radical scavenging assays are used to determine the antioxidant capacity of the compounds. The following three assays were chosen for their simplicity, common occurrence in the literature, solubility of the compounds and reproducibility.

### 3.2.1 DPPH radical scavenging assay

The 2,2-diphenyl-1-picrylhydrazyl (DPPH) assay is commonly reported in the antioxidant literature. It examines the radical scavenging activity of a compound as it scavenges the DPPH radical. It is a commercially available stable radical species. The assay is typically performed in methanol or ethanol, but it has also been carried out in water / alcohol mixtures, such as 50% aqueous ethanol<sup>21,24,220,222</sup>. The DPPH absorbs in the UV-Vis range at approximately 519 nm wavelength, with the decline in absorbance

recorded as compounds scavenge the radical. In solution, the color changes from the oxidized DPPH (purple) to reduced DPPH (yellow) (Fig. 12).

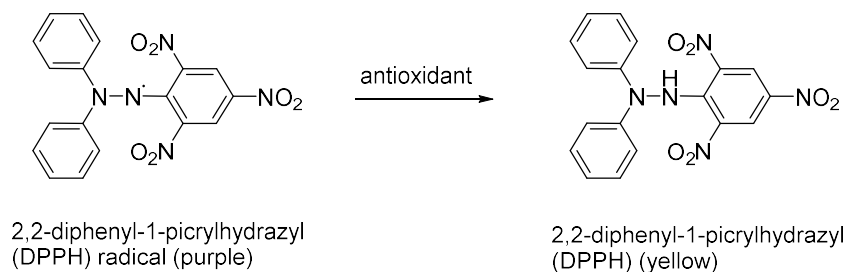


Fig. 12: The net chemical reaction of the DPPH radical scavenging assay.

The antioxidant scavenges the purple DPPH radical converting it to its non-radical form, which is yellow in color. A loss of absorbance is monitored at a wavelength of 519 nm.

Percent radical scavenging was determined using Eq. 1.

$$[\text{Eq. 1}] \text{ Percent Radical Scavenging} = \frac{(Abs_c - Abs_t)}{Abs_c} \times 100$$

$Abs_c$  is the control absorbance of the DPPH alone.  $Abs_t$  is the absorbance of the DPPH with the test compound.

The DPPH assay requires time to complete, with some studies running the assay from 30 min to 24 h. The interaction between the radical and radical scavengers can vary significantly depending on the solvents used and the form of the radical scavenger (extracts or single compounds). In my work, readings were recorded every 15 min for 1 h, but the 30 min readings were determined to provide the least significant variation in the data while also allowing for sufficient time to scavenge the radical. The DPPH assay is a mixed mode assay and is effective primarily with compounds that act through the

SET and HAT mechanisms, depending on the antioxidant's mode of action and solvent effect<sup>21</sup>.

### 3.2.2 ABTS radical scavenging assay

The 2,2'-azino-bis(3-ethylbenzothiazoline-6-sulfonic acid) (ABTS) (or Trolox equivalence antioxidant capacity (TEAC)) assay utilizes the ABTS radical generated prior to its use by reaction with an oxidizing agent (such as:  $K_2S_2O_8$ )<sup>21,220</sup>. The ABTS radical is green in color and absorbs in the UV-Vis range at approximately 734 nm.

Percent radical scavenging was determined using Eq. 1.

$$\text{[Eq. 1] Percent Radical Scavenging} = \frac{(Abs_c - Abs_t)}{Abs_c} \times 100$$

$Abs_c$  is the control absorbance of the ABTS alone.  $Abs_t$  is the absorbance of the ABTS with the test compound.

As the ABTS radical is scavenged, the non-radical product turns colorless. Thus, the decrease in the absorbance appears to be related to the antioxidant capacity of the sample (Fig. 13).

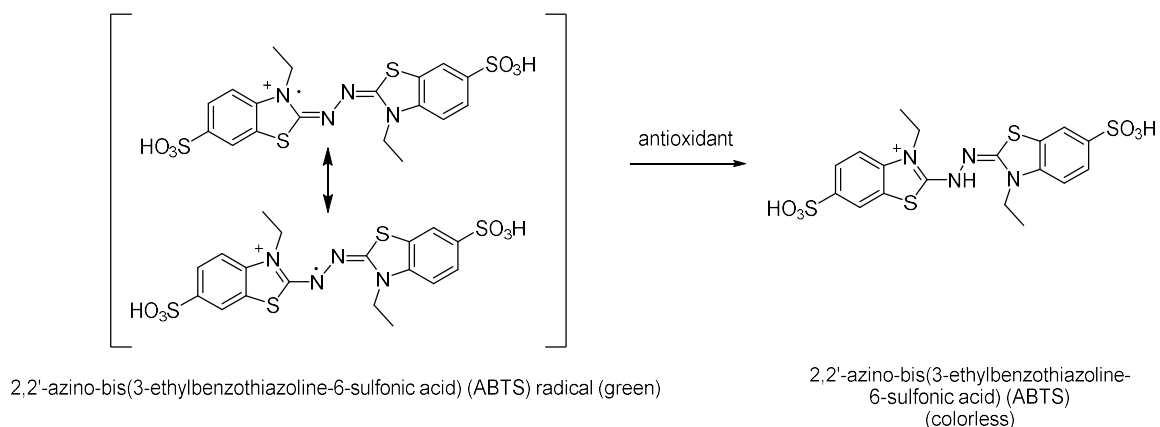


Fig. 13: The chemical reaction of the ABTS radical scavenging assay. The antioxidant scavenges the green ABTS radical converting it to its non-radical form, which is colorless. A loss of absorbance is monitored at 734 nm.

This assay was originally developed for standardization of the antioxidant activity of plant-based extracts, reporting the results in Trolox equivalence amounts. This was meant to give the scientific community working with plant-based extracts a way to standardize and compare the results obtained in different labs. Unlike other radical scavenging assays, the ABTS assay requires 12 min to complete, with readings taken at 0, 6 and 12 min, as the interaction between the radical and radical scavengers is complete within 12 min.

The ABTS assay is a mixed mode assay and is effective primarily with compounds that act through the SET and HAT mechanisms, depending on the antioxidant's mode of action<sup>21</sup>.

### 3.2.3 ORAC radical scavenging assay

The oxygen radical absorbance capacity (ORAC) assay has been widely used to analyze the antioxidant capacity of food samples. It uses the 2-hydroperoxy-2-methylpropanimidamide radical that is much smaller than the DPPH and ABTS radicals. The antioxidant scavenges the peroxy radical generated by the reaction of AAPH with  $O_2$  and is converted to its peroxide form (Fig. 14).

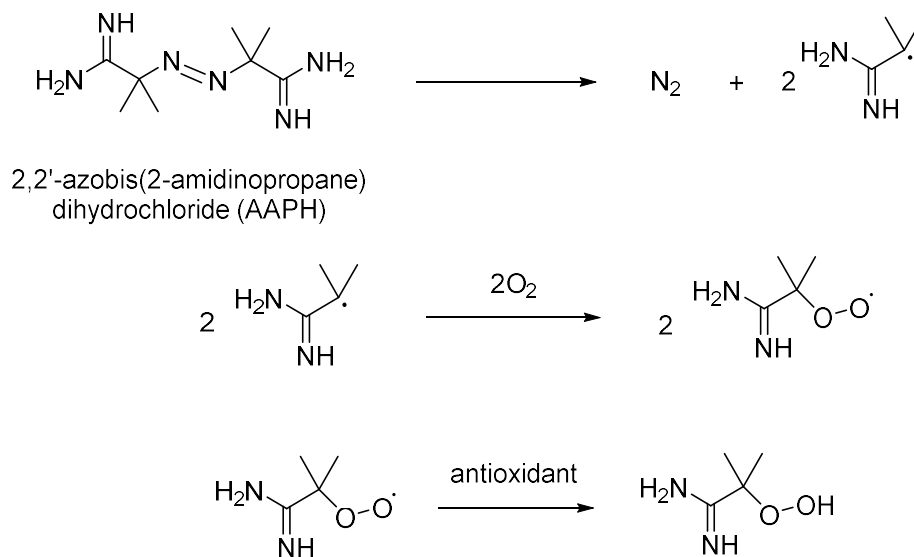


Fig. 14: Preparation of the radical and its quenching by the antioxidant in the oxygen radical absorbance capacity (ORAC) radical scavenging assay.

By scavenging the peroxy radical, the fluorescein dye is unaffected and continues to fluoresce. The lack of antioxidant activity allows the radical to oxidize the dye and thus decrease the fluorescence. The sample is getting excited at 485 nm and the loss of fluorescence is monitored at 520 nm over the course of 60 min.

The ORAC assay was conducted at a concentration of 0.612  $\mu$ M fluorescein and 19.125 mM AAPH with the compound concentration of 10  $\mu$ M and screened at an excitation and

emission wavelength of 485 and 520 nm respectively. Fluorescent intensity was calculated by Eqs. 2 and 3.

$$\text{[Eq. 2] } Net\ AUC = 0.5 + \sum_{0-29} \frac{f_i}{f_0} + \left( 0.5 * \frac{f_{30}}{f_0} \right)$$

The parameters are defined as followed:  $f_i$  is the fluorescence intensity at reading 1 to 29,  $f_0$  is the initial fluorescence intensity at reading zero and  $f_{30}$  is the fluorescence intensity at reading 30.

$$\text{[Eq. 3] } Percent\ Radical\ Scavenging = \frac{(Net\ AUC_t - Net\ AUC_c)}{Net\ AUC_{f\_max}} \times 100$$

Net AUC<sub>c</sub> is the net area under the curve as defined in Eq. 2 in case of the control with fluorescein and radical. Net AUC<sub>t</sub> with the test compound. Net AUC<sub>f\_max</sub> with the fluorescein alone.

This assay is effective primarily with compounds that act through the HAT mechanism for free radical scavenging<sup>21,223</sup>. Originally, the ORAC assay was developed to use  $\beta$ -phycoerythrin ( $\beta$ -PE) fluorescent protein isolated from *Porphyridium cruentum* as the fluorescent probe oxidized by 2,2'-azobis(2-methylpropionamidine) dihydrochloride (AAPH)<sup>224,225</sup>. However, the fluorescence decay of  $\beta$ -PE fluorescent protein was too quick and it was eventually replaced with fluorescein to provide better long term stability of the fluorescent probe (Fig. 15)<sup>228</sup>.

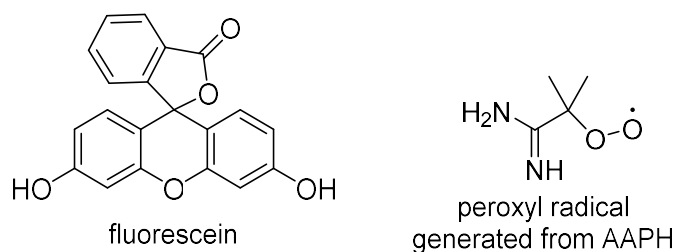


Fig. 15: Fluorescein is the fluorescent probe currently used to detect the AAPH radical in the ORAC assay.

This procedure was modified for high-throughput studies using a COBAS FARA II analyzer to provide larger sets of data. The automation of the ORAC assay allowed for the assessment of the length of radical scavenging activity and antioxidant capacity through kinetic measurements of many different samples at a time<sup>21</sup>. The ORAC readings can be further processed in comparison with a Trolox dilution series<sup>21</sup>. By standardizing the results, the data collected will be comparable to other data in the literature. The ORAC is a useful tool in the arsenal of free radical scavenging assays to analyze the activity of single compounds and plant derived extracts. The ORAC assay has been shown to provide higher activity readings to radical scavenging compounds with slower kinetic profiles<sup>220</sup>.

### 3.3 In vitro protein fibril aggregation

Protein structure is a string of amino acids that are arranged in a three-dimensional space by various inter- and intra-molecular forces such as hydrogen bonding, disulfide bonds and hydrophobic interactions, to name some examples. In solution, the three-dimensional structure of a protein will adapt to the lowest energy conformation possible, even if that folded state is only slightly more stable than the unfolded state<sup>106,107,227</sup>. In the case of

amyloidogenic proteins, the amyloid fibril state is highly stable and low energy resulting in protein structures that are rich in hydrophobic  $\beta$ -sheet structures. These structures interact with each other in solution and aggregate. This aggregation develops from single monomers to oligomer and fibrillar species through nucleation driven events (Fig. 16)<sup>22,228</sup>.

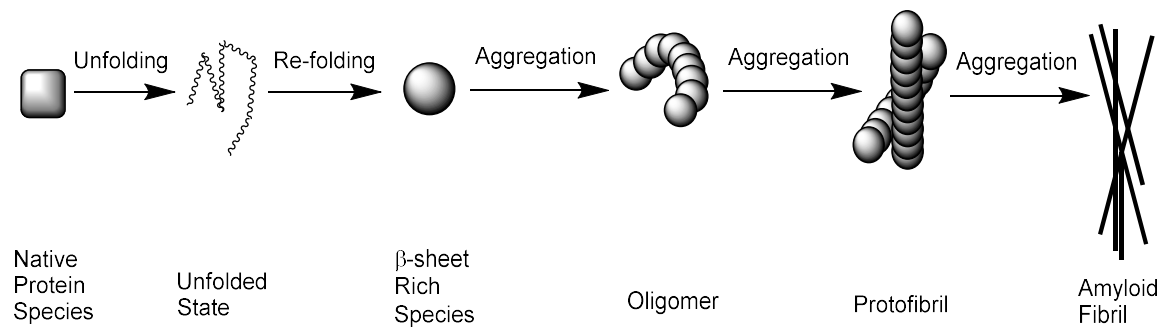


Fig. 16: Simplified amyloid fibril formation process.

Protein misfolding, aggregation and amyloid formation can be a highly varied process. Although it is protein dependent, acidic conditions have traditionally been the simplest method to generate fibrils of amyloidogenic proteins<sup>28,29</sup>; however, the process readily occurs under physiological conditions as well<sup>29</sup>.

### 3.4 Monitoring amyloid fibril formation by Thioflavin T fluorescence spectroscopy

Due to the high  $\beta$ -sheet content of amyloid fibrils, their formation can be spectroscopically monitored through the use of a specific amyloid binding dyes (such as Congo red or Thioflavin T (ThT)). The ThT dye is widely used to identify and quantify the formation of amyloid fibrils in vitro<sup>229,230</sup>. By itself, ThT has very little fluorescence



with an excitation (417 nm) and emission (480 nm) maxima<sup>231</sup>. However, when ThT binds to  $\beta$ -sheet rich domains of amyloid fibrils (Fig. 17), such as A $\beta$  fibrils, its excitation (440 nm) and an emission maxima (490 nm) shift and the fluorescence intensity is significantly increased<sup>231</sup>.

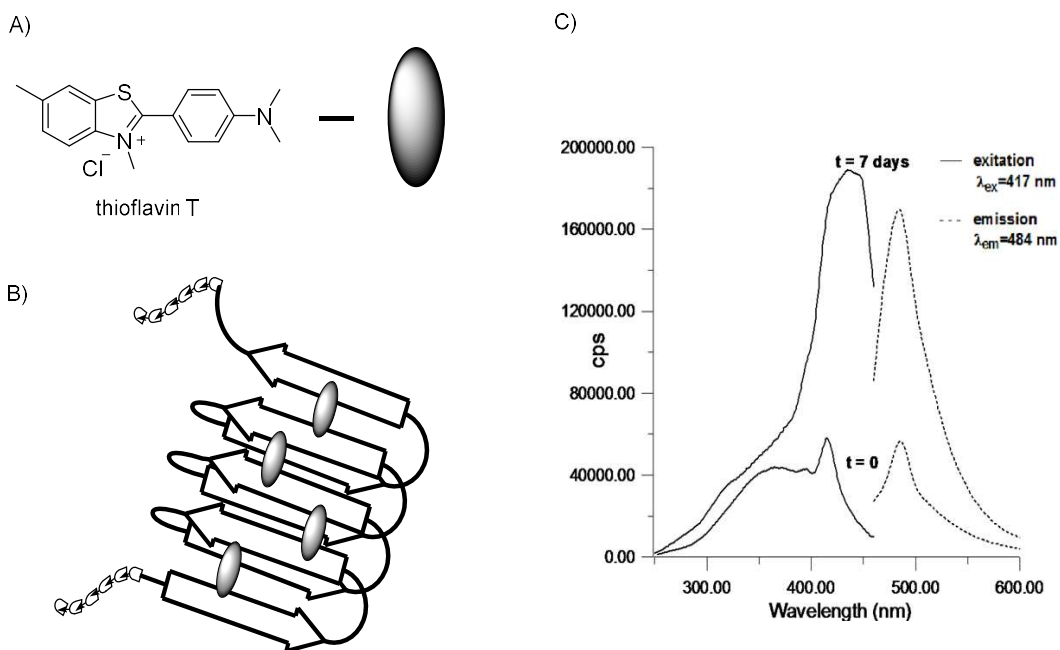


Fig. 17: (A) ThT and its interaction (B) with the  $\beta$ -sheet rich domains of amyloid fibrils. (C) Fluorescence shift for ThT binding to A $\beta$  fibril species (seven-day incubation) vs. monomeric (zero days incubation) protein.

If the protein aggregates analyzed do not consist of mostly  $\beta$ -sheet rich structures (e.g. amorphous deposits), the ThT will not bind and fibril formation will not be identified<sup>232</sup>. The ThT assay provides a valuable tool in quantifying the formation of amyloid fibrils from native protein monomers; however, just as with all research, additional evidence of fibril formation needs to be collected by using electron microscopy (EM) or atomic force microscopy (AFM) for example<sup>229</sup>. During tests of fibrillogenesis inhibitors, control sets

without the protein species should be run to determine if the compounds alone may fluoresce under the conditions of the ThT assay. At the same time, when this assay is used for assessing the fibril inhibition or disassembly, the compounds examined, such as curcumin and resveratrol, may displace the ThT from the binding sites<sup>233,234</sup>. The displacement of the ThT on the  $\beta$ -sheet rich structures results in decreased fluorescence signal, which suggests less amyloid fibril formation than what is present. Therefore, the ThT assay should be coupled with other methods confirming the formation of amyloid fibrils, such as EM or AFM.

### **3.5 Atomic force microscopy of amyloid fibril formations**

Atomic force microscopy produces detailed 3D high-resolution images of biochemical samples, such as proteins and cells<sup>235</sup>. By utilizing the natural attractive and repulsive forces of the sample, a probe can be run across the surface in question to generate an image of it. There are three modes of operation for scanning the surfaces of different samples: non-contact, contact and tapping modes<sup>236</sup>. Contact mode is the most commonly used method for AFM scanning of the surface of a sample<sup>237</sup>. The strong repulsive forces give excellent resolution; however, these forces can damage delicate biological samples<sup>235</sup>. Non-contact mode measures the van der Waals forces between the tip and sample while maintaining the integrity of the sample; this technique is of low resolution<sup>235</sup>. The tapping mode, which combines the functionality of the contact and non-contact modes, provides the best features of contact and non-contact modes<sup>235</sup> for biological samples. This allows the probe to only briefly come into close contact with the sample in order to provide a detailed picture without disrupting the surface of the sample.

AFM has been widely used to investigate the fibril formation of amyloidogenic proteins<sup>237</sup>.

### **3.6 Synthesis of a library of small molecules**

The small molecules **1 – 16, 31 – 45 and 78 – 93** tested in this work were synthesized in Bela Török's lab. The general synthesis of the compounds is provided in their respective chapters.

The small molecules **17 – 30** were provided by the group of Donald Sikazwe at the

University of the Incarnate Word, San Antonio, Texas. The general synthesis of these compounds is provided in chapter 9.

## CHAPTER 4

### MATERIALS AND EXPERIMENTAL METHODS

#### 4.1 Chemicals and enzymes

The phenol and aniline derivatives, ACh, BuCh, DMSO, DPPH, AAPH, ABTS, DTNB, fluorescein, Trolox, resveratrol, galantamine, ThT, ethanol, acetonitrile, TritonX-100, HEPES, potassium persulfate, monobasic sodium phosphate, dibasic sodium phosphate, NaCl, AChE from *Electrophorus electricus*/electric eel (catalog number: C2888-500UN), BuChE from equine serum (catalog number: C4290-1KU) and human insulin (catalog number: 11061-68-0) were all purchased from Sigma Aldrich. Lysozyme from chicken egg white (210083405), muscovite mica V-2 (50-949-111), 1/8" diameter Teflon beads (1298222) and ascorbic acid were all purchased from Thermo Fisher Scientific. Magnetic discs (20 mm specimen metal discs for AFM 75010-20) were purchased from Electron Microscopy Sciences. The AFM tips (standard tapping mode AFM Probe PPNCHR-10) were purchased from NanoAndMore USA. A $\beta$  was purchased from Anaspec. HCl was purchased from EMD chemicals.

#### 4.2 Amyloid fibril inhibition and disassembly procedures

##### 4.2.1 Lysozyme amyloid fibril formation

###### *Fibril preparation in 80% ethanol*

Hen egg white lysozyme (HEWL) protein (3.0 mg) with a molecular weight of 14,307 g/mol was dissolved in 200  $\mu$ L deionized water and stirred with a small magnetic stir bar for 10 min in a glass screw-cap vial. Then 800  $\mu$ L 100% ethanol was added. The 80% ethanol HEWL sample was left with constant agitation for 2 weeks at room temperature

to form amyloid fibrils. The 80% ethanol lysozyme fibril sample was diluted with deionized water at 1:50 ratio to prepare the AFM sample.

#### *Preparation of heat denatured lysozyme aggregates*

For the preparation of heat denatured aggregates, 3.0 mg of HEWL (14,307 g/mol) protein was dissolved in 1.0 mL deionized water and stirred with a small magnetic stir bar for 10 min in an Eppendorf tube. The sample was then placed into a boiling (100 °C) water bath for 15 min and then cooled to room temperature and used without further dilution.

#### **4.2.2 Insulin amyloid fibril formation**

##### *Physiological buffer*

For the preparation of the buffer, NaCl (0.137 mol), KCl (0.0027 mol), Na<sub>2</sub>HPO<sub>4</sub> (0.0081 mol) and KH<sub>2</sub>PO<sub>4</sub> (0.00147 mol) were dissolved in 900 mL of de-ionized (DI) water. The pH was adjusted to 7.5 with phosphoric acid and sodium hydroxide. The final solution was then diluted to 1 L with DI water and stored at 4 °C until use<sup>238</sup>.

##### *Acetic acid solution*

For the preparation of the acetic acid solution, NaCl (0.100 mol) was dissolved in 800 mL of DI water. 200 mL of acetic acid was added and the solution was stored at 4 °C until use<sup>239</sup>.

##### *Insulin stock solution*

Insulin (14.2 mg) was dissolved in 350 µL of 1.0 M HCl.

#### *Amyloid fibril formation of insulin under physiological pH conditions*

The stock solution of insulin (50  $\mu$ L) was neutralized with 50  $\mu$ L of 1.0 M NaOH in a screw cap microcentrifuge tube. The solution was diluted with 900  $\mu$ L of PBS and was vortexed to ensure mixing. A 1/8" diameter Teflon bead was added to the microcentrifuge tube as a nucleation initiation to help the insulin fibril formation begin. The sample was incubated at 37 °C and shaken at 700 rpm. Samples were analyzed after 2 days for amyloid fibril formation.

#### *Acidic conditions 70 °C*

The stock solution of insulin (5  $\mu$ L) was diluted with 95  $\mu$ L of acetic acid solution and the mixture was vortexed to ensure mixing. The sample was incubated at 70 °C. Samples were analyzed after two days for amyloid fibril formation.

#### **4.2.3 Thioflavin T binding assay**

Thioflavin T solution was freshly prepared by dissolving 1.0 mg ThT in 63.75 mL of 10 mM phosphate buffer solution at pH 7.4 and 3  $\mu$ L of the lysozyme solution were diluted with 960  $\mu$ L of ThT solution. Background solutions with the samples were made replacing the ThT solution with the 10 mM phosphate buffer pH 7.4 solution. The fluorescence intensity of all samples was recorded with a Hitachi F-2500 fluorescence spectrophotometer and the FL Solutions 2.0 software at the excitation and emission wavelengths of 460 nm and 480 nm respectively.

#### **4.2.4 Atomic force microscopy**

##### *Sample preparation*

A magnetic disc sample holder was used for mounting the mica on the AFM stage. The mica was cut into a small square disc using double-sided tape. The top layer of mica was peeled off in order to have a surface free of imperfections. 2  $\mu$ l of the diluted HEWL amyloid solution was placed on the center of the mica. After 2 min, to allow for adsorption onto the surface of the mica, the sample was rinsed with DI water, removing any unbound protein from the sample. The samples were left to air dry.

##### *Atomic force microscopy image collection*

The AFM images of the samples were taken with using a Bruker Innova Atomic Force Microscope in tapping mode with these parameters: resolution: 256 \* 256 pixels (for quick scans) or 512 \* 512 pixels (high resolution images), scan range: 200 nm to 100  $\mu$ m, scan rate: between 0.3 to 1 kHz (adjustable for each sample). Analysis of AFM images was conducted with Image J software<sup>240,241</sup>.

#### **4.3 Ellman's method for enzyme inhibition**

##### *HEPES buffer (20 mM) pH 8.0 (0.1% tritonX-100) preparation*

For the preparation of the buffer, HEPES (0.9532 g) was added to 190 mL of DI water. The pH was adjusted to 8.0 with phosphoric acid and sodium hydroxide. The final solution was then diluted to 200 mL with DI water and 200  $\mu$ L of TritonX-100 was added. The solution was stored at 4  $^{\circ}$ C until use.

*Phosphate buffer (0.1 M) pH of 8.0 preparation (buffer A)*

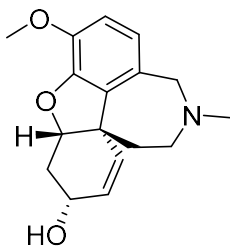
For the preparation of the buffer,  $\text{NaH}_2\text{PO}_4$  (0.0140 mol) and  $\text{Na}_2\text{HPO}_4$  (0.0860 mol) were dissolved in 900 mL of DI water. The pH was adjusted to 8.0 with phosphoric acid and sodium hydroxide. The final solution was then diluted to 1 L with DI water and stored at 4 °C until use.

*Phosphate buffer (0.1 M) pH of 7.0 preparation (buffer B)*

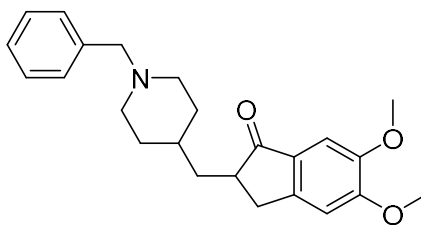
For the preparation of the buffer,  $\text{NaH}_2\text{PO}_4$  (0.0619 mol) and  $\text{Na}_2\text{HPO}_4$  (0.0381 mol) were dissolved in 900 mL of DI water. The pH was adjusted to 7.0 with phosphoric acid and sodium hydroxide. The final solution was then diluted to 1 L with DI water and stored at 4 °C until use.

**4.3.1 Acetylcholinesterase inhibition assay preparation**

The AChE solution was prepared in aliquots of 6 U/mL (activity units/mL) in a 20 mM HEPES buffer at a pH of 8 (0.1% TritonX-100). The enzyme was stored at -20 °C and used when needed. Stock solutions of the inhibitors (experimental compounds and the controls galantamine and donepezil (Fig. 18)) were prepared at 10 mM in DMSO.



galantamine



donepezil



Fig.18: Control compounds for the AChE and BuChE inhibition. Experimental compounds were run at the  $IC_{50}$  of galantamine for each enzyme.

Buffers A and B were incubated at 37 °C for 2 h. The inhibitor stocks were diluted to a 0.15 mM solution through a co-solvent method using buffer A and acetonitrile (50% buffer A and 48.5% acetonitrile, with the remaining 1.5% being the DMSO solution of the compounds). The DTNB dye was dissolved in buffer B to a concentration of 10.24 mM and then further diluted with buffer A to 0.4331 mM. The inhibitors were added to a 96 well plate to reach a concentration in the final assay of 2.0  $\mu$ M. The DTNB solution was added to the 96 well plate into every well to a final assay concentration of 0.3410 mM. The 96 well plate was incubated for 20 min. The AChE enzyme was diluted with buffer A (0.02 U/mL) and added to wells of the 96 well plate as seen in Fig. 19.

Acetylthiocholine was dissolved in buffer A to a concentration of 4.124 mM and 20  $\mu$ L was added to every well in the 96 well plate (Fig. 19). A Versa<sub>max</sub> microplate reader with SoftMax Pro software was used in kinetic mode at a wavelength of 412 nm at a temperature of 37 °C. Measurements were taken every 15 s for 15 min with shaking for 5 s before every read.



### 4.3.2 Butyrylcholinesterase inhibition assay preparation

The BuChE enzyme was prepared in aliquots of 6 U/mL (activity units/mL) in a 20 mM HEPES buffer at a pH of 8 (0.1% Triton X-100). The enzyme was stored at -20 °C and used when needed. Stock solutions of the inhibitors (experimental compounds and galantamine) were prepared at 10 mM in DMSO. Buffers A and B were incubated at 37 °C for 2 h. The inhibitor stocks were diluted to a 0.15 mM solution through a co-solvent method using buffer A and acetonitrile (50% buffer A and 48.5% acetonitrile with the remaining 1.5% being the DMSO solution of the compounds). The DTNB dye was dissolved in buffer B to a concentration of 10.24 mM and then further diluted with buffer A to 0.4331 mM. The inhibitors were added to a 96 well plate to reach a final concentration of 10 µM. The DTNB solution was added to the 96 well plate into every well to a final assay concentration of 0.3410 mM. The 96 well plate was incubated for 20 min. the BuChE enzyme was diluted with buffer A (0.02 U/mL) and added to wells of the 96 well plate as seen in Fig. 20. Butyrylthiocholine was dissolved in buffer A to a concentration of 4.124 mM and 20 µL was added to every well in the 96 well plate (Fig. 20). A Versa<sub>max</sub> microplate reader with SoftMax Pro software was used in kinetic mode at a wavelength of 412 nm at a temperature of 37 °C. Measurements were taken every 15 s for 15 min with shaking for 5 s before every read.



#### **4.4 Free radical scavenging assays**

##### *Preparation of 75mM phosphate and 50mM NaCl buffered solution with a pH 7.4 (PBS)*

For the preparation of the buffer, NaCl (0.05 mol), NaH<sub>2</sub>PO<sub>4</sub> (0.0294 mol) and Na<sub>2</sub>HPO<sub>4</sub> (0.0456 mol) were dissolved in 900 mL of DI water. The pH was adjusted to 7.4 with phosphoric acid and sodium hydroxide. The final solution was then diluted to 1 L with DI water and stored at 4°C until use.

##### *Preparation of 75mM phosphate buffered solution with a pH 7.4*

For the preparation of the buffer, NaH<sub>2</sub>PO<sub>4</sub> (0.0294 mol) and Na<sub>2</sub>HPO<sub>4</sub> (0.0456 mol) were dissolved in 900 mL of DI water. The pH was adjusted to 7.4 with phosphoric acid and sodium hydroxide. The final solution was then diluted to 1 L with DI water and stored at 4 °C until use.

##### *Preparation of compound stock solutions*

Stock solutions of all experimental compounds were prepared at 50 mM in DMSO and known antioxidants Trolox (ethanol), resveratrol (ethanol) and ascorbic acid (water) were prepared at 10 mM. The stocks were further diluted to a working solution with ethanol for each of the antioxidant assays.

#### **4.4.1 DPPH radical scavenging assay**

The DPPH assay was carried out to assess the radical scavenging activity of a large group of compounds<sup>21,24,220,222</sup>. All compound and control stock solutions were diluted to 0.2 mM with ethanol prior to evaluation. The 50% aqueous ethanol was incubated at 37 °C for 2 h and the DPPH was dissolved in 50% aqueous ethanol at a concentration of 105.3 µM. It was further stirred for 1 h to ensure full dissolution. Water (100 µL) was added to the rows A and B as well as columns 1 and 12 of the 96 well plates to prevent solvent

evaporation during incubation. The control antioxidants and experimental compounds (5  $\mu\text{L}$ ) were added to a 96 well plate, respectively, followed by 95  $\mu\text{L}$  of the DPPH solution, or 50 % aqueous ethanol as can be seen in Fig. 21. The final concentrations of the compounds were 10  $\mu\text{M}$  and the DPPH concentration was 100  $\mu\text{M}$ . A Versa<sub>max</sub> plate reader set to 37 °C and 519 nm coupled with SoftMax Pro 5 software (Molecular Devices) recorded the absorbance of the wells every 15 min for 60 min with shaking for 5 s before every reading.

	1	2	3	4	5	6	7	8	9	10	11	12
<b>A</b>	100 $\mu$ L H <sub>2</sub> O	100 $\mu$ L H <sub>2</sub> O	100 $\mu$ L H <sub>2</sub> O	100 $\mu$ L H <sub>2</sub> O	100 $\mu$ L H <sub>2</sub> O	100 $\mu$ L H <sub>2</sub> O	100 $\mu$ L H <sub>2</sub> O	100 $\mu$ L H <sub>2</sub> O	100 $\mu$ L H <sub>2</sub> O	100 $\mu$ L H <sub>2</sub> O	100 $\mu$ L H <sub>2</sub> O	100 $\mu$ L H <sub>2</sub> O
		Blank	DPPH Control	Ascorbic Acid	Resveratrol	Trolox	Compound 1	Compound 2	Compound 3	Compound 4	Compound 5	
	100 $\mu$ L H <sub>2</sub> O	95 $\mu$ L 50% Ethanol	95 $\mu$ L DPPH	95 $\mu$ L DPPH	95 $\mu$ L DPPH	95 $\mu$ L DPPH	95 $\mu$ L DPPH	95 $\mu$ L DPPH	95 $\mu$ L DPPH	95 $\mu$ L DPPH	95 $\mu$ L DPPH	95 $\mu$ L DPPH
<b>B</b>		5 $\mu$ L Ethano/DMSO	5 $\mu$ L Ethano/DMSO	5 $\mu$ L Compound	5 $\mu$ L Compound	5 $\mu$ L Compound	5 $\mu$ L Compound	5 $\mu$ L Compound	5 $\mu$ L Compound	5 $\mu$ L Compound	5 $\mu$ L Compound	
<b>C</b>	100 $\mu$ L H <sub>2</sub> O	Blank	DPPH Control	Ascorbic Acid	Resveratrol	Trolox	Compound 1	Compound 2	Compound 3	Compound 4	Compound 5	
		95 $\mu$ L 50% Ethanol	95 $\mu$ L DPPH	95 $\mu$ L DPPH	95 $\mu$ L DPPH	95 $\mu$ L DPPH	95 $\mu$ L DPPH	95 $\mu$ L DPPH	95 $\mu$ L DPPH	95 $\mu$ L DPPH	95 $\mu$ L DPPH	100 $\mu$ L H <sub>2</sub> O
		5 $\mu$ L Ethano/DMSO	5 $\mu$ L Ethano/DMSO	5 $\mu$ L Compound	5 $\mu$ L Compound	5 $\mu$ L Compound	5 $\mu$ L Compound	5 $\mu$ L Compound	5 $\mu$ L Compound	5 $\mu$ L Compound	5 $\mu$ L Compound	
<b>D</b>	100 $\mu$ L H <sub>2</sub> O	Blank	DPPH Control	Ascorbic Acid	Resveratrol	Trolox	Compound 1	Compound 2	Compound 3	Compound 4	Compound 5	
		95 $\mu$ L 50% Ethanol	95 $\mu$ L DPPH	95 $\mu$ L DPPH	95 $\mu$ L DPPH	95 $\mu$ L DPPH	95 $\mu$ L DPPH	95 $\mu$ L DPPH	95 $\mu$ L DPPH	95 $\mu$ L DPPH	95 $\mu$ L DPPH	100 $\mu$ L H <sub>2</sub> O
		5 $\mu$ L Ethano/DMSO	5 $\mu$ L Ethano/DMSO	5 $\mu$ L Compound	5 $\mu$ L Compound	5 $\mu$ L Compound	5 $\mu$ L Compound	5 $\mu$ L Compound	5 $\mu$ L Compound	5 $\mu$ L Compound	5 $\mu$ L Compound	
<b>E</b>	100 $\mu$ L H <sub>2</sub> O	Blank	DPPH Control	Compound 6	Compound 7	Compound 8	Compound 9	Compound 10	Compound 11	Compound 12	Compound 13	
		95 $\mu$ L 50% Ethanol	95 $\mu$ L DPPH	95 $\mu$ L DPPH	95 $\mu$ L DPPH	95 $\mu$ L DPPH	95 $\mu$ L DPPH	95 $\mu$ L DPPH	95 $\mu$ L DPPH	95 $\mu$ L DPPH	95 $\mu$ L DPPH	100 $\mu$ L H <sub>2</sub> O
		5 $\mu$ L Ethano/DMSO	5 $\mu$ L Ethano/DMSO	5 $\mu$ L Compound	5 $\mu$ L Compound	5 $\mu$ L Compound	5 $\mu$ L Compound	5 $\mu$ L Compound	5 $\mu$ L Compound	5 $\mu$ L Compound	5 $\mu$ L Compound	
<b>F</b>	100 $\mu$ L H <sub>2</sub> O	Blank	DPPH Control	Compound 6	Compound 7	Compound 8	Compound 9	Compound 10	Compound 11	Compound 12	Compound 13	
		95 $\mu$ L 50% Ethanol	95 $\mu$ L DPPH	95 $\mu$ L DPPH	95 $\mu$ L DPPH	95 $\mu$ L DPPH	95 $\mu$ L DPPH	95 $\mu$ L DPPH	95 $\mu$ L DPPH	95 $\mu$ L DPPH	95 $\mu$ L DPPH	100 $\mu$ L H <sub>2</sub> O
		5 $\mu$ L Ethano/DMSO	5 $\mu$ L Ethano/DMSO	5 $\mu$ L Compound	5 $\mu$ L Compound	5 $\mu$ L Compound	5 $\mu$ L Compound	5 $\mu$ L Compound	5 $\mu$ L Compound	5 $\mu$ L Compound	5 $\mu$ L Compound	
<b>G</b>	100 $\mu$ L H <sub>2</sub> O	Blank	DPPH Control	Compound 6	Compound 7	Compound 8	Compound 9	Compound 10	Compound 11	Compound 12	Compound 13	
		95 $\mu$ L 50% Ethanol	95 $\mu$ L DPPH	95 $\mu$ L DPPH	95 $\mu$ L DPPH	95 $\mu$ L DPPH	95 $\mu$ L DPPH	95 $\mu$ L DPPH	95 $\mu$ L DPPH	95 $\mu$ L DPPH	95 $\mu$ L DPPH	100 $\mu$ L H <sub>2</sub> O
		5 $\mu$ L Ethano/DMSO	5 $\mu$ L Ethano/DMSO	5 $\mu$ L Compound	5 $\mu$ L Compound	5 $\mu$ L Compound	5 $\mu$ L Compound	5 $\mu$ L Compound	5 $\mu$ L Compound	5 $\mu$ L Compound	5 $\mu$ L Compound	
<b>H</b>	100 $\mu$ L H <sub>2</sub> O	100 $\mu$ L H <sub>2</sub> O	100 $\mu$ L H <sub>2</sub> O	100 $\mu$ L H <sub>2</sub> O	100 $\mu$ L H <sub>2</sub> O	100 $\mu$ L H <sub>2</sub> O	100 $\mu$ L H <sub>2</sub> O	100 $\mu$ L H <sub>2</sub> O	100 $\mu$ L H <sub>2</sub> O	100 $\mu$ L H <sub>2</sub> O	100 $\mu$ L H <sub>2</sub> O	100 $\mu$ L H <sub>2</sub> O

Fig. 21: 96-well plate set up for DPPH radical scavenging activity screening.

#### 4.4.2 ABTS radical scavenging assay

The ABTS assay was carried out to provide more information on the total antioxidant capacity of the experimental compounds<sup>21,24,220,222</sup>. The ABTS radical solution was prepared by dissolving ABTS and K<sub>2</sub>S<sub>2</sub>O<sub>8</sub> in water to a concentration of 7 and 2.45 mM respectively and stored in the dark at room temperature 16 h before performing the assay. The 75mM PBS pH 7.4 with 50 mM NaCl solution was incubated at 37 °C for 2 h. Every experimental compound and antioxidant standard was further diluted to 0.5 mM with ethanol. The concentrated ABTS solution was diluted with a 75 mM PBS pH 7.4 with 50 mM NaCl solution to an absorbance reading of 0.7. Compounds and controls were plated in a 96 well plate at a final concentration of 10 μM (4 μL of diluted compound) and 196 μL of the ABTS or buffer solution was added as seen in Fig. 22. Measurements were recorded using a Versa<sub>max</sub> plate reader set to 37 °C and 734 nm coupled with SoftMax Pro 5 software (Molecular Devices). Absorbance readings were recorded at the zero, six and twelve-minute time points.



	1	2	3	4	5	6	7	8	9	10	11	12
<b>A</b>	Blank	Blank	Blank	Blank	Blank	Blank	Control	Control	Control	Control	Control	Control
	196 $\mu$ L Buffer	196 $\mu$ L Buffer	196 $\mu$ L Buffer	196 $\mu$ L Buffer	196 $\mu$ L Buffer	196 $\mu$ L Buffer	196 $\mu$ L ABTS	196 $\mu$ L ABTS	196 $\mu$ L ABTS	196 $\mu$ L ABTS	196 $\mu$ L ABTS	196 $\mu$ L ABTS
<b>B</b>	Ethanol/DMSO	Ethanol/DMSO	Ethanol/DMSO	Ethanol/DMSO	Ethanol/DMSO	Ethanol/DMSO	Ethanol/DMSO	Ethanol/DMSO	Ethanol/DMSO	Ethanol/DMSO	Ethanol/DMSO	Ethanol/DMSO
	4 $\mu$ L	4 $\mu$ L	4 $\mu$ L	4 $\mu$ L	4 $\mu$ L	4 $\mu$ L	4 $\mu$ L	4 $\mu$ L	4 $\mu$ L	4 $\mu$ L	4 $\mu$ L	4 $\mu$ L
<b>C</b>	Ascorbic Acid	Ascorbic Acid	Ascorbic Acid	Resveratrol	Resveratrol	Resveratrol	Trolox	Trolox	Trolox	25 $\mu$ M Trolox	25 $\mu$ M Trolox	25 $\mu$ M Trolox
	196 $\mu$ L ABTS	196 $\mu$ L ABTS	196 $\mu$ L ABTS	196 $\mu$ L ABTS	196 $\mu$ L ABTS	196 $\mu$ L ABTS	196 $\mu$ L ABTS	196 $\mu$ L ABTS	196 $\mu$ L ABTS	196 $\mu$ L ABTS	196 $\mu$ L ABTS	196 $\mu$ L ABTS
<b>D</b>	4 $\mu$ L Compound	4 $\mu$ L Compound	4 $\mu$ L Compound	4 $\mu$ L Compound	4 $\mu$ L Compound	4 $\mu$ L Compound	4 $\mu$ L Compound	4 $\mu$ L Compound	4 $\mu$ L Compound	4 $\mu$ L Compound	4 $\mu$ L Compound	4 $\mu$ L Compound
	Compound 1	Compound 1	Compound 1	Compound 2	Compound 2	Compound 2	Compound 3	Compound 3	Compound 3	Compound 3	Compound 3	Compound 3
<b>E</b>	196 $\mu$ L ABTS	196 $\mu$ L ABTS	196 $\mu$ L ABTS	196 $\mu$ L ABTS	196 $\mu$ L ABTS	196 $\mu$ L ABTS	196 $\mu$ L ABTS	196 $\mu$ L ABTS	196 $\mu$ L ABTS	196 $\mu$ L ABTS	196 $\mu$ L ABTS	196 $\mu$ L ABTS
	4 $\mu$ L Compound	4 $\mu$ L Compound	4 $\mu$ L Compound	4 $\mu$ L Compound	4 $\mu$ L Compound	4 $\mu$ L Compound	4 $\mu$ L Compound	4 $\mu$ L Compound	4 $\mu$ L Compound	4 $\mu$ L Compound	4 $\mu$ L Compound	4 $\mu$ L Compound
<b>F</b>	Compound 7	Compound 7	Compound 7	Compound 8	Compound 8	Compound 8	Compound 9	Compound 9	Compound 9	Compound 9	Compound 9	Compound 9
	196 $\mu$ L ABTS	196 $\mu$ L ABTS	196 $\mu$ L ABTS	196 $\mu$ L ABTS	196 $\mu$ L ABTS	196 $\mu$ L ABTS	196 $\mu$ L ABTS	196 $\mu$ L ABTS	196 $\mu$ L ABTS	196 $\mu$ L ABTS	196 $\mu$ L ABTS	196 $\mu$ L ABTS
<b>G</b>	4 $\mu$ L Compound	4 $\mu$ L Compound	4 $\mu$ L Compound	4 $\mu$ L Compound	4 $\mu$ L Compound	4 $\mu$ L Compound	4 $\mu$ L Compound	4 $\mu$ L Compound	4 $\mu$ L Compound	4 $\mu$ L Compound	4 $\mu$ L Compound	4 $\mu$ L Compound
	Compound 10	Compound 10	Compound 10	Compound 11	Compound 11	Compound 11	Compound 12	Compound 12	Compound 12	Compound 12	Compound 12	Compound 12
<b>H</b>	196 $\mu$ L ABTS	196 $\mu$ L ABTS	196 $\mu$ L ABTS	196 $\mu$ L ABTS	196 $\mu$ L ABTS	196 $\mu$ L ABTS	196 $\mu$ L ABTS	196 $\mu$ L ABTS	196 $\mu$ L ABTS	196 $\mu$ L ABTS	196 $\mu$ L ABTS	196 $\mu$ L ABTS
	4 $\mu$ L Compound	4 $\mu$ L Compound	4 $\mu$ L Compound	4 $\mu$ L Compound	4 $\mu$ L Compound	4 $\mu$ L Compound	4 $\mu$ L Compound	4 $\mu$ L Compound	4 $\mu$ L Compound	4 $\mu$ L Compound	4 $\mu$ L Compound	4 $\mu$ L Compound
<b>I</b>	Compound 16	Compound 16	Compound 16	Compound 17	Compound 17	Compound 17	Compound 18	Compound 18	Compound 18	Compound 18	Compound 18	Compound 18
	196 $\mu$ L ABTS	196 $\mu$ L ABTS	196 $\mu$ L ABTS	196 $\mu$ L ABTS	196 $\mu$ L ABTS	196 $\mu$ L ABTS	196 $\mu$ L ABTS	196 $\mu$ L ABTS	196 $\mu$ L ABTS	196 $\mu$ L ABTS	196 $\mu$ L ABTS	196 $\mu$ L ABTS
<b>J</b>	4 $\mu$ L Compound	4 $\mu$ L Compound	4 $\mu$ L Compound	4 $\mu$ L Compound	4 $\mu$ L Compound	4 $\mu$ L Compound	4 $\mu$ L Compound	4 $\mu$ L Compound	4 $\mu$ L Compound	4 $\mu$ L Compound	4 $\mu$ L Compound	4 $\mu$ L Compound
	Compound 16	Compound 16	Compound 16	Compound 17	Compound 17	Compound 17	Compound 18	Compound 18	Compound 18	Compound 18	Compound 18	Compound 18

Fig. 22: 96-well plate set up for ABTS radical scavenging activity screening.

#### 4.4.3 ORAC radical scavenging assay

To provide a further refined profile of the compounds as radical scavengers a third antioxidant assay, the ORAC assay, was conducted<sup>21,24,226</sup>. A fluorescein stock solution was prepared at a 4.19  $\mu\text{M}$  concentration in a pH 7.4, 75 mM phosphate buffered solution. This fluorescein solution was diluted to 0.0816  $\mu\text{M}$  solution fresh daily before performing the assay. The pH 7.4, 75 mM phosphate buffered solution and fluorescein working solution was incubated at 37 °C for 2 h. The stock solutions of the compounds and known antioxidants were diluted to 80  $\mu\text{M}$  in ethanol prior to screening the compounds. An AAPH solution was prepared in 4 °C pH 7.4, 75 mM phosphate buffer at a concentration of 153 mM prior to screening the compounds and stored on ice. A 25  $\mu\text{L}$  solution of the compounds and control antioxidants were plated in a black 96 well plate and 150  $\mu\text{L}$  of the working fluorescein solution was added to the wells of the 96 well plates (Fig. 23). The plate was incubated at 37 °C for 15 min after which, 25  $\mu\text{L}$  of AAPH was added to the wells (Fig. 23). A SpectraMax i3x plate reader in kinetic mode set to 37 °C with excitation and emission wavelengths at 485 nm and 520 nm, respectively, was used to record the fluorescence of the wells every 2 min for 60 min.



#### **4.5 Calculation of physical descriptors of synthetic antioxidants and model compounds by Gaussian 09 for structure activity relationship studies**

The calculations were run in collaboration with Swarada Peerannawar in Bela Török's lab. Frequency calculations for all compounds were performed to confirm the minima on potential energy surfaces. The effect of solvent (water) has also been studied for selected compounds to confirm their stability. The  $^1\text{H}$  NMR chemical shifts ( $\delta\text{H}$ ) in DMSO for hydrazone and its azo tautomer were modeled by self-consistent reaction field (SCRF) calculations<sup>242</sup> by incorporating the polarizable continuum model (PCM). The chemical shifts were calculated by subtracting the nuclear magnetic shielding tensors of protons in the hydrazone and its tautomer from those of the tetramethylsilane (reference) using the gauge-independent atomic orbital (GIAO) method<sup>243</sup>.

The electronic structures of the phenol and aniline derivatives were determined using density functional theory (DFT)<sup>244,245</sup>. Calculations were carried out at the B3LYP/6-31G(d,p) level of theory using the Gaussian09 program suite<sup>246</sup>. The sum of the energies for the radical and the hydrogen atom in the starting compound were calculated. The N-H (and O-H for the compounds **62** - **78** and **90** - **93**) bond dissociation energy (BDE) for the compounds was determined by subtracting the two energies. Additional parameters were also calculated to identify any experimental correlations between the compounds and their experimental antioxidant activities: N-H (as well as O-H bond distances for some compounds), dipole moments, logP values, HOMO and LUMO orbital energies, band gap energies, radical spin densities, proton affinities, ionization potentials. The experimentally derived Hammett constants, which were also used for assessment, were experimentally determined and obtained from the literature<sup>247</sup>.

## CHAPTER 5

### $\beta$ -CARBOLINES AS POTENTIAL MULTI-FUNCTIONAL ALZHEIMER'S DISEASE THERAPUTIC AGENTS

#### 5.1 Introduction

The  $\beta$ -carboline core structure (Fig. 24) was extensively explored for drug development in diverse areas such as cancer therapy, anti-malarial agents, Alzheimer's therapy, etc.

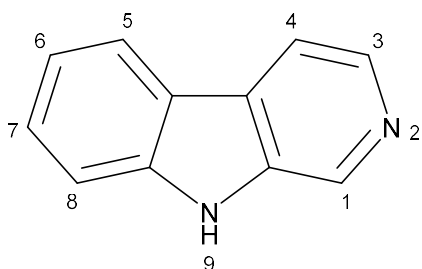


Fig. 24:  $\beta$ -carboline core structure.

Work on  $\beta$ -carboline alkaloids such as harmine (Fig. 25) has shown these compounds to be highly toxic to cancer cells<sup>248</sup>. The Chen lab further investigated 1-(4-hydroxy-3-methoxyphenyl)- $\beta$ -carboline-3-carboxyl-Trp-Trp-AA-OBzl derivatives (Fig. 25) as anti-cancer agents with approximately 50% tumor inhibition reported<sup>249</sup>. Novel 3,9-substituted  $\beta$ -carboline derivatives (Fig. 25) were also investigated as anti-cancer agents showing promising results with several compounds having an  $IC_{50}$  of less than 10  $\mu$ M against several cancer lines<sup>250</sup>. The efficiency of  $\beta$ -carbolines as anti-malarial and anti-leishmanial agents have also been explored. They appeared to selectively target the parasites, having little to no cytotoxic effects on human cell lines<sup>144, 251, 252</sup>. 1-

Benzyl-1,2,3,4-tetrahydro- $\beta$ -carboline (Fig. 25) inhibits the N-methyl-D-aspartate (NMDA) receptors which are important for synaptic plasticity and memory function<sup>253</sup>. Inhibition of this receptor prevents the increase in intra cellular  $\text{Ca}^{2+}$  concentrations by blocking the voltage-dependent channel permeable to  $\text{Ca}^{2+}$  and  $\text{Na}^+$ .<sup>253</sup> Methyl-6,7-dimethoxy-4-ethyl- $\beta$ -carboline-3-carboxylate (DMCM) (Fig. 25) is used as a promoter of the  $\text{GABA}_A$  receptor<sup>254</sup>. Simple  $\beta$ -carbolines are also excellent antioxidants (Fig.25)<sup>255</sup>.

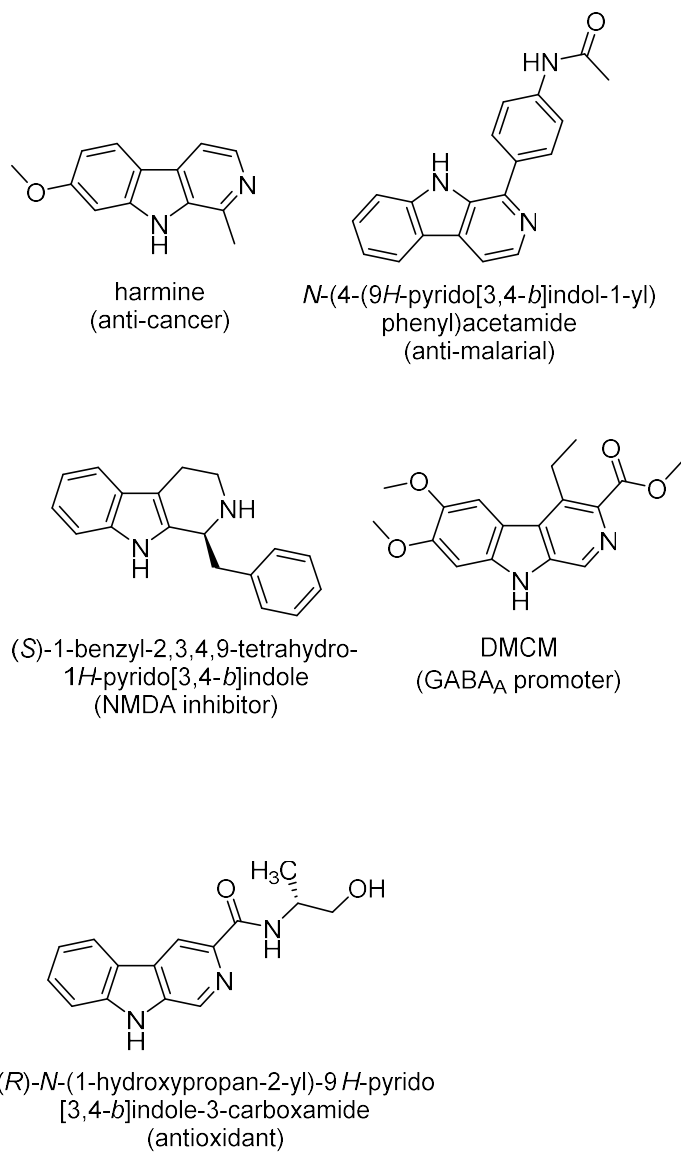


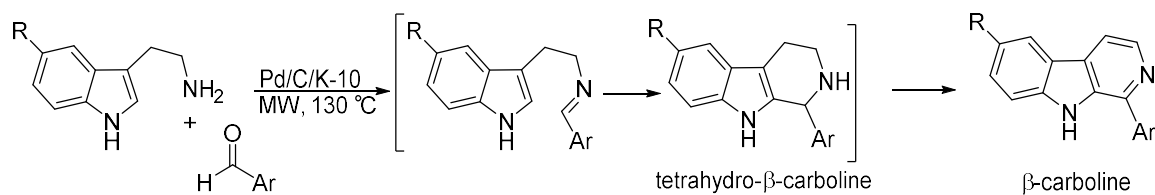
Fig. 25: Examples of  $\beta$ -carboline derivatives with different activities as drug candidates.

The structural analysis of a large set of A $\beta$  self-assembly inhibitors<sup>122,144</sup> indicated the importance of extended aromatic structure as well as the presence of H-donor and H-acceptor units in binding to the A $\beta$  peptide. In addition, analyzing the structures of

cholinesterase inhibitors, it appears paramount to have a relatively extended structure that is able to span the active center of the cholinesterases involving a variety of hydrophobic units. The basic  $\beta$ -carboline skeleton fulfills these criteria. Thus, we have considered  $\beta$ -carboline derivatives as potential multi-functional AD agents. Based on earlier findings, the original three ring system has been extended with an additional aromatic ring either directly or via a carbonyl linker to test the role of molecular flexibility on the efficacy of anti-cholinesterase activity. The extended aromatic structures are also expected to contribute to the potential antioxidant activity.

## 5.2 Synthesis

The  $\beta$ -carboline derivatives were synthesized in the Bela Török lab at the University of Massachusetts Boston by the following general procedure by applying a 3-step-one pot domino reaction by using a special mixture of commercially available 5% Pd/C and K-10 montmorillonite as a bifunctional catalyst (Scheme 1). The first condensation step between the aldehyde and tryptamine was catalyzed by the solid acid K-10. The imine formed immediately underwent a cyclization also by K-10 catalysis. The resulting tetrahydro- $\beta$ -carbolines were dehydrogenated by the Pd metal to provide the aromatic  $\beta$ -carbolines. Each product was characterized by  $^1\text{H}$  and  $^{13}\text{C}$  NMR spectroscopy and mass spectrometry (GC-MS). The spectroscopic characterization of the compounds was in agreement with their structures and the literature data<sup>256</sup>.

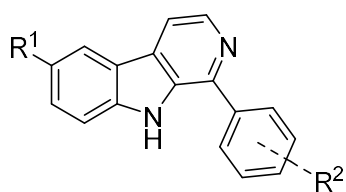


Scheme 1. Synthesis of  $\beta$ -carboline derivatives.



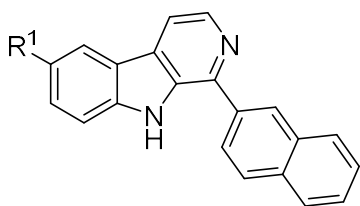
### 5.3 Results

Sixteen  $\beta$ -carboline derivatives were used in an effort to investigate the activity and potency of these compounds as potential multi-target drug candidates for Alzheimer's disease. These included compounds with electron donating and withdrawing groups and hydrophobic substituents (Fig. 26), with more prominent aromatic units (Fig. 27) and compounds with having a carbonyl group as a linker between the  $\beta$ -carboline core and the additional aromatic unit (Fig. 28).



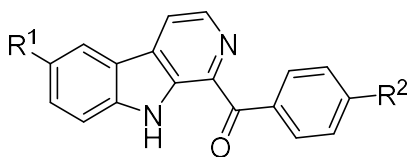
<u>Compound</u>	<u>R<sup>1</sup></u>	<u>R<sup>2</sup></u>
<b>1</b>	H	H
<b>2</b>	H	4-F
<b>3</b>	H	4-CH <sub>3</sub>
<b>4</b>	H	2-CH <sub>3</sub>
<b>5</b>	CH <sub>3</sub>	H
<b>6</b>	CH <sub>3</sub>	4-CF <sub>3</sub>
<b>7</b>	OCH <sub>3</sub>	H
<b>8</b>	OCH <sub>3</sub>	4-F
<b>9</b>	OCH <sub>3</sub>	4-CH <sub>3</sub>

Fig. 26: Compounds **1-9** are simple  $\beta$ -carbolines with an aromatic extension.



<u>Compound</u>	$R^1$
<b>10</b>	H
<b>11</b>	OCH <sub>3</sub>

Fig. 27: Compounds **10** and **11** are  $\beta$ -carbolines with a more prominent aromatic extension to ideally provide increased compound surface for interaction in the active site of cholinesterases.



<u>Compound</u>	$R^1$	$R^2$
<b>12</b>	H	H
<b>13</b>	H	F
<b>14</b>	H	CF <sub>3</sub>
<b>15</b>	OCH <sub>3</sub>	F
<b>16</b>	OCH <sub>3</sub>	CF <sub>3</sub>

Fig. 28: Compounds **12-16** are  $\beta$ -carboline derivatives where the aromatic extension has been linked via a carbonyl group.

The biochemical assays in this section ( $A\beta$  fibril and oligomer formation, AChE and BuChE, ABTS, DPPH and ORAC assays) outline the tests carried out on the  $\beta$ -carboline to assess their potential as multi-target drug candidates.

### **5.3.1 Inhibition of $A\beta$ fibril formation**

As multi-target drug candidates,  $\beta$ -carboline should be able to inhibit the formation of the toxic  $A\beta$  plaques that build up in the brains of Alzheimer's patients. The data indicate that several compounds had a moderate inhibiting effect on the fibril formation of  $A\beta$  as tabulated in Table 2.

Table 2: Inhibition of A $\beta$  fibril formation by  $\beta$ -carboline **1-16**. Negative inhibition data indicate that those compounds promoted the fibril formation compared to the inhibitor-free control.

compound	A $\beta$ fibril Inhibition (%)
<b>1</b>	-4
<b>2</b>	37
<b>3</b>	-7
<b>4</b>	17
<b>5</b>	-
<b>6</b>	34
<b>7</b>	19
<b>8</b>	12
<b>9</b>	10
<b>10</b>	39
<b>11</b>	-
<b>12</b>	20
<b>13</b>	-
<b>14</b>	11
<b>15</b>	6
<b>16</b>	-5

### 5.3.2 Inhibition of A $\beta$ oligomer formation

The activity of  $\beta$ -carboline derivatives were also assessed as inhibitors of A $\beta$  oligomer formation by the Harry Levine III group (University of Kentucky, Medical School) by the biotinyl-A $\beta$  single-site streptavidin-based assay<sup>257</sup>. As the data in Table 3 show, the compounds were highly active in preventing the formation of soluble neurotoxic A $\beta$  oligomers.

Table 3: Inhibition of A $\beta$  oligomer formation by  $\beta$ -carboline derivatives (**1-16**).

compound	A $\beta$ oligomer inhibition (%)
<b>1</b>	79
<b>2</b>	22
<b>3</b>	6
<b>4</b>	45
<b>5</b>	-
<b>6</b>	82
<b>7</b>	58
<b>8</b>	-
<b>9</b>	63
<b>10</b>	58
<b>11</b>	-
<b>12</b>	-
<b>13</b>	-
<b>14</b>	-
<b>15</b>	82
<b>16</b>	84

### 5.3.3 Inhibition of cholinesterase activity (AChE, BuChE)

As described earlier, cholinesterases cleave ACh (or BuCh), an important neurotransmitter. Inhibition of these enzymes increases the amount of ACh in the synaptic cleft which leads to improved cognitive function. I have used the widely accepted Ellman's method that follows the production of choline with the DTNB indicator to evaluate the kinetic activity of the enzyme (Chapter 4.3.2)<sup>217</sup>. Decreased reaction rate compared to the uninhibited control identifies compounds as inhibitors of the cholinesterase enzymes. The cholinesterase enzymes (AChE and BuChE) have different substrates (ACh and BuCh respectively) and inhibitors often show specificity, but some compounds may inhibit both AChE and BuChE (such as galantamine or donepezil). The activity of  $\beta$ -carboline against AChE and BuChE was investigated at concentrations of 2  $\mu$ M (AChE) and 10  $\mu$ M (BuChE), respectively, as described in Chapter 3.1. As shown in Table 4, the  $\beta$ -carboline has negligible effect on the activity of AChE. In contrast, the compounds were highly active in the inhibition of BuChE. After the initial assays,  $IC_{50}$  values were determined using a dilution series from 4.0 nM to 10  $\mu$ M.

Table 4: Inhibition of AChE and BuChE by  $\beta$ -carbolines and  $IC_{50}$  for BuChE activity is shown below. The initial assays were carried out at 2  $\mu$ M (AChE) and 10  $\mu$ M (BuChE) concentrations of the tested  $\beta$ -carbolines. The values here represent the mean  $\pm$  the standard deviation of the data (n = 2–6).

compound	AChE inhibition (%)	BuChE inhibition (%)	BuChE $IC_{50}$ ( $\mu$ M)
<b>galantamine</b>	50 $\pm$ 3	29 $\pm$ 2	10
<b>1</b>	1 $\pm$ 0	39 $\pm$ 13	> 10
<b>2</b>	1 $\pm$ 2	76 $\pm$ 2	4 $\pm$ 1
<b>3</b>	1 $\pm$ 2	95 $\pm$ 2	3 $\pm$ 1
<b>4</b>	-9 $\pm$ 3	5 $\pm$ 8	> 10
<b>5</b>	-9 $\pm$ 5	53 $\pm$ 2	> 10
<b>6</b>	1 $\pm$ 6	5 $\pm$ 6	> 10
<b>7</b>	3 $\pm$ 1	63 $\pm$ 2	5 $\pm$ 0
<b>8</b>	4 $\pm$ 6	32 $\pm$ 4	> 10
<b>9</b>	1 $\pm$ 1	29 $\pm$ 3	> 10
<b>10</b>	0 $\pm$ 3	95 $\pm$ 1	0.225 $\pm$ 0.030
<b>11</b>	-2 $\pm$ 3	14 $\pm$ 8	> 10
<b>12</b>	-2 $\pm$ 2	14 $\pm$ 6	> 10
<b>13</b>	-2 $\pm$ 3	-1 $\pm$ 2	> 10
<b>14</b>	-6 $\pm$ 8	69 $\pm$ 3	1 $\pm$ 0
<b>15</b>	1 $\pm$ 1	48 $\pm$ 5	> 10
<b>16</b>	1 $\pm$ 2	18 $\pm$ 5	1 $\pm$ 1

#### **5.3.4 Free radical scavenging activity (ABTS, DPPH, ORAC)**

Since oxidative stress is a widely accepted contributor to AD progression, the ABTS, DPPH and ORAC<sup>21,220,224</sup> (Chapter 3.2.1-3.2.3) assays were performed to investigate the radical scavenging activity of the compounds. The data collected in the radical scavenging assays suggested different modes of action by the investigated compounds, based on the differences in radical scavenging activity between the different assays. Several compounds showed comparable low activity in both the ABTS and DPPH assays (Table 5). The  $\beta$ -carbolines were most active against the relatively small peroxy radical used in the ORAC assay and several surpassed the activity of the controls. Since peroxy radicals are a common form of ROS, this observation is encouraging.



Table 5: Free radical scavenging activity of the  $\beta$ -carboline derivatives against the DPPH<sup>a</sup>, ABTS<sup>b</sup> and peroxy radicals<sup>c</sup>. The values here represent the mean  $\pm$  the standard deviation of the data (n = 2–6).

compound	ABTS radical scavenging (%)	DPPH radical scavenging (%)	ORAC radical scavenging (%)
<b>ascorbic acid</b>	28 $\pm$ 2	15 $\pm$ 7	15 $\pm$ 10
<b>resveratrol</b>	95 $\pm$ 2	28 $\pm$ 5	97 $\pm$ 4
<b>Trolox</b>	24 $\pm$ 1	23 $\pm$ 4	91 $\pm$ 2
<b>1</b>	12 $\pm$ 2	-7 $\pm$ 6	10 $\pm$ 7
<b>2</b>	22 $\pm$ 5	-3 $\pm$ 5	54 $\pm$ 9
<b>3</b>	13 $\pm$ 3	-7 $\pm$ 4	24 $\pm$ 9
<b>4</b>	15 $\pm$ 4	-0 $\pm$ 3	58 $\pm$ 6
<b>5</b>	10 $\pm$ 1	2 $\pm$ 4	10 $\pm$ 11
<b>6</b>	-	-	-
<b>7</b>	16 $\pm$ 2	-6 $\pm$ 8	35 $\pm$ 7
<b>8</b>	15 $\pm$ 1	-13 $\pm$ 4	41 $\pm$ 6
<b>9</b>	13 $\pm$ 1	-12 $\pm$ 6	28 $\pm$ 9
<b>10</b>	14 $\pm$ 1	-6 $\pm$ 5	0 $\pm$ 11
<b>11</b>	17 $\pm$ 3	-4 $\pm$ 6	12 $\pm$ 11
<b>12</b>	6 $\pm$ 2	-3 $\pm$ 6	6 $\pm$ 10
<b>13</b>	2 $\pm$ 1	-17 $\pm$ 6	-1 $\pm$ 8
<b>14</b>	7 $\pm$ 2	-1 $\pm$ 4	-10 $\pm$ 13
<b>15</b>	3 $\pm$ 1	2 $\pm$ 4	5 $\pm$ 8
<b>16</b>	5 $\pm$ 2	-4 $\pm$ 5	5 $\pm$ 11

a: Calculation for DPPH radical scavenging activity can be seen in Chapter 3.2.1. Eq. 1 b: Calculation for ABTS radical scavenging activity can be seen in Chapter 3.2.2. Eq. 1. c: Calculation for ORAC radical scavenging activity can be seen in Chapter 3.2.3. Eqs. 2 and 3.

## 5.4 Discussion

The larger structures (**2**, **4**, **6**, **10**, **12** and **14**) acted as moderately active A $\beta$  fibril formation inhibitors with the best performances shown by **2** (39%) and **10** (40%), which represents an approximately 110  $\mu$ M EC<sub>50</sub> value.

A majority of the compounds produced more than 50% oligomer formation inhibition (**1**, **6**, **7**, **9**, **10**, **15** and **16**). The activity comparison of the compounds in the A $\beta$  fibril and oligomer formation inhibition assays are in agreement with previous findings; namely that a compound is either a fibril or an oligomer formation inhibitor<sup>257,258</sup>. This is shown by the respective behaviors of **1**, **15** and **16** that have A $\beta$  fibril inhibition values of -4, -5 and 6 while having A $\beta$  oligomer inhibition values of 79, 84 and 82. However, compounds **6** and **10** appear to provide a reasonable protection against the formation of oligomeric and fibrilized states of A $\beta$  self-assemblies with A $\beta$  fibril inhibition values of 34 and 39 as well as A $\beta$  oligomer inhibition values of 82 and 58.

Electrospray-ionization mass spectrometry data revealed convincing evidence that **10**, which can block both fibril (39%) and oligomer (58%) formation of A $\beta$ , forms a complex with the peptide in the solution (Fig. 29). The most typical complex appears to be the 1:1 ratio of A $\beta$ :**10**, although another complex with higher ratio (1:2) can be observed. The spectrum, however, shows that A $\beta$  is still overwhelmingly in an un-complexed form, indicating that a limited amount of inhibitor could modify the self-assembly process by partially complexing/blocking the peptide.

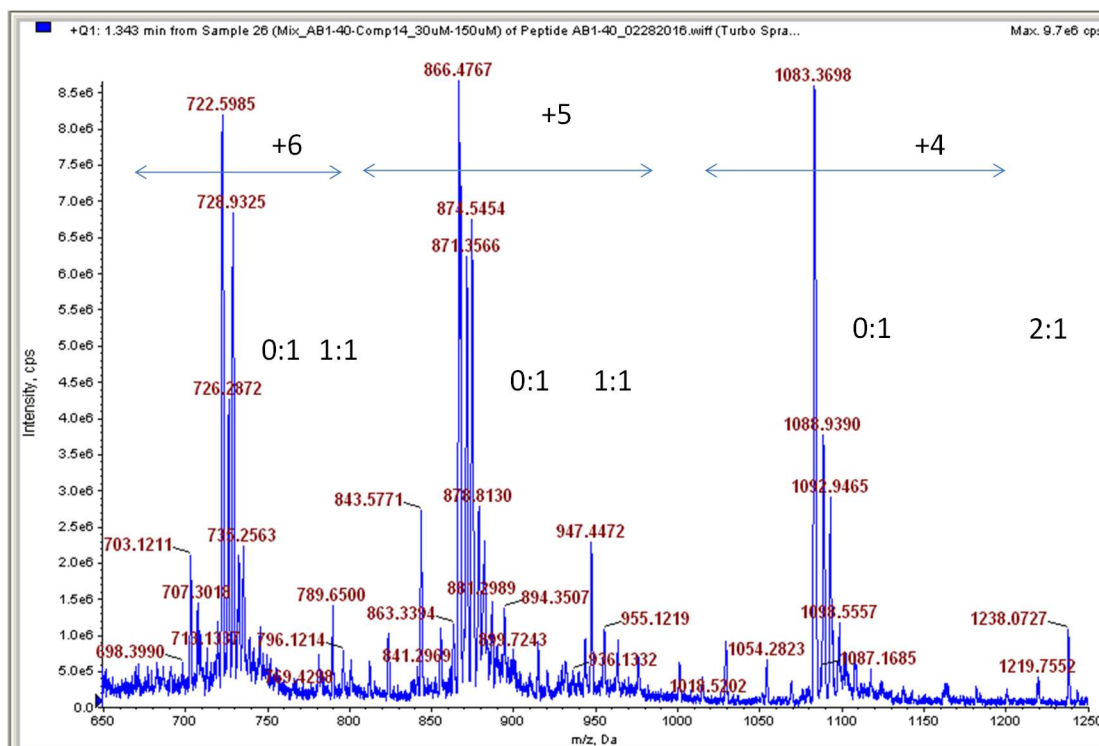


Fig. 29: Electrospray ionization (ESI) mass spectrum of the A $\beta$ <sub>1-40</sub>-peptide-**10** mixture (30  $\mu$ M to 150  $\mu$ M). The relevant signals indicate 1:1 A $\beta$ <sub>1-40</sub><sup>5+</sup> (947.4472 m/z) and 1:2 A $\beta$ <sub>1-40</sub><sup>4+</sup> (1238.0727 m/z) complex formations between the peptide and inhibitor compound. The intervals highlight the relevant peaks of the charged A $\beta$  carrying 4 to 6 positive charges.

As shown in Table 4 the  $\beta$ -carbolines have negligible effect on the activity of AChE. In contrast, the compounds were highly active in the inhibition of BuChE; over 60% of the studied compounds appear to be a better inhibitor of BuChE than the control, galantamine. Several of them (e.g. **3**, **10**) show above 80% inhibition of the enzyme at 10  $\mu$ M concentration (the IC<sub>50</sub> of galantamine).

To compare the potency of the compounds to others in the literature the  $IC_{50}$  values of compounds that showed >50% inhibition at 10  $\mu$ M concentration were determined. The following  $IC_{50}$  values were obtained: **2**– $4.27 \pm 1.30 \mu$ M, **3**– $3.06 \pm 1.27 \mu$ M, **7**– $4.48 \pm 0.27 \mu$ M, **10**– $225 \pm 30$  nM, **14**– $1.29 \pm 0.25 \mu$ M, **16**– $1.42 \pm 0.73 \mu$ M. The data show that, as expected, these compounds in fact possess a better  $IC_{50}$  than the reference compound. Compound **10** was found to be the best inhibitor of BuChE; its 225 nM  $IC_{50}$  value is of practical importance for further lead development. While at this level of the research it is difficult to make structure activity relationship predictions it appears that the presence of an electron-donating substituents ( $CH_3$ ,  $OCH_3$ ) on the  $\beta$ -carboline ring positively affects the BuChE inhibition. In addition, considering the lower, additional ring, the bulkier the group, the better the effect. Compound **10** with the quite large naphthyl group was found to be by far the most effective inhibitor.

With the aim of understanding the BuChE inhibition property of these molecules, two among the best compounds (**10** and **16**) were docked in the active site of BuChE (PDB code: 1P0I42) using the Glide module of the Schrodinger package<sup>259</sup>. The superimposition of compound **10** and **16** with donepezil and galantamine (known BuChE inhibitors) in the active site of the enzyme is shown in Figs. 30 and 31.

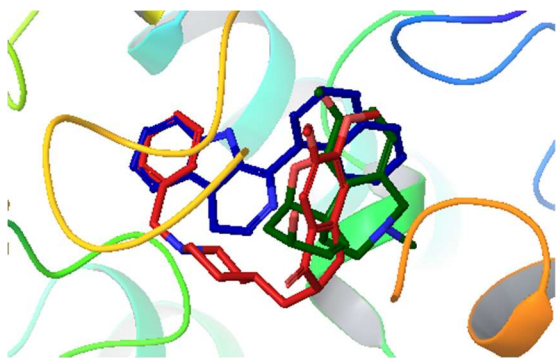


Fig. 30: Superimposition of compound **10** (blue) with donepezil (red) and galantamine (dark green) in the active site of huBuChE (PDB ID: 1P0I). (hydrogens are concealed for clarity).

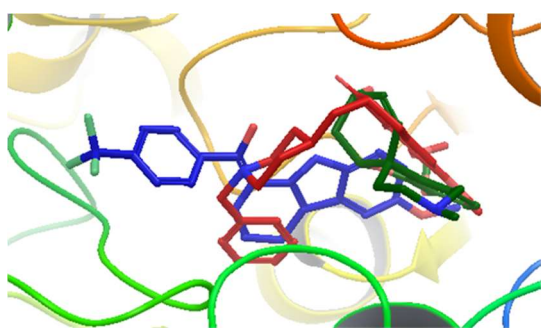


Fig. 31: Superimposition of molecule **16** (blue) with donepezil (red) and galantamine (dark green) in the active site of huBuChE (PDB ID: 1P0I). (hydrogens are concealed for clarity).

The analysis of the docked structures revealed that while **16** is extended through the active site of BuChE the reference compounds galantamine and donepezil appear to bind in the right side of the active site in 1P0I (Figs. 30 and 31). The N-H at position nine of **16** shows a hydrogen bonding interaction with the Pro285 and Thr120 residues,

respectively. In addition to that, the methoxy oxygen of **16** interacts with the Glu197 residue of the active site. In contrast, compound **10** appears to bind to the enzyme very similarly to donepezil, which is one of the best-known inhibitors of AChE as well as BuChE. The binding of **10** stretched through the active site explains the IC<sub>50</sub> that is an order of magnitude lower than that of **16**. The N-H at position nine of **10** shows hydrogen bonding interaction with the hydroxyl group of Ser198. In addition to that two  $\pi$ - $\pi$  stacking interactions were observed, first between the phenyl ring of indole and residue Trp231 and the second one between the naphthalene ring of compound **10** and residue His438. Likewise, a cation- $\pi$  interaction was noticed between quaternary nitrogen of **10** and residue Trp231.

Since the compounds appear to act as selective BuChE inhibitors, a docking study was carried out with **15** and AChE to observe whether the compound-enzyme interaction would reveal the reasons for the negligible effect. Fig. 32 shows that the orientation of **15** is significantly different from that of donepezil and galantamine. The molecule stretches completely through the active site while galantamine only occupies the right side of the pocket and donepezil also appears on the right side and turns back to the center. Although **15** shows hydrogen bonding interaction with residues Phe295, Tyr124 as well as  $\pi$ - $\pi$  interaction with Trp286, The338 and Tyr337 residues, it is likely, that several of these interactions do not block residues that possess a role in the catalytic action.

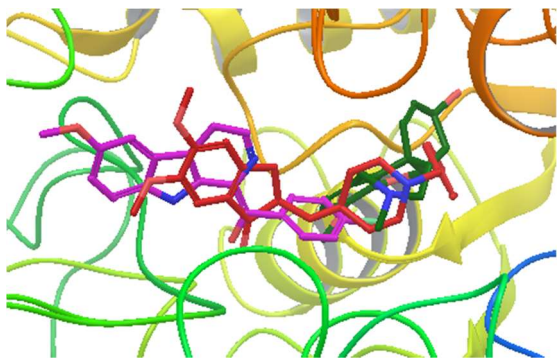


Fig. 32: Superimposition of molecule **15** (purple) with donepezil (red) and galantamine (dark green) in the active site of huAChE (PDB ID-4EY7) (hydrogens are concealed for clarity).

It was observed that, ABTS radical scavenging activity was low for the  $\beta$ -carbolines with a range of 2% to 21% radical scavenging; comparatively low to the reference compounds. Similar tendency was observed from the DPPH assays; the scavenging activity was mostly uniform, but low and several compounds resulted in increases in DPPH absorbance (Table 5). This could be for one of three reasons: the compound has background absorption at the wavelength checked, the compound regenerated some of the degraded DPPH in solution, or the molecular interactions of the compound with the radical developed a species that has a higher molar absorptivity at the wavelength screened. Compound blanks with no DPPH were screened at the assay wavelength to rule out the background absorption of the molecules. While the results from the ABTS and DPPH assays did not reveal high activity, the scavenging data from the ORAC assay provided a different picture of the  $\beta$ -carbolines. In this assay most of the  $\beta$ -carbolines performed the same or better than the control antioxidants, with radical scavenging

percentages from 0% to 58% (Table 5). The large differences in the activity of the compounds between the three assays can provide some insight into the activity of the  $\beta$ -carbolines. ORAC has historically been known to provide higher values to compounds that scavenge radicals at a slower rate (with the assay not differentiating between rate and efficiency of radical scavenging due to the in vitro generation of peroxy species) and thus show up as lower activity in radical scavenging assays with shorter timescales<sup>21</sup>. The fact that the  $\beta$ -carbolines perform significantly better in the ORAC assay than in the ABTS and DPPH assays suggests they may be slow acting antioxidants, due to their high activity in the ORAC assay, but poor activity in the ABTS and DPPH assays. While slow radical scavenging activity is not ideal in an environment with a high rate of ROS activity, in a cellular system slower acting radical scavengers could potentially boost the endogenous antioxidant systems allowing them to continue to maintain the redox homeostasis within the cell.

With the promising results for  $\beta$ -carbolines as A $\beta$  fibril and oligomer inhibitors as well as their selectivity for inhibiting butyrylcholinesterase coupled with the strong activity in scavenging peroxy radicals, the  $\beta$ -carbolines appear to be excellent candidates for further multi-target drug development for Alzheimer's disease.



## CHAPTER 6

### COMPUTER AIDED DRUG DESIGN OF MULTI-FUNCTIONAL HYDRAZIDE AND NIPECOTIC ACID DERIVATIVES

This section focuses on the development of cholinesterase inhibitors developed computer aided by computational modeling and docking studies. A library of 14 hydrazide and nipecotic acid derivatives were designed through molecular docking with AChE to mimic the electrostatic characteristics of donepezil, a potent AChE inhibitor. The results below are the culmination of these findings.

#### **6.1 Introduction**

Computer aided drug design is a growing field in the pharmaceutical industry<sup>260</sup>. Aided by the increase in expression and identification of new protein species coupled with crystallography techniques, computational modeling of compounds at the active sites of enzymes has become a booming industry<sup>19</sup>. Computational modeling coupled with high-throughput screening has allowed the compounds identified in the modeling studies to be efficiently investigated for activity<sup>260</sup>. Hydrazide–hydrazone derivatives have been investigated as standalone and hybrid drug candidates for a wide variety of ailments. For example, (2-Oxobenzoxazoline-3-yl) acetohydrazide<sup>261</sup> derivatives (Fig. 33) are used clinically as anticonvulsants and many antibacterial agents currently in use contain a hydrazide–hydrazone moiety<sup>262</sup>. Imidazo[1,2-a]pyrazine-2-carboxylic acid arylidene-hydrazides (Fig. 33) have also been investigated as potential anti-fungal agents<sup>263</sup>. Hydrazones have also been identified as potential antioxidants (Fig. 33)<sup>264</sup>.

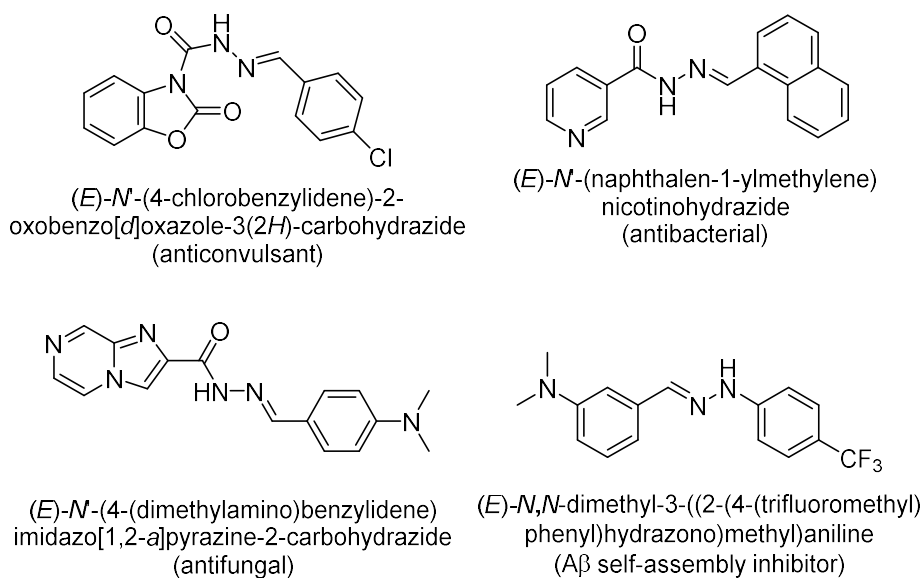


Fig. 33: Examples of hydrazone and hydrazide derivatives with different activities as drug candidates.

Nipecotic acid derivatives have also been investigated as drug candidates. Acting as an anticonvulsant, nipecotic acid (Fig. 34) inhibits GABA uptake in neuronal and glial cells<sup>265</sup>. New prodrug derivatives of nipecotic acid (Fig. 34) have been used as anticonvulsants<sup>266</sup>. Nipecotic acid derivatives with 4-substitution (Fig. 34) have been investigated as inhibitors of the GABA transporter mGAT1, which controls the glycosylation of proteins in the Golgi of developing sperm, to increase the overall sperm production<sup>267</sup>.

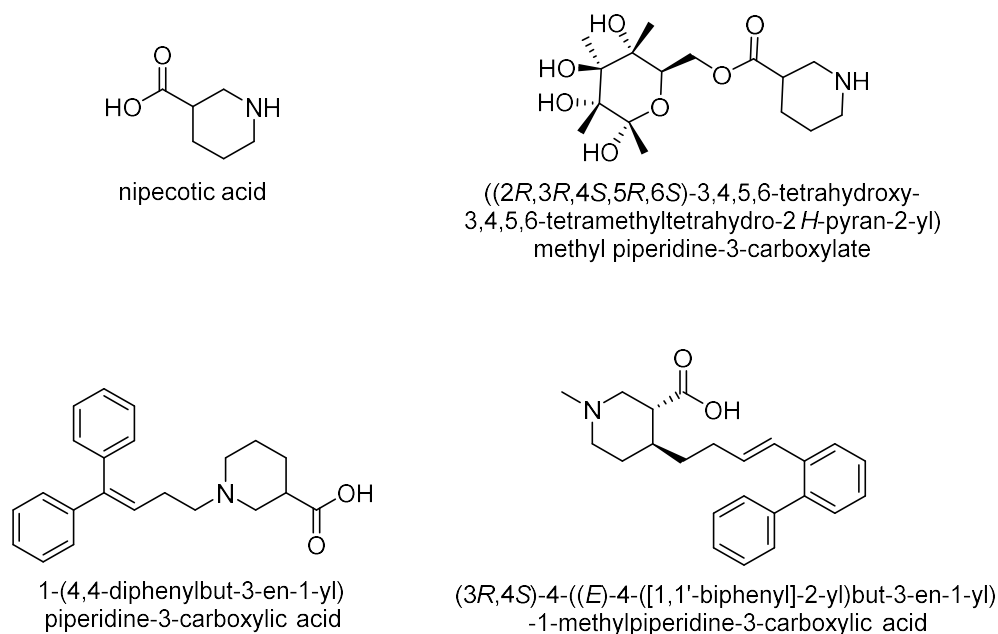


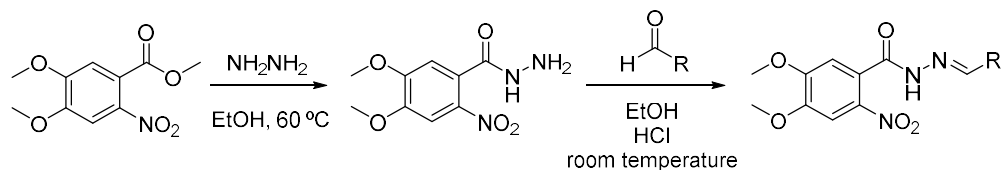
Fig. 34: Examples of nipecotic acid and derivatives with different activities as drug candidate anticonvulsants.

The compounds 4,5-dimethoxy-2-nitrobenzohydrazide or hydrazones and 1-(1-benzylpiperidin-4-yl)ethan-1-one or nipecotic acid derivatives were investigated due to their abilities to donate or accept hydrogen<sup>268</sup>. They can be readily derivatized with diverse hetero-/non-hetero aromatic groups to generate multi-functional drug candidates<sup>269,270</sup>. The molecules were designed to contain at least two hetero-aryl moieties spaced by a 2 to 3 carbonylated atom linker to electrostatically mimic donepezil<sup>271-273</sup>.

## 6.2 Synthesis

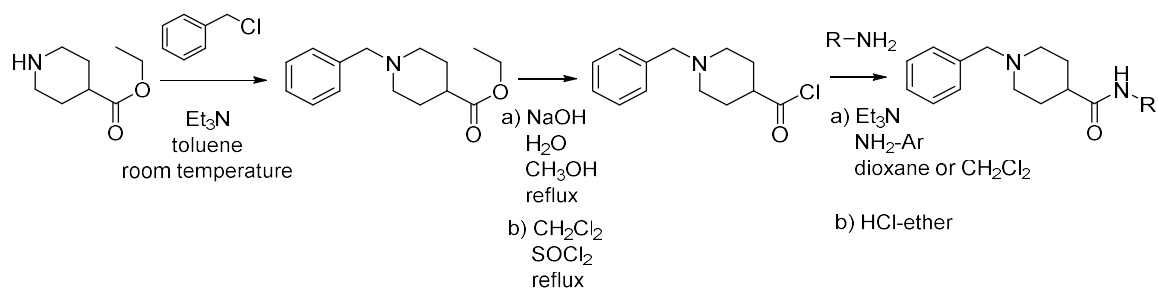
Hydrazide synthesis was conducted by the Sikazwe lab (University of the Incarnate World, San Antonio, Texas) by the following general procedure. Hydrazide synthesis occurred in two steps (Scheme 2)<sup>269,270,274</sup>. Step one involved refluxing methyl 4,5-

dimethoxy-2-nitrobenzoate and excess hydrazine monohydrate in absolute ethanol and afforded intermediate. In step two, this intermediate was condensed with a variety of aromatic aldehydes to form arylated hydrazones.



Scheme 2. General synthesis of hydrazide derivatives.

Exploratory arylated nipecotic acid derivatives **28** – **30** (Fig. 36) were prepared beginning with the trimethylamine-facilitated N-benylation of isonipecotate ethyl ester in toluene (Scheme 3)<sup>275</sup>. Ester hydrolysis, under basic reflux, led to the carboxylic acid intermediate, which was promptly converted to the acyl chloride via the dropwise addition of  $\text{SOCl}_2$ . Finally, acyl chloride treatment with appropriate amines, in step three (Scheme 3), afforded target products **28–30**.



Scheme 3. General synthesis of nipecotic acid derivatives.

### 6.3 Results

Several of the fourteen 4,5-dimethoxy-2-nitrobenzohydrazide or hydrazones (Fig. 35) and 1-(1-benzylpiperidin-4-yl)ethan-1-one or nipecotic acid derivatives (Fig. 36) exhibited potent antioxidant properties and modest AChE / BuChE inhibition (Table 6).

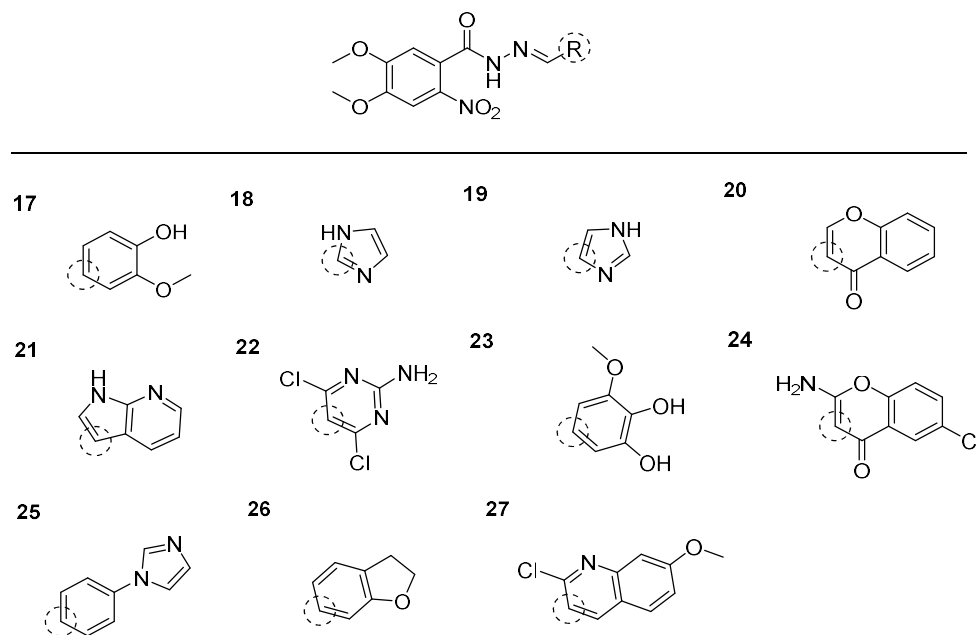


Fig. 35: Structures of the synthesized hydrazides 17 – 27.

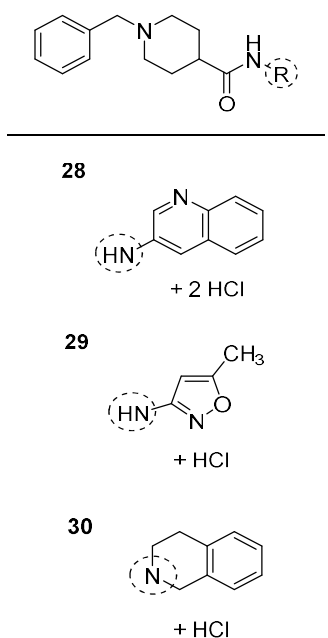


Fig. 36: Structures of the synthesized nipecotic acid derivatives **28** – **30**.

### 6.3.1 Cholinesterase (AChE, BuChE) docking studies using AutoDock Tools

Since I participated in this study as a collaborator, I was not involved in the development of the hydrazide compounds investigated here. The compounds investigated were derived from AChE docking studies and designed to mimic the electrostatic profile of donepezil, a well-known inhibitor of both AChE and BuChE. Compound structures were identified through docking studies done by the Sikazwe lab (University of the Incarnate World, San Antonio, Texas) with AChE (PDB ID: 1EVE)<sup>272</sup>, using AutoDock Tools (Version 1.5.6) software and the correct protonation state of each ligand was determined at pH 7.4 using MarvinSketch (Version 17.2.27 ChemAxon, Cambridge, MA, USA)<sup>276</sup>.

### **6.3.2 Inhibition of cholinesterase activity (AChE, BuChE)**

The activity of the hydrazone-hydrazide derivatives **17** – **30** against AChE and BuChE were carried out at concentration of 2  $\mu$ M (AChE) and 10  $\mu$ M (BuChE) respectively.

Most analogs poorly inhibited the enzymes. The exception was the nipecotic acid derivatives **28** and **30**, which showed modest inhibition of both AChE and BuChE. The data are tabulated in Table 6.

Table 6: Inhibition of AChE and BuChE activity by the hydrazide and nipecotic acid derivatives. Galantamine (Ga) and donepezil (Do) were used as control compounds for cholinesterase inhibition. The values here represent the mean  $\pm$  the standard deviation of the data (n = 2–6).

compound	AChE inhibition (%)	BuChE inhibition (%)
<b>Ga</b>	57 $\pm$ 2	36 $\pm$ 4
<b>Do</b>	98 $\pm$ 0	58 $\pm$ 1
<b>17</b>	-0 $\pm$ 4	4 $\pm$ 3
<b>18</b>	-3 $\pm$ 6	-4 $\pm$ 2
<b>19</b>	-1 $\pm$ 2	-6 $\pm$ 2
<b>20</b>	8 $\pm$ 1	-1 $\pm$ 1
<b>21</b>	4 $\pm$ 1	-0 $\pm$ 2
<b>22</b>	-1 $\pm$ 2	2 $\pm$ 3
<b>23</b>	-3 $\pm$ 6	-3 $\pm$ 3
<b>24</b>	7 $\pm$ 1	-1 $\pm$ 3
<b>25</b>	2 $\pm$ 4	-3 $\pm$ 3
<b>26</b>	-1 $\pm$ 5	-1 $\pm$ 4
<b>27</b>	3 $\pm$ 1	-2 $\pm$ 1
<b>28</b>	10 $\pm$ 2	10 $\pm$ 4
<b>29</b>	3 $\pm$ 4	-1 $\pm$ 2
<b>30</b>	4 $\pm$ 7	14 $\pm$ 3



### **6.3.3 Free radical scavenging activity (ABTS, DPPH, ORAC)**

The hydrazide and nipecotic acid derivatives were investigated as radical scavengers in an effort to elucidate their potential multi-functional characteristics. Their activity in the DPPH, ABTS and ORAC assays can be seen in Table 7.

Table 7: Free radical scavenging activity of the hydrazide derivatives against the DPPH<sup>a</sup>, ABTS<sup>b</sup> and peroxy radicals<sup>c</sup>. The values here represent the mean  $\pm$  the standard deviation of the data (n = 2–6).

compound	ABTS radical scavenging (%)	DPPH radical scavenging (%)	ORAC radical scavenging (%)
<b>ascorbic acid</b>	40 $\pm$ 1	21 $\pm$ 2	30 $\pm$ 8
<b>resveratrol</b>	10 $\pm$ 0	30 $\pm$ 2	95 $\pm$ 5
<b>Trolox</b>	44 $\pm$ 42	20 $\pm$ 3	90 $\pm$ 5
<b>17</b>	50 $\pm$ 2	13 $\pm$ 4	88 $\pm$ 2
<b>18</b>	14 $\pm$ 1	8 $\pm$ 2	15 $\pm$ 6
<b>19</b>	3 $\pm$ 2	2 $\pm$ 1	11 $\pm$ 3
<b>20</b>	15 $\pm$ 6	12 $\pm$ 4	80 $\pm$ 2
<b>21</b>	18 $\pm$ 15	9 $\pm$ 11	30 $\pm$ 2
<b>22</b>	1 $\pm$ 0	12 $\pm$ 7	58 $\pm$ 3
<b>23</b>	35 $\pm$ 2	18 $\pm$ 2	87 $\pm$ 2
<b>24</b>	20 $\pm$ 0	4 $\pm$ 3	-1 $\pm$ 3
<b>25</b>	9 $\pm$ 3	1 $\pm$ 3	18 $\pm$ 2
<b>26</b>	6 $\pm$ 1	-2 $\pm$ 9	11 $\pm$ 1
<b>27</b>	2 $\pm$ 1	-1 $\pm$ 4	7 $\pm$ 2
<b>28</b>	7 $\pm$ 1	7 $\pm$ 4	23 $\pm$ 2
<b>29</b>	1 $\pm$ 0	8 $\pm$ 6	29 $\pm$ 1
<b>30</b>	5 $\pm$ 2	9 $\pm$ 2	9 $\pm$ 2

a: Calculation for DPPH radical scavenging activity can be seen in Chapter 3.2.1. Eq. 1 b: Calculation for ABTS radical scavenging activity can be seen in Chapter 3.2.2. Eq. 1. c: Calculation for ORAC radical scavenging activity can be seen in Chapter 3.2.3. Eqs. 2 and 3.

Unlike the AChE and BuChE data, these compounds showed excellent activity in the ORAC assays, suggesting they are effective free radical scavengers.

#### **6.4 Discussion**

The hydrazone-hydrazide derivatives were designed to mimic the structural and electronic properties of donepezil in an effort to design new AD drugs with multi-target functionality. These derivatives were not potent inhibitors of AChE or BuChE as donepezil is. Compounds **28** and **30** were the most active cholinesterase inhibitors with activity from 10-20% which is far less than the activity of the controls galantamine (56% for AChE and 36% for BuChE) and donepezil (97% AChE and 57% BuChE). Despite the low enzyme inhibitory effect, the antioxidant activity of these derivatives was promising. The hydrazone-hydrazide derivatives were most active against the comparatively small peroxy radical used in the ORAC assay and several compounds surpassed the activity of the controls. Compounds **17**, **20**, **22** and **23** all performed >10% in the DPPH assay. The compounds exhibited reasonable activity in the ABTS assay with **17** and **22** all with >30% radical scavenging activity, performing just as good or better than the reference compounds ascorbic acid and Trolox. In the ORAC assay the compounds screened had a much higher radical scavenging activity with values obtained higher than 50% for compounds **17**, **20**, **22** and **23**. Compounds **17**, **20** and **22** were by far the best radical scavengers of all three antioxidant assays.

These compounds are clearly not multi-target drug candidates for AD treatment.

However, they showed strong antioxidant activity and several of them provided some degree of inhibition against AChE and BuChE. Further refinement of the structures of

compounds **28** and **30** for cholinesterase inhibition could potentially lead to stronger inhibitors and ultimately better drug candidates.

CHAPTER 7  
STRUCTURE ACTIVITY RELATIONSHIP OF HYDRAZONES AS RADICAL  
SCAVENGERS

Building upon our earlier efforts on potential multi-target inhibitors<sup>264</sup>, the hydrazone core structure that yielded several excellent inhibitors against A $\beta$  fibril and oligomer formation was further investigated. It was decided to explore the effects on the radical scavenging activity of these compounds with emphasis on finding a structure-activity relationship (SAR). Structural and energetic features of a series of fifteen diarylhydrazone derivatives were calculated by density functional theory (DFT). The major goal was to identify key features that most likely contribute to their antioxidant effect. The following section describes the work performed to form a SAR study using the radical scavenging activity correlated with the characteristics of the compounds.

### 7.1 Introduction

Hydrazone derivatives have been applied in a multitude of medical applications. A number of acetylhydrazones<sup>277</sup>, oxamoylhydrazones<sup>277</sup> and hydrazones<sup>278</sup> have been investigated and used clinically as anticonvulsants (Fig. 37). Several N-acylarylhydrazone derivative Ca<sup>2+</sup> chelators<sup>270</sup> and 2-(2-formylfuryl)pyridylhydrazones<sup>279</sup> have shown promise as anti-inflammatory drugs (Fig. 37).

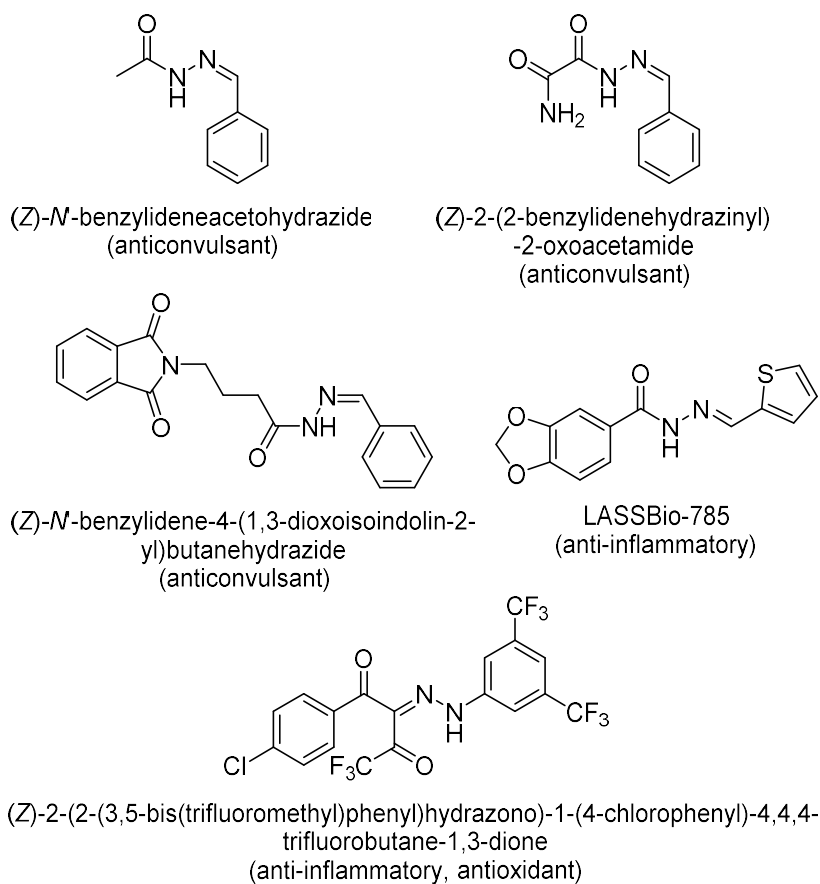
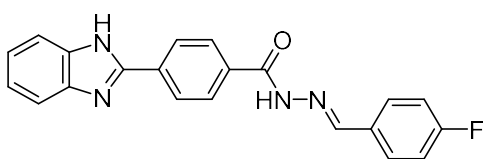


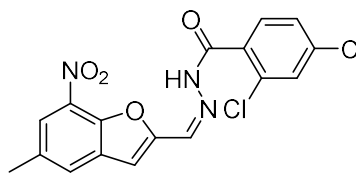
Fig. 37: Examples of biologically active hydrazones.

Hydrazones have gained attention in the pharmaceutical field and are being included in hybrid drugs to create more potent therapeutics<sup>24-26</sup>. A good example of this is that current research being done to synthesize new antibacterial drugs with several research groups working on combining pharmacophore properties of other antimicrobial drugs with a hydrazone backbone. Several benzimidazole derivatives containing a hydrazone moiety<sup>280</sup> and hydrazone derivatives of benzofuran<sup>281</sup> have been used as antibacterial agents (Fig. 38). Hydrazone derivatives of quinolone and their respective  $\text{Cu}^{2+}$  and  $\text{Zn}^{2+}$  complexes are used to treat tuberculosis<sup>282</sup> (Fig. 38). Drugs derived from 4-methyl-1,2,3-

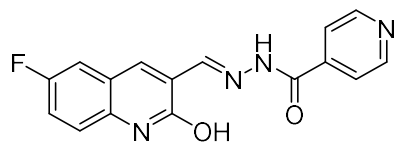
thiadiazole-5-carboxaldehyde benzoyl hydrazone<sup>283</sup> have been used as antiviral agents and 2-hydroxy-1-naphthylaldehyde isonicotinoyl hydrazone<sup>284</sup> has been used to fight malaria. Not only do hydrazones have a wide range of biological activities, but they have also been identified as potential antioxidants (Fig. 38)<sup>264</sup>. Due to their outstanding activity and multifunctional capabilities, hydrazones are excellent candidates for multi-target drug development.



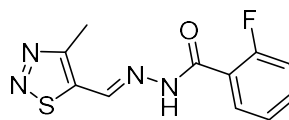
(*E*)-4-(1*H*-benzo[*d*]imidazol-2-yl)-*N*-(4-fluorobenzylidene)benzohydrazide  
(antibacterial)



(*Z*)-2,4-dichloro-*N*-((5-methyl-7-nitrobenzofuran-2-yl)methylene)benzohydrazide  
(antibacterial)



(*E*)-*N*-((6-fluoro-2-hydroxyquinolin-3-yl)methylene)isonicotinohydrazide  
(tuberculosis treatment)

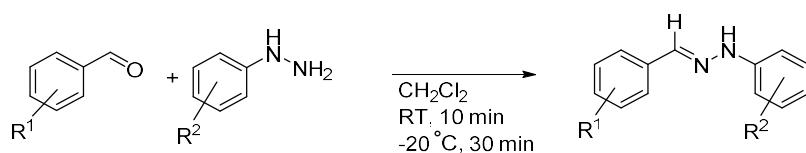


(*E*)-2-fluoro-*N*-((4-methyl-1,2,3-thiadiazol-5-yl)methylene)benzohydrazide  
(anti-malarial)

Fig. 38: Additional examples of biologically active hydrazones.

## 7.2 Synthesis

The hydrazone derivatives were synthesized in the Bela Török lab at the University of Massachusetts Boston by the following general procedure (Scheme 4). General synthesis of the hydrazones was carried out in a 25-mL Erlenmeyer flask; 1 mmol of benzaldehyde and 1 mmol of phenyl hydrazine were dissolved in 2 ml of dichloromethane. The reaction mixture was stirred for 10 min at room temperature, then it was cooled to  $-20\text{ }^{\circ}\text{C}$  for 30 min to crystallize the products. The crystalline product was filtered and air-dried for 12 h. The purity was verified using GC-MS and NMR. Impurities were removed by recrystallization or preparative TLC to yield at least 98 % purity product.

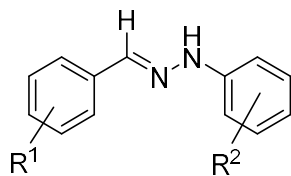


Scheme 4: Synthesis of the applied hydrazone derivatives.

## 7.3 Results

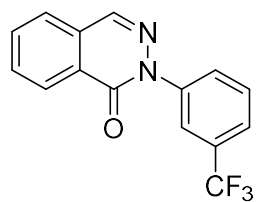
Fifteen hydrazone derivatives were selected from the Török lab's earlier work on hydrazones as multi-target candidates for AD treatment<sup>264</sup> in an effort to investigate their free radical scavenging activity. Compounds **31** – **42** were selected from this earlier study while compounds **43** – **45** have not yet been investigated. The antioxidant data was coupled with structural data determined using density functional theory (DFT) calculations. The list of compounds included molecules with electron withdrawing groups (such as CF<sub>3</sub>), hydrophobic residues, cyclized hydrazone structures and extended hydrazone structures (Fig. 39 and 40).



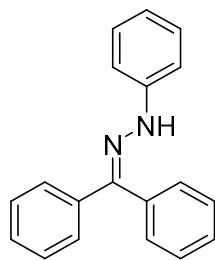


<u>compound</u>	<u>R<sup>1</sup></u>	<u>R<sup>2</sup></u>
<b>31</b>	3-Cl	H
<b>32</b>	4-CF <sub>3</sub>	H
<b>33</b>	2-Br	4-NO <sub>2</sub>
<b>34</b>	3,4-di(OMe)	2-CF <sub>3</sub>
<b>35</b>	2-Br	2-CF <sub>3</sub>
<b>36</b>	4-CF <sub>3</sub>	2-CF <sub>3</sub>
<b>37</b>	2-OH 4-OMe	2-CF <sub>3</sub>
<b>38</b>	2-OH 4-OMe	3-CF <sub>3</sub>
<b>39</b>	3-OH	H
<b>40</b>	4-N(Me) <sub>2</sub>	3-CF <sub>3</sub>
<b>41</b>	4-NO <sub>2</sub>	3-CF <sub>3</sub>
<b>42</b>	4-N(Me) <sub>2</sub>	2-CF <sub>3</sub>

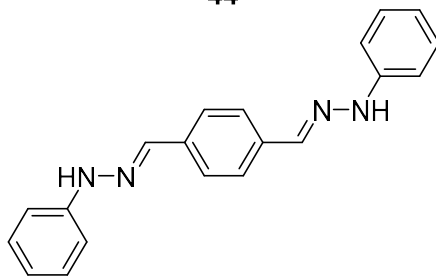
Fig. 39: Compounds **31** - **42** are hydrazones derivatized that have halogen and other electron withdrawing substituents.



**43**



**44**



**45**

Fig. 40: Compound **43** is a hydrazone that has cyclized through reaction of the hydrazone center with one of the substituents. Compound **44** is a hydrazone prepared from benzophenone and compound **45** is a simple double diarylhydrazone molecule prepared from 1,4-phthalaldehyde.

### **7.3.1 Free radical scavenging activity (ABTS, DPPH, ORAC)**

In the experimental studies, ABTS, DPPH and ORAC<sup>21,220,224</sup> (Chapter 3) assays were all performed to investigate the radical scavenging activity of the hydrazones. The activity profile of the compounds appeared different in the three assays. Several compounds (**37**, **38**, **40** and **42**) showed comparable activity to the reference compounds ascorbic acid and Trolox in all three assays (Table 8).

Table 8: Free radical scavenging activity of the hydrazone derivatives **31** – **45** against the DPPH<sup>a</sup>, ABTS<sup>b</sup> and peroxy radicals<sup>c</sup>. The compounds were screened at 10 μM for all three assays. The values here represent the mean ± the standard deviation of the data (n = 2–6).

compound	ABTS radical scavenging (%)	DPPH radical scavenging (%)	ORAC radical scavenging (%)
ascorbic acid	13 ± 2	12 ± 5	16 ± 8
resveratrol	75 ± 3	35 ± 3	97 ± 2
Trolox	15 ± 2	16 ± 7	89 ± 6
<b>31</b>	33 ± 1	17 ± 6	73 ± 5
<b>32</b>	27 ± 2	18 ± 6	82 ± 2
<b>33</b>	48 ± 3	7 ± 7	46 ± 4
<b>34</b>	18 ± 2	29 ± 12	67 ± 4
<b>35</b>	26 ± 1	16 ± 6	46 ± 4
<b>36</b>	8 ± 1	15 ± 4	56 ± 3
<b>37</b>	36 ± 2	47 ± 3	85 ± 3
<b>38</b>	30 ± 1	54 ± 8	87 ± 2
<b>39</b>	70 ± 1	12 ± 9	80 ± 2
<b>40</b>	28 ± 2	28 ± 1	83 ± 7
<b>41</b>	42 ± 4	24 ± 3	55 ± 16
<b>42</b>	35 ± 1	32 ± 2	86 ± 5
<b>43</b>	-2 ± 1	-1 ± 4	-4 ± 4
<b>44</b>	20 ± 0	27 ± 4	79 ± 3
<b>45</b>	31 ± 1	38 ± 5	78 ± 3

a: Calculation for DPPH radical scavenging activity can be seen in Chapter 3.2.1. Eq. 1 b: Calculation for ABTS radical scavenging activity can be seen in Chapter 3.2.2. Eq. 1. c: Calculation for ORAC radical scavenging activity can be seen in Chapter 3.2.3. Eqs. 2 and 3.

The data reveal that the compounds showed a broad range of activity in the DPPH assay. Compound **43** exhibited no effect; several compounds appear to possess higher activities than those of the reference compounds (**37**, **38**, **45**) and the rest of the compounds showed moderate effect, similar to resveratrol; however, their radical scavenging is still higher than that of ascorbic acid and Trolox. The data are somewhat similar in the ABTS assay; here, resveratrol is a very strong radical scavenger; however, according to the literature, this assay often reports false high radical scavenging for this compound due to several issues such as kinetic rates of phenol oxidation or the generation of secondary products<sup>21</sup>. It was observed that only compound **39** is better than resveratrol, while the rest of the compounds showed varying effect (from 10 to 50 %) yet; most are more effective than ascorbic acid and Trolox. The ORAC data diverges from the previous two sets. The hydrazones were most active against the smallest peroxy radical used in the ORAC assay, surpassing the activity of the controls. Since the peroxy radical in the ORAC assay is closest in nature to naturally occurring reactive oxygen species, this observation is encouraging. In this assay, the hydrazones appeared to be highly active and although their radical scavenging is still somewhat lower than those of resveratrol and Trolox, the activity values range from 50 to 88 % (except **43**, which remained inactive in the latter two assays as well).

As a first observation, one can say that the compounds exhibit a strong structure-activity relationship in the DPPH and ABTS assays, while the studied limited variations of the substituents of the hydrazone core structure affect the antioxidant activity only in a moderate extent in the ORAC assay. It is important to note that compound **43** possessing a structure with no N–H bond uniformly did not exhibit any measurable effect.

### **7.3.2 Physicochemical parameter determination using the Gaussian09 program suite**

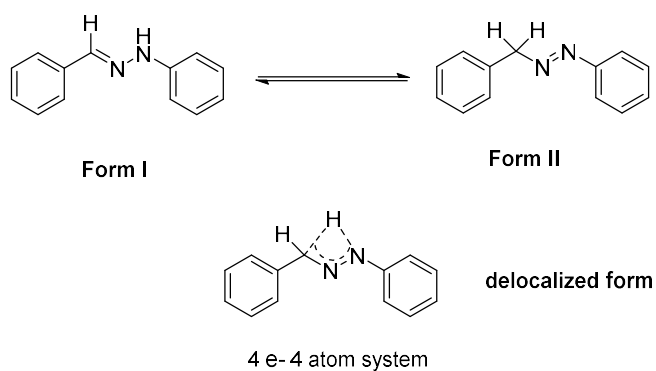
In an effort to understand the relationship between the hydrazone structural motifs and antioxidant activity, a more detailed structure-activity relationship (SAR) study was conducted. The electronic structures of the hydrazones were determined using density functional theory (DFT). Calculations were carried out at the B3LYP/6-31G(d,p) level of theory using the Gaussian09 program suite. The DFT calculations were performed in gas phase, calculating 10 different parameters (O-H bond distances, dipole moments, logP values, HOMO and LUMO orbital energies, band gap energies, radical spin densities, proton affinities, ionization potentials and bond dissociation energies) to conduct the SAR study (Table 9).

Table 9: Theoretical parameters of the hydrazones investigated. Values were determined using Gaussian09. (a - Å, b - hartree, c - eV, d - kcal/mol).

	<u>N-H distance<sup>a</sup></u>	<u><math>\mu</math> (D)</u>	<u>LogP</u>	<u>HOMO<sup>b</sup></u>	<u>LUMO<sup>b</sup></u>	<u>Band gap<sup>c</sup></u>	<u>BDE<sup>d</sup></u>	<u>PA<sup>d</sup></u>	<u>Ionization potential<sup>d</sup></u>	<u>Ionization potential<sup>e</sup></u>
31	1.017	3.570	3.62	-0.19413	-0.05095	3.89	66.85	209.4	6.76	155.97
32	1.017	3.402	4.44	-0.19775	-0.05814	3.79	67.25	210.4	6.85	158.06
33	1.017	8.315	3.10	-0.21650	-0.08302	3.63	69.27	199.4	7.24	167.00
34	1.016	4.658	4.44	-0.18963	-0.04327	3.98	66.29	214.8	6.44	148.58
35	1.014	1.748	4.77	-0.20307	-0.05814	3.94	69.90	210.8	6.92	159.70
36	1.015	2.054	5.24	-0.20854	-0.06511	3.90	70.19	207.3	7.08	163.47
37	1.014	3.580	3.68	-0.19371	-0.04857	3.94	64.75	211.5	6.58	151.85
38	1.014	3.053	3.68	-0.19202	-0.04656	3.95	64.02	212.5	6.54	150.90
39	1.016	0.804	2.48	-0.18701	-0.04027	3.99	66.68	213.3	6.56	151.45
40	1.016	5.728	4.75	-0.17504	-0.03387	3.84	98.6	218	6.07	140.13
41	1.017	5.812	3.51	-0.21777	-0.09755	3.2	68.59	198	7.32	168.97
42	1.014	3.891	4.77	-0.17452	-0.033	3.85	67.86	221.05	6.05	139.55
43	N/A	5.449	4.08	-0.22997	-0.06666	4.44	87.4	193.84	7.65	176.43
44	1.02	2.276	5.51	-0.19515	-0.03277	4.41	92.02	232.6	6.44	148.59
45	1.017	0.197	4.37	-0.17781	-0.05797	3.26	89.86	218	5.99	138.16

## 7.4 Discussion

In regard to the contribution of the structural features, it is believed that the antioxidant activity of resveratrol is partially due to its phenolic OH groups as well as its conjugated structure. As the hydrazones possess a similar structure to resveratrol, the possible contribution of the NH group as well as the partial conjugation was considered. The extended conjugation is a common characteristic in many natural antioxidants, such as lycopene (tomato),  $\beta$ -carotene (carrot), or curcumin (turmeric)<sup>285</sup>. It is proposed that the partial conjugation is achieved by the rapid equilibrium of the two potential tautomers of the hydrazones<sup>286</sup> as illustrated in Scheme 5.



Scheme 5: Tautomers and the potential delocalized form of diarylhydrazones.

First, the potential tautomeric forms of benzylidene-phenyl hydrazone (Scheme 5) have been investigated to reveal the stable form of the molecule, which would be the candidate for further calculations. The optimized geometry, electronic energy and relative stabilization energy of the two tautomeric forms were calculated by Gaussian at the B3LYP/6-31G(d,p) level (Fig. 41).



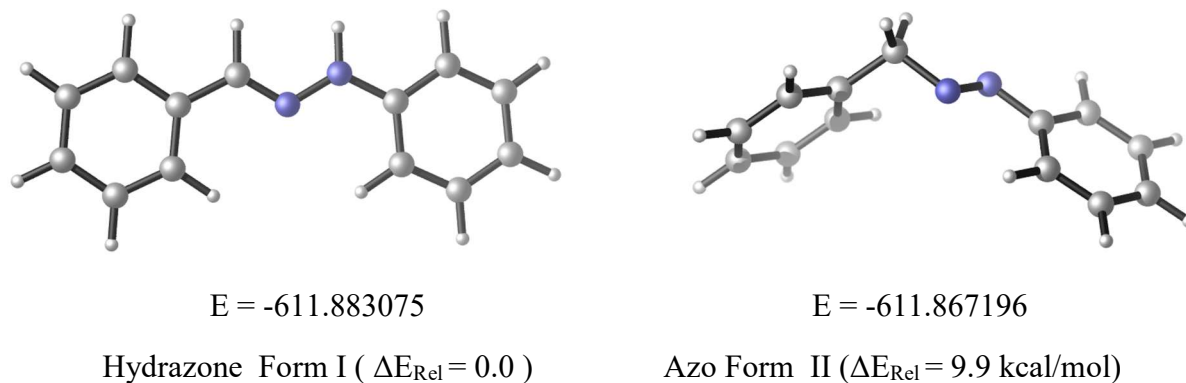
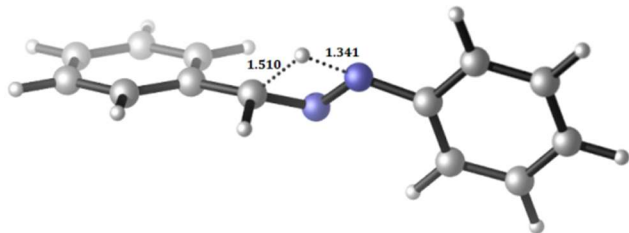


Fig. 41: B3LYP/6-31G(d,p) optimized geometries of hydrazone Form I and azo Form II of benzylidene-phenylhydrazine. Electronic energy ( $E$ ) is given in hartrees. Relative stabilization energies ( $\Delta E_{\text{Rel}}$ ), expressed in kcal/mol, are given in parenthesis.

The calculated relative stabilization energy data of the two resonance forms show that Form I with the  $\text{-C=N-NH-}$  unit is more stable than Form II with the  $\text{-CH}_2\text{-N=N-}$  unit by 9.9 kcal/mol. This energy difference between the tautomers is significant. Calculations revealed that the activation energy barrier between the Form I and Form II is  $E_{\text{A}} = 62.26$  kcal/mol, which is relatively high and supports the stabilization of hydrazone (Form I) over its azo tautomer (Form II). The structure of the transition state (Fig. 42 A) and the intrinsic reaction coordinate diagram (Fig. 42 B) are shown in Fig. 42.

(A)



(B)

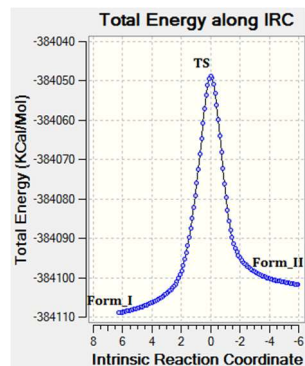


Fig. 42: The structure of the transition state of between the two diarylhydrazone tautomers (A) and the intrinsic reaction coordinate diagram for the tautomerization (B).

Since the overall electron delocalization may also play a role in the antioxidant effect, the electrostatic potential map of the tautomers has also been determined (Fig. 43) in order to identify potential electron-rich or electron-deficient areas in the tautomers.

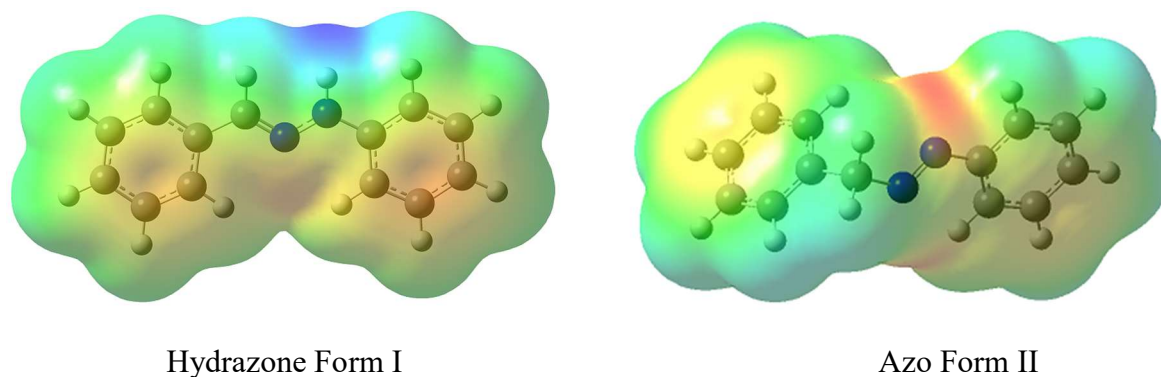


Fig. 43: Hydrazone Form I and azo Form II of benzylidene-phenyl hydrazine at isovalue 0.0004. The blue region shows electron-poor areas and the red region shows electron-rich surfaces.

The electron density distribution appears to be significantly different in the case of the two tautomeric forms. Form I has more even electron distribution on the aromatic rings and the vicinity of the N–H bond shows an electron-poor character. In contrast, Form II has an electron-rich area in the vicinity of the N=N bond due to the presence of the double bond as well as the lone pairs of the N atoms. As a result, however, both aromatic rings exhibit a partially electron-poor character. In order to investigate the tautomeric equilibrium both experimentally and theoretically, the  $^1\text{H}$  NMR spectrum of the benzylidene-phenyl hydrazine has been determined in  $\text{DMSO-}d_6$  and calculated for both tautomeric forms. The data are shown in Fig. 44.

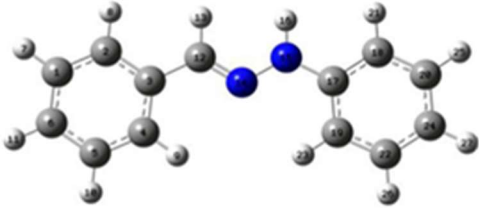
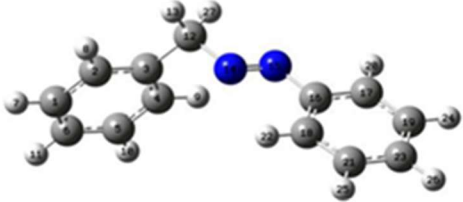
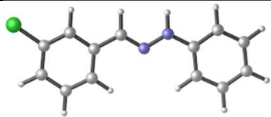
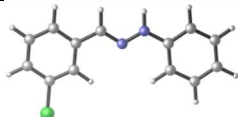
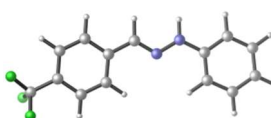
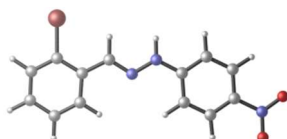
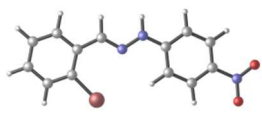
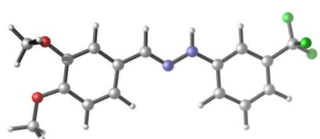
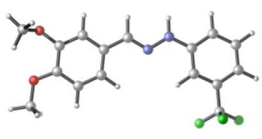
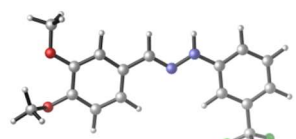
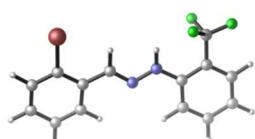
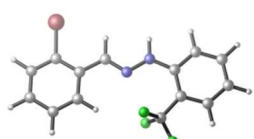
Hydrazone Form I		Azo Form II		Structures
H-atom number	$\delta_{\text{H-CALC}}$ (ppm)	H-atom number	$\delta_{\text{H-CALC}}$ (ppm)	
8	7.4	8	8.2	<i>Form I</i> 
7	7.6	7	7.8	
11	7.5	11	7.6	
10	7.6	10	7.6	
9	8.3	9	7.5	
21	6.8	22	7.8	
25	7.5	25	7.7	<i>Form II</i> 
27	7.0	26	7.8	
26	7.5	24	7.9	
23	7.6	20	8.3	
13	7.5	13	5.9	
16	7.9	17	4.9	

Fig. 44: Calculated  $^1\text{H}$  NMR chemical shifts of the hydrazone form I and azo form II of benzylidene-phenyl hydrazine in DMSO.

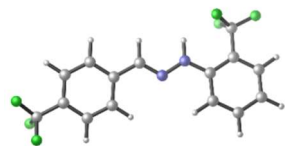
The experimental spectrum is very similar to the calculated chemical shifts of the hydrazone form. The azo tautomer is only visible to a strongly limited extent; a small singlet appears at 5.750 ppm that could represent the  $\text{CH}_2$  protons of the azo form. Therefore, the comparison of the theoretical and experimental  $^1\text{H}$  NMR data suggests that while the presence of the azo form is supported by the experimental spectrum, the contribution of this form appears to be negligible (less than 1 %). Thus, while the tautomeric equilibrium may contribute to a partially delocalized electron distribution, it likely is not a significant species in the radical scavenging processes that are related to the traditional mechanisms<sup>220</sup>. Based on the above studies, the hydrazone form was selected for further investigations.

As these molecules contain a variety of substituents in altering positions, a conformational analysis was carried out to determine the lowest energy conformers that would be used to calculate the parameters of the compounds for the structure-activity relationship studies. The optimized geometries and electronic energies of selected conformers are shown in Table 10. The comparison of the electronic energies allowed the selection of the most stable conformers that were used to calculate the parameters of the compounds that we applied in the structure activity relationship studies. In several cases, the identification was a rather simple task when the symmetry of the compound strongly favored a particular conformer. An interesting observation was made, however, when compounds with an -OH substituent were investigated. The minimum energy structure of hydrazones **37** and **38** (Table 13, entries **37**, **38**, conformer 3) exposed an intramolecular hydrogen bonding interaction between the hydroxyl group and the sp<sup>2</sup>-hybrid nitrogen from the hydrazone. As the phenolic OH group also participates in radical scavenging activity, this hydrogen bond might affect its ability to perform that function. The calculations revealed a similar trend in conformational stability both in aqueous solution as well as in the gas phase, indicating that the interaction with the water molecules does not disrupt the hydrogen bonding. Finally, based on the data in Table 10, the lowest energy structures for each compound were selected for calculating the different parameters of the compounds to be used in the structure activity relationship studies.

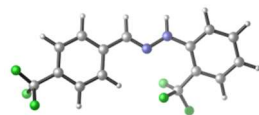
Table 10: Electronic energy (E) are given in hartree while the relative stabilization energies ( $\Delta E_{\text{Rel}}$ ) are in parenthesis in kcal/mol units.

compound	conformer 1	conformer 2	conformer 3	selected conformer
31	 E=-1071.487170 ( $\Delta E_{\text{Rel}}$ =0.005)	 E=-1071.487178 ( $\Delta E_{\text{Rel}}$ =0.0)		2
32	 E=-948.914773			1
33	 E=-3387.496664 ( $\Delta E_{\text{Rel}}$ =0.0)	 E=-3387.492026 ( $\Delta E_{\text{Rel}}$ =2.910)		1
34	 E=-1177.893122 ( $\Delta E_{\text{Rel}}$ =0.0)	 E=-1177.893017 ( $\Delta E_{\text{Rel}}$ =0.060)	 E=-1177.892232 ( $\Delta E_{\text{Rel}}$ =0.492)	1
35	 E=-3520.02675 ( $\Delta E_{\text{Rel}}$ =0.0)	 E=-3520.018558 ( $\Delta E_{\text{Rel}}$ =5.140)		1

36



E=-1285.945827

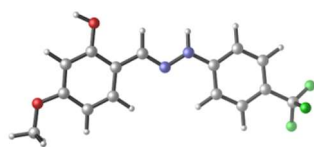
 $(\Delta E_{\text{Rel}}=0.0)$ 

E=-1285.937467

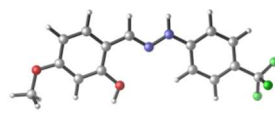
 $(\Delta E_{\text{Rel}}=5.245)$ 

1

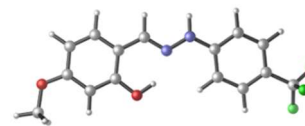
37



E=-1138.625669

 $(\Delta E_{\text{Rel}}=6.113)$ 

E=-1138.620439

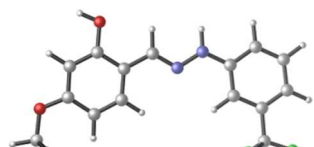
 $(\Delta E_{\text{Rel}}=9.395)$ 

E=-1138.635412

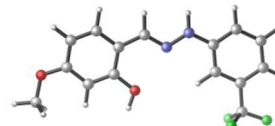
 $(\Delta E_{\text{Rel}}=0.0)$ 

3

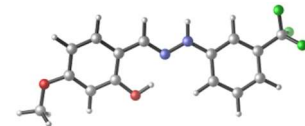
38



E=-1138.624073

 $(\Delta E_{\text{Rel}}=6.304)$ 

E=-1138.618971

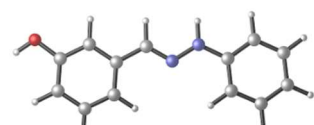
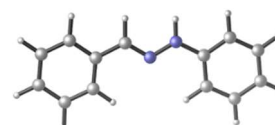
 $(\Delta E_{\text{Rel}}=9.506)$ 

E=-1138.63412

 $(\Delta E_{\text{Rel}}=0.0)$ 

3

39

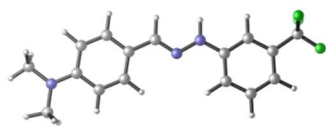
E=-687.099116  $(\Delta E_{\text{Rel}}=0.0)$ 

E=-687.098919

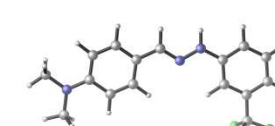
 $(\Delta E_{\text{Rel}}=0.123)$ 

1

40



E=-1082.817095

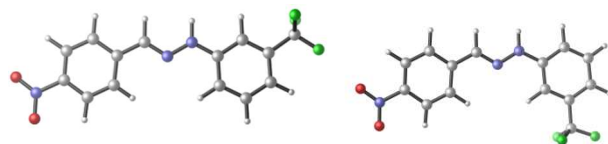
 $(\Delta E_{\text{Rel}}=0.0)$ 

E=-1082.816944

 $(\Delta E_{\text{Rel}}=0.094)$ 

1

41



E=-1153.412616

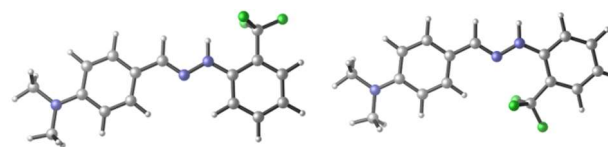
( $\Delta E_{\text{Rel}}=0.0$ )

E=-1153.412329

( $\Delta E_{\text{Rel}}=0.180$ )

1

42



E=-1082.817245

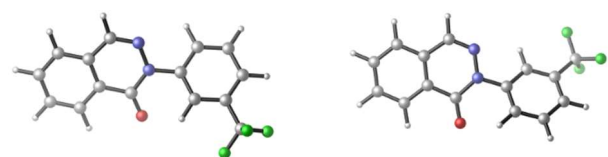
( $\Delta E_{\text{Rel}}=0.0$ )

E=-1082.807854

( $\Delta E_{\text{Rel}}=5.892$ )

1

43



E=-1061.073094

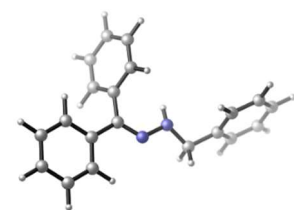
( $\Delta E_{\text{Rel}}=0.1$ )

E=-1061.073402

( $\Delta E_{\text{Rel}}=0.0$ )

2

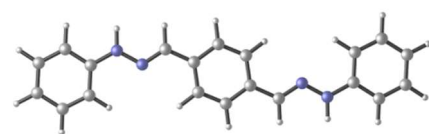
44



E=-882.140343

1

45



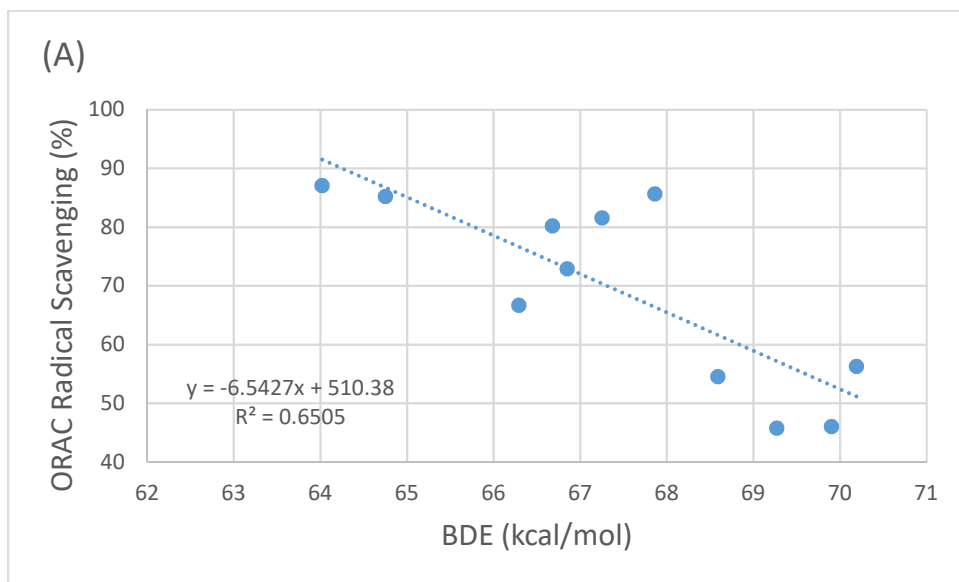
E=-991.609857

1



Several parameters such as N–H distance, dipole moment, logP value, HOMO-LUMO energies, band gap, bond dissociation energy, proton affinity and ionization potential of the above selected were calculated. The data are tabulated in Table 9.

In order to uncover the potential contribution of the above calculated parameters to the radical scavenging activity, the relation of the parameters to the experimental data has been assessed. The analysis of the activity vs. property plots revealed that several parameters appear to influence the antioxidant activity (Figs. 45 and 46) while others seem to have no or only non-characteristic effects (not shown).



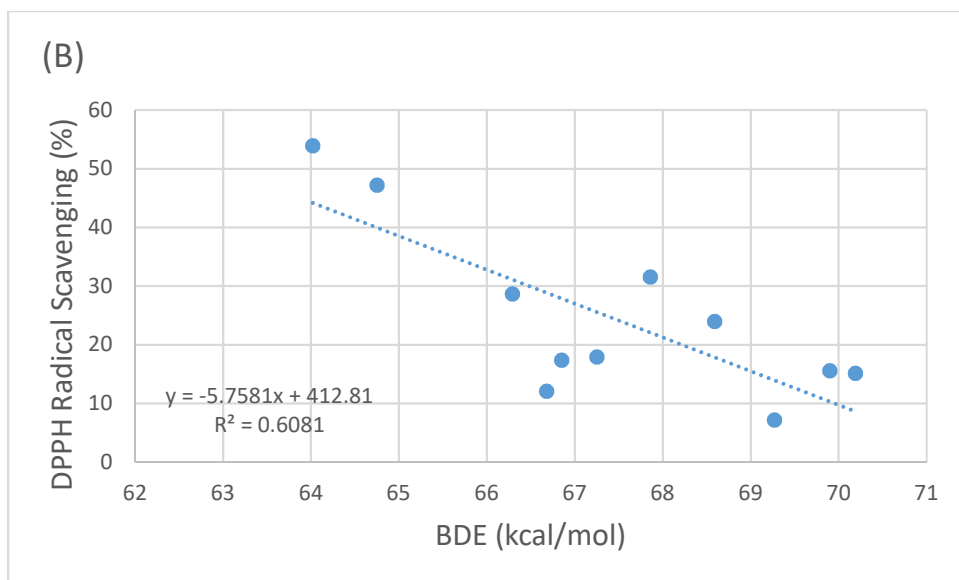
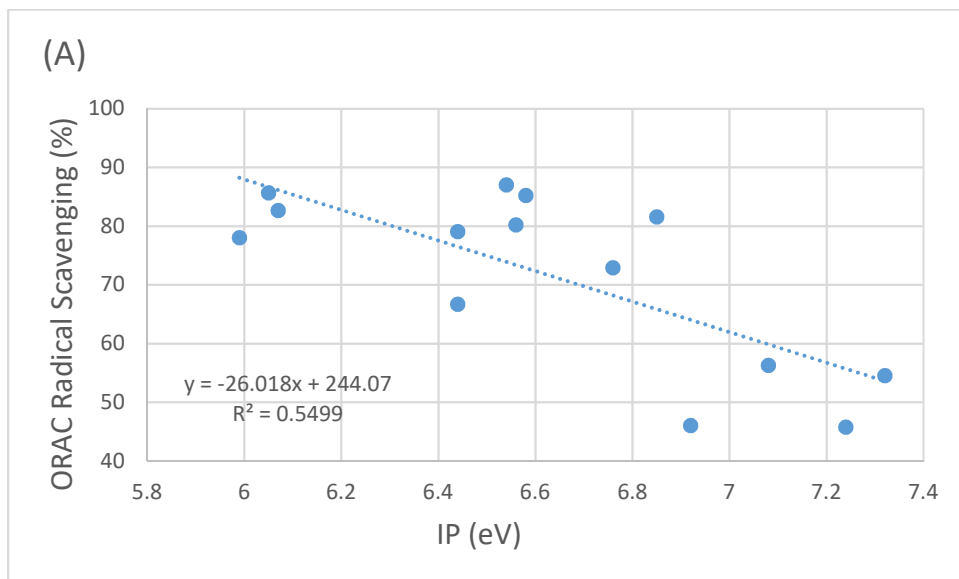


Fig. 45: Selected radical scavenging activity vs. BDE plots to illustrate the effect of the BDE on the activity of the hydrazones. Compound **43** was removed due to the cyclized structure and compounds with antioxidant activity higher than 80% (**40**, **44** and **45**) were removed (see appendix - B).



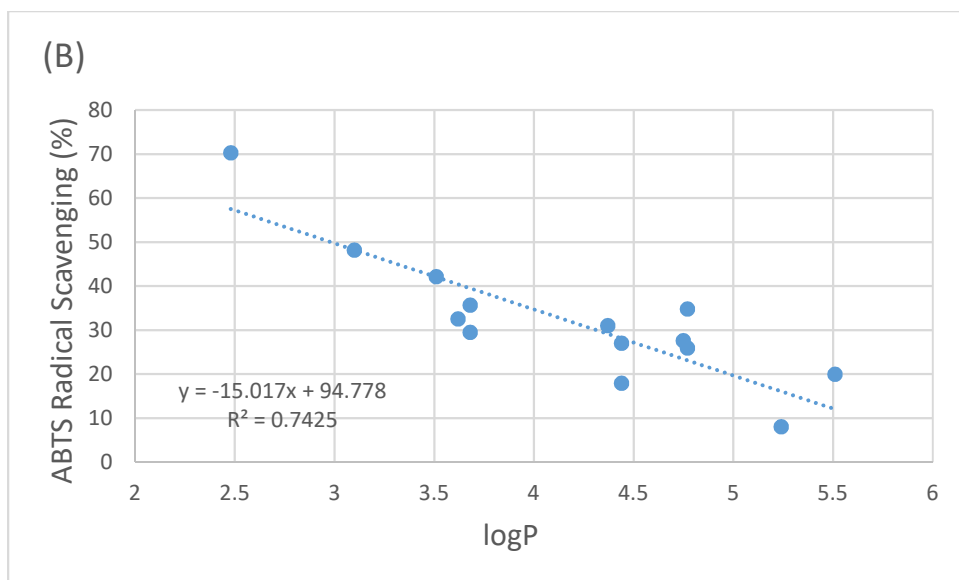


Fig. 46: Selected radical scavenging activity vs. IP and logP plots to illustrate the effect of the parameters on the radical scavenging activity of the hydrazones.

Foremost, the N–H bond dissociation energies (BDE) showed a correlation with the antioxidant activity. Based on the plots, obtained for the ORAC ( $R^2=0.6505$ ) and DPPH ( $R^2=0.6081$ ) assays (Fig. 45 A and B respectively), a linear relationship describes the effect of N–H BDE on the antioxidant activity, suggesting that decreasing BDE values result in increasing radical scavenging activity. The BDE effect is a clear indication that the hydrazones, at least partially, act via the hydrogen atom transfer (HAT) mechanism as described in Eq. 4.

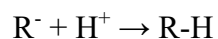
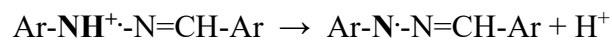
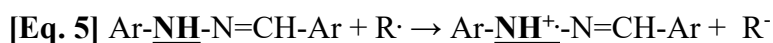


The HAT mechanism is the most common mechanism considered for the natural antioxidant polyphenols<sup>287</sup>. However, the poor correlation for the highest activity

compounds also indicates that while BDE is a strong contributing factor to the activity, it likely is not the only important characteristic.

The underlying principle of the HAT mechanism is that low BDE indicates weak X–H bonds (X=N, O) which facilitate homolytic bond cleavage, thus providing H atoms to scavenge the target radical. Such a relationship is often observed for phenol derivatives, although the type of correlation varies<sup>288</sup>. It is important to note that compound **43**, which does not possess an N–H bond, did not show any activity in either assay, a clear indication that the presence of the N–H bond is a necessary feature in these compounds. When comparing the calculated BDE with the experimentally observed antioxidant activity, it was found that compounds **37 - 39** and **42** show high experimental activities and have a low BDE. However, there are compounds, such as **40**, **44** and **45**, which have high BDE but also high activity in the assays and were removed from the plot due to poor sample size and correlation (see appendix- B). It must be noted that as the target radicals vary in the three assays, so does the correlation. Compounds **37 - 39** represent a specific group in which the compounds also possess a phenolic OH group in addition to the NH group of the hydrazone linkage. Similarly, in three-ring, hydrazone-like compounds, the phenolic OH group was claimed to be primary antioxidant, despite obtaining lower BDE values for the NH bond than for the OH bond<sup>289</sup>. Thus, to evaluate the reactivity of the NH–and OH groups in these compounds, BDE of the OH bond was calculated. The obtained BDE values for the –O–H bonds are 77.5 (**37**), 77.1 (**38**) and 73.8 (**39**) kcal/mol. These values are comparatively higher than those calculated for the N–H bond in the same compounds: 64.75 (**7**), 64.02 (**38**) and 66.18 (**39**) kcal/mol. In addition, several compounds (e.g., **32**, **40**, **42** and **44**) that do not have phenolic OH substituent exhibit

similar or better antioxidant activities than those with it. Thus, our data provide further support to the earlier observations regarding the relative N–H vs O–H BDE values; however, in contrast to the earlier suggestion<sup>289</sup>, we found that the NH group is more efficient in the hydrogen atom transfer than the OH in these compounds. It is worth noting that just like molecules **37** - **39**, compound **45** also contains multiple X–H bonds (two N–H) that may contribute positively to the antioxidant effect. The BDE of **45** (89.85kcal/mol) is one of the highest in the studied groups despite that **45** exhibits one of the best activities. It is in line with the obtained exponential correlation. However, it also highlights that the number of active groups plays an important role. Another important feature appears to be the ionization potential (IP). A representative plot is shown in Fig. 46 A for the ORAC assay; however, similar correlation was observed in the other assays as well. The data indicate a linear relationship ( $R^2=0.5499$ ) between IP and the antioxidant activity, namely, the activity decreases with increasing IP. This finding suggests that the radical scavenging by hydrazones is partially due to their participation in the single electron transfer (SET) mechanism<sup>290</sup>. This pathway occurs in three steps as shown in Eq. 5.



According to the data and Eq. 5, the increasing IP value will decrease the extent of the formation of the  $\text{Ar-NH}^+\cdot\text{-N=CH-Ar}$  radical cation and thus result in diminishing antioxidant activity. Compounds with low IP values, such as **40**, **42**, **44** and **45**, either

having no additional substituents or the presence of electron withdrawing and electron donating substituents is balanced, have high activities. In contrast, the exclusive presence of electron withdrawing groups on both rings of the hydrazones in **33** (Br, NO<sub>2</sub>), **35** (Br, CF<sub>3</sub>), **36** (CF<sub>3</sub>, CF<sub>3</sub>) and **42** (NO<sub>2</sub>, CF<sub>3</sub>) decreases the possibility of electron transfer from the parent compound, hence decreases the antioxidant activity. In addition to the above-discussed molecular features, the logP value that describes the partition of the compounds in aqueous and organic media is a common factor to consider in structure-activity relationship studies. As an example, the effect of logP on the antioxidant activity is shown in Fig. 46 B, which indicates that increasing lipophilicity (or logP) results in decreasing antioxidant effect ( $R^2=0.7425$ ). This effect can be explained by the assay conditions; all assays are carried out in hydrophilic medium, either in aqueous buffers or 50 % aq. ethanol solution. Thus, compound **39** with a hydrophilic OH substituent showed the highest activity in the ABTS assay. However, when considering the logP factor, one must remember that for compounds to be considered as drug candidates, they must also possess a reasonable lipophilicity as well. The analysis of the other calculated characteristics did not reveal significant correlation with the antioxidant activity. The above results highlight clear and firm relationships between the structural and energetic features and their contribution to antioxidant activity for the studied group of hydrazones. However, it must be noted that an extended study with a broader group of hydrazones bearing more diverse substituents is needed to propose a quantitative description of the effect of these features that would make possible the rational design of antioxidants for potential therapeutic use.

## CHAPTER 8

### EFFECT OF STRUCTURAL PARAMETERS OF PHENOL AND ANILINE MODEL COMPOUNDS ON THEIR RADICAL SCAVENGING ACTIVITY

#### 8.1 Introduction

As mentioned earlier in Chapter 2, free radical damage has been identified as a common factor in the progression of many neurological diseases and radical scavenging could be incorporated into the design of multi-functional drug therapeutics. The most abundant plant-based antioxidants are polyphenols, which have a large structural variety<sup>291,292</sup>. A majority of the literature is primarily focused on the extraction, identification and quantification of their bioactivity<sup>57-61</sup>. Natural polyphenols may have excellent in vitro activity; however, their poor bioavailability limits their practical applications in biological systems<sup>57,73-77</sup>.

In the above experimental and DFT studies investigating the free radical scavenging activity of diarylhydrazones, it was established that the -NH group of the hydrazones provided significant free radical scavenging activity for these compounds<sup>245</sup>. Since there are several N-containing natural antioxidants (e.g. betalain, bilirubin or uric acid),<sup>64</sup> it prompted us to evaluate the comparative activity of the -OH vs. the -NH groups. To avoid structural features that unnecessarily complicate the DFT studies (e.g. the possibility of conformational or E-Z isomers) we decided to focus on simple substituted phenols and anilines.

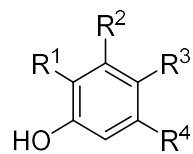
The major aim of this work is to gain new insights to the fundamental mode of action of complex radical scavengers. Therefore, the experimental radical scavenging activity of

simple phenol and aniline model compounds was compared to investigate the effects of structural features. The selected compounds are simple, single ring structures that allow a direct comparison of the electronic and steric properties. While these molecules are not practical antioxidants, their simple structures offer a better opportunity to reveal important structural features that significantly affect their activity. In this work, our major goals were to (i) compare the antioxidant activity of similar phenol (-OH) and aniline (-NH) derivatives and (ii) identify the effect of a broad variety of structural features (iii) to better understand the antioxidants' mode of action.

## **8.2 Results**

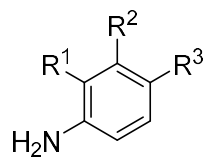
Thirty-two phenol and aniline model compounds were investigated through a SAR study to identify structural features resulting in increased radical scavenging activity. The compounds analyzed are commercially available and chosen to have a broad variety of substituents from the strongly electron withdrawing (EW) to electron donating (ED) groups and can be seen in Figs. 47, 48 and 49





	$R^1$	$R^2$	$R^3$	$R^4$
46	H	H	H	H
47	H	H	CH <sub>3</sub>	H
48	CH <sub>2</sub> CH <sub>3</sub>	H	H	H
49	H	H	OH	H
50	H	H	(CH <sub>2</sub> ) <sub>2</sub> H <sub>3</sub>	H
51	H	CH <sub>3</sub>	Br	H
52	H	H	COOH	H
53	H	H	CHO	H
54	CHO	H	OCH <sub>3</sub>	H
55	H	H	COPh	H
56	OH	COOH	H	H
57	H	COOH	OH	H
58	COOH	OH	H	H
59	OH	H	COOH	H
60	H	OH	H	COOH
61	H	OCH <sub>2</sub>	OH	H
62	Ph	H	OH	H

Fig. 47: The structures of phenol model compounds (46 - 62) investigated.



	$\underline{R}^1$	$\underline{R}^2$	$\underline{R}^3$
<b>63</b>	H	H	H
<b>64</b>	F	H	H
<b>65</b>	H	Cl	H
<b>66</b>	H	CF <sub>3</sub>	H
<b>67</b>	H	H	Cl
<b>68</b>	H	H	Br
<b>69</b>	H	H	F
<b>70</b>	H	H	NO <sub>2</sub>
<b>71</b>	H	H	CH <sub>2</sub> CH <sub>3</sub>
<b>72</b>	H	H	CH <sub>2</sub> CH <sub>2</sub> CH <sub>3</sub>
<b>73</b>	H	CH <sub>3</sub>	Br

Fig. 48: The structures of aniline model compounds (**63** - **73**) investigated.

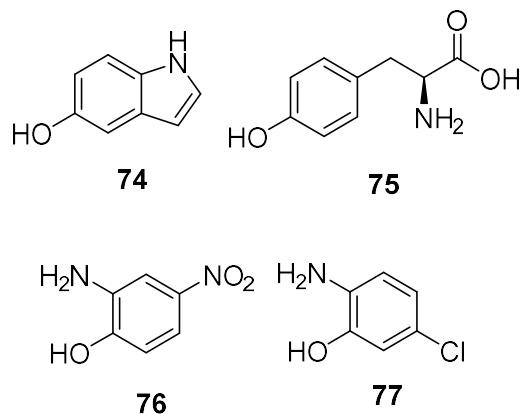


Fig. 49: The structures of phenol model compounds with an -NH group (74 - 77) investigated.

Compounds **46 - 62** contain a phenolic -OH group while compounds **63 - 73** all contain a -NH<sub>2</sub> group. Compound **74** is a hydroxyindole and is distinctly different than the other compounds in this study. Compounds **76** and **77** have both an -OH and -NH<sub>2</sub> on the same phenyl ring. Compound **75** is tyrosine. The biochemical assays in this section (ABTS, DPPH and ORAC assays) were completed to identify compounds with radical scavenging activity. The experimental activity of these compounds was utilized in a SAR study to identify the structural parameters that are important for radical scavenging activity of phenol and aniline model compounds.

### 8.2.1 Free radical scavenging activity of the model compounds (ABTS, DPPH, ORAC)

Due to the high radical scavenging activity of polyphenols<sup>66-70</sup> and the antioxidant activity of the hydrazones described in Chapter 7, this work was designed to investigate the activity of not just the substituted phenols, but also the effects of substituents on the activity of anilines as well. The experimental activities were determined using three

commonly applied and widely accepted assays; the DPPH, ABTS and ORAC protocols. Many of these compounds showed activity in all three of the radical scavenging assays (Tables 11 and 12).

Table 11: Free radical scavenging activity of the phenol model compounds **46 – 61** against the DPPH<sup>a</sup>, ABTS<sup>b</sup> and peroxy radicals<sup>c</sup>. The values here represent the mean  $\pm$  the standard deviation of the data (n = 2–6).

compound	ABTS radical scavenging (%)	DPPH radical scavenging (%)	ORAC radical scavenging (%)
<b>ascorbic acid</b>	9 $\pm$ 7	36 $\pm$ 5	29 $\pm$ 8
<b>resveratrol</b>	51 $\pm$ 6	37 $\pm$ 5	97 $\pm$ 1
<b>Trolox</b>	20 $\pm$ 1	35 $\pm$ 1	71 $\pm$ 11
<b>46</b>	28 $\pm$ 1	1 $\pm$ 12	59 $\pm$ 1
<b>47</b>	81 $\pm$ 3	0 $\pm$ 12	54 $\pm$ 4
<b>48</b>	64 $\pm$ 8	2 $\pm$ 10	42 $\pm$ 1
<b>49</b>	21 $\pm$ 1	31 $\pm$ 10	93 $\pm$ 3
<b>50</b>	48 $\pm$ 3	6 $\pm$ 6	40 $\pm$ 4
<b>51</b>	45 $\pm$ 3	10 $\pm$ 7	82 $\pm$ 2
<b>52</b>	31 $\pm$ 5	-3 $\pm$ 8	74 $\pm$ 1
<b>53</b>	3 $\pm$ 4	2 $\pm$ 5	83 $\pm$ 4
<b>54</b>	19 $\pm$ 6	5 $\pm$ 8	84 $\pm$ 2
<b>55</b>	22 $\pm$ 5	-2 $\pm$ 7	88 $\pm$ 2
<b>56</b>	28 $\pm$ 1	44 $\pm$ 10	91 $\pm$ 1
<b>57</b>	18 $\pm$ 1	26 $\pm$ 6	92 $\pm$ 1
<b>58</b>	44 $\pm$ 2	-5 $\pm$ 10	36 $\pm$ 8
<b>59</b>	20 $\pm$ 1	31 $\pm$ 9	97 $\pm$ 1
<b>60</b>	60 $\pm$ 4	4 $\pm$ 8	79 $\pm$ 2
<b>61</b>	50 $\pm$ 1	47 $\pm$ 12	88 $\pm$ 0

a: Calculation for DPPH radical scavenging activity can be seen in Chapter 3.2.1. Eq. 1 b: Calculation for ABTS radical scavenging activity can be seen in Chapter 3.2.2. Eq. 1. c: Calculation for ORAC radical scavenging activity can be seen in Chapter 3.2.3. Eqs. 2 and 3.

Table 12: Free radical scavenging activity of the phenol and aniline model compounds **62**

- **77** against the DPPH<sup>a</sup>, ABTS<sup>b</sup> and peroxy radicals<sup>c</sup>. The values here represent the mean  $\pm$  the standard deviation of the data (n = 2–6).

compound	ABTS radical scavenging (%)	DPPH radical scavenging (%)	ORAC radical scavenging (%)
ascorbic acid	9 $\pm$ 7	36 $\pm$ 5	29 $\pm$ 8
resveratrol	51 $\pm$ 6	37 $\pm$ 5	97 $\pm$ 1
Trolox	20 $\pm$ 1	35 $\pm$ 1	71 $\pm$ 11
<b>62</b>	4 $\pm$ 2	-1 $\pm$ 4	80 $\pm$ 1
<b>63</b>	17 $\pm$ 8	7 $\pm$ 8	85 $\pm$ 3
<b>64</b>	9 $\pm$ 7	-9 $\pm$ 11	73 $\pm$ 2
<b>65</b>	14 $\pm$ 5	-2 $\pm$ 6	82 $\pm$ 2
<b>66</b>	5 $\pm$ 4	-4 $\pm$ 7	61 $\pm$ 3
<b>67</b>	22 $\pm$ 5	-1 $\pm$ 6	91 $\pm$ 1
<b>68</b>	25 $\pm$ 4	-2 $\pm$ 11	87 $\pm$ 2
<b>69</b>	17 $\pm$ 5	2 $\pm$ 14	88 $\pm$ 3
<b>70</b>	2 $\pm$ 5	-2 $\pm$ 9	5 $\pm$ 4
<b>71</b>	41 $\pm$ 5	10 $\pm$ 7	92 $\pm$ 1
<b>72</b>	38 $\pm$ 10	0 $\pm$ 8	86 $\pm$ 5
<b>73</b>	31 $\pm$ 3	8 $\pm$ 10	93 $\pm$ 2
<b>74</b>	67 $\pm$ 8	42 $\pm$ 5	91 $\pm$ 5
<b>75</b>	37 $\pm$ 7	4 $\pm$ 2	98 $\pm$ 3
<b>76</b>	43 $\pm$ 8	31 $\pm$ 6	91 $\pm$ 3
<b>77</b>	28 $\pm$ 8	32 $\pm$ 6	6 $\pm$ 4

a: Calculation for DPPH radical scavenging activity can be seen in Chapter 3.2.1. Eq. 1 b: Calculation for ABTS radical scavenging activity can be seen in Chapter 3.2.2. Eq. 1. c: Calculation for ORAC radical scavenging activity can be seen in Chapter 3.2.3. Eqs. 2 and 3.

The three general mechanisms describing how antioxidants scavenge free radical species<sup>220,221</sup>: hydrogen atom transfer (HAT), sequential electron transfer (SET) and sequential proton loss electron transfer (SPLET) were reported in Fig. 10 in Chapter 3.2. The data reveals that although phenols have higher radical scavenging activity, anilines are also able to scavenge the investigated radicals. The data showed that almost every compound performed extremely well in the ORAC assay, with radical scavenging percentages almost always above 80% (Tables 11 and 12) except for compounds **70** and **77** which had minimal activity in all three free radical scavenging assays. Compounds with high activity in the ORAC experiment are thought to primarily react through the HAT mechanism<sup>21</sup>. In contrast, the compounds exhibited uniformly negligible activity in the DPPH assay (Tables 11 and 12). Due to the uniform activity profiles that provided minimal variations, neither the DPPH nor the ORAC data were appropriate for the SAR analysis. In contrast, the radical scavenging of ABTS, which may occur through the SET and HAT mechanisms<sup>21</sup>, provided the most viable dataset for the compounds investigated (Tables 11 and 12). Thus, all further discussion will be based on the ABTS assay. It was observed that phenols generally performed better than anilines. Free radical scavenging assays, such as the ABTS assay, are known to report higher activities for compounds with multiple -OH groups<sup>220</sup>, which does not appear to be the case with our compounds (e.g. **56**, **57** and **59**). While we noticed similar trends to those seen in the literature, it was found that the position of the -OH on the aromatic ring affects the activity of the compound more than the number of the -OH groups.

### **8.2.2 Determination of physicochemical parameters using the Gaussian09 program suite**

The electronic structures of the phenol and aniline derivatives were determined using density functional theory (DFT). Calculations were carried out at the B3LYP/6-31G(d,p), level of theory using the Gaussian09 program suite. The sum of the energies for the radical and the hydrogen atom in the starting compound were calculated. The O-H and N-H bond dissociation energy (BDE) for the thirty-two compounds was determined by subtracting the two energies. Additional parameters (Table 13) were also calculated to identify any experimental correlations between the phenols and anilines and their experimental radical scavenging activities: N-H and O-H bond distances, dipole moments, logP values, HOMO and LUMO orbital energies, band gap energies, radical spin densities, proton affinities, ionization potentials and the experimentally derived Hammett constants<sup>24</sup>



Table 13: Theoretical parameters of the substituted phenols and anilines investigated. Values were determined using Gaussian09. (a - Å, b - hartree, c - eV, d - kcal/mol).

	N-H distance <sup>a</sup>	O-H distance <sup>a</sup>	$\mu$ (D)	LogP	HOMO <sup>b</sup>	LUMO <sup>b</sup>	Band gap <sup>c</sup>	BDE[NH] <sup>d</sup>	BDE[OH] <sup>d</sup>	Spin density radical	Spin density O-radical	P <sup>h</sup> <sub>v</sub>	Ionization potential <sup>d</sup>	Ionization potential <sup>e</sup>	$\sigma$ (meta)	$\sigma$ (para)
46	NA	0.966	1.335	1.45	-0.2193	0.00054	5.98	NA	74.405	NA	0.444	182.57	184.85	8.01	NA	NA
47	NA	0.966	1.312	1.94	-0.2111	0.0019	5.79	NA	72.669	NA	0.643	185.24	176.71	7.66	NA	-0.17
48	NA	0.966	1.079	2.11	-0.21309	0.00753	6	NA	71.97	NA	0.631	185.45	177.4	7.69	NA	-0.15
49	NA	0.965	0	0.79	-0.19904	-0.00286	5.33	NA	69.815	NA	0.624	182.76	170.285	7.38	NA	-0.37
50	NA	0.965						NA		NA					NA	
51	NA	0.966	1.333	2.23	-0.21129	0.00178	5.79	NA	72.937	NA	0.642	185.81	175.54	7.61	NA	-0.13
52	NA	0.966	2.385	2.59	-0.2184	-0.00933	5.68	NA	73.739	NA	0.638	178.73	178.298	7.73	-0.07	0.23
53	NA	0.966	1.481	0.57	-0.2357	-0.0382	5.37	NA	76.72	NA	0.427	NA	190.67	8.27	NA	0.45
54	NA	0.966	2.491	1.34	-0.2387	-0.0536	5.03	NA	76.59	NA	0.412	NA	192.96	8.37	NA	0.42
55	NA	0.966	4.099	1.16	-0.2289	-0.2386	-0.26	NA	76.33	NA	0.645	NA	182.71	7.92	0.12	NA
56	NA	0.966	4.458	2.21	-0.231	-0.057	4.73	NA	75.69	NA	0.417	NA	179.89	7.8	NA	0.43
57	NA	0.986	2.796	0.84	-0.21279	-0.0504	4.41	NA	82.7082	NA	0.587	214.262	174.755	7.57	0.37	NA
58	NA	0.966						NA		NA						
59	NA	0.972	1.813	0.77	-0.21016	-0.05145	4.31	NA	77.7172	NA	0.598	190.782	173.808	7.53	0.37	-0.37
60	NA	0.965						NA	71.1245	NA	0.636	180.705			NA	NA
61	NA	0.971	1.909	1.58	-0.21749	-0.05513	4.41	NA	78.7922	NA	0.588	186.352	178.095	7.72	0.12	NA
62	NA	0.983						NA	84.4566	NA	0.592	206.926			NA	NA
63	NA	0.968	4.572	0.02	-0.22166	-0.03815	4.99	NA	76.0503	NA	0.642	183.553	181.231	7.85	NA	0.45
64	NA	0.965						NA	75.5494	NA	0.567	182.504			NA	NA
65	NA	0.966	2.98	-0.03	-0.22448	-0.0471	4.82	NA	75.354	NA	0.651	176.31	182.521	7.91	0.37	NA
66	NA	0.966						NA		NA					NA	NA
67	NA	0.966	3.233	1.33	-0.21334	-0.05039	4.43	NA	68.7372	NA	0.586	179.092	175.36	7.6	0.376	NA
68	NA	0.966						NA	73.1405	NA	0.644	183.815			NA	NA
69	NA	0.965	0.246	1.92	-0.1978	-0.02317	4.75	NA	67.3182	NA	0.597	195.762	161.775	7.01	0.109	-0.37
70	NA	0.965						NA	70.2375	NA	0.621	188.035			NA	NA
71	1.011	NA	1.27	0.9	-0.1981	0.0085	5.63	79.34	NA	0.634	NA	214.36	166.96	7.24	NA	0
72	1.01	NA	1.719	0.99	-0.2034	0.0041	5.65	78.9	NA	0.63	NA	211.95	169.94	7.37	NA	NA
73	0.966	NA	3.165	1.81	-0.2105	-0.0059	5.57	80.55	NA	0.639	NA	209.14	172.59	7.48	0.37	NA
74	1.01	NA	3.153	2.11	-0.2145	-0.019	5.32	80.88	NA	0.642	NA	207.55	175.46	7.61	0.43	NA
75	1.01	NA	2.251	1.88	-0.2046	-0.0074	5.36	104.04	NA	0.619	NA	209.87	168.09	7.29	NA	0.23
76	1.01	NA	2.325	1.83	-0.2036	-0.0075	5.34	79.42	NA	0.617	NA	210.25	166.77	7.23	NA	0.23
77	1.011	NA	3.316	1.8	-0.1992	-0.0044	5.3	78.19	NA	0.627	NA	212.09	166.76	7.23	NA	0.06
78	1.008	NA	5.802	1.56	-0.2294	-0.0716	4.29	83.4	NA	0.619	NA	199.62	185.09	8.03	NA	0.78
79	1.011	NA	0.736	1.81	-0.1926	0.0089	5.49	78.37	NA	0.62	NA	217.2	160.09	6.94	NA	-0.15
80	1.011	NA	1.525	2.11	-0.1925	0.00902	5.48	78.373	NA	0.771	NA	217.52	159.282	6.9	NA	-0.13
81	1.01	NA	3.25	2.29	-0.20083	-0.00186	5.41	79.29	NA	0.901	NA	212.51	163.653	7.09	-0.07	0.23
82	1.006	0.965	3.329	1.65	-0.191	-0.0052	5.05	78.78	70.3	0.395	0.426	205.55	162.21	7.03	NA	NA
83	1.017	0.973	1.55	-1.88	-0.2164	-0.0053	5.74	88.17	73.51	0.967	0.43	223.91	171	7.41	NA	NA
84	1.01	0.966	6.404	-0.2	-0.2105	-0.0059	5.57	80.48	65.56	0.629	0.28	207.99	174.87	7.58	NA	0.78
85	1.01	0.965	2.75	0.83	-0.1957	-0.00002	5.33	77.56	63.55	0.31	0.37	215.75	161.53	7	0.37	NA

### 8.3 Discussion

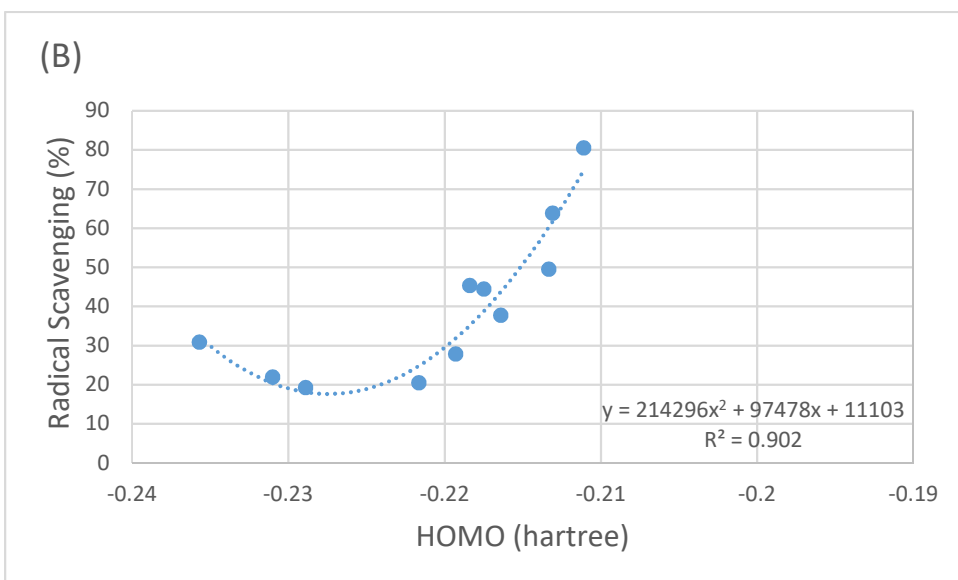
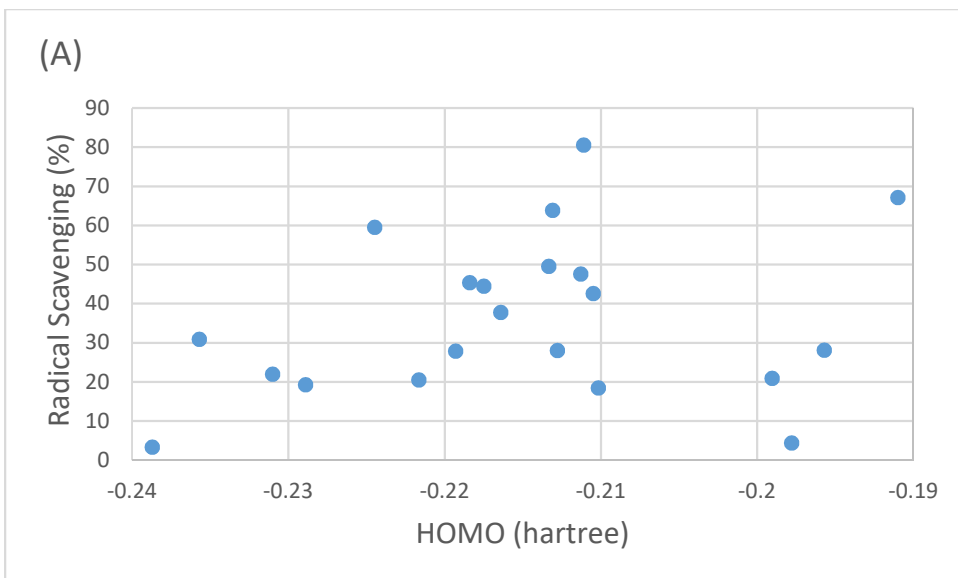
The ABTS data suggests a few key points. While the phenolic compounds have higher free radical scavenging activity, it is worth noting that compounds **66**, **74** and **75** from the aniline set also have comparable activity to the best phenols. Additionally, benzoic acid compounds having -OH groups in different positions were also studied. If compounds possess higher activity solely by the number of -OH groups, compounds **52** - **60** should all have similarly high activity. Instead, varying activity was observed across these compounds with the highest activity belonging to benzoic acids with -OH groups located in the 1,3 positions. Another interesting trend with the ABTS data suggests that electron donating groups on the phenyl ring promote radical scavenging activity, e.g. compounds **48** (Et) and **50** (Pr), respectively. The experimental data alone suggests that it is not just the amount of -OH groups present in the compound that correlate to activity, but there are other properties which significantly contribute to the activity of these phenol and aniline models.

Correlating the theoretical properties of the compounds to the ABTS activity data led to several important observations. As these compounds have similar chemical structures, their experimental activity data and structural parameter values were expected to be related. Thus, the experimentally determined ABTS radical scavenging data have been plotted as a function of each calculated parameter set respectively. Then the obtained plots were analyzed in order to reveal potential relationships between the experimental activity and the characteristics. It was observed that several properties seem to have little to no effect on the activity of the compounds. -OH distance, -NH distance, logP, LUMO, spin density of O-radical, spin density of N-radical, proton affinity and Hammett

constants (meta) all appeared to be irrelevant as modulators to the radical scavenging activity (data not shown). Along with this observation, correlating the calculated properties with experimental activity using the complete compound set did not reveal any reasonable correlations with the data. (Data not shown) It suggests that comparing phenols and anilines in a single unified set is not a sufficient approach. Thus, it was decided to analyze the compounds in two separate groups as defined by their parent compounds, phenols and anilines.

### *Phenols*

Phenols investigated in this set (**46 - 62** and **74 - 77**) showed several reasonable correlations between the ABTS radical scavenging data and the physicochemical properties examined. The HOMO energies are used to determine the likelihood of an electron to be donated by a compound<sup>79</sup>. Elevated HOMO values indicate that the compound is likely to donate electrons. The effect of the HOMO energies on the experimental activity of the phenols is depicted in Fig. 50.



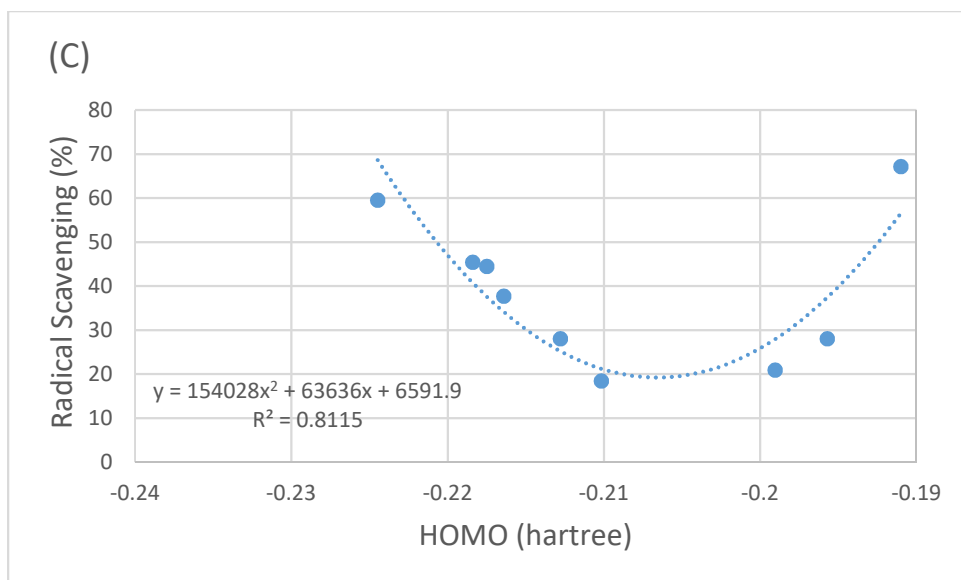


Fig. 50: (A) Effect of the HOMO energies of phenols on the radical scavenging activity of the compounds. (B) Activity vs. HOMO correlation for compounds **46 - 48, 51, 52, 54, 55, 58, 59, 61** and **75** which correspond to the left parabola on (A). (C) Activity vs. HOMO correlation for compounds **49, 51, 56 - 58, 60, 74, 75** and **77** which correspond to the right parabola.

Two activity wells can be identified in Fig. 50 A where the activity of the phenols drops between -0.20 and -0.21 hartree as well as between -0.22 and -0.23 hartree. These wells appear as two distinct but overlapping parabolic functions when all phenols are included. Compounds **46 - 48, 51, 52, 54, 55, 58, 59, 61** and **75** can be seen forming the left parabola (Fig. 50 B), while compounds **49, 51, 56 - 58, 60, 74, 75** and **77** form the right parabola (Fig. 50 C) The  $R^2$  values indicate a reasonable fit between the calculated functions and the data. Compounds **74** and **75** appear to be part of both functions. The compounds that form the left parabola (Fig. 50 B) are primarily consisted of single -OH

containing molecules, while compounds in the right parabola (Fig. 50 C) generally include molecules with multiple -OH groups.

The LUMO energies for the phenols were found to be far too similar to identify a specific trend within the data set (Table 13). Similar to the above observations, the effect of the band gap energy on the activity yielded two distinct relationships (Fig. 51).

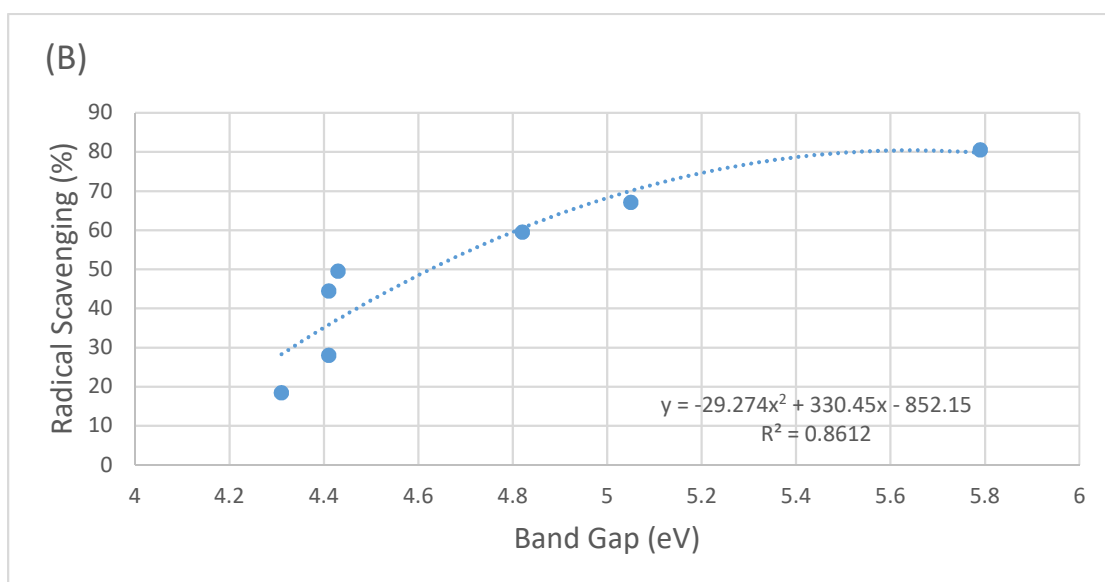
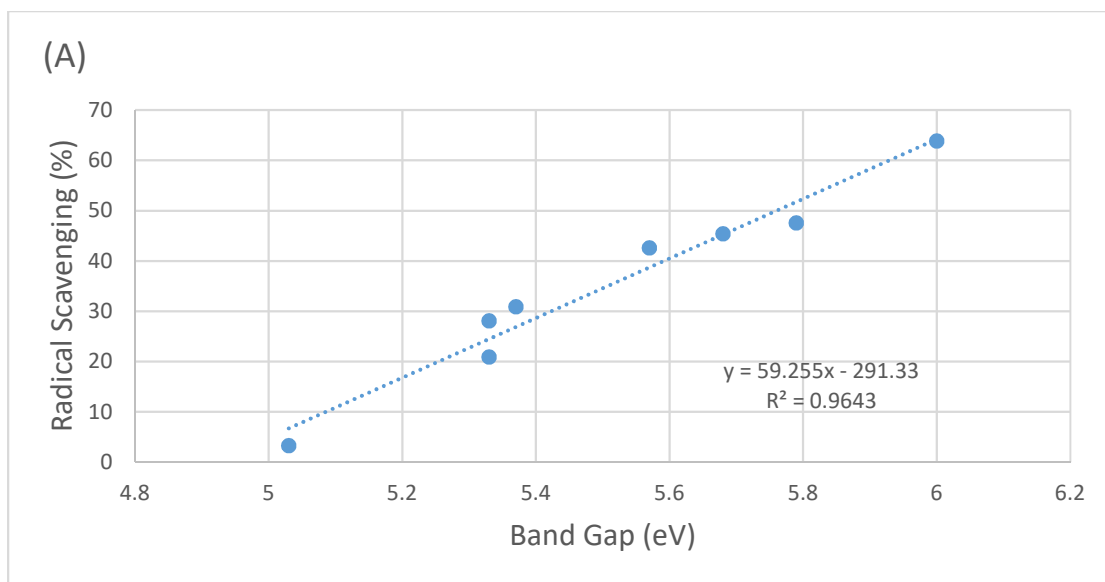


Fig. 51: Free radical scavenging activity vs band gap functions of (A) compounds **48 - 53, 76 and 77** and (B) compounds **47, 56 - 58, 60, 61 and 74**.

Band gap energy is a common theoretical factor used to predict radical scavenging activity and to help determine stability of the spent antioxidant. In Fig. 51 A, for compounds **48 - 53, 76 and 77** the activity vs. band gap energy relationship corresponds

to a linear function. The molecules that are plotted in Fig. 51 A are all compounds with a single -OH group. In contrast, compounds with multiple -OH substituents (**47**, **56 - 58**, **60**, **61** and **74**) plotted in Fig. 51 B, the activity vs. band gap energy function show an exponential relationship. Both functions can be characterized by reasonable  $R^2$  values, the linear relationships being an excellent fit ( $R^2=0.964$ ). Whether exponentially or linearly related, it seems clear that increasing band gap energy results in enhanced radical scavenging activity. When this band gap energy data is coupled with the HOMO energy correlations it suggests that phenols with high radical scavenging activity react primarily through the HAT mechanism where they donate a hydrogen atom to the radical species. The bond dissociation energy (BDE) is also a common feature to interpret the radical scavenging activity of an antioxidant<sup>293-295</sup>. This feature is often associated with the HAT mechanism; the stronger this bond, the less likely the antioxidant will react with the radical species in solution<sup>295</sup>. This is probably the best predictor of compounds that will react by the HAT mechanism, which involves the transfer of a hydrogen atom to the radical. The BDE calculations are usually restricted to X-H bonds, such as O-H and N-H<sup>72</sup>. The activity vs. BDE data are depicted in Fig. 52.



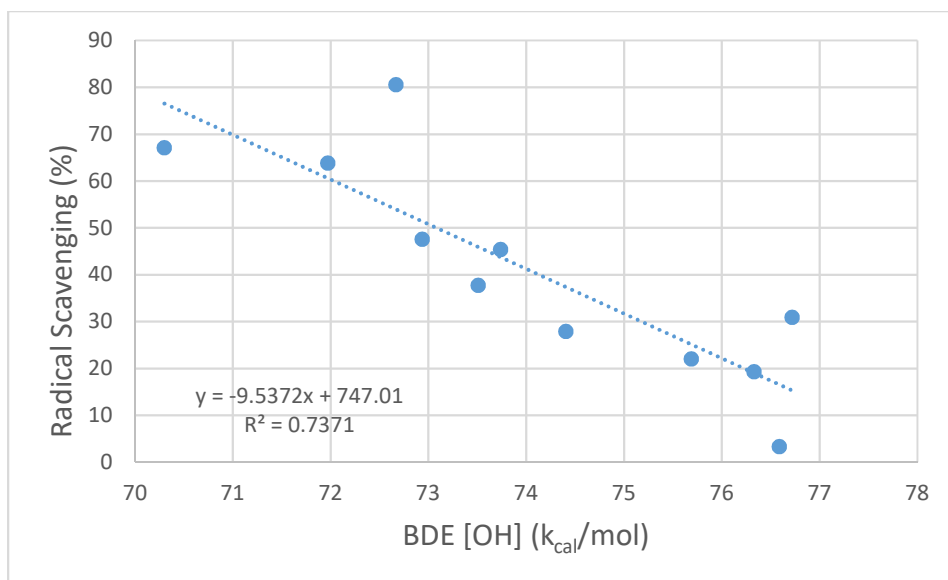


Fig. 52: Effect of bond dissociation energy (BDE) of the phenols **46 - 48**, **50 - 55**, **74** and **75** on their corresponding radical scavenging activity.

Fig. 52 shows a less characteristic relationship as compared to Figs. 50 and 51. While the general trend indicates that BDE has an inverse relationship with the scavenging activity, the low  $R^2$  value suggests a relatively modest correlation. This could be due to experimental limitations; compounds with a greater number of -OH groups tend to be more reactive in these free radical scavenging assays than they would be in biologically relevant systems<sup>220</sup>. Removing all of the compounds with more than one -OH group (**56 - 63**) as well as compounds **76** and **77** (dual -OH/NH) produces Fig. 52. The linear correlation of the BDE data with the ABTS scavenging activity of the single -OH compounds (**46 - 48**, **50 - 55**, **74** and **75**) shows that the lower the BDE of the -OH, the better free radical scavenger the compound will be. It indicates that the compound will likely donate a hydrogen atom that would terminate free radical species in solution.

Properties such as the LUMO and spin density of the O-radical did not show correlation with radical scavenging activity. However, where correlation between the properties and ABTS data exist, they are typically high (HOMO, band gap energy, BDE). All three of these properties suggest that the most important factor for phenols to be a free radical scavenger is the stability of the spent antioxidant. There is extensive literature available about polyphenols being potent free radical scavengers because they have more -OH groups present to scavenge the radical<sup>296,297</sup>. However, our investigations with the above model compounds suggest it is not necessarily the amount of -OH groups, rather the position of the -OH groups that is important. Fig. 53 highlights eight of our models with single and multiple hydroxyl groups along with the experimental ABTS scavenging activity.

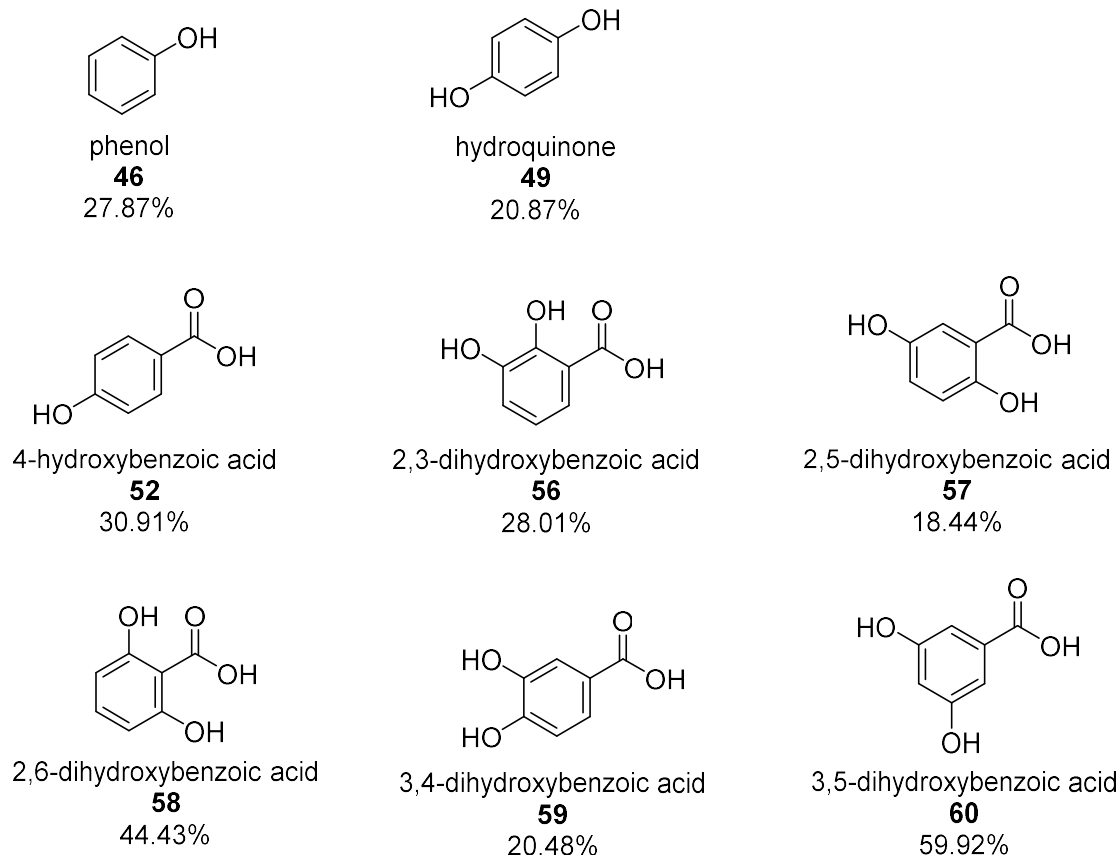


Fig. 53: The structure and ABTS activity data of compounds **46**, **49**, **52** and **56 - 60**.

If the -OH content alone was responsible for the activity of the compounds, then compound **49** should have significantly lower activity than compound **46** and compound **52** should have lower activity than compounds **56 - 60**. This is not necessarily the case. Instead, the position of the phenolic -OH groups appears to be important in determining the activity. Hydroquinone (**49**) should be higher in activity than the phenol (**46**) and our study indicates this is not true, instead the single -OH phenol possess 1.4 times higher activity than hydroquinone. Several benzoic acids were also part of our analysis and the results led to the same conclusion. Most of the benzoic acids that have more than one phenolic -OH group (**56**, **57** and **59**) have lower activity than 4-hydroxybenzoic acid (**52**).

However, compounds **58** and **60**, where the -OH groups are in relative 1,3-positions respectively, have higher activity than compound **52**. This suggests that the placement of the phenolic -OH groups is of primary importance; the 1,3 arrangement helps boost the radical scavenging activity. In fact, many of the potent polyphenols commonly investigated in the literature have this 1,3 – dihydroxy motif (resveratrol, cyanidin, catechin, quercetin, tannin, etc.)<sup>56,61,67</sup>.

#### *Anilines and other NH-containing compounds*

As the joint analysis of phenols and anilines did not result in coherent a SAR, it was decided to analyze the potential relationship between their calculated properties and experimental radical scavenging activity separately. Accordingly, we shift the discussion to primary amino group containing aromatics (anilines) and other –NH containing compounds. Consisting of compounds **63 – 73**, **76** and **77**, these models showed widespread correlations between the ABTS scavenging data and their properties. Anilines (**67 - 72**) had significant correlation between their ABTS scavenging data and dipole moment (Fig. 54).

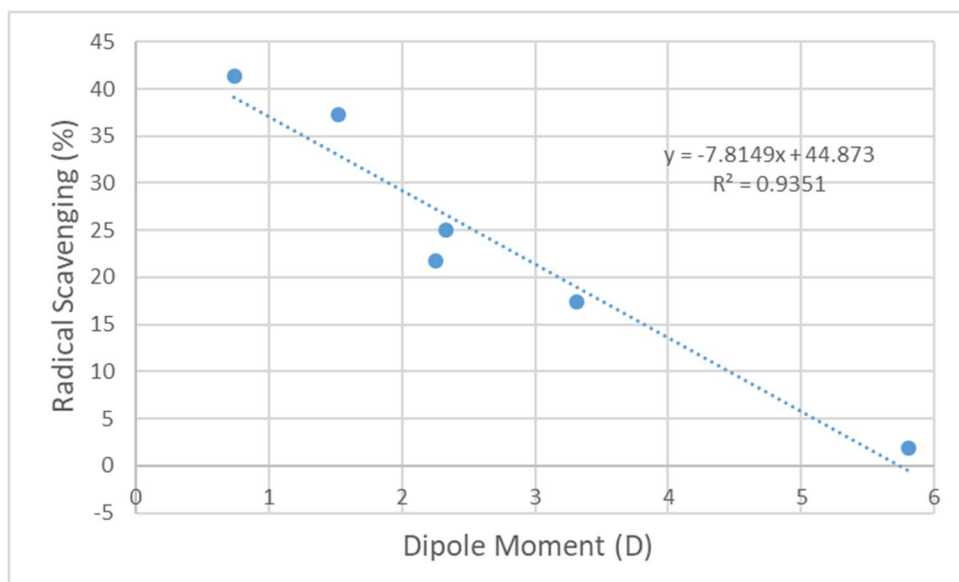


Fig. 54: Effect of dipole moment on the ABTS scavenging activity of anilines **67 - 72**.

The dipole moment of a potential radical scavenger may offer information on the potential stability of the spent antioxidant that is often another radical<sup>295</sup>. Anilines, unlike substituted phenols, showed a linear trend upon further refining the data (Fig. 54) by removing aniline (**79**) and a few of the compounds with groups that may sterically hinder the interaction of the -NH<sub>2</sub> with the bulky radical species (**64 - 66**, **73**, **76** and **77**). A low dipole moment suggests more pronounced delocalization in the molecule that can contribute to the stabilization of the lone electron left on the spent antioxidant. Stability of the spent antioxidant is important to prevent the antioxidant from behaving like an active radical.

Similar to the phenols it appears that the radical scavenging activity of anilines is also affected by their HOMO energy. In Fig. 55 compounds **63 - 73** and **77** can be seen forming an exponential relationship with activity.

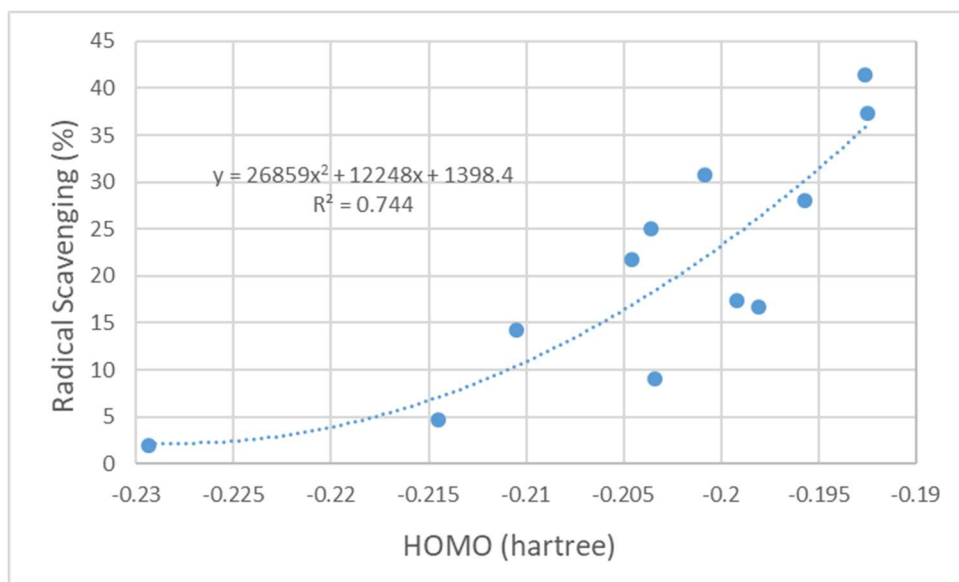


Fig. 55: The effect of HOMO energies of the anilines (**63** - **73** and **77**) on their scavenging activity.

Unlike the phenols, the activity of anilines grew with increasing HOMO energy, suggesting that the more likely the anilines were to share the electrons, the better the antioxidant they were, which would be expected for compounds reacting through the SET mechanism. Based on previously outlined mechanisms of free radical scavenging activity the ability for anilines to share electrons explains their activity in the ABTS assay. As it was the case with phenols, the LUMO energies for the anilines were also too similar to be able to identify a specific trend in the data (Table 13).

An exponentially growing trend was identified in the band gap energy data for anilines **66** - **68**, **71** - **73**, **76** and **77** (Fig. 56). Much like the band gap energy-activity relationship of the phenols stabilization of the spent antioxidant is very important<sup>298</sup>.

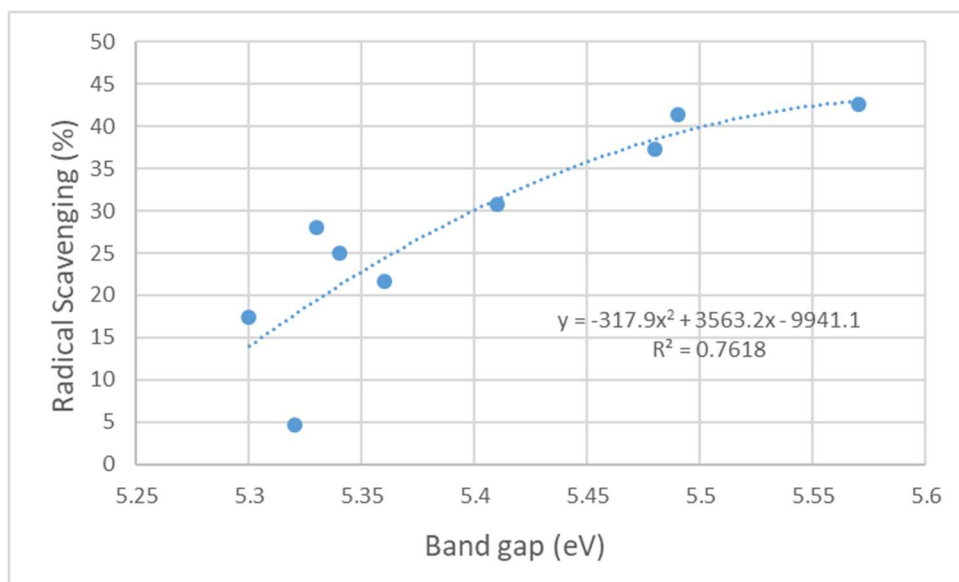


Fig. 56: Effect of band gap energy of the anilines on their radical scavenging activity with compounds **63** - **65** and **70** removed.

The activity vs. BDE plot of the anilines also appears relevant and shows a correlation with the ABTS activity data (Fig. 57). The exponentially declining activity as a function of BDE is in agreement with expectations and with the well-established HAT – mechanism, in which a direct H-atom transfer from the antioxidant to the radical would ensure the radical scavenging effect.

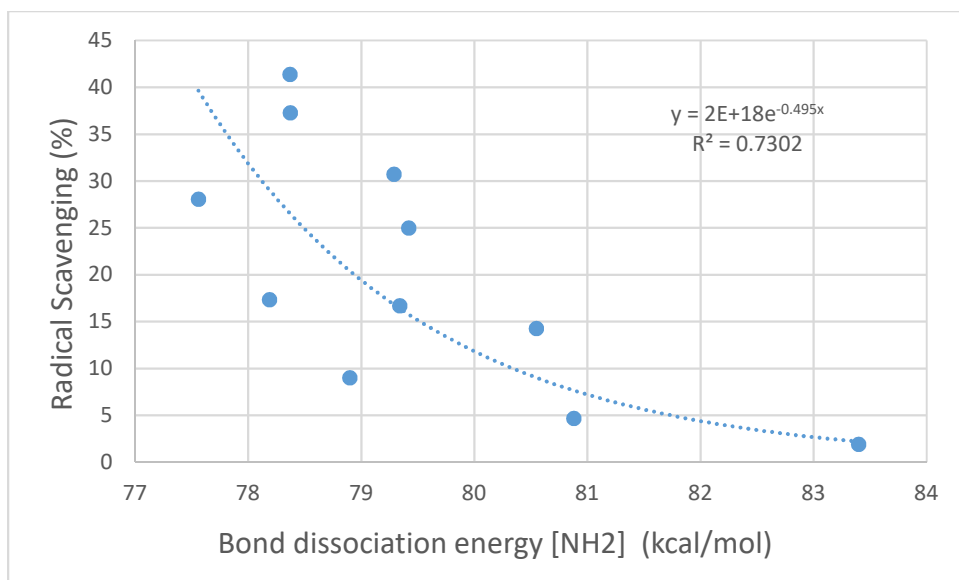


Fig. 57: Radical scavenging of anilines as a function of their bond dissociation energy (BDE) with compounds **67** and **76** removed.

Ionization potential (IP) is important for the evaluation of antioxidants, as the electron transfer from the scavengers to the radical species is an essential step in the SET mechanism<sup>296</sup>. Anilines show an inverse linear correlation between free radical scavenging activity and the ionization potential. The ionization potential (Fig. 58) of the compound decreases as their free radical scavenging activity increases. This is in direct agreement with the literature which suggests that the first step in SET mechanism (the donation of an electron from the antioxidant compound to the radical species) is favorable for these anilines<sup>295,298</sup>.



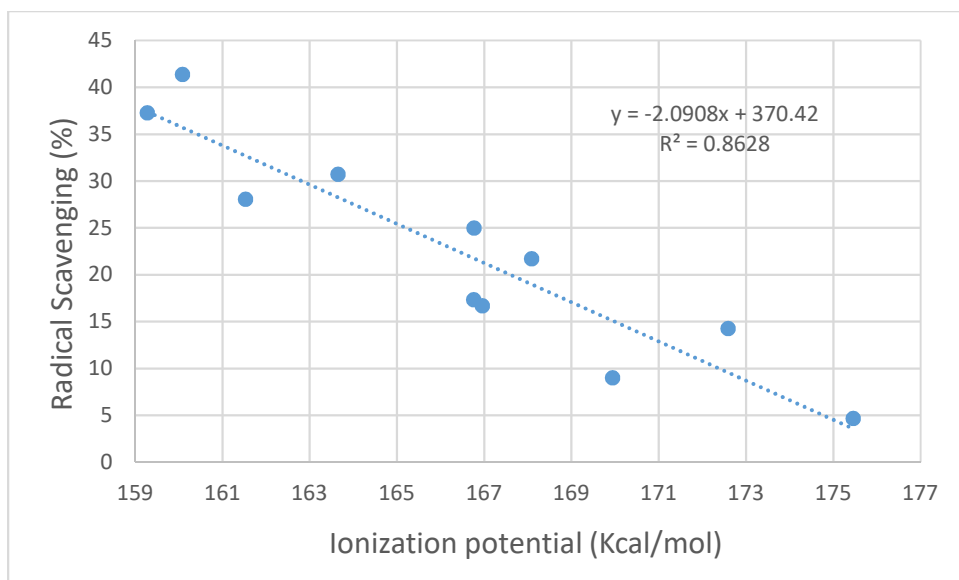


Fig. 58: Effect of ionization potential (IP) of the anilines on their experimental radical scavenging activity with the compounds **70** and **76** removed.

Activity vs. proton affinity (PA) plots can be used to determine the likelihood of a compound scavenging the radical species through the SPLET mechanism<sup>286</sup>. Elevated proton affinity values suggest that the molecule may undergo heterolytic cleavage and release an H<sup>+</sup> to solution (first step of SPLET mechanism)<sup>299</sup>. In Fig. 59 the data show that anilines have proton affinity values higher than 200 kcal/mol and as the proton affinity increases the free radical scavenging activity also increases. The data suggest that anilines do not operate solely under one mechanism rather, they interact with radicals through a variety of pathways, likely SET and SPLET.

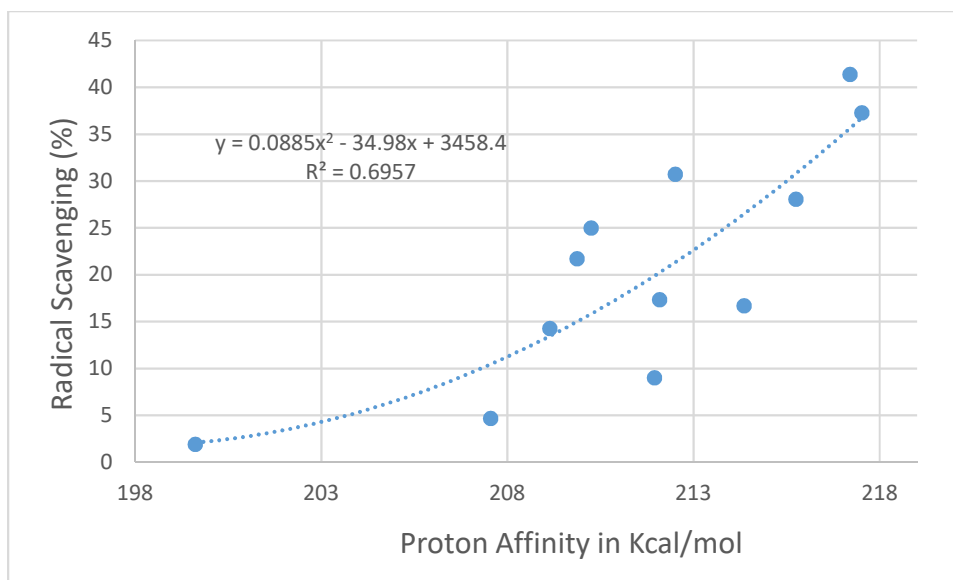


Fig. 59: Effect of proton affinity (PA) of anilines on the ABTS radical scavenging activity with the compound **76** removed.

Hammett constants ( $\sigma$ ) were investigated to identify possible inductive or resonance effects on the free radical scavenging activity of the anilines<sup>247</sup>. Using compounds with a similar backbone that have varying substituents allows us to investigate the effects the substituents may have on the overall electron density of the compound and ultimately investigate the stability of the spent antioxidant<sup>286</sup>. The substituents in both the *meta* and *para* positions in the phenols are mostly other -OH groups, so the data collected for phenols does not provide much useful information. The data collected from anilines shows a more interesting trend. Fig. 60 exhibits a linear correlation between the *para* Hammett constants and the ABTS radical scavenging activity suggesting that electron donating substituents such as ethyl and propyl increase that free radical scavenging activity of the anilines. A trend does not develop with the *meta* Hammett constants.

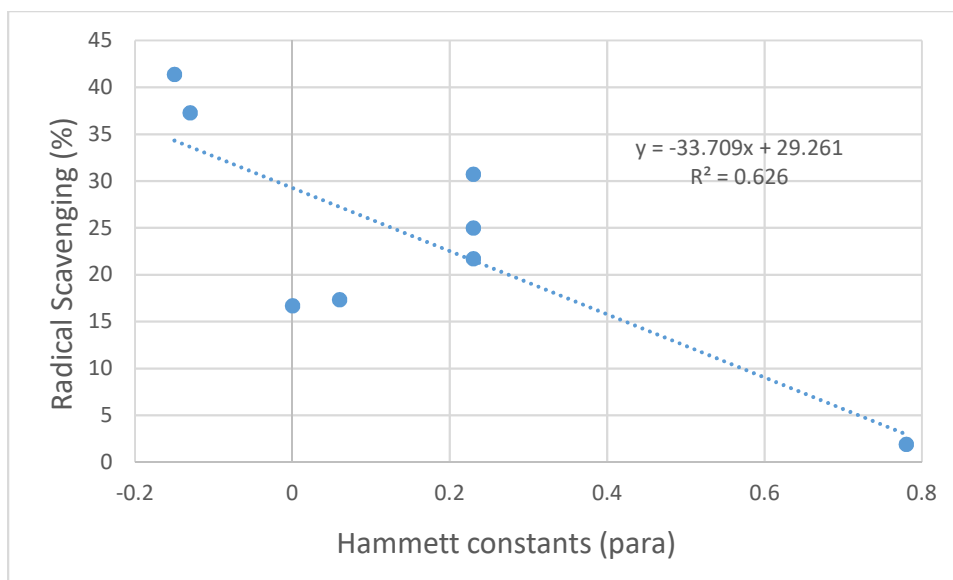


Fig. 60: Radical scavenging of anilines as a function of their Hammett constants (*para*) with compound **76** removed.

Electron withdrawing groups such as  $-CF_3$  and  $-NO_2$  have had a tremendous impact on the free radical scavenging activity of the anilines. The  $-NO_2$  containing compounds were removed from most data sets to provide a better estimate of the correlation of the ABTS activity with the theoretical properties of the molecule. Interestingly enough, the 2-amino-4-nitrophenol still retained a 43% radical scavenging activity in the ABTS assay. This is most likely due to the presence of the  $-OH$  on the phenyl ring. Summarizing the above analysis, the factors that appeared to have meaningful effect on the ABTS radical scavenging activity are tabulated in Tables 14 and 15.

Table 14: Major properties of phenols that the show considerable fit with the experimental ABTS radical scavenging data.

Parameter	Function	Fit (R <sup>2</sup> value)	Note
HOMO energy	$y = 214296x^2 + 97478x + 11103$	0.902	mono-phenols
HOMO energy	$y = 154028x^2 + 63636x + 6591.9$	0.812	dihydroxy compounds
Band gap	$y = 59.255x - 291.33$	0.964	mono-phenols
Band gap	$y = -29.274x^2 - 330.45x - 852.15$	0.861	dihydroxy compounds
Bond dissociation energy (BDE)	$y = -9.5372x + 747.01$	0.737	

Table 15: Major properties of anilines that the show considerable fit with the experimental ABTS radical scavenging data.

Parameter	Function	Fit (R <sup>2</sup> value)	Note
Dipole moment	$y = -7.8149x + 44.873$	0.935	
HOMO energy	$y = 26859x^2 + 12248x + 1398.4$	0.744	
Band gap	$y = -317.9x^2 - 3563.2x - 9941.1$	0.762	
Bond dissociation energy (BDE)	$y = 2E+18e^{-0.495x}$	0.730	
Ionization potential (IP)	$y = 2.0908x + 370.42$	0.863	
Proton affinity (PA)	$y = 0.0885x^2 - 34.98x + 3458.4$	0.696	
Hammett constants ( $\sigma$ )	$y = 33.709x + 29.261$	0.626	$\sigma_{para}$ only

It appears that while the phenols and anilines used do not form a unified model set that result in coherent picture, analyzing them separately yields valuable information. HOMO, band gap and bond dissociation energy data are of high importance to determine the radical scavenging activity of both groups. Interestingly, these are the only parameters that seem to contribute to the activity of phenols. During the analysis, it was found, that even monophenols and dihydroxy derivatives cannot/should not be handled together.

When evaluated separately, these two groups resulted in meaningful fits between the experimental data and calculated HOMO and band gap energies. Based on the data obtained phenols appear to act predominantly via HAT mechanism. The experimental radical scavenging data of aniline derivatives reveal strong free radical scavenging properties that are competitive with those of phenols. The theoretical analysis of their properties, however, indicates that while anilines also act via HAT mechanism, their mode of action is somewhat more complicated. Reasonable fits with ionization potential and proton affinity values suggest that these compounds at least partially scavenge radicals via the SET and SPLET mechanisms as well. This complex mode of action could contribute to the versatility of aniline-NH-containing natural and synthetic antioxidants and make them novel candidates in antioxidant-based therapeutic applications.

## CHAPTER 9

### HYDRAZONES AS MULTI-FUNCTIONAL CK2 ENZYME INHIBITORS

As described above (Chapter 7) among other effects, hydrazones have free radical scavenging activity and cholinesterase enzyme inhibition. The SAR relationship study (Chapter 7) was the phase 1 of our development of multi-functional CK2 enzyme inhibitors. Fluorinated hydrazone derivatives (phase 2) were designed and synthesized based on preliminary CK2 enzyme inhibition data obtained from the phase 1 compounds to further investigate the activity of hydrazones as a new class of CK2 inhibitors. The following work aims to introduce this previously unexplored class of compounds as potential multi-functional inhibitors of CK2. At this time this work is still in progress and here I will focus on the relevant antioxidant data.

#### **9.1 Introduction**

Casein kinase II (CK2) is a ubiquitous serine/threonine kinase, which is known to influence cell survival, growth and death<sup>191-193</sup>. The expression of CK2 can suppress apoptosis leading to cell survival and is elevated in almost all types of cancer<sup>192,193,195</sup>. A defining factor of CK2 inhibitors is the presence of a hydroxyl, nitro, amino, or halogen substituents, which interact at the ATP binding site or through other possible modes of inhibition<sup>216</sup>. Examples of known inhibitors of CK2 can be seen in Figs. 6 and 7 in Chapter 2.

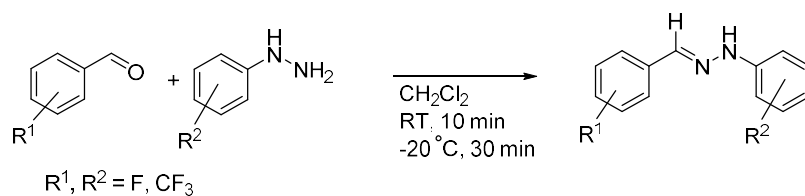
To further improve the pharmacokinetic properties of drug candidates they should also have features that allow for better absorption and distribution within the body. Addition of fluorine has been shown to enhance the ADME properties of drug candidates<sup>300,301</sup>.

Single fluorine incorporation or the replacement of a methyl group with a trifluoromethyl group is commonly used to improve metabolic stability, bioavailability and protein–ligand interactions<sup>300,301</sup>. The introduction of fluorine to a molecule has been shown to decrease the pK<sub>a</sub> of a compound, due to fluorine’s electronegativity<sup>300,301</sup>. It also increases the bioavailability of the compounds in the body<sup>300,301</sup>. Aromatic fluorination has also been shown to increase the lipophilicity of drug candidates<sup>300,301</sup>. Fluorine-carbon bonds are highly stable and improve the overall metabolic stability and resist oxidation by cytochrome P450 enzymes reducing the clearance rates of compounds in the body further increasing their distribution times<sup>300</sup>. As such there has been interest in adding or replacing parts of existing and developmental drug candidates with F atom or CF<sub>3</sub> group<sup>301,302</sup>. Additionally, the inclusion of radioactive fluorine in compounds also allows for direct imaging of the compound’s distribution in the body through in vivo fluorine magnetic resonance<sup>301,303</sup>. This is essential for understanding the distribution, namely mapping where specific drug candidates are being delivered in the body.

## 9.2 Synthesis

The fluorinated hydrazone derivatives (phase 2) were synthesized in the Bela Török lab at the University of Massachusetts Boston by the following general procedure (Scheme 6). General synthesis of the hydrazones was carried out in a 25-mL Erlenmeyer flask; 1 mmol of benzaldehyde and 1 mmol of phenyl hydrazine were dissolved in 2 ml of dichloromethane. The reaction mixture was stirred for 10 min at room temperature, then it was cooled to –20 °C for 30 min to crystallize the products. The crystalline product was filtered and air-dried for 12 h. The purity was verified using GC-MS and NMR.

Impurities were removed by recrystallization or preparative TLC to yield at least 98 % purity product.

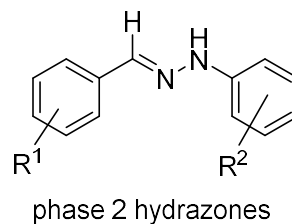
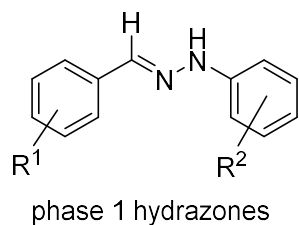


Scheme 6. Synthesis of the fluorinated hydrazone derivatives.

### 9.3 Results

Sixteen hydrazone derivatives were developed based on CK2 enzyme inhibition findings from the phase 1 compounds (Chapter 7) conducted by the Baier lab at the John Paul II Catholic University, Lublin. Both phase 1 and phase 2 hydrazones can be seen in Figs. 61 and 62. To assess their multi-functional capabilities phase 2 derivatives were screened for radical scavenging activity. Based on the experimental data from the phase 1 assays and feedback from the collaborator the design of extensively halogenated derivatives was carried out. Since C-Br, C-Cl bonds are easier to cleave and thus produce toxic byproducts we focused on organofluorine compounds. The extensive fluorination is believed to foster a better small molecule-enzyme interaction; hence stronger inhibition of the enzyme activity.





<u>compound</u>	<u>R<sup>1</sup></u>	<u>R<sup>2</sup></u>	<u>compound</u>	<u>R<sup>1</sup></u>	<u>R<sup>2</sup></u>
<b>31</b>	3-Cl	H	<b>78</b>	4-N(Me) <sub>2</sub>	4-CF <sub>3</sub>
<b>32</b>	4-CF <sub>3</sub>	H	<b>79</b>	4-N(Me) <sub>2</sub>	3,4- di(CF <sub>3</sub> )
<b>33</b>	2-Br	4-NO <sub>2</sub>	<b>80</b>	4-N(Me) <sub>2</sub>	2, 3, 4, 5, 6 - penta F
<b>34</b>	3,4- di(OMe)	2-CF <sub>3</sub>	<b>81</b>	2-OH 4-OMe	4-CF <sub>3</sub>
<b>35</b>	2-Br	2-CF <sub>3</sub>	<b>82</b>	2-OH 4-OMe	3,4- di(F)
<b>36</b>	4-CF <sub>3</sub>	2-CF <sub>3</sub>	<b>83</b>	2-OH 4-OMe	2, 3, 4, 5, 6 - penta F
<b>37</b>	2-OH 4-OMe	2-CF <sub>3</sub>	<b>84</b>	2, 3, 4, 5, 6 - penta F	2-CF <sub>3</sub>
<b>38</b>	2-OH 4-OMe	3-CF <sub>3</sub>	<b>85</b>	2, 3, 4, 5, 6 - penta F	3-CF <sub>3</sub>
<b>39</b>	3-OH	H	<b>86</b>	2, 3, 4, 5, 6 - penta F	4-CF <sub>3</sub>
<b>40</b>	4-N(Me) <sub>2</sub>	3-CF <sub>3</sub>	<b>87</b>	2, 3, 4, 5, 6 - penta F	3,4- di(CF <sub>3</sub> )
<b>41</b>	4-NO <sub>2</sub>	3-CF <sub>3</sub>	<b>88</b>	2, 3, 4, 5, 6 - penta F	2, 3, 4, 5, 6 - penta F
<b>42</b>	4-N(Me) <sub>2</sub>	2-CF <sub>3</sub>			

Fig. 61: Phase 1 compounds **31 - 42** are hydrazones identified with those from the SAR study on radical scavenging activity from Chapter 7. Phase 2 compounds **78 - 88** are heavily fluorinated hydrazones with varying substituents.

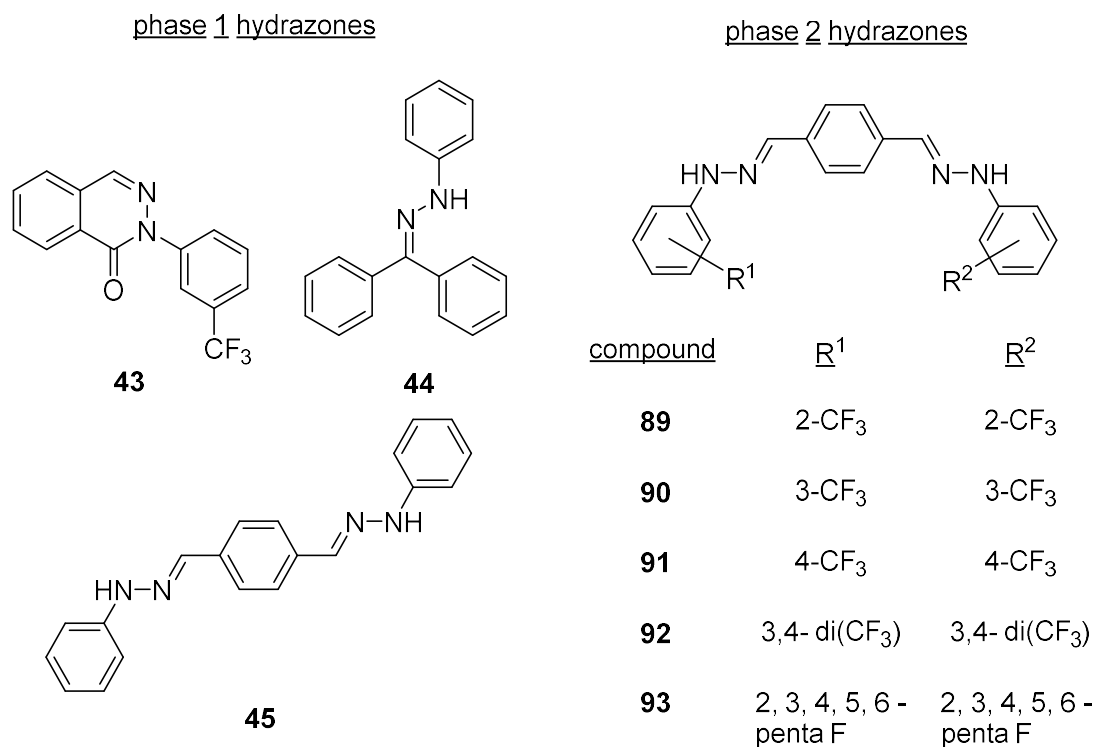


Fig. 62: Phase 1 compounds **43** – **45** are hydrazones identified with those from the SAR study on radical scavenging activity from Chapter 7. Phase 2 compounds **89** – **93** are double hydrazone derivatives which have been heavily fluorinated.

### 9.3.1 Free radical scavenging activity (ABTS, DPPH, ORAC)

From Chapter 7 the radical scavenging activity of the phase 1 hydrazones was already determined and described. It was observed that these hydrazones were most active against the smallest peroxy type radical used in the ORAC assay surpassing the activity of the controls with activity values ranging from 50 to 88% for all compounds except **43**, the cyclized hydrazone which lacks an N-H bond. Phase 2 hydrazone derivatives **78** - **93** are heavily fluorinated, with the idea that the increased halogenation may provide better interaction of these compounds within the active site of the CK2 holoenzyme. The radical

scavenging feature of the compounds has been assessed by the DPPH, ABTS and ORAC assays. The data are tabulated in Table 16. Many compounds showed comparable or better activity to the reference compounds ascorbic acid and Trolox in all three assays. Unlike the phase 1 hydrazones the data for compounds **78 – 93** are not as uniform and may provide more insights into the radical scavenging activity of these hydrazones.

Table 16: Free radical scavenging activity of the phase 2 hydrazone derivatives against the DPPH<sup>a</sup>, ABTS<sup>b</sup> and peroxy radicals<sup>c</sup>. The values here represent the mean  $\pm$  the standard deviation of the data (n = 2–6).

compound	ABTS radical scavenging (%)	DPPH radical scavenging (%)	ORAC radical scavenging (%)
<b>ascorbic acid</b>	24 $\pm$ 1	30 $\pm$ 8	35 $\pm$ 8
<b>resveratrol</b>	90 $\pm$ 1	43 $\pm$ 7	98 $\pm$ 2
<b>Trolox</b>	19 $\pm$ 2	46 $\pm$ 7	55 $\pm$ 3
<b>78</b>	34 $\pm$ 4	44 $\pm$ 8	88 $\pm$ 5
<b>79</b>	33 $\pm$ 3	42 $\pm$ 5	93 $\pm$ 4
<b>80</b>	34 $\pm$ 1	38 $\pm$ 7	94 $\pm$ 4
<b>81</b>	40 $\pm$ 5	51 $\pm$ 6	83 $\pm$ 2
<b>82</b>	31 $\pm$ 1	40 $\pm$ 6	53 $\pm$ 2
<b>83</b>	36 $\pm$ 6	39 $\pm$ 6	49 $\pm$ 9
<b>84</b>	35 $\pm$ 9	23 $\pm$ 8	32 $\pm$ 1
<b>85</b>	34 $\pm$ 5	28 $\pm$ 9	21 $\pm$ 4
<b>86</b>	53 $\pm$ 2	25 $\pm$ 10	62 $\pm$ 3
<b>87</b>	50 $\pm$ 1	19 $\pm$ 10	45 $\pm$ 1
<b>88</b>	53 $\pm$ 4	27 $\pm$ 9	12 $\pm$ 13
<b>89</b>	27 $\pm$ 2	29 $\pm$ 8	32 $\pm$ 11
<b>90</b>	30 $\pm$ 4	45 $\pm$ 5	36 $\pm$ 6
<b>91</b>	36 $\pm$ 1	41 $\pm$ 9	59 $\pm$ 5
<b>92</b>	23 $\pm$ 1	30 $\pm$ 6	17 $\pm$ 5
<b>93</b>	34 $\pm$ 2	40 $\pm$ 8	28 $\pm$ 1

a: Calculation for DPPH radical scavenging activity can be seen in Chapter 3.2.1. Eq. 1 b: Calculation for ABTS radical scavenging activity can be seen in Chapter 3.2.2. Eq. 1. c: Calculation for ORAC radical scavenging activity can be seen in Chapter 3.2.3. Eqs. 2 and 3.

The phase 2 hydrazone derivatives **78 - 93** all had activity in the DPPH assay with **78, 79, 90, 91** and **93** showing approximately the same radical scavenging activity as the three controls. The fluorinated hydrazones (**78 – 93**) all had radical scavenging activity, in the ABTS assay as well, higher than that of ascorbic acid and Trolox except for **92**, with derivatives **86 – 88** all above 50%. In the ORAC assay, compounds **78 – 93**, all exhibited radical scavenging activity greater than 10% with compounds **78 – 81** all at above 80% free radical scavenging and compounds **82, 83, 87** and **91** all having radical scavenging activity higher than 45%.

### **9.3.2 CK2 enzyme inhibition**

The phase 1 hydrazones were investigated as CK2 holoenzyme inhibitors in an effort to determine their viability as potential multi-target therapeutic agents for the treatment of cancer. Currently, only the monomeric CK2 $\alpha$  and CK2 $\alpha'$  subunits have been investigated for enzyme inhibition with hydrazones **31 – 45**. From these enzyme studies IC<sub>50</sub> values were determined for the active compounds. None of the investigated hydrazones had any inhibitory effect on the monomeric CK2 $\alpha$ , however they exhibited inhibitory activity, with IC<sub>50</sub> values from 1 to 15  $\mu$ M, for compounds **31, 36, 37, 38, 40, 42** and **45** on monomeric CK2 $\alpha'$ . This suggests that these hydrazones are selective inhibitors for the CK2 $\alpha'$  subunit. The link between effective halogenated inhibitors and CK2 $\alpha'$  inhibition led to the development of the fluorinated hydrazones in phase 2. Studies are still being conducted on the CK2 $\alpha_2\beta_2$  and CK2 $\alpha'_2\beta_2$  holoenzyme structures. The phase 1 hydrazone derivatives with CK2 $\alpha'$  inhibition also have moderate antioxidant activity in all three of the antioxidant assays, except for compound **36** which has an ABTS scavenging activity

of 8%. This suggests that hydrazones could be investigated as multi-functional candidates.

#### 9.4 Discussion

Hydrazone derivatives were selected in an effort to develop multi-functional drug candidates for the inhibition of the CK2 holoenzyme. Based on my earlier work, 15 hydrazone compounds (discussed in Chapter 7) was analyzed through a SAR study to correlate the physicochemical properties of the compounds to their radical scavenging activity. These derivatives **31 – 45**, showed excellent activity in the ORAC assay with radical scavenging values ranging from 50 to 88% for all compounds except **43**, a cyclized hydrazone. Most of the hydrazones in phase 1 showed moderate activity in the DPPH and ABTS assays with radical scavenging activity for most compounds lower than 30% in both assays. The structure of phase 2 hydrazone derivatives were designed with one goal; to increase the amount of halogen substituents, mainly F, on the aryl rings. The reasoning for this is two-fold: halogenated hydrazones from phase 1 showed lower IC<sub>50</sub> values than others suggesting that halogenation is important for the hydrazone's ability to inhibit CK2 $\alpha'$  and to improve the ADME properties<sup>301</sup> of the compounds. While these compounds have yet to be assessed for CK2 inhibition, their radical scavenging activity was determined through the ABTS, DPPH and ORAC assays.

The phase 2 hydrazones exhibited different radical scavenging profiles than their counterparts in phase 1. The ORAC scavenging activity had significantly decreased with only the 4-N, N dimethyl compounds (**78 – 81**) showing activity higher than 80%. At the same time, the ABTS and DPPH activity profiles of these compounds were also enhanced with most compounds showing higher than 30% activity in the ABTS assay (with the

exception of compounds **89** and **92**) and higher than 25% in the DPPH assay (with the exception of compounds **84** and **87**). The addition of the electron withdrawing fluorine groups has altered the radical scavenging activity of these compounds. We can see by looking at compounds **84** to **88** (which have fluorine substituents in every available position on at least one of the aromatic rings of the hydrazone) that in general the antioxidant activity decreases. However, compound **86** still seems to retain some activity, likely due to the 4-CF<sub>3</sub> group present in the R<sup>2</sup> position which also seems to provide activity to compounds **39**, **42** and **91**. This data suggests that hydrazones have potential as multi-functional therapeutics functioning as free radical scavengers, CK2 $\alpha$ ' inhibitors and as potential AD therapeutic agents (discussed in Chapter 7). This work is still in progress and after the full profile of the hydrazones as CK2 inhibitors is completed more work still needs to be done.

CHAPTER 10  
METHOD DEVELOPMENT OF AMYLOID FIBRIL FORMATION FOR  
EDUCATION AND RESEARCH

### **10.1 Introduction**

Amyloidogenic structures have been identified in the misfolded states of many different proteins such as lysozyme, insulin, A $\beta$ ,  $\alpha$ -synuclein and many others<sup>304</sup>. These structures are rich in tightly packed  $\beta$ -sheet formations held together by hydrogen bonding between the backbone N-H group on one strand to the backbone C=O group on the adjacent strand, as well as other intramolecular forces such as hydrophobic interactions<sup>305</sup>. The nature of the interactions explains why so many different protein structures can adopt the amyloid fibril conformation. Amyloid fibrils have been implicated in numerous neurodegenerative diseases such as AD, Parkinson's disease and Creutzfeldt-Jakob disease just to name a few. The formation of amyloid fibrils from native protein folds is not completely understood, yet it is commonly accepted that the process is a nucleation driven event and when one protein adopts the amyloidogenic fold, it can re-fold other native proteins into amyloid structures<sup>229</sup>. The amyloid structures will aggregate as more are formed and begin to oligomerize and continue aggregating forming the insoluble fibrillar structure.

In an effort to understand and inhibit the process of amyloid fibril formation, research has investigated inhibitors of fibril formation and disassembly agents to reduce the concentration of fibrillar protein deposits. To investigate the inhibition of fibril formation or disassembly, we must first generate amyloid fibrils in vitro. Although strongly protein



dependent, traditionally, the methods for fibril formations prioritized acidic conditions, preferably pH 1.5-2.5 and elevated temperatures which generate fibrillar species without the need for sample agitation<sup>306,307</sup>. Acidic and elevated temperature conditions help break apart the tertiary and secondary structure of a protein without denaturing the sample<sup>228</sup>. The protein is then free to re-arrange to a new lower energy conformation, which, for these proteins, results in the formation of amyloid fibrils. While many publications on amyloid fibril disassembly compounds rely on these in vitro generated protein structures, very little is known about how they compare to in vivo fibril species. It is well documented that amyloid fibril formation can result in slightly different structures depending on growth methodology<sup>304</sup>. Several studies have investigated generating amyloid fibrils in concentrated ethanol solutions<sup>308</sup> and under physiological pH with shaking<sup>239</sup>. However, many of these reports are not consistent, with different conditions reported between labs, to provide reproducible fibril formation. The fibril formation, when performed as an assay for finding suitable inhibitors of the process for drug development, should have parameters that mimic physiological conditions. Acidic and physiological growth conditions may have different impacts on fibril formation and drug stability. This section aims to investigate several methods for growing amyloid fibril species of lysozyme<sup>309,310</sup> and insulin and comparing the fibril species generated to their counterparts generated in acidic conditions. Specifically, the lysozyme project looks to investigate fibril formation conditions that could easily be replicated in a teaching lab setting for students to work with an AFM, while the insulin project aims to develop a reliable assay for fibril development under physiological pH for use in future drug development.

## **10.2 Results**

### **10.2.1 Lysozyme**

In order to investigate lysozyme amyloid fibril formation for the development of an upper level biochemistry lab, lysozyme fibrils were grown in various concentrations of (50% to 90%) ethanol. The goal was to generate lysozyme fibrils reproducibly and in a way that fits the time-frame and schedule of the laboratory exercises. Samples (1.0 mL) were incubated at room temperature with constant agitation with a magnetic stir bar. The samples were monitored for amyloid fibril formation for one and two weeks through ThT fluorescence intensity and AFM. The amount of fibril formation increased with the percentage of ethanol in the solution according to the ThT data for seven and fourteen days of incubation (Tables 17 and 18).

Table 17: ThT intensity and AFM dimension values of lysozyme fibrils grown in concentrated ethanol solutions after 7 days.

conditions	ThT fluorescence (cps)	AFM fibril height (nm)	AFM fibril length (nm)	AFM fibril diameter (nm)
<b>50% ethanol</b>	254.6	1.450	853	38
<b>70% ethanol</b>	319.5	4.010	1263	41
<b>80% ethanol</b>	436.3	18.320	2166	99 - 506
<b>90% ethanol</b>	623.3	12.183	2876	116 - 271

Table 18: ThT intensity and AFM dimension values of lysozyme fibrils grown in concentrated ethanol solutions after 14 days.

conditions	ThT fluorescence (cps)	AFM fibril height (nm)	AFM fibril length (nm)	AFM fibril diameter (nm)
<b>50% ethanol</b>	491.7	3.405	1578	105
<b>70% ethanol</b>	417.8	11.105	2971	67
<b>80% ethanol</b>	1057.3	8.043	538	36
<b>90% ethanol</b>	593.3	9.383	679	41

However, the AFM results suggest that the percentage of ethanol in the solution has a big impact on the size of the amyloid fibrils, not just their quantity. Ethanol at an 80% concentration was identified as the most consistent and simplistic procedure to generate amyloid fibrils by this method.

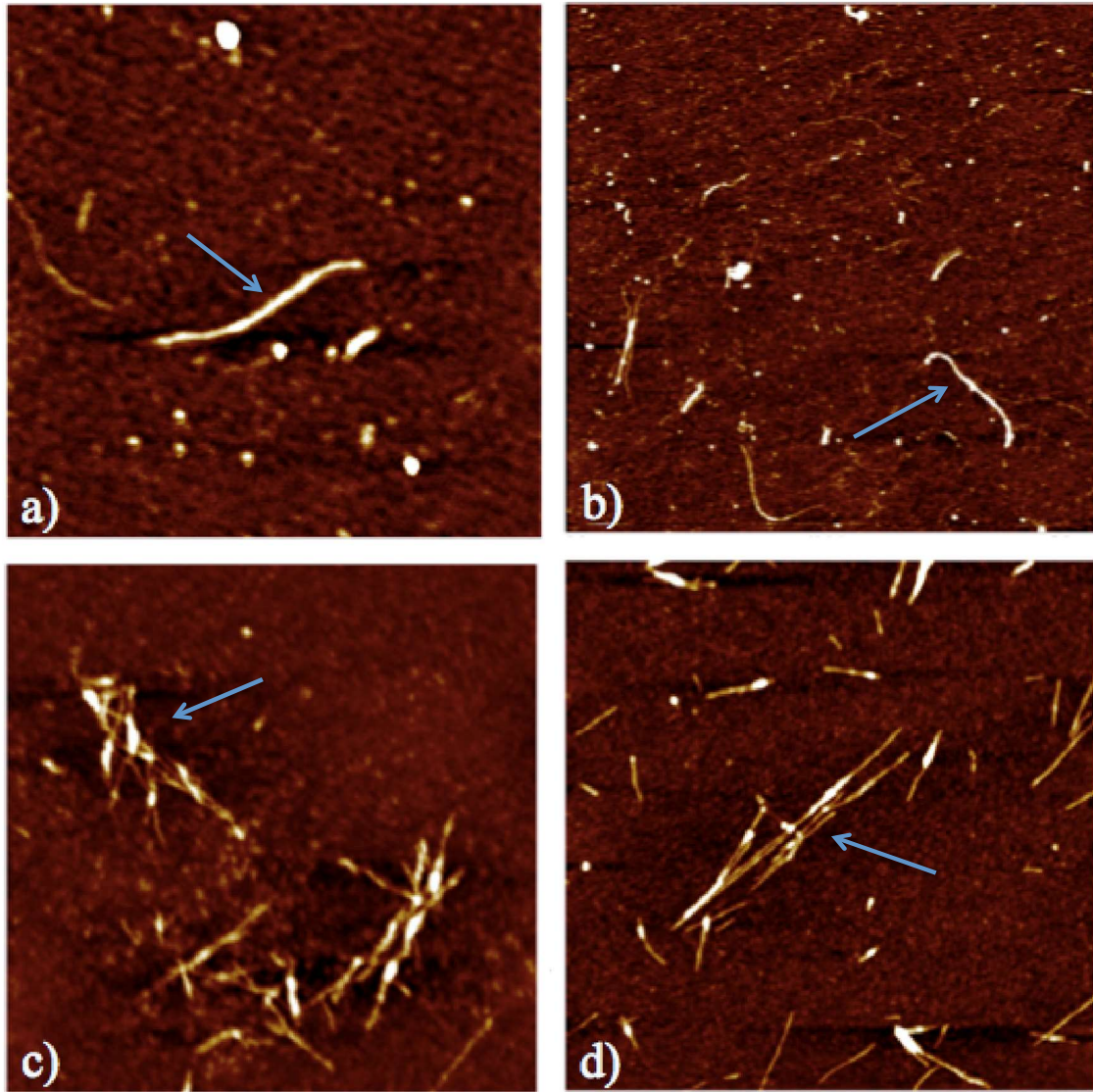


Fig. 63: Representative AFM images of prepared lysozyme samples after 7 days of incubation. a)  $2\ \mu\text{m} \times 2\ \mu\text{m}$  scan of lysozyme fibril formed under 50% ethanol concentration b)  $5\ \mu\text{m} \times 5\ \mu\text{m}$  scan of lysozyme fibril formed under 70% ethanol concentration c)  $5\ \mu\text{m} \times 5\ \mu\text{m}$  scan of lysozyme fibrils formed under 80% ethanol concentration d)  $5\ \mu\text{m} \times 5\ \mu\text{m}$  scan of lysozyme fibrils formed under 90% ethanol concentration.

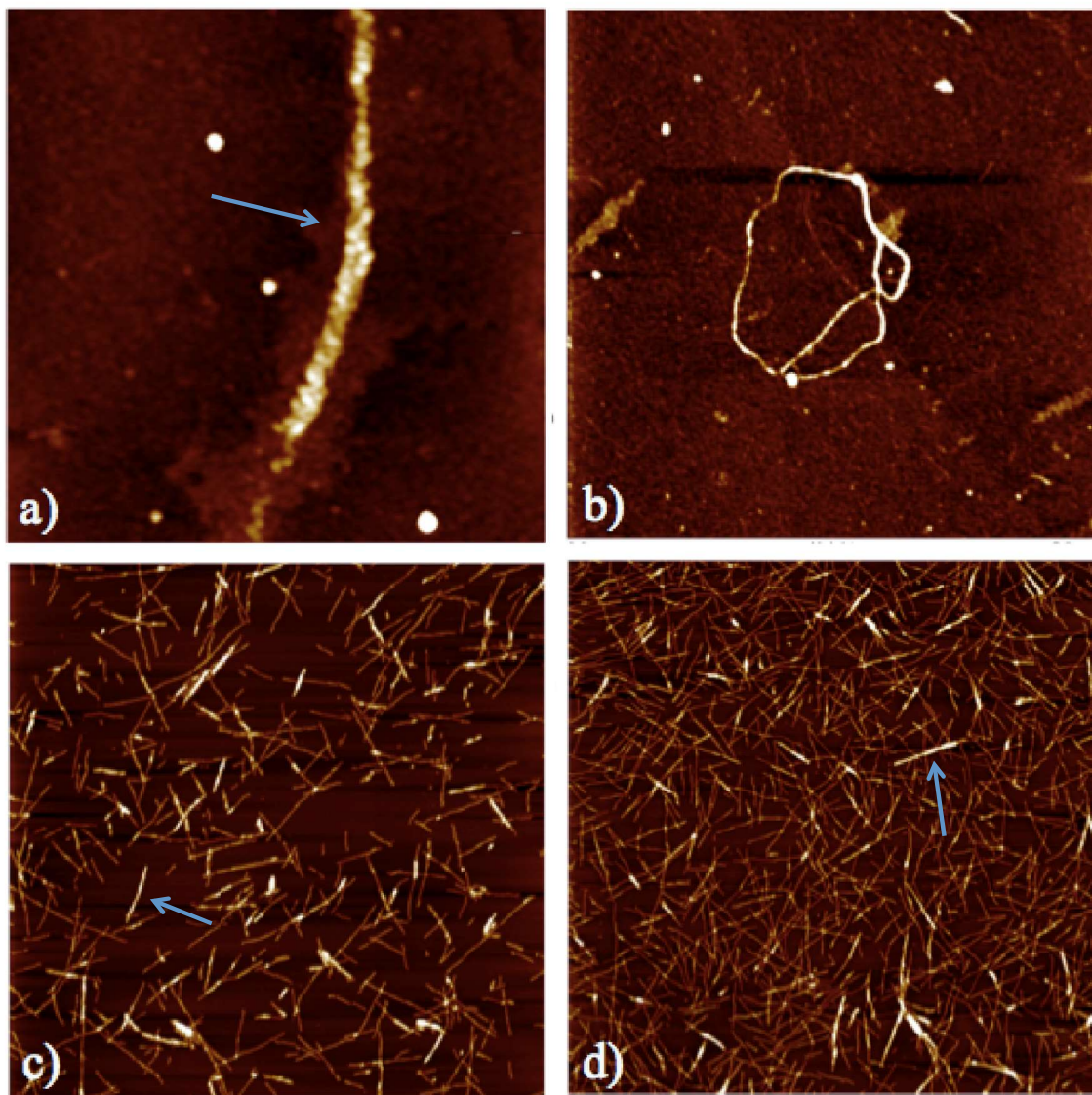


Fig. 64: Representative AFM images of prepared lysozyme samples after 14 days of incubation. a)  $2\mu\text{m} \times 2\mu\text{m}$  scan of a lysozyme fibril formed under 50% ethanol concentration b)  $2\mu\text{m} \times 2\mu\text{m}$  scan of a lysozyme fibril formed under 70% ethanol concentration c)  $5\mu\text{m} \times 5\mu\text{m}$  scan of lysozyme fibrils formed under 80% ethanol concentration d)  $5\mu\text{m} \times 5\mu\text{m}$  scan of lysozyme fibrils formed under 90% ethanol concentration

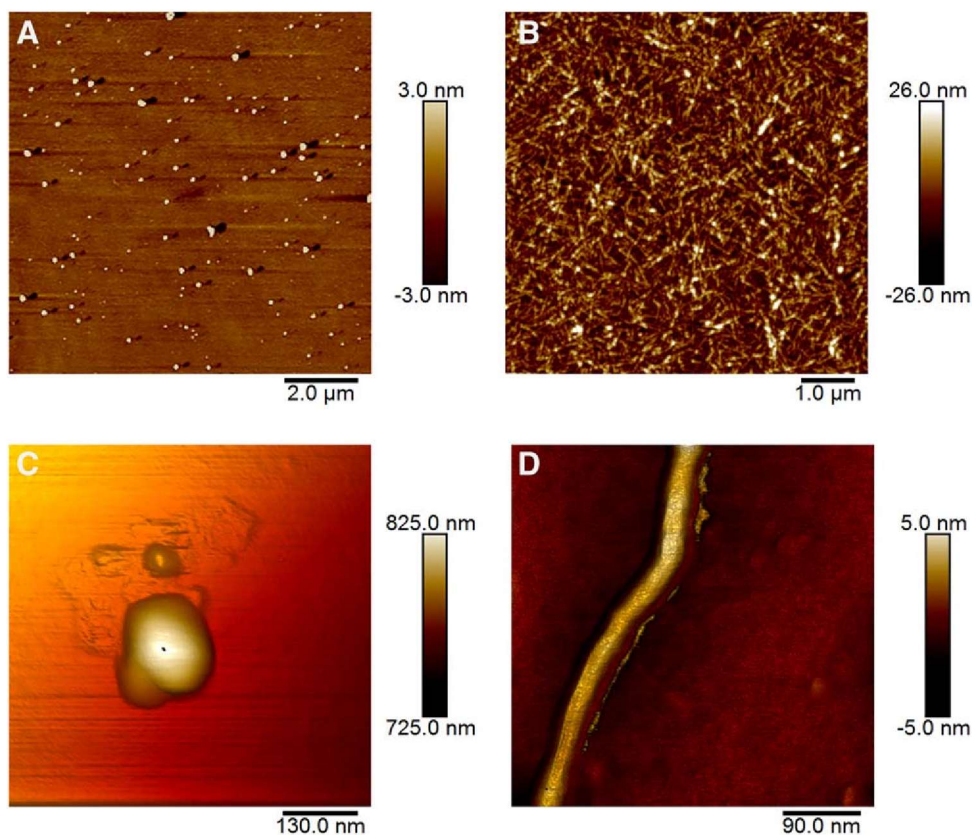


Fig. 65: Representative AFM images of denatured lysozyme samples (A: 256 x 256 pixel resolution, C: 512 x 512 pixel resolution) compared to the 80% ethanol sample after 14 days of incubation (B: 256 x 256 pixel resolution, D: 512 x 512 pixel resolution).

A control of denatured lysozyme was used as a comparison to show that the fibrillar species identified were unique and not just denatured protein.

### 10.2.2 Insulin

Insulin fibrils are typically grown under acidic (pH 1.6) and high temperature (70 °C) conditions. However, the results of fibril formation inhibition and disassembly studies using acidic conditions may not represent amyloid fibril species generated under physiological conditions. In addition, the classical form of the inhibitors/disassembly agents could be altered under strong acidic conditions (e.g. protonation, decomposition, etc.). To identify variations in insulin amyloid fibril formation, the protein was processed through the following conditions: acidic (1.6 pH and 70 °C)<sup>240</sup>, physiological (PBS and 37 °C), physiological with shaking (PBS and 37 °C at 300 rpm), physiological with shaking and high temperature (PBS and 70 °C at 300 rpm) and physiological pH and temperature containing a Teflon bead with shaking (PBS and 37 °C at 700 rpm). The data are tabulated in Table 19.

Table 19: ThT intensity values of insulin fibrils grown in various conditions. The ThT values were followed for at most four days.

conditions	pH	temperature °C	RPM	time (days)	ThT fluorescence (cps)
20% acetic acid	1.6	70	300	4	391.5
PBS	7.4	37	300	2	1.843
PBS	7.4	70	300	3	4.266
PBS w/ teflon ball	7.4	37	700	3	53.63

The results of the ThT studies for the insulin fibril formation under different growth conditions can be seen in Table 19 and representative ThT spectra can be seen in appendix - A. The results from these experiments concluded that under physiological pH

conditions insulin forms fibrillar species in the presence of a nucleation agent, such as a Teflon bead. The acidic procedure provided the highest fibril content seen in this study. However, as the goal in this case was to investigate optimal conditions for fibril inhibition studies, the physiological pH conditions are promising. Under these conditions, amyloid fibril formation did not occur unless there was a nucleation agent present in the sample (such as a bead, or fibril seeding). AFM images for the acidic and physiological pH sample with the Teflon ball can be seen in Figs. 66 and 67.

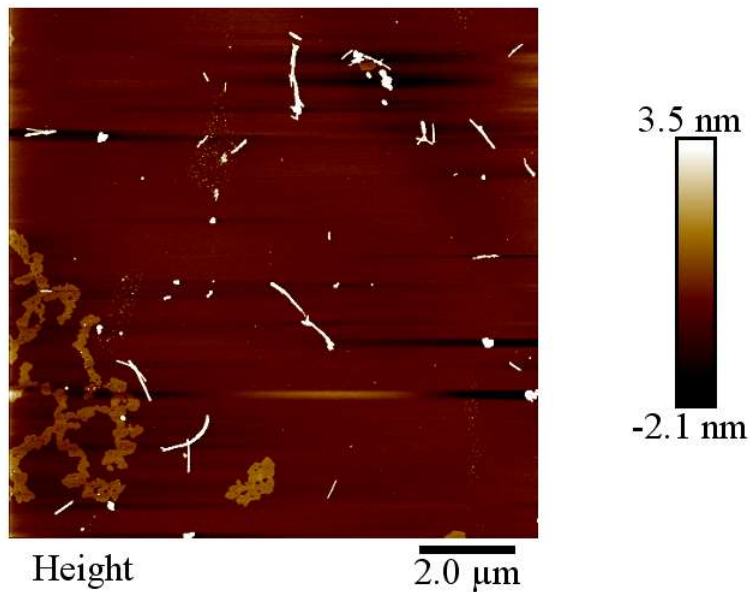


Fig. 66: Representative AFM image of prepared insulin fibrils after 3 days of incubation in PBS and 37 °C with shaking at 700 rpm and the addition of a 1/8 in. diameter Teflon bead.



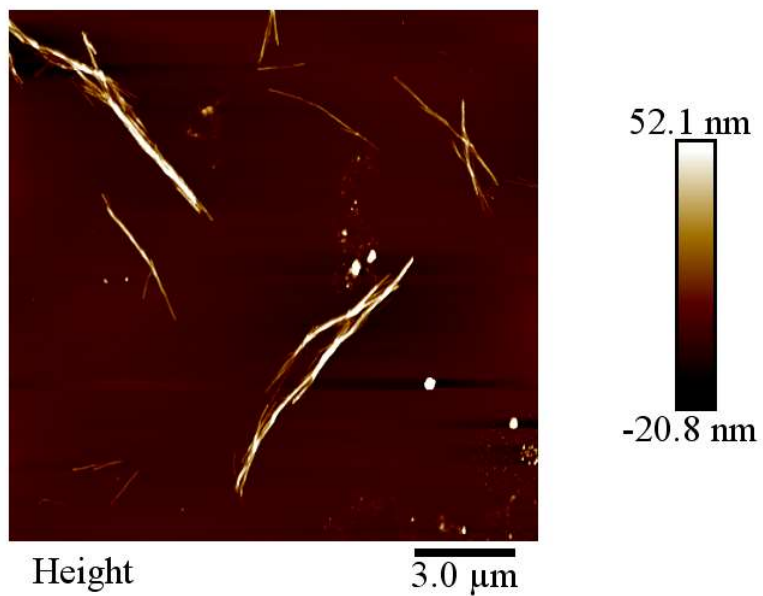


Fig. 67: Representative AFM image of prepared insulin fibrils after 4 days of incubation under acidic conditions and 70 °C with shaking at 300 rpm.

### 10.3 Discussion

#### *Lysozyme*

The ThT intensities were recorded after one week for the lysozyme samples grown in ethanol solutions. The fluorescence intensity and AFM dimensions of the lysozyme fibril samples increased as the concentrations of ethanol increased, as can be seen in Tables 17 and 18, suggesting that amyloid fibril formation was occurring quicker in the solutions with higher concentrations of ethanol as a solvent. This was corroborated by the AFM data seen in Fig. 63. The generation of amyloid fibrils has increased for lysozyme sample preparation in the 80% and 90% ethanol (Fig. 64). Readings of ThT fluorescence were collected at week two to determine if the amyloid fibril growth continued for all samples. The data recorded after fourteen days of incubation of lysozyme in concentrated ethanol solutions further exemplifies the fact that lysozyme forms fibrils under these conditions. The fluorescence intensity and AFM dimensions of the lysozyme fibril samples increased from the previous week for all samples except the 90% ethanol as can be seen in Table 18 and Fig. 64. It was observed that the 80% and 90% ethanol AFM images, seen in Fig. 64, look very similar and yet the ThT intensities are drastically different. This is likely because the 90% ethanol solution has a greater density of amyloid fibrils than what can be seen in the 80% ethanol sample. This can cause scattering of the fluorescence light produced by exciting the bound ThT due to the large number of fibril species in solution, providing a lower fluorescence intensity than what would be expected. The lysozyme fibril formation in 80% ethanol was concluded to be the best representation of fibril growth for this study. Heat denatured lysozyme samples were used as a control to ensure that the species present in the AFM images was not just denatured lysozyme. As can be

seen in Fig. 65, the heat denatured lysozyme does not resemble the ordered structures that can be seen for the fibrils formed in the concentrated ethanol solutions.

### *Insulin*

The insulin samples were prepared under different conditions. The aim of this work was to investigate and compare the growth of insulin amyloid fibrils under acidic and physiological conditions. The results from this experiment concluded that under physiological conditions insulin may not be able to form fibrillar species at 37 °C and at 70 °C it may denature. Insulin fibrils were readily formed after four days of incubation at 37 °C with shaking at 700 rpm under physiological pH conditions. The important factor that helped the growth of the amyloid fibrils was the addition of a nucleation agent, a 1/8 in. diameter Teflon bead. Examples of the fibril formation analyzed by AFM can be seen in Fig. 66. The acidic procedure also provided the highest fibril content seen in this study, but the fibril species were distinctly different than those identified in the physiological pH samples (Fig. 67).

## CHAPTER 11

### CONCLUSIONS

The above detailed description and analysis of the collected data allowed me to draw several major conclusions from my studies. The major findings of my work are as follows.

#### **11.1 $\beta$ -carbolines as multi-functional drug candidates**

We have identified  $\beta$ -carbolines as promising drug candidates for further development of multi-functional AD therapeutics. The most promising compound that could serve as lead for drug discovery would be compound **10**. Having 40% A $\beta$  fibril formation inhibition activity and an EC<sub>50</sub> value of 110  $\mu$ M, and oligomer formation inhibition activity of 58% highlights the compounds ability to not only inhibit the formation of A $\beta$  fibrils, but to prevent the buildup of the toxic oligomeric species as well. The selectivity for butyrylcholinesterase for all of the  $\beta$ -carbolines (IC<sub>50</sub> = 225  $\pm$  30 nM for compound **10**) coupled with the strong activity in scavenging of peroxy radicals suggests these compounds are excellent candidates for further multi-target drug development for AD.

#### **11.2 Hydrazide and nipecotic acid derivatives as multi-functional drug candidates**

I have contributed to a collaborative work on hydrazide and nipecotic acid derivatives investigated as cholinesterase inhibitors. These derivatives were identified through computer aided drug discovery<sup>19</sup>. The aim is to develop drugs based on the molecular interactions expected to occur at the active site of an enzyme so that the drug will bind efficiently and fit into the protein. Fourteen compounds were developed based on the docking studies, mimicking the electrostatic interactions of donepezil. While the

compounds did not retain significant activity in the in vitro assays, they were identified as potential radical scavenging compounds. Compounds **17**, **20** and **22** had the highest radical scavenging activity in the ORAC assay with scavenging values of 88%, 80% and 56%. Development of these compounds should be continued, with an emphasis on understanding why they were not functional inhibitors. The fact that they showed radical scavenging activity suggests that they may be useful in the development of multi-functional drug candidates.

### **11.3 SAR study of hydrazones as radical scavenging agents**

The results from the hydrazone radical scavenging SAR identifies clear and firm relationships between the structural and energetic features (BDE, ionization potential and logP) and their contribution to radical scavenging activity. Compound **43**, which possesses a structure with no N–H bond, uniformly did not exhibit any measurable effect highlighting the importance of the N-H bond for radical scavenging activity. The rest of the hydrazones were most active against the smallest peroxy radical used in the ORAC assay surpassing the activity of the controls with activity values ranging from 50 to 88%. The linear correlation of the ORAC ( $R^2=0.6505$ ) and DPPH ( $R^2=0.6081$ ) data with the BDE suggests the compounds react through the HAT mechanism, via homolytic bond cleavage and the H atoms scavenge the radical species. The trend between ionization potential and the ORAC data also suggests the radical scavenging by hydrazones is partially due to their participation in the single electron transfer (SET) mechanism. The SAR correlation with logP suggests that the scavenging activity improved with increasing hydrophobicity. The results of this SAR study highlight common notions seen in the literature where BDE<sup>294-296</sup> and IP<sup>226,229</sup> are generally correlated with antioxidant activity.

An extended study with a broader group of hydrazones bearing more diverse substituents is needed to propose a quantitative description of the effect of these features that would make possible the rational design of antioxidants for potential therapeutic use.

#### **11.4 SAR study on radical scavenging activity of phenol and aniline model compounds**

Based on the SAR study with hydrazones in Chapter 7, it was decided to analyze the radical scavenging activity of phenol and aniline models as a function of their calculated properties. The goal was to provide a better understanding of the contributing factors on the radical scavenging capabilities of these compounds. It was observed that phenols, on average, possess higher radical scavenging activity than anilines. However, several anilines showed much higher activity than the majority of phenols, thus the activity ranges overlap, indicating that anilines are comparable radical scavengers to phenols.

Regarding phenols, it has been found that increasing the number of -OH groups does not necessarily result in parallel enhancement in radical scavenging activity. It was observed however, that the position of the multiple -OH groups is of particular importance; having them in 1,3 position results in significant synergistic increase in activity, in contrast to 1,2 or 1,4-positions. The study identified several physical properties that likely govern the free radical scavenging activity of both phenols and anilines, such as the HOMO energies, band gap and BDE. Anilines, on the other hand, appear to act via more complex pathways as the ionization potential, dipole moment and proton affinity all have considerable effect on their radical scavenging properties.

## 11.5 Hydrazones as multi-functional drug candidates

Hydrazones, which have already been studied as potential anti- AD agents, were investigated for their potential function as CK2 holoenzyme inhibitors to treat cancer. The hydrazones from Chapter 7 were investigated and determined to have promising activity against the CK2 $\alpha'$  monomer of CK2. Compounds **31**, **36**, **37**, **38**, **40**, **42** and **45** were determined to have IC<sub>50</sub> values from 1 to 15  $\mu$ M. It was observed that hydrazones with halogen, particularly fluorine, were good inhibitors of CK2 $\alpha'$ . This information served as a foundation and led to the design and synthesis of phase 2 hydrazone derivatives which include more fluorines. The phase 2 hydrazones exhibited different radical scavenging profiles than their phase 1 counterparts; with the ABTS and DPPH activity profiles of these compounds increased and the ORAC activity was ultimately lower and less uniform than that of the phase 1 compounds. This work is still in progress and the full profile determination of these hydrazones as CK2 inhibitors is currently underway.

## **11.6 Optimization of the conditions for the formation of amyloid fibrils**

It is clear from our work that conditions maintained during amyloid fibril formation are crucially important. When generating amyloid fibril species, the protein in question needs an environment that is unfavorable to its natively folded state in order to initiate the protein to adopt the amyloid state. In addition, when the fibril formation is performed as an assay for finding suitable inhibitors of the process for drug development purposes it is important that the parameters mimic physiological conditions. In practice, one has to consider the goal of an assay and optimize the conditions accordingly. During my work I optimized the fibril formation process of two amyloidogenic proteins: lysozyme and insulin. Lysozyme fibril formation optimization was investigated to provide fibril formation conditions that could easily be replicated in a teaching lab setting for students to work with an AFM. Since the lysozyme project was not investigating self-assembly inhibitors, the conditions for amyloid fibril formation did not need to be physiological. I was also able to optimize the formation of insulin amyloid fibrils under physiological conditions which required the facilitation of the seeding in the sample. As amyloid fibril formation is already understood to be a nucleation driven process<sup>229</sup> this is in agreement with earlier findings regarding other proteins. The differences in fibril structure seen between the acidic and physiological pH preparation methods clearly show the importance of investigations on amyloid fibril formation prior to studying self-assembly inhibitors and disassembly agents. My optimized protocol will allow the testing of insulin self-assembly inhibitors under physiological pH and temperature.



The results of the studies in this work have all been published or are in preparation for publication in various peer reviewed journals. The publications are listed below.

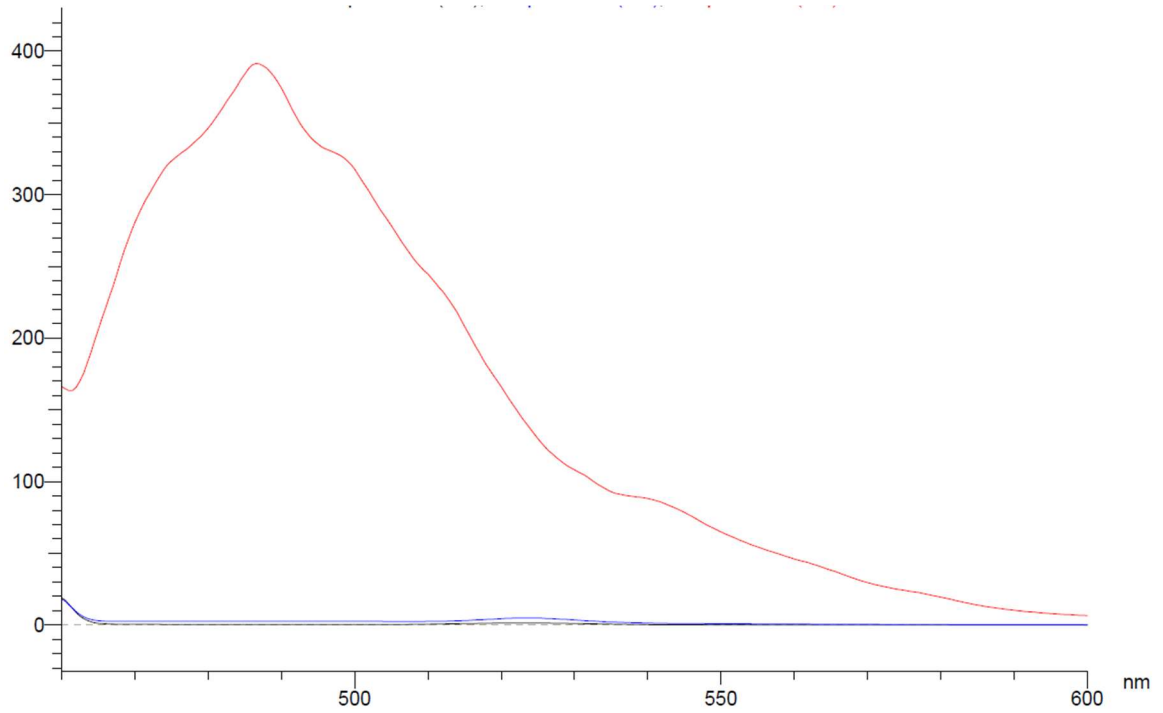
1. **Horton, W.**; Peerannawar, S.; Török, B. and Török, M. “Theoretical and Experimental Analysis of the Antioxidant Features of Substituted Phenol and Aniline Model Compounds,” *Org. Biomol. Chem.* **2018** (submitted)
2. Gokalp, S.; **Horton, W.**; Jonsdottir, E.; Foster, M. and Török, M. “Laboratory Exercise for Studying the Morphology of Heat-denatured and Amyloid Aggregates of Lysozyme by Atomic Force Microscopy,” *Biochem. Mol. Biol. Ed.* **2018**, doi: 10.1002/bmb.21101. (in press)
3. Banu, R.; Gerding, J.; Franklin, C.; Sikazwe, D.; **Horton, W.**; Török, M.; Davis, J.; Cheng, K.H.; Nakazwe, M. and Mochona, B. “4,5-dimethoxy-2-nitrobenzohydrazides and 1-(1-benzylpiperidin-4-yl)ethan-1-ones as potential antioxidant/cholinergic endowed small molecule leads,” *Sci. Pharm.* **2017**, *86*, doi: 10.3390/scipharm86010002.
4. Peerannawar, S.; **Horton, W.**; Kokel, A.; Török, F.; Török, M and Török, B. “Theoretical and Experimental Analysis of the Antioxidant Features of Diarylhydrazones,” *Struct. Chem.* **2017**, *28*, 391-402.
5. **Horton, W.**; Sood, A.; Peerannawar, S.; Kugyela, N.; Kulkarni, A.; Tulsan, R.; Tran, C.D.; Soule, J.; LeVine, H. III.; Török, B. and Török, M. “Synthesis and application of  $\beta$ -carbolines as novel multi-functional anti-Alzheimer’s disease agents,” *Bioorg. Med. Chem. Lett.* **2017**, *27*, 232-236.

**Other related publications:**

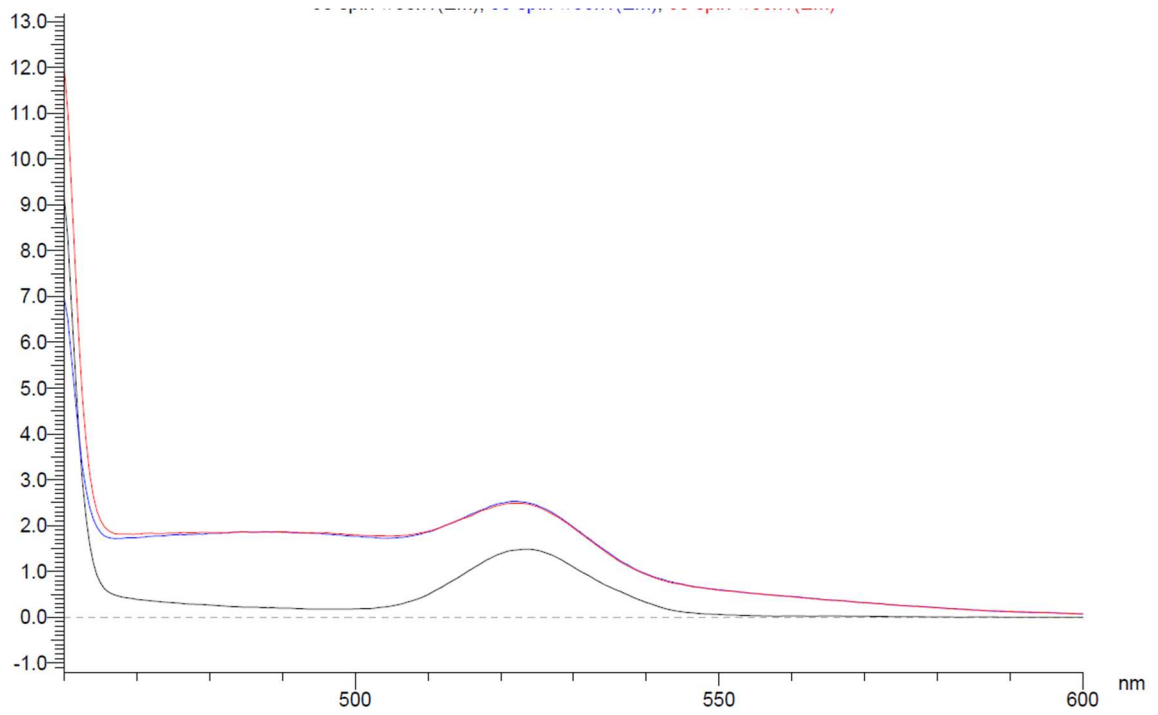
1. **Horton, W.** and Török, M. “Natural and nature-inspired synthetic small molecule antioxidants in the context of green chemistry,” in *Green chemistry: an inclusive approach*, (Török, B., Dransfield eds.). **2018**, Chp 3.27, pp 963-979, Elsevier, Oxford.
2. Ackerman, S. and **Horton, W.** “Effects of Environmental Factors on DNA: damage and mutations,” in *Green chemistry: an inclusive approach*, (Török, B., Dransfield eds.). **2018**, Chp 2.4, pp 109-128, Elsevier, Oxford.

## APPENDIX

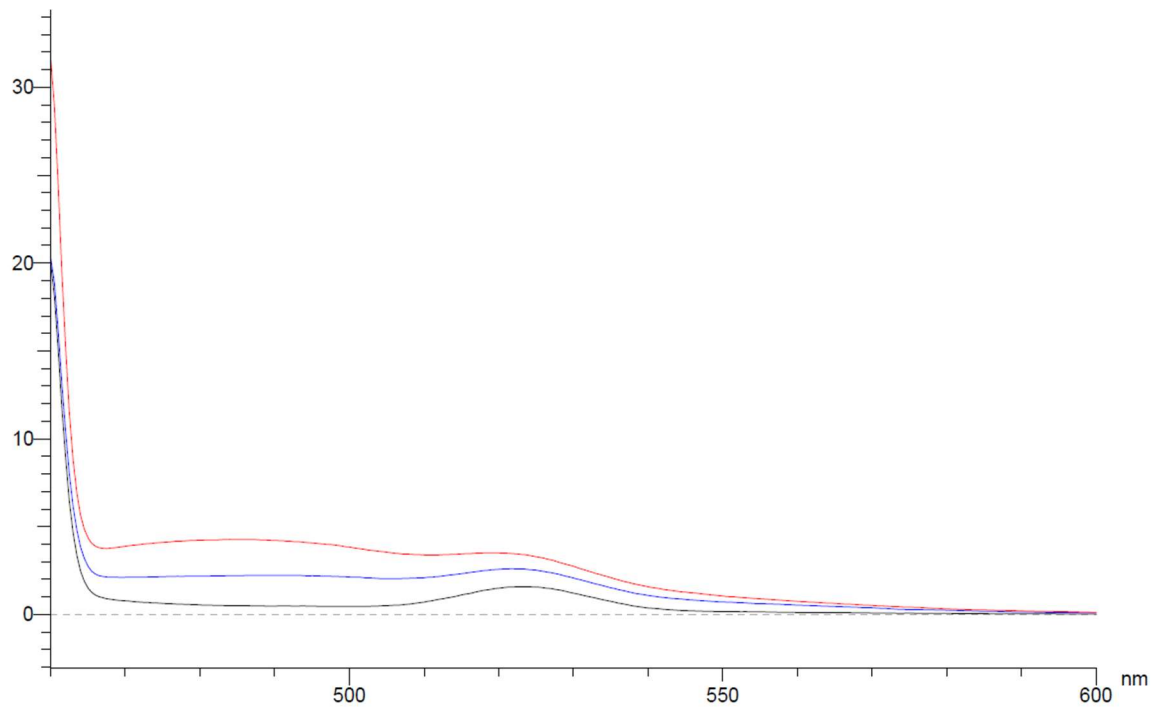
### A. SELECTED THIOFLAVIN T EMISSION SPECTRA FOR INSULIN FIBRIL FORMATION



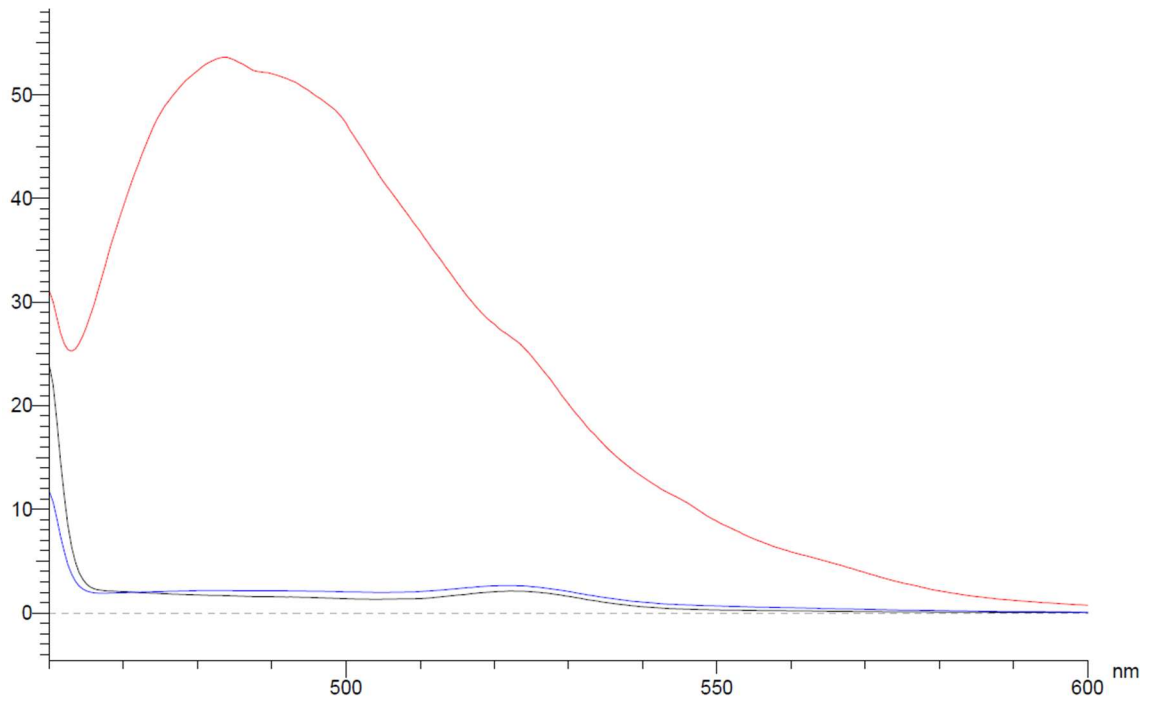
ThT emission spectra for insulin fibrils formed under acidic conditions after 2 days. (red: insulin + ThT, blue: ThT, black: insulin)



ThT emission spectra for insulin fibrils formed under physiological conditions at 37 °C and 300 rpm after 3 days. (red: insulin + ThT, blue: ThT, black: insulin)

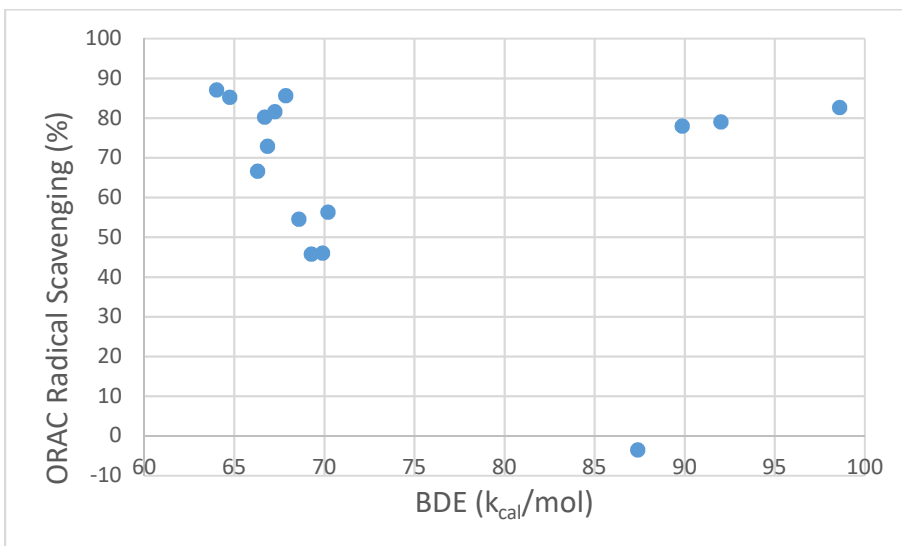


ThT emission spectra for insulin fibrils formed under physiological conditions at 70 °C and 300 rpm after 3 days. (red: insulin + ThT, blue: ThT, black: insulin)

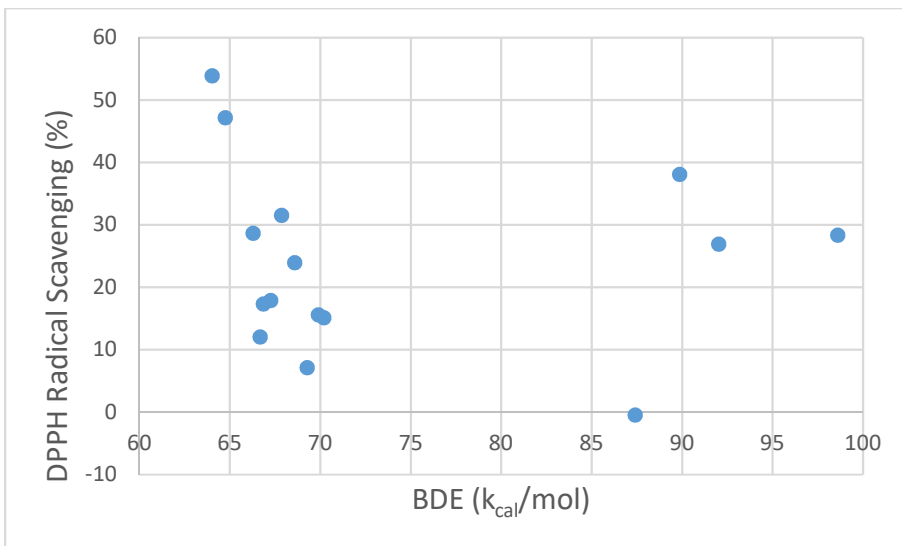


ThT emission spectra for insulin fibrils formed under physiological conditions at 37 °C, 700 rpm and a Teflon ball added after 3 days. (red: insulin + ThT, blue: ThT, black: insulin)

B. PLOT OF BDE ENERGY VS. RADICAL SCAVENGING ACTIVITY FOR SAR OF HYDRAZONES



ORAC radical scavenging activity vs. BDE plot to illustrate the effect of the BDE on the activity of all hydrazones investigated in the SAR study.



DPPH radical scavenging activity vs. BDE plot to illustrate the effect of the BDE on the activity of all hydrazones investigated in the SAR study.

## ENDNOTES

1. <https://www.alz.org/facts/#personalFinancialImpact> (accessed on 03-19-2018).
2. <http://www.diabetes.org/diabetes-basics/statistics/> (accessed on 03-19-2018)
3. Siegel, R.L.; Miller, K.D. and Jemal, A. "Cancer Statistics, 2018," *CA: Cancer J. Clin.* **2018**, *68*, doi: 10.3322/caac.21442
4. Kandimalla, R.; Thirumala, V. and Reddy, P.H. "Is Alzheimer's disease a Type 3 Diabetes A critical appraisal," *Biochim. Biophys. Acta Mol. Basis Dis.* **2017**, *1863*, 1078-1089.
5. Larner, A.J. "Cholinesterase inhibitors: beyond Alzheimer's disease," *Expert Rev. Neurother.* **2010**, *10*, 1699-1705.
6. Francis, P.T.; Ramirez, M.J. and Lai, M.K. "Neurochemical basis for symptomatic treatment of Alzheimer's disease," *Neuropharmacol.* **2010**, *59*, 221-229.
7. Darvesh, H. Hopkins, D.A. and Geula, C. "Neurobiology of butyrylcholinesterase," *Nat. Rev. Neurosci.* **2003**, *4*, 131-138.
8. Riviere, C.; Delaunay, J.C.; Immel, F.O.; Cullin, C. and Monti, J.P. "The polyphenol piceid destabilizes preformed amyloid fibrils and oligomers in vitro: hypothesis on possible molecular mechanisms," *Neurochem. Res.* **2009**, *34*, 1120-1128.
9. Ono, K.; Hirohata, M. and Yamada, M. "Ferulic acid destabilizes preformed  $\beta$  amyloid fibrils in vitro," *Biochem. Biophys. Res. Commun.* **2005**, *336*, 444-449.
10. Matsunaga, S. Kishi, T. and Iwata, N. "Combination therapy with cholinesterase inhibitors and memantine for Alzheimer's disease: a systematic review and meta-analysis," *Int. J. Neuropsychopharmacol.* **2014**, *18*, doi: 10.1093/ijnp/pyu115.
11. Atri, A.; Shaughnessy, L.W.; Locascio, J.J. and Growdon, J.H. "Long-term course and effectiveness of combination therapy in Alzheimer disease," *Alzheimer Dis. Assoc. Disord.* **2008**, *22*, 209-221.
12. Schmitt, B.; Bernhardt, T.; Moeller, H.J.; Heuser, I. and Frölich, L. "Combination therapy in Alzheimer's disease: a review of current evidence," *CNS Drugs* **2004**, *18*, 827-844.
13. Vogelstein, B. and Kinzler, K.W. "Cancer genes and the pathways they control," *Nat. Med.* **2004**, *10*, 789-799.



14. Reya, T.; Morrison, S.J.; Clarke, M.F. and Weissman, I.L. "Stem cells, cancer and cancer stem cells," *Nature* **2001**, *414*, 105-111.
15. Hanahan, D. and Weinberg, R.A. "Hallmarks of cancer: the next generation," *Cell* **2011**, *144*, 646-674.
16. Wang, J.; Liu, Q.; Yuan, S.; Xie, W.; Liu, Y.; Xiang, Y.; Wu, N.; Wu, L.; Ma, X.; Cai, T.; Zhang, Y.; Sun, Z. and Li, Y. "Genetic predisposition to lung cancer: comprehensive literature integration, meta-analysis and multiple evidence assessment of candidate-gene association studies," *Sci. Rep.* **2017**, *7*, doi:10.1038/s41598-017-07737-0.
17. Ramsay, R.R; Popovic-Nikolic, M.R.; Nikolic, K.; Uliassi, E. and Bolognesi, M.L. "A perspective on multi-target drug discovery and design for complex diseases," *Clin. Transl. Med.* **2018**, *7*, doi: 10.1186/s40169-017-0181-2.
18. Bag, S.; Ghosh, S.; Tulsan, R.; Sood, A.; Zhou, W.; Schifone, C. and Foster, M. "Design, Synthesis and Biological Activity of Multifunctional  $\alpha,\beta$ -Unsaturated Carbonyl Scaffolds for Alzheimer's Disease," *Bioorg. Med. Chem. Lett.* **2013**, *23*, 2614-2618.
19. Schüttelkopf, A.W. and van Aalten, D.M. "PRODRG: a tool for high-throughput crystallography of protein-ligand complexes," *Acta Crystallogr. D. Biol. Crystallogr.* **2004**, *60*, 1355-1363.
20. Kumar, P.; Kadyan, K.; Duhan, M.; Sindhu, J.; Singh, V. and Saharan, B.S. "Design, synthesis, conformational and molecular docking study of some novel acyl hydrazone based molecular hybrids as antimalarial and antimicrobial agents," *Chem. Cent. J.* **2017**, *11*, doi: 10.1186/s13065-017-0344-7.
21. Apak, R.; Özyürek, M.; Güçlü, K. and Çapanoğlu, E. "Antioxidant Activity/Capacity Measurement. 2. Hydrogen Atom Transfer (HAT)-Based, Mixed-Mode (Electron Transfer (ET)/HAT) and Lipid Peroxidation Assays.," *J. Agric. Food. Chem.* **2016**, *64*, 1028-1045.
22. Valko, M.; Leibfritz, D.; Moncol, J.; Cronin, M.T.D.; Mazur, M. and Telser, J. "Free radicals and antioxidants in normal physiological functions and human disease," *Int. J. Biochem. Cell. Biol.* **2007**, *39*, 44-84.
23. Forman, H.J.; Augusto, O.; Brigelius-Flohe, R.; Dennery, P.A.; Kalyanaraman, B.; Ischiropoulos, H.; Mann, G.E.; Radi, R.; Roberts, L.J. 2<sup>nd</sup>; Vina, J. and Davies, K.J. "Even free radicals should follow some rules: a guide to free radical research terminology and methodology," *Free. Radic. Biol. Med.* **2015**, *78*, 233-235.

24. Peerannawar, S.; Horton, W.; Kokel, A.; Török, F.; Török, M and Török, B. "Theoretical and Experimental Analysis of the Antioxidant Features of Diarylhydrazones," *Struct. Chem.* **2017**, *28*, 391-402.
25. Gorantla, V.; Gundla, R.; Jadav, S.S.; Anugu, S.R.; Chimakurthy, J.; Nidasanametlab, S.K. and Korupolu, R. "Molecular hybrid design, synthesis and biological evaluation of N-phenyl sulfonamide linked N-acyl hydrazone derivatives functioning as COX-2 inhibitors: new anti-inflammatory, anti-oxidant and anti-bacterial agents," *New J. Chem.* **2017**, *41*, 13516-13532.
26. Domalaon, R.; Idowu, T.; Zhanel, G.G. and Schweizer, F. "Antibiotic hybrids: the next generation of agents and adjuvants against gram-negative pathogens?," *Clin. Microbiol. Rev.* **2018**, *31*, doi: 10.1128/CMR.00077-17.
27. Ferchtat, L.L and Makhove, N.N. "Molecular hybridization tools in the development of furoxan-based NO-donor prodrugs," *ChemMedChem.* **2017**, *12*, doi: 10.1002/cmdc.201700113.
28. Moaedzadeh, S.; Madadlou, A. and Khosrowshahi asl, A. "Formation mechanisms, handling and digestibility of food protein nanofibrils," *Trends Food Sci. Technol.* **2015**, *45*, 50-59.
29. McAllister, C.; Karymov, M.; Kawano, Y.; Lushnikov, A.Y.; Mikheykin, A.; Uversky, V. and Lyubchenko, Y. "Protein Interactions and Misfolding Analyzed by AFM Force Spectroscopy," *J. Mol. Biol.* **2006**, *354*, 1028-1042.
30. Murray, R.K.; Bender, D.A.; Botham, K.M.; Kennely, P.J. Rodwell, V.W. and Weil, P.A. "Free radicals and antioxidant nutrients," *Harper's Illustrated Biochemistry*. McGraw-Hill Companies, Inc; **2012**, p. 543-548.
31. Pisoschi, A.M. and Pop, A. "The role of antioxidants in the chemistry of oxidative stress: a review," *Eur. J. Med. Chem.* **2015**, *97*, 55-74.
32. Delanty, N. and Dichter, M.A. "Oxidative injury in the nervous system," *Acta Neurol. Scand.* **1998**, *98*, 145-153.
33. Foyer, C.H "Redox homeostasis and antioxidant signaling: a metabolic interface between stress perception and physiological responses," *Plant Cell* **2005**, *17*, 1866-1875.
34. Rajendran, P.; Nandakumar, N.; Rengarajan, T.; Palaniswami, R.; Gnanadhas, E.N.; Lakshminarasiah, U.; Gopas, J. and Nishigaki, I. "Antioxidants and human diseases," *Clin. Chim. Acta.* **2014**, *436*, 332-347.

35. Halliwell, B. and Gutteridge, J.M. "Role of free radicals and catalytic metal ions in human disease: an overview," *Methods Enzymol.* **1990**, *186*, 1-85.
36. Lin, M. and Beal, M.F. "Mitochondrial dysfunction and oxidative stress in neurodegenerative diseases," *Nature* **2006**, *443*, 787-795.
37. Ames, B.; Shigenaga, M. and Hagen, T. "Oxidants, antioxidants and the degenerative diseases of aging," *Proc. Natl. Acad. Sci. U.S.A.* **1993**, *90*, 7915-7922.
38. Reuter, S.; Gupta, S.; Chaturvedi, M.M. and Aggarwal, B.B. "Oxidative stress, inflammation and cancer: how are they linked?" *Free Radic. Biol. Med.* **2010**, *49*, 1603-1616.
39. Kelsey, N.A.; Wilkins, H.M. and Linseman, D.A. "Nutraceutical antioxidants as novel neuroprotective agents," *Molecules* **2010**, *15*, 7792-7814.
40. Galkina, O.V. "The specific features of free-radical processes and the antioxidant defense in the adult brain," *Neurochem. J.* **2013**, *7*, 89-97.
41. Dröge, W. "Free Radicals in the Physiological Control of Cell Function," *Physiol. Rev.* **2002**, *82*, 47-95.
42. Knight, J.A. "Review: Free radicals, antioxidants and the immune system," *Ann. Clin. Lab Sci.* **2000**, *30*, 145-158.
43. Hensley, K.; Robinson, K.A.; Gabbita, S.P.; Salsman, S. and Floyd, R.A. "Reactive oxygen species, cell signaling and cell injury." *Free Radic. Biol. Med.* **2000**, *28*, 1456-1462.
44. Denu, J. M. and Tanner, K. G. "Specific and reversible inactivation of protein tyrosine phosphatases by hydrogen peroxide: evidence for a sulfenic acid intermediate and implications for redox regulation," *Biochemistry* **1998**, *37*, 5633–5642.
45. Lee, S.R.; Kwon, K.S.; Kim, S.R. and Rhee, S.G. "Reversible inactivation of protein-tyrosine phosphatase 1B in A431 cells stimulated with epidermal growth factor," *J. Biol. Chem.* **1998**, *273*, 15366–15372.
46. Sundaresan, M.; Yu, Z.X.; Ferrans, V.J.; Irani, K. and Finkel, T. "Requirement for generation of H<sub>2</sub>O<sub>2</sub> for platelet-derived growth factor signal transduction," *Science* **1995**, *270*, 296–299.

47. Lawrence, T. "The nuclear factor NF-kappaB pathway in inflammation," *Cold Spring Harb. Perspect. Biol.* **2009**, *1*, doi: 10.1101/cshperspect.a001651.
48. Robinson, K.; Stewart, C.A.; Pye, Q.N.; Nguyen, X.; Kenney, L.; Salsman, S.; Floyd, R. A. and Hensley, K. "Redox sensitive protein phosphatase activity regulates the phosphorylation state of p38 protein kinase in primary astrocyte culture," *J. Neurosci Res.* **1999**, *55*, 724-732.
49. Pryor, W.A. "Biological effects of cigarettes smoke, wood smoke and the smoke from plastics – the use of electron spin resonance," *Free Radic. Biol. Med.* **1992**, *13*, 659–676.
50. Riley, P.A. "Free radicals in biology – oxidative stress and the effects of ionizing radiation," *Int. J. Radiat. Biol.* **1994**, *65*, 27–33.
51. Benedetti, M.; Giuliani, M.E. and Regoli, F. "Oxidative metabolism of chemical pollutants in marine organisms: molecular and biochemical biomarkers in environmental toxicology," *Ann. N.Y. Acad. Sci.* **2015**, *1340*, 8–19.
52. Bode1, A.M.; Dong, Z. and Wang, H. "Cancer prevention and control: alarming challenges in China," *Natl. Sci. Rev.* **2016**, *3*, 117-127.
53. Horton, W. and Török, M. "Natural and nature-inspired synthetic small molecule antioxidants in the context of green chemistry," in *Green chemistry: an inclusive approach* (Török, B., Dransfield eds.). **2018**, Chp 3.27, pp 963-979, Elsevier, Oxford.
54. Bouayed, J. and Bohn, T. "Exogenous antioxidants--double-edged swords in cellular redox state: health beneficial effects at physiologic doses versus deleterious effects at high doses," *Oxid. Med. Cell Longev.* **2010**, *3*, 228-237.
55. Panieri, E. and Santoro, M.M. "ROS homeostasis and metabolism: a dangerous liason in cancer cells," *Cell Death Dis.* **2016**, *7*, doi:10.1038/cddis.2016.105.
56. Slimen, I.; Najar, T. and Abderrabba, M. "Chemical and Antioxidant Properties of Betalains," *J. Agric. Food Chem.* **2017** *65*, 675-689.
57. Halake, K.; Birajdar, M. and Lee, J. "Structural implications of polyphenolic antioxidants," *J. Ind. Eng. Chem. Res.* **2016**, *35*, 1-7.
58. Poljšak, B. and Fink, R. "The protective role of antioxidants in the defence against ROS/RNS-mediated environmental pollution," *Oxid. Med. Cell Longev.* **2014**, doi: 10.1155/2014/671539.

59. Neto, C.C. "Cranberry and blueberry: evidence for protective effects against cancer and vascular diseases," *Mol. Nutr. Food Res.* **2007**, *51*, 652-664.
60. Neto, C.C. "Cranberries: ripe for more cancer research?," *J. Sci. Food Agric.* **2011**, *91*, 2303-2307.
61. Xia, E.; Deng, G.; Guo, Y. and Li, H. "Biological activities of polyphenols from grapes," *Int. J. Mol. Sci.* **2010**, *11*, 622-646
62. Azeredo, H. "Betalains: properties, sources, applications and stability – a review," *Int. J. Food Sci. Nutr.* **2009**, *44*, 2365-2376.
63. Butera, D.; Tesoriere, L.; Gaudio, F.; Bongiorno, A.; Allegra, M.; Pintaudi, A.M.; Kohen, R. and Livrea, M.A. "Antioxidant activities of sicilian prickly pear (*Opuntia ficus indica*) fruit extracts and reducing properties of its betalains: betanin and indicaxanthin," *J. Agric. Food. Chem.* **2002**, *50*, 6895-6901.
64. Gengatharan, A.; Dykes, G. and Choo, W. "Betalains: Natural plant pigments with potential application in functional foods," *LWT-Food Sci. Technol.* **2015**, *64*, 645-649.
65. Swieca, M.; Gawlik-Dziki, U.; Dziki, D. and Baraniak, B. "Wheat bread enriched with green coffee - In vitro bioaccessibility and bioavailability of phenolics and antioxidant activity," *Food Chem.* **2017**, *221*, 1451-1457.
66. Foti, M. and Amorati, R. "Non-phenolic radical-trapping antioxidants," *J. Pharm. Pharmacol.* **2009**, *61*, 1435-1448.
67. Shahidi, F. and Ambigaipalan, P. "Phenolics and polyphenolics in foods, beverages and spices: Antioxidant activity and health effects: A review," *J. Funct. Foods* **2015**, *18*, 820-897.
68. Sarmadi, B. and Ismail, A. "Antioxidative peptides from food proteins: a review," *Peptides* **2010**, *31*, 1949-1956.
69. Dai, J. and Mumper, R. "Plant phenolics: extraction, analysis and their antioxidant and anticancer properties," *Molecules* **2010**, *15*, 7313-7352.
70. Manach, C.; Scalbert, A.; Morand, C.; Rémésy, C. and Jiménez, L. "Polyphenols: food sources and bioavailability," *Am. J. Clin. Nutr.* **2004**, *79*, 727-747.
71. Forman, H.J.; Davies, K.J. and Ursini, F. "How do nutritional antioxidants really work: nucleophilic tone and para-hormesis versus free radical scavenging in vivo," *Free Radic. Biol. Med.* **2014**, *66*, 24-35.

72. Kanner, J.; Harel, S. and Granit, R. "Betalains - a new class of dietary cationized antioxidants," *J. Agric. Food. Chem.* **2001**, *49*, 5178-5185.
73. Manach, C.; Williamson, G.; Morand, C.; Scalbert, C. and Rémésy, C. "Bioavailability and bioefficacy of polyphenols in humans. I. Review of 97 bioavailability studies," *Am. J. Clin. Nutr.* **2005**, *81(suppl)*, 230S-242S.
74. Manach, C.; Williamson, G.; Morand, C.; Scalbert, C. and Rémésy, C. "Bioavailability and bioefficacy of polyphenols in humans. II. Review of 93 intervention studies," *Am. J. Clin. Nutr.* **2005**, *81(suppl)*, 243S-255S.
75. Hollman, P.C. "Unravelling of the health effects of polyphenols is a complex puzzle complicated by metabolism," *Arch. Biochem. Biophys.* **2014**, *559*, 100-105.
76. Crozier, A.; Jaganath, I.B. and Clifford, M.N. "Dietary phenolics: chemistry, bioavailability and effects on health," *Nat. Prod. Rep.* **2009**, *26*, 1001-1043.
77. Scalbert, A. and Williamson, G. "Dietary intake and bioavailability of polyphenols," *J. Nutr.* **2000**, *130*, 2073S-2085S.
78. Walle, T.; Hsieh, F.; DeLegge, M.; Oatis, J. and Walle, K. "High absorption but very low bioavailability of oral resveratrol in humans," *Drug Metab. Dispos.* **2004**, *32*, 1377-1382.
79. Albanes, D.; Heinonen, O.P.; Taylor, P.R.; Virtamo, J.; Edwards B.K.; Rautalahti, M.; Hartman, A.M.; Palmgren, J.; Freedman, L.S.; Haapakoski, J.; Barrett, M.J.; Pietinen, P.; Malila, N.; Tala, E.; Liippo, K.; Salomaa, E.R.; Tangrea, J.A.; Teppo, L.; Askin, F.B.; Taskinen, E.; Erozan, Y. Greenwald, P. and Huttunen, J.K. "Alpha-tocopherol and beta-carotene supplements and lung cancer incidence in the alpha-tocopherol, beta-carotene cancer prevention study: effects of baseline characteristics and study compliance," *J. Natl. Cancer Inst.* **1996**, *88*, 1560-1570.
80. Heinonen, O.P.; Albanes, D.; Virtamo, J.; Taylor, P.R.; Huttunen, J.K.; Hartman, A.M.; Haapakoski, J.; Malila, N.; Rautalahti, M.; Ripatti, S.; Mäenpää, H.; Teerenhovi, L.; Koss, L.; Virolainen, M. and Edwards, B.K. "Prostate cancer and supplementation with alpha-tocopherol and beta-carotene: incidence and mortality in a controlled trial," *J. Natl. Cancer Inst.* **1998**, *90*, 440-446.
81. Bolognesi, M.L. "Polypharmacology in a single drug: multitarget drugs," *Curr. Med. Chem.* **2013**, *20*, 1639-1645.
82. Bolognesi, M.L. and Cavalli, A. "Multitarget drug discovery and polypharmacology," *ChemMedChem.* **2016**, *11*, 1190-1192.

83. Talevi, A. “Multi-target pharmacology: possibilities and limitations of the “skeleton key approach” from a medicinal chemist perspective,” *Front Pharmacol.* **2015**, doi: 10.3389/fphar.2015.00205.
84. Morphy, R.; Kay, C. and Rankovic, Z. “From magic bullets to designed multiple ligands,” *Drug Discov. Today* **2004**, *9*, 641–651.
85. Youdim, M.B.H. and Buccafusco, J.J. (2005) Multi-functional drugs for various CNS targets in the treatment of neurodegenerative disorders,” *Trends Pharm. Sci.* **2005**, *26*, 27–35.
86. Roth, B.L.; Sheffler, D.J. and Kroeze, W.K. “Magic shotguns versus magic bullets: selectively non-selective drugs for mood disorders and schizophrenia,” *Nat. Rev. Drug Discov.* **2004**, *3*, 353–359.
87. Lin, H.H.; Zhang, L.L.; Yan, R.; Lu, J.J. and Hu, Y.J. (2017) “Network analysis of drugtarget interactions: a study on FDA-approved new molecular entities between 2000 to 2015,” *Sci. Rep.* **2017**, *7*, doi: 10.1038/s41598-017-12061-8.
88. Zimmermann, G.R.; Lehár, J. and Keith, C.T. “Multi-target therapeutics: when the whole is greater than the sum of the parts,” *Drug Discov. Today* **2007**, *12*, 34–42.
89. Xie, L. and Bourne, P.E. “Developing multi-target therapeutics to fine-tune the evolutionary dynamics of the cancer ecosystem,” *Front Pharmacol.* **2015**, *6*, doi: 10.3389/fphar.2015.00209.
90. Cavalli, A.; Bolognesi, M.L.; Minarini, A.; Rosini, M.; Tumiatti, V.; Recanatini, M. and Melchiorre, C. “Multi-target-directed ligands to combat neurodegenerative diseases,” *J. Med. Chem.* **2008**, *51*, 347–372.
91. Viayna, E.; Sola, I.; Di Pietro, O. and Munoz-Torrero, D. (2013) “Human disease and drug pharmacology, complex as real life,” *Curr. Med. Chem.* **2013**, *20*, 1623–1634.
92. Morphy, R. and Rankovic, Z. “Design of multitarget ligands,” in Lead generation approaches in drug discovery. (Morphy, R. and Rankovic, Z.). **2010**, Wiley, Hoboken, 141–164.
93. Morphy, R. and Rankovic, Z. “Designing multiple ligands—medicinal chemistry strategies and challenges,” *Curr. Pharm. Des.* **2009**, *15*, 587–600.

94. Felice, D.; Gardier, A.M.; Sanchez, C. and David, D.J. (2017) “Innovative solutions to the development of novel antidepressants,” *Frontiers Drug Disc.* **2017**, *2*, 1-40.
95. Bannwart, L.M.; Carter, D.S.; Cai, H.Y.; Choy, J.C.; Greenhouse, R.; Jaime-Figueroa, S.; Iyer, P.S.; Lin, C.J.; Lee, E.K.; Lucas, M.C.; Lynch, S.M.; Madera, A.M.; Moore, A.; Ozboya, K.; Raptova, L.; Roetz, R.; Schoenfeld, R.C.; Stein, K.A.; Steiner, S.; Villa, M.; Weikert, R.J. and Zhai, Y. “Novel 3,3-disubstituted pyrrolidines as selective triple serotonin/norepinephrine/dopamine reuptake inhibitors,” *Bioorg. Med. Chem. Lett.* **2008**, *18*, 6062–6066.
96. Morphy, R. and Rankovic, Z. “Designed multiple ligands. An emerging drug discovery paradigm,” *J. Med. Chem.* **2005**, *48*, 6523–6543.
97. Sliwoski, G.; Kothiwale, S.; Meiler, J. and Lowe, E.W. Jr. “Computational methods in drug discovery,” *Pharmacol. Rev.* **2014**, *66*, 334–395.
98. Cherkasov, A.; Muratov, E.N.; Fourches, D.; Varnek, A.; Baskin I.I.; Cronin M.; Dearden, J.; Gramatica, P.; Martin, Y.C.; Todeschini, R.; Consonni, V.; Kuz'min, V.E.; Cramer, R.; Benigni, R.; Yang, C.; Rathman, J.; Terfloth, L.; Gasteiger, J.; Richard, A. and Tropsha, A. “QSAR modeling: where have you been? Where are you going to?,” *J. Med. Chem.* **2014**, *57*, 4977–5010.
99. Danishuddin and Khan, A.U. “Descriptors and their selection methods in QSAR analysis: paradigm for drug design,” *Drug Discov. Today.* **2016**, *21*, 1291–1302.
100. Morris, G.M.; Huey, R.; Lindstrom, W.; Sanner, M.F.; Belew, R.K.; Goodsell, D.S. and Olson, A.J. “AutoDock4 and AutoDockTools4: automated docking with selective receptor flexibility,” *J. Comput. Chem.* **2009**, *30*, 2785–2791.
101. Meng, X.Y.; Zhang, H.X.; Mezei, M. and Cui, M. “Molecular docking: a powerful approach for structure-based drug discovery,” *Curr. Comput. Aided Drug Des.* **2011**, *7*, 146–157.
102. Hua, Q.X. and Weiss, M.A. “Mechanism of insulin fibrillation: the structure of insulin under amyloidogenic conditions resembles a protein-folding intermediate,” *J. Biol. Chem.* **2004**, *179*, 21499-21460.
103. Hartl, F.U. “Protein misfolding diseases,” *Annu. Rev. Biochem.* **2017**, *86*, 21-26.
104. Chaudhuri, T.K. and Paul, S. “Protein-misfolding diseases and chaperone-based therapeutic approaches,” *FEBS J.* **2006**, *273*, 1331-1349.
105. Horwich, A.L.; Neupert, W. and Hartl, F.U. “Protein-catalysed protein folding,” *Trends in Biotech.* **1990**, *8*, 126-131.



106. Creighton, T.E. "Protein folding," *Biochem. J.* **1990**, *270*, 1-16.
107. Privalov, P.L. "Stability of proteins: small globular proteins," *Adv. Protein Chem.* **1979**, *33*, 167-241.
108. Page, M.I. and Jencks, W.P. "Entropic Contributions to Rate Accelerations in Enzymic and Intramolecular Reactions and the Chelate Effect," *Proc. Natl. Acad. Sci. U.S.A.* **1971**, *68*, 1678-1683.
109. Smith, R.C.; Rosen, K.M.; Pola, R. and Magrané, J. "Stress proteins in Alzheimer's disease," *Int. J. Hyperthemia* **2005**, *21*, 421-431.
110. Kelley, B.J. and Petersen, R.C. "Alzheimer's disease and mild cognitive impairment," *Neur. Clin.* **2007**, *25*, 577-609.
111. Ballard, C.; Gauthier, S.; Corbett, A.; Brayne, C.; Aarsland, D. and Jones, E. "Alzheimer's disease," *Lancet* **2011**, *377*, 1019-1031.
112. Chen, X.; Tikhonova, I.G. and Decker, M. "Probing the mid-gorge of cholinesterases with spacer-modified bivalent quinazolinimines leads to highly potent and selective butyrylcholinesterase inhibitors," *Bioorg. Med. Chem.* **2011**, *19*, 1222-1235.
113. Jakob-Roetne, R. and Jacobsen, H. "Alzheimer's disease: from pathology to therapeutic approaches," *Angew. Chem. Int. Ed.* **2009**, *121*, 3030-3059.
114. Neugroschl, J. and Sano, M. "An update on treatment and prevention strategies for Alzheimer's disease," *Curr. Neurol. Neurosci. Rep.* **2009**, *5*, 368-376.
115. Bolognesi, M.L.; Matera, R.; Minarini, A.; Rosini, M. and Melchiorre, C. "Alzheimer's disease: new approaches to drug discovery," *Curr. Opin. Chem. Biol.* **2009**, *13*, 303-308.
116. Relkin, N.R. "Beyond symptomatic therapy: a re-examination of acetylcholinesterase inhibitors in Alzheimer's disease," *Expert. Rev. Neurother.* **2007**, *7*, 735-748.
117. Bartus, R.T.; Dean III, R.L.; Beer, B. and Lippa, A.S. "The cholinergic hypothesis of geriatric memory dysfunction," *Science* **1982**, *217*, 408-414.
118. Belinson, H.; Kariv-Inbal, Z.; Kaye, R.; Masliah, E. and Michaelson, D.M. "Following activation of the amyloid cascade, apolipoprotein E4 drives the in vivo oligomerization of amyloid- $\beta$  resulting in neurodegeneration," *J. Alz. Dis.* **2010**, *22*, 959-970.

119. Selkoe, D.J. "The cell biology of beta-amyloid precursor protein and presenilin in Alzheimer's disease," *Trends Cell Biol.* **1998**, *8*, 447-453.
120. Selkoe, D.J. "Alzheimer's disease genes, proteins and therapy," *Physiol. Rev.* **2001**, *81*, 741-766.
121. Török, B.; Bag, S.; Sarkar, M.; Dasgupta, S. and Török, M "Structural features of small molecule amyloid-beta self-assembly inhibitors," *Curr. Bioact. Comp.* **2013**, *9*, 37-63.
122. Adamski-Werner, S.L.; Palaninathan, S.K.; Sacchettini, J.C. and Kelly, J.W. "Diflunisal analogues stabilize the native state of transthyretin. potenti of amyloidogenesis," *J. Med. Chem.* **2004**, *47*, 355-374.
123. Byeon, S.R.; Lee, J.H.; Sohn, J.H.; Kim, D.C.; Shin, K.J.; Yoo, K.H.; Mook-Jung, I.; Lee, W.K. and Kim, D.J. "Bis-styrylpyridine and bis-styrylbenzene derivatives as inhibitors for A $\beta$  fibril formation," *Bioorg. Med. Chem. Lett.* **2007**, *17*, 1466-1470.
124. Török, M.; Abid, M.; Mhadgut, S.C. and Török, B. "Organofluorine inhibitors of amyloid fibrillogenesis," *Biochemistry* **2006**, *45*, 5377-5383.
125. Török, B.; Sood, A.; Bag, S.; Kulkarni, A.; Borkin, D.; Lawler, E.; Dasgupta, S.; Landge, S.M.; Abid, M.; Zhou, W.; Foster, M.; LeVine III, H. and Török, M. "Structure-activity relationship of organofluorine inhibitors of amyloid-beta self-assembly," *ChemMedChem* **2012**, *7*, 910-919.
126. Ono, K.; Yoshiike, Y.; Takashima, A.; Hasegawa, K.; Naiki, H. and Yamada, M. "Potent anti-amiloidogenic and fibril-destabilizing effects of polyphenols *in vitro*: implications for the prevention and therapeutics of Alzheimer's disease," *J. Neurochem.* **2003**, *87*, 172-81.
127. Porat, Y.; Abramowitz, A. and Gazit, E. "Inhibition of amyloid fibril formation by polyphenols: structural similarity and aromatic interactions as common Inhibition mechanism," *Chem. Biol. Drug. Des.* **2006**, *67*, 27-37.
128. Taniguchi, S.; Suzuki, N.; Masuda, M.; Hisanaga, S.; Iwatsubo, T.; Goedert, M. and Hasegawa, M. "Inhibition of heparin-induced tau filament formation by phenothiazines, polyphenols and porphyrins," *J. Biol. Chem.* **2005**, *280*, 7614-7623.
129. Riviere, C.; Richard, T.; Vitrac, X.; Merillon, J.M.; Walls, J. and Monti, J.P. "New polyphenols active on  $\beta$ -amyloid aggregation," *Bioorg. Med. Chem. Lett.* **2008**, *18*, 828-831.

130. Ono, K.; Hasegawa, K.; Naiki, H. and Yamada, M. "Anti-amyloidogenic activity of tannic acid and its activity to destabilize Alzheimer's  $\beta$ -amyloid fibrils in vitro," *Biochim. Biophys. Acta* **2004**, *1690*, 193-202.
131. Hirohata, M.; Hasegawa, K.; Tsutsumi-Yasuhara, S.; Ohhashi, Y.; Ookoshi, T.; Ono, K.; Yamada, M. and Naiki, H. "The anti- amyloidogenic effect is exerted against Alzheimer's  $\beta$ -amyloid fibrils in vitro by preferential and reversible binding of flavonoids to the amyloid fibril atructure," *Biochemistry* **2007**, *46*, 1888-1899.
132. Heo, H.J.; Kim, D.O.; Shin, S.C.; Kim, M.J.; Kim, B.G. and Shin, D.H. "Effect of antioxidant flavanone, naringenin, from citrus junos on neuroprotection," *J. Agric. Food Chem.* **2004**, *52*, 1520-25.
133. Cosentino, U.; Vari, M.R.; Saracino, A.A.G.; Pieta, D.; Moro, G. and Salmona, M. "Tetracycline and its analogues as inhibitors of amyloid fibrils: searching for a geometrical pharmacophore by theoretical investigation of their conformational behavior in aqueous solution," *J. Mol. Model.* **2005**, *11*, 17-25.
134. Lenhart, J.A.; Ling, X.; Gandhi, R.; Guo, T.L.; Gerk, P.M.; Brunzell, D.H. and Zhang, S. "Clicked" Bivalent ligands containing curcumin and cholesterol as multifunctional A $\beta$  oligomerization inhibitors: design, synthesis and biological characterization," *J. Med. Chem.* **2010**, *53*, 6198-209.
135. Ortega, A.; Rincón, A.; Jiménez-Aliaga, K.L.; Bermejo-Bescós, P.; Martín-Aragón, S.; Molina, M.T. and Csáky, A.G. "Synthesis and evaluation of arylquinones as BACE1 inhibitors,  $\beta$ -amyloid peptide aggregation inhibitors and destabilizers of preformed  $\beta$ -amyloid fibrils," *Bioorg. Med. Chem. Lett.* **2011**, *21*, 2183-2187.
136. Soto-Ortega, D.D.; Murphy, B.P.; Gonzalez-Velasquez, F.J.; Wilson, K.A.; Xie, F.; Wangb, Q. and Moss, M.A. "Inhibition of amyloid- $\beta$  aggregation by coumarin Analogs can be manipulated by functionalization of the aromatic center," *Bioorg. Med. Chem.* **2011**, *19*, 2596-2602.
137. Hamley, I.W. "Peptide Fibrillization," *Angew. Chem. Int. Ed.* **2007**, *46*, 8128-8147.
138. Broersen, K.; Rouaaeau, F. and Schymkowitz, J. "The culprit behind amyloid beta peptide related neurotoxicity in Alzheimer's disease: oligomer size or conformation?," *Alzheimers Res. Ther.* **2010**, *2*, doi: 10.1186/alzrt36.
139. Galzitskay, O.V.; Galushko, E.I. and Selivanova, O.M. "Studies of the process of amyloid formation by A $\beta$  peptide," *Biokhimiya* **2018**, *83 (suppl)*, S62-S80.

140. Kayed, R.; Canto, I.; Breydo, L.; Rasool, S.; Lukacsovich, T.; Wu, J.; Albay III, R.; Pensalfini, A.; Yeung, S.; Head, E.; Marsh, J.L. and Glabe, C. "Conformation dependent monoclonal antibodies distinguish different replicating strains or conformers of prefibrillar A $\beta$  oligomers," *Mol. Neurodegener.* **2010**, *5*, 57-67.
141. Shankar, G.M.; Leissring, M.A.; Adame, A.; Sun, X.; Spooner, E.; Masliah, E.; Selkoe, D.J.; Lemere, C.A. and Walsh, D.M. "Biochemical and immunohistochemical analysis of an Alzheimer's disease mouse model reveals the presence of multiple cerebral A $\beta$  assembly forms throughout life," *Neurobiol. Dis.* **2009**, *36*, 293-302.
142. Zhao, W.Q.; Santini, F.; Breese, R.; Ross, D.; Zhang, X.D.; Stone, D.J.; Ferrer, M.; Townsend, M.; Wolfe, A.L.; Seager, M.A.; Kinney, G.G.; Shughrue, P.J. and Ray, W.J. "Inhibition of calcineurin-mediated endocytosis and alpha-amino-3-hydroxy-5-methyl-4-isoxazolepropionic acid (AMPA) receptors prevents amyloid beta oligomer-induced synaptic disruption," *J. Biol. Chem.* **2010**, *285*, 7619-7632.
143. Kaye, R.; Head, E.; Thompson, J.L.; McIntire T.M.; Milton, S.C.; Cotman, C.W. and Glabe, C.G. "Common structure of soluble amyloid oligomers implies common mechanism of pathogenesis," *Science* **2003**, *300*, 486-489.
144. Török, B.; Dasgupta, S. and Török, M. "Chemistry of small molecule inhibitors in self-assembly of Alzheimer's disease related amyloid-beta peptide," *Curr. Bioact. Comp.* **2008**, *4*, 159-174.
145. Verma, M.; Vats, A. and Taneja, V. "Toxic species in amyloid disorders: oligomers or mature fibrils," *Ann. Indian Acad. Neurol.* **2015**, *18*, 138-145.
146. DeKosky, S.T. and Scheff, S.W. "Synapse loss in frontal cortex biopsies in Alzheimer's disease: correlation with cognitive severity," *Ann. Neurol.* **1990**, *27*, 457-464.
147. Ferreira-Vieira, T.H.; Guimaraes, I.M.; Silva, F.R. and Ribeiro, F.M. "Alzheimer's disease: targeting the cholinergic system," *Curr. Neuropharmacol.* **2016**, *14*, 101-115.
148. Butterfield, D.A. "A review, amyloid  $\beta$ -peptide (1-42)-induced oxidative stress and neurotoxicity implications for neurodegeneration in Alzheimer's disease brain," *Free Radic. Res.* **2002**, *36*, 1307-1313.
149. Barnham, K.J.; Masters, C.L. and Bush, A.I. "Neurodegenerative diseases and oxidative stress," *Nat. Rev.* **2004**, *3*, 205-214.

150. Huang, X.; Moir, R.D.; Tanzi, R.E.; Bush, A.I. and Rogers, J.T. "Redox-active metals, oxidative stress and Alzheimer's disease pathology," *Ann. N.Y. Acad. Sci.* **2004**, *1012*, 153-163.
151. Wollen, K.A. "Alzheimer's disease: the pros and cons of pharmaceutical, nutritional, botanical and stimulatory therapies, with a discussion of treatment strategies from the perspective of patients and practitioners," *Alt. Med. Rev.* **2010**, *15*, 223-244.
152. Bolognesi, M.L.; Simoni, E.; Rossini, M.; Minarini, A.; Tumiatti, V. and Melchiorre, C. "Multitarget-directed ligands: innovative chemical probes and therapeutic tools against Alzheimer's disease," *Curr. Top Med. Chem.* **2011**, *11*, 2797-2806.
153. Butterfield, D.A.; Di Domenico, F. and Barone, E. "Elevated risk of type 2 diabetes for development of Alzheimer disease a key role for oxidative stress in brain," *Biochim. Biophys. Acta* **2014**, *1842*, 1693-1706.
154. Guzior, N.; Więckowska, A.; Panek, D. and Malawska, B. "Recent development of multifunctional agents as potential drug candidates for the treatment of Alzheimer's disease," *Curr. Med. Chem.* **2015**, *22*, 373-404.
155. Ashcroft, F.M. and Rorsman, P. "Diabetes mellitus and the  $\beta$  cell: the last ten years," *Cell* **2012**, *6*, 1160-1171.
156. Guo, S. "Insulin signaling, resistance and the metabolic syndrome: insights from mouse models to disease mechanisms," *J. Endocrinol.* **2014**, *220*, T1-T23.
157. Pozzilli, P.; Battelino, T.; Danne, T.; Hovorka, R.; Jarosz-Chobot, P. and Renard, E. "Continuous subcutaneous insulin infusion in diabetes: patient populations, safety, efficacy and pharmacoeconomics," *Diabetes Metab. Res. Rev.* **2016**, *32*, 21-39.
158. Eckel, R.H.; Kahn, S.E.; Ferrannini, E.; Goldfine, A.B.; Nathan, D.M.; Schwartz, M.W.; Smith, R.J. and Smith, S.R. "Obesity and type 2 diabetes: what can be unified and what needs to be individualized?," *J. Clin. Endocrinol. Metab.* **2011**, *96*, 1654-1663.
159. Pomytkin, I.A. "H<sub>2</sub>O<sub>2</sub> signalling pathway: a possible bridge between insulin receptor and mitochondria," *Curr. Neuropharmacol.* **2012**, *10*, 311-320.
160. Kaur, R.; Dahiya, L. and Kumar, M. "Fructose-1,6-bisphosphatase inhibitors: A new valid approach for management of type 2 diabetes mellitus," *Eur. J. Med. Chem.* **2017**, *141*, 473-505.

161. Bie, J.; Liu, S.; Zhou, J.; Xu, B. and Shen, Z. "Design, synthesis and biological evaluation of 7-nitro-1H-indole-2-carboxylic acid derivatives as allosteric inhibitors of fructose-1,6-bisphosphatase," *Bioorg. Med. Chem.* **2014**, *22*, 1850-1862.
162. Bie, J.; Liu, S.; Li, Z.; Mu, Y.; Xu, B. and Shen, Z. "Discovery of novel indole derivatives as allosteric inhibitors of fructose-1, 6-bisphosphatase," *Eur. J. Med. Chem.* **2014**, *90*, 394-405.
163. Dang, Q.; Kasibhatla, S.R.; Xiao, W.; Liu, Y.; DaRe, J.; Taplin, F.; Reddy, K.R.; Scarlato, G.R.; Gibson, T.; van Poelje, P.D.; Potter, S.C. and Erion, M.D. "Fructose-1,6-bisphosphatase inhibitors. 2. design, synthesis and structure-activity relationship of a series of phosphonic acid containing benzimidazoles that function as 5'-adenosinemonophosphate (AMP) mimics," *J. Med. Chem.* **2010**, *53*, 441-451.
164. Rudnitskaya, A.; Borkin, D.A.; Huynh, K.; Török, B. and Stieglitz, K. "Rational design, synthesis and potency of N-substituted indoles, pyrroles and triarylpyrazoles as potential fructose 1,6-bisphosphatase inhibitors," *ChemMedChem* **2010**, *5*, 384-389.
165. Kahn, S.E.; Cooper, M.E. and Del Prato, S. "Pathophysiology and treatment of type 2 diabetes: perspectives on the past, present and future," *Lancet* **2014**, *383*, 1068-1083.
166. de la Monte, S.M. "Insulin resistance and Alzheimer's disease," *BMB Rep.* **2009**, *42*, 475-481.
167. Zhao, W.Q. and Townsend, M. "Insulin resistance and amyloidogenesis as common molecular foundation for type 2 diabetes and Alzheimer's disease," *Biochim. Biophys. Acta* **2009**, *1792*, 482-496.
168. Craft, S. "Insulin resistance syndrome and Alzheimer's disease: age- and obesity-related effects on memory, amyloid and inflammation," *Neurobiol. Aging* **2005**, *26*, 65-69.
169. Schulingkamp, R.J.; Pagano, T.C.; Hung, D. and Raffa, R.B. "Insulin receptors and insulin action in the brain: review and clinical implications," *Neurosci. Biobehav. Rev.* **2000**, *24*, 855-872.
170. Banks, W.A.; Jaspan, J.B. and Kastin, A.J. "Selective, physiological transport of insulin across the blood-brain barrier: novel demonstration by species-specific radioimmunoassays," *Peptides* **1997**, *18*, 1257-1262.

171. Gray, S.M.; Meijer, R.I. and Barrett, E.J. “Insulin Regulates Brain Function, but How Does It Get There?,” *Diabetes* **2014**, *63*, 3992-3997.
172. Baskin, D.G.; Figlewicz, D.P.; Woods, S.C.; Porte Jr. D. and Dorsa, D.M. “Insulin in the brain,” *Annu. Rev. Physiol.* **1987**, *49*, 335–347.
173. Gasparini, L.; Gouras, G.K.; Wang, R.; Gross, R.S.; Beal, M.F.; Greengard, P. and Xu, H. “Stimulation of beta-amyloid precursor protein trafficking by insulin reduces intraneuronal beta-amyloid and requires mitogen-activated protein kinase signaling,” *J. Neurosci.* **2001**, *21*, 2561-2570.
174. Solano, D.C.; Sironi, M.; Bonfini, C.; Solerte, S.B.; Govoni, S. and Racchi, M. “Insulin regulates soluble amyloid precursor protein release via phosphatidyl inositol 3 kinase-dependent pathway,” *FASEB J.* **2000**, *14*, 1015–1022.
175. Malito, E.; Hulse, R.E. and Tang, W.J. “Amyloid beta-degrading cryptidases: insulin degrading enzyme, presequence peptidase and neprilysin,” *Cell Mol. Life Sci.* **2008**, *65*, 2574–2585.
176. Lesort, M. and Johnson, G.V. “Insulin-like growth factor-1 and insulin mediate transient site-selective increases in tau phosphorylation in primary cortical neurons,” *Neurosci.* **2000**, *99*, 305–316.
177. Lesort, M.; Jope, R.S. and Johnson, G.V. “Insulin transiently increases tau phosphorylation: involvement of glycogen synthase kinase-3beta and Fyn tyrosine kinase,” *J. Neurochem.* **1999**, *72*, 576–584.
178. Pani, G.; Giannoni, E.; Galeotti, T. and Chiarugi, P. “Redox-based escape mechanism from death: the cancer lesson,” *Antioxid. Redox Signal.* **2009**, *11*, 2791–2806.
179. Menendez, J.A.; Joven, J.; Cufí S.; Corominas-Faja, B.; Oliveras-Ferraros, C.; Cuyàs, E.; Martín-Castillo, B.; López-Bonet, E.; Alarcón, T. and Vazquez-Martin, A. “The warburg effect version 2.0: metabolic reprogramming of cancer stem cells,” *Cell Cycle* **2013**, *12*, 1166–1179.
180. Pacini, N. and Borziani, F. “Cancer stem cell theory and the warburg effect, two sides of the same coin?,” *Int. J. Mol. Sci.* **2014**, *15*, 8893-8930.
181. Warburg, O. “On the origin of cancer cells,” *Science* **1956**, *123*, 309–314.
182. Liou, G.Y. and Storz, P. “Reactive oxygen species in cancer,” *Free Radic. Res.* **2010**, *44*, 1-31.

183. Afanas'ev, I. "Reactive oxygen species signaling in cancer," *Aging Dis.* **2011**, *2*, 219-230.
184. Peng, X. and Gandhi, V. "ROS-activated anticancer prodrugs: a new strategy for tumor-specific damage," *Ther. Deliv.* **2012**, *3*, 823-833.
185. Ding, S.; Li, C.; Cheng, N.; Cui, X.; Xu, X. and Zhou, G. "Redox regulation in cancer stem cells," *Oxid. Med. Cell Longev.* **2015**, *2015*, doi: 10.1155/2015/750798.
186. Qanungo, S.; Das, M.; Haldar, S. and Basu, A. "Epigallocatechin-3-gallate induces mitochondrial membrane depolarization and caspase-dependent apoptosis in pancreatic cancer cells," *Carcinogenesis* **2005**, *26*, 958–967.
187. Zhang, R.; Humphreys, I.; Shau, R.P.; Shi, Y. and Srivastava, S.K. "In vitro and in vivo induction of apoptosis by capsaicin in pancreatic cancer cells is mediated through ROS generation and mitochondrial death pathway," *Apoptosis* **2008**, *13*, 1465–1478.
188. Donadelli, M.; Costanzo, C.; Beghelli, S.; Scupoli, M.T.; Dandrea, M.; Bonora, A.; Piacentini, P.; Budillon, A.; Caraglia, M.; Scarpa, A. and Palmieri, M. "Synergistic inhibition of pancreatic adenocarcinoma cell growth by trichostatin A and gemcitabine," *Biochim. Biophys. Acta* **2007**, *1773*, 1095–1106.
189. Sahu, R.P.; Zhang, R.; Batra, S.; Shi, Y. and Srivastava, S.K. "Benzyl isothiocyanate mediated generation of reactive oxygen species causes cell cycle arrest and induces apoptosis via activation of MAPK in human pancreatic cancer cells," *Carcinogenesis* **2009**, *30*, 1744-1753.
190. Carew, J.S.; Zhou, Y.; Albitar, M.; Carew, J.D.; Keating, M.J. and Huang, P. "Mitochondrial DNA mutations in primary leukemia cells after chemotherapy: clinical significance and therapeutic implications," *Leukemia* **2003**, *17*, 1437–1447.
191. Ampofo, E.; Rudzitis-Auth, J.; Dahmke, I.N.; Rössler, O.G.; Thiel, G.; Montenarh, M.; Menger, M.D. and Laschke, M.W. "Inhibition of protein kinase CK2 suppresses tumor necrosis factor (TNF)- $\alpha$ -induced leukocyte-endothelial cell interaction," *Biochim. Biophys. Acta.* **2015**, *1852*, 2123-2136.
192. Janeczko, M.; Orzesko, A.; Kazimierczuk, Z.; Szyszka, R. and Baier, A. "CK2 $\alpha$  and CK2 $\alpha'$  subunits differ in their sensitivity to 4, 5,6,7-tetrabromo- and 4,5,6,7 tetraiodo-1H-benzimidazole derivatives," *Eur. J. Med. Chem.* **2012**, *47*, 345-350.



193. Najda-Bernatowicz, A.; Lebska, M.; Orzesko, A.; Kopańska, K.; Krywińska, E.; Muszyńska, G. and Bretner, M. "Synthesis of new analogs of benzotriazole, benzimidazole and phthalimide—potential inhibitors of human protein kinase CK2," *Bioorg. Med. Chem.* **2009**, *17*, 1573-1578.
194. Ryu, S.Y. and Kim, S. "Evaluation of CK2 inhibitor (E)-3-(2, 3,4,5-tetrabromophenyl) acrylic acid (TBCA) in regulation of platelet function," *Eur. J. Pharmacol.* **2013**, *720*, 391-400.
195. Guerra, B. and Issinger, O.G. "Protein kinase CK2 and its role in cellular proliferation, development and pathology," *Electrophoresis* **1999**, *20*, 391-408.
196. Ahmed, K.; Gerber, D.A. and Cochet, C. "Joining the cell survival squad: an emerging role for protein kinase CK2," *Trends Cell Biol.* **2002**, *12*, 226-230.
197. Litchfield, D.W. "Protein kinase CK2: structure, regulation and role in cellular decisions of life and death," *Biochem. J.* **2003**, *369*, 1-15.
198. Pinna, L.A. "Protein kinase CK2: a challenge to canons," *J. Cell. Sci.* **2002**, *115*, 3873-3878.
199. Seldin, D. C. and Leder, P. "Casein kinase 2 alpha-induced murine lymphoma: relation to Teilleriosis in cattle," *Science* **1995**, *267*, 894-897.
200. Orlandini, M.; Semplici, F.; Ferruzzi, R.; Meggio, F.; Pinna, L.A. and Oliviero, S. "Protein kinase CK2alpha' is induced by serum as a delayed early gene and cooperates with Ha-ras in fibroblast transformation," *J. Biol. Chem.* **1998**, *273*, 21291-21297.
201. Lebrin, F.; Chambaz, E.M. and Bianchini, L. "A role for protein kinase CK2 in cell proliferation: evidence using a kinaseinactive mutant of CK2 catalytic subunit R," *Oncogene* **2001**, *20*, 2010-2022.
202. Meggio, F. and Pinna, L.A. "One-thousand-and-one substrates of protein kinase CK2?," *FASEB J.* **2003**, *17*, 349-368.
203. Wang, S. and Jones, K.A. "CK2 controls the recruitment of Wnt regulators to target genes in vivo," *Curr. Biol.* **2006**, *16*, 2239-2244.
204. Lin, C.Y.; Navarro, S.; Reddy, S. and Comai, L. "CK2-mediated stimulation of Pol I transcription by stabilization of UBF-SL1 interaction," *Nucleic Acids Res.* **2006**, *34*, 4752-4766.

205. Duncan, J.S.; Gyenis, L.; Lenehan, J.; Bretner, M.; Graves, L.M.; Haystead, T.A. and Litchfield, D.W. "An unbiased evaluation of CK2 inhibitors by chemoproteomics: characterization of inhibitor effects on CK2 and identification of novel inhibitor targets," *Mol. Cell. Proteom.* **2008**, *7*, 1077-1088.
206. Schaefer, S.; Svenstrup, T.H.; Fischer, M. and Guerra, B. "D11-Mediated Inhibition of Protein Kinase CK2 Impairs HIF-1 $\alpha$ -Mediated Signaling in Human Glioblastoma Cells," *Pharmaceuticals (Basel)* **2017**, *10*, doi: 10.3390/ph10010005.
207. Trembley, J.H.; Wang, G.; Unger, G.; Slaton, J. and Ahmed, K. "Protein kinase CK2 in health and disease: CK2: A key player in cancer biology," *Cell. Mol. Life Sci.* **2009**, *66*, 1858–1867.
208. Guerra, B.; Issinger, O.-G. "Protein kinase CK2 in human diseases," *Curr. Med. Chem.* **2008**, *15*, 1870–1886.
209. Lolli, G.; Cozza, G.; Mazzorana, M.; Tibaldi, E.; Cesaro, L.; Donella-Deana, A.; Meggio, F.; Venerando, A.; Franchin, C.; Sarno, S.; Battistutta, R. and Pinna, L.A. "Inhibition of Protein Kinase CK2 by Flavonoids and Tyrphostins. A Structural Insight," *Biochemistry* **2012**, *51*, 6097-6107.
210. Sarno, S.; de Moliner, E.; Ruzzene, M.; Pagano, M.A.; Battistutta, R.; Bain, J.; Fabbro, D.; Schoepfer, J.; Elliott, M.; Furet, P.; Meggio, F.; Zanotti, G. and Pinna, L.A. "Biochemical and three-dimensional-structural study of the specific inhibition of protein kinase CK2 by [5-oxo-5, 6-dihydroindolo-(1,2-a)quinazolin-7-yl]acetic acid (IQA)," *Biochem. J.* **2003**, *374*, 639-646.
211. Critchfield, J.W.; Coligan, J.E.; Folks, T.M. and Butera, S.T. "Casein kinase II as a selective target of HIV-1 transcriptional inhibitors," *Proc. Natl. Acad. Sci. U.S.A.* **1997**, *94*, 6110–6115.
212. Yim, H.; Lee, Y.H.; Lee, C.H. and Lee, S.K. "Emodin, an anthraquinone derivative isolated from the rhizomes of *Rheum palmatum*, selectively inhibits the activity of casein kinase II as a competitive inhibitor," *Planta Med.* **1999**, *65*, 9–13.
213. Janeczko, M.; Maslyk, M.; Kubiński, K. and Golczyk, H. "Emodin, a natural inhibitor of protein kinase CK2, suppresses growth, hyphal development and biofilm formation of *Candida albicans*," *Yeast* **2017**, *34*, 253-265.
214. Sarno, S.; Reddy, H.; Meggio, F.; Ruzzene, M.; Davies, S.P.; Donella-Deana, A.; Shugar, D. and Pinna, L.A. "Selectivity of 4,5,6,7-tetrabromobenzotriazole, an ATP site-directed inhibitor of protein kinase CK2 ('casein kinase-2')," *FEBS Lett.* **2001**, *496*, 44-48.

215. Pagano, M.A.; Andrzejewska, M.; Ruzzene, M.; Sarno, S.; Cesaro, L.; Bain, J.; Elliott, M.; Meggio, F.; Kazimierczuk, Z. and Pinna, L. A. "Optimization of protein kinase CK2 inhibitors derived from 4,5,6,7-tetrabromobenzimidazole," *J. Med. Chem.* **2004**, *47*, 6239-6247.
216. Meggio, F.; Pagano, M.A.; Moro, S.; Zagotto, G.; Ruzzene, M.; Sarno, S.; Cozza, G.; Bain, J.; Elliott, M.; Deana, A.D.; Brunati, A.M. and Pinna, L.A. "Inhibition of protein kinase CK2 by condensed polyphenolic derivatives. An in vitro and in vivo study," *Biochemistry* **2004**, *43*, 12931-12936.
217. Ellman, G.L.; Courtney, K.D.; Andres, B.J. and Featherstone, R.M. "A new and rapid colorimetric determination of acetylcholinesterase activity," *Biochem. Pharmacol.* **1961**, *7*, 88-95.
218. Komersova, A.; Komersa, K. and Cegan, A. "New findings about Ellman's method to determine cholinesterase activity," *Z Naturforsch C.* **2007**, *62*, 150-154.
219. Walmsley, T.A.; Abernethy, M.H. and Fitzgerald, H.P. "Effect of daylight on the reaction of thiols with Ellman's reagent, 5,5'-dithiobis(2-nitrobenzoic acid)," *Clin. Chem.* **1987**, *33*, 1928-1931.
220. Apak, R.; Özyürek, M.; Güçlü, K. and Çapanoğlu, E. "Antioxidant Activity/Capacity Measurement. 1. Classification, Principles, Mechanisms and Electron Transfer (ET)-Based Assays," *J. Agric. Food. Chem.* **2016**, *64*, 997-1027.
221. Mayer, J.M.; Hrovat, D.A.; Thomas, J.L. and Borden, W.T. "Proton-coupled electron transfer versus hydrogen atom transfer in benzyl/toluene, methoxyl/methanol and phenoxyl/ phenol self-exchange reactions," *J. Am. Chem. Soc.* **2002**, *124*, 11142-11147.
222. Lu, J.M.; Lin, P.; Yao, Q. and Chen, C. "Chemical and molecular mechanisms of antioxidants: experimental approaches and model systems," *J. Cell. Mol. Med.* **2010**, *14*, 840-860.
223. Ou, B.; Huang, D.; Hampsch-Woodill, M.; Flanagan, J.A. and Deemer, E.K. "Analysis of antioxidant activities of common vegetables employing oxygen radical absorbance capacity (ORAC) and ferric reducing antioxidant power (FRAP) assays: a comparative study," *J. Agric. Food Chem.* **2002**, *50*, 3122-3128.
224. Glazer, A. N. "Phycoerythrin fluorescence-based assay for reactive oxygen species," *Methods Enzymol.* **1990**, *186*, 161-168.

225. Cao, G.; Alessio, H.M. and Cutler, R.G. "Oxygen-radical absorbance capacity assay for antioxidants," *Free Radic. Biol. Med.* **1993**, *14*, 303– 311.
226. Huang, D.; Ou, B.; Hampsch-Woodill, M.; Flanagan, J.A. and Prior, R.L. "High-Throughput Assay of Oxygen Radical Absorbance Capacity (ORAC) Using a Multichannel Liquid Handling System Coupled with a Microplate Fluorescence Reader in 96-Well Format," *J. Agric. Food Chem.* **2002**, *50*, 4437-4444.
227. Schmittschmitt, J.P. and Scholtz, J.M. "The role of protein stability, solubility and net charge in amyloid fibril formation," *J. Mol. Biol.* **1996**, *256*, 870–877.
228. Hortschansky, P.; Schroeckh, V.; Christopeit, T.; Zandomenighi, G. and Fandrich, M. "The aggregation kinetics of Alzheimer's  $\beta$ -Amyloid peptide is controlled by stochastic nucleation," *Prot. Sci.* **2005**, *14*, 1753-1759.
229. Lomakin, A.; Teplow, D.B.; Kirschner, D.A. and Benedek, G.B. "Kinetic theory of fibrillogenesis of amyloid  $\beta$ -protein," *Proc. Natl. Acad. Sci. USA* **1997**, *94*, 7942-7947.
230. Iannuzzi, C.; Borriello, M.; Portaccio, M. Irace, G. and Sirangelo, I. "Insights into insulin fibril assembly at physiological and acidic pH and related amyloid intrinsic fluorescence," *Int. J. Mol. Sci.* **2017**, *18*, doi: 10.3390/ijms18122551.
231. Bolder, S.G.; Sagis, L.M.; Venema, P. and van der Linden, E. "Thioflavin T and birefringence assays to determine the conversion of proteins into fibrils," *Langmuir* **2007**, *23*, 4144–4147.
232. Hawe, A.; Sutter, M. and Jiskoot, W. "Extrinsic fluorescent dyes as tools for protein characterization," *Pharm. Res.* **2008**, *25*, 1487–1499.
233. LeVine III, H. "Thioflavine T interactions with amyloid  $\beta$ -sheet structures," *Amyloid* **1995**, *2*, 1–6.
234. Krebs, M.R.H.; Bromley, E.H.C. and Donald, A.M. "The binding of thioflavin-T to amyloid fibrils: localization and implications," *J. Struct. Biol.* **2005**, *149*, 30-37.
235. Hudson, S.A.; Ecroyd, H.; Kee, T.W. and Carver, J.A. "The Thioflavin-T fluorescence assay for amyloid fibril detection can be biased by the presence of exogenous compounds," *FEBS J.* **2009**, *276*, 5960-5972.
236. Eisert, R.; Felau, L. and Brown, L. "Methods for enhancing the accuracy and reproducibility of Congo red and thioflavin-T assays," *Anal. Biochem.* **2006**, *353*, 144-146.

237. Morton, K.C. and Baker, L.A. "Atomic force microscopy-based bioanalysis for the study of disease," *Anal. Methods* **2014**, *6*, 4932–4955.
238. Eaton, P. and West P. "Atomic Force Microscopy," in *Atomic Force Microscopy* (Eaton, P. and West P.). **2010**, Oxford University Press.
239. Stine, W.B.; Snyder, S.W.; Ladrer, U.S.; Wade, W.S.; Miller, M.F.; Perun, T.J.; Holzman, T.F. and Kraftt, G.A. "The nanometer-scale structure of amyloid-beta visualized by atomic force microscopy," *J. Protein Chem.* **1996**, *15*, 193-203.
240. Iannuzzi, C.; Borriello, M.; Irace, G.; Cammarota, M. and Sirangelo, I. "Vanillin affects amyloid aggregation and non-enzymatic glycation in human insulin," *Sci. Rep.* **2017**, *7*, doi: 10.1038/s41598-017-15503-5.
241. Yoshihara, H.; Saito, J.; Tanabe, A.; Amada, T.; Kitagawa, K. and Asada, S. "Characterization of novel insulin fibrils that show strong cytotoxicity under physiological pH," *J. Pharm. Sci.* **2016**, *105*, 1419-1426.
242. <http://rsbweb.nih.gov/ij/download.html> (accessed on 03-19-2018).
243. <https://imagej.nih.gov/ij/docs/guide/user-guide.pdf> (accessed on 03-19-2018).
244. Mierts, S.; Scrocco, E. and Tomasi, J. "Electrostatic interaction of a solute with a continuum. A direct utilization of AB initio molecular potentials for the prevision of solvent effects," *Chem. Phys.* **1981**, *55*, 117–129.
245. Wolinski, K.; Hilton, J.F. and Pulay, P. "Efficient implementation of the gauge-independent atomic orbital method for NMR chemical shift calculations," *J. Am. Chem. Soc.* **1990**, *112*, 8251–8260.
246. Hansch, C.; Leo, A. and Taft, W. "A survey of Hammett substituent constants and resonance and field parameters," *Chem. Rev.* **1991**, *91*, 165-195.
247. Becke, A.D. "Density-functional exchange-energy approximation with correct asymptotic behavior," *Phys. Rev. A.* **1988**, *38*, 3098-3100.
248. Lee, C.; Yang, W. and Parr, R.G. "Development of the Colle-Salvetti correlation-energy formula into a functional of the electron density," *Phys. Rev. A.* **1988**, *37*, 785-789.

249. Gaussian 16, Revision B.01, Frisch, M. J.; Trucks, G. W.; Schlegel, H. B.; Scuseria, G. E.; Robb, M. A.; Cheeseman, J. R.; Scalmani, G.; Barone, V.; Petersson, G. A.; Nakatsuji, H.; Li, X.; Caricato, M.; Marenich, A. V.; Bloino, J.; Janesko, B. G.; Gomperts, R.; Mennucci, B.; Hratchian, H. P.; Ortiz, J. V.; Izmaylov, A. F.; Sonnenberg, J. L.; Williams-Young, D.; Ding, F.; Lipparini, F.; Egidi, F.; Goings, J.; Peng, B.; Petrone, A.; Henderson, T.; Ranasinghe, D.; Zakrzewski, V. G.; Gao, J.; Rega, N.; Zheng, G.; Liang, W.; Hada, M.; Ehara, M.; Toyota, K.; Fukuda, R.; Hasegawa, J.; Ishida, M.; Nakajima, T.; Honda, Y.; Kitao, O.; Nakai, H.; Vreven, T.; Throssell, K.; Montgomery, J. A., Jr.; Peralta, J. E.; Ogliaro, F.; Bearpark, M. J.; Heyd, J. J.; Brothers, E. N.; Kudin, K. N.; Staroverov, V. N.; Keith, T. A.; Kobayashi, R.; Normand, J.; Raghavachari, K.; Rendell, A. P.; Burant, J. C.; Iyengar, S. S.; Tomasi, J.; Cossi, M.; Millam, J. M.; Klene, M.; Adamo, C.; Cammi, R.; Ochterski, J. W.; Martin, R. L.; Morokuma, K.; Farkas, O.; Foresman, J. B.; Fox, D. J. Gaussian, Inc., Wallingford CT, 2016.
250. Ishida, J.; Wang, H.K.; Bastow, K.F.; Hu, C.Q. and Lee, K.H. "Antitumor agents 201. Cytotoxicity of harmine and beta-carboline analogs," *Bioorg. Med. Chem. Lett.* **1999**, *9*, 3319-3324.
251. Chen, H.; Gao, P.; Zhang, M.; Liao, W. and Zhang, J. "Synthesis and biological evaluation of a novel class of  $\beta$ -carboline derivatives," *New J. Chem.* **2014**, *38*, 4155-4166.
252. Chen, Y.F.; Lin, Y.C.; Chen, J.P.; Chan, H.C.; Hsu, M.H.; Lin, H.Y.; Kuo, S.C. and Huang, L.J. "Synthesis and biological evaluation of novel 3,9-substituted  $\beta$ -carboline derivatives as anticancer agents," *Bioorg. Med. Chem. Lett.* **2015**, *25*, 3873-3877.
253. Gohil, V.M.; Brahmabhatt, K.G.; Loiseau, P.M. and Bhutani, K.K. "Synthesis and anti-leishmanial activity of 1-aryl- $\beta$ -carboline derivatives against *Leishmania donovani*," *Bioorg. Med. Chem. Lett.* **2012**, *22*, 3905-3907.
254. Gellis, A.; Dumètre, A.; Lanzada, G.; Hutter, S.; Ollivier, E.; Vanelle, P. and Azas, N. "Preparation and antiprotozoal evaluation of promising  $\beta$ -carboline alkaloids," *Biomed. Pharmacother.* **2012**, *66*, 339-347.
255. Espinoza-Moraga, M.; Caballero, J.; Gaube, F.; Winckler, T. and Santos, L.S. "1-Benzyl-1,2,3,4-Tetrahydro- $\beta$ -Carboline as Channel Blocker of N-Methyl-d-Aspartate Receptors," *Chem. Biol. Drug Des.* **2012**, *79*, 594-599.
256. May, A.C.; Fleischer, W.; Kletke, O.; Haas, H.L. and Sergeeva, O.A. "Benzodiazepine-site pharmacology on GABAA receptors in histaminergic neurons," *Br. J. Pharmacol.* **2013**, *170*, 222-232.

257. Francik, R.; Kazek, G.; Cegla, M. and Stepniewski, M. "Antioxidant activity of beta-carboline derivatives," *Acta Pol. Pharm.* **2011**, *68*, 185-189.
258. Kulkarni, A.; Abid, M.; Török, B. and Huang, X. "A direct synthesis of [beta]-carbolines via a three-step one-pot domino approach with a bifunctional Pd/C/K-10 catalyst," *Tetrahedron Lett.* **2009**, *50*, 1791-1794.
259. LeVine III, H. "Biotin-avidin interaction-based screening assay for Alzheimer's beta-peptide oligomer inhibitors," *Anal. Biochem.* **2006**, *356*, 265-272.
260. LeVine III, H. Ding, Q. Walker, J.A. Voss, R.S. and Augelli-Szafran, C.E. "Clioquinol and other hydroxyquinoline derivatives inhibit A beta(1-42) oligomer assembly," *Neurosci Lett.* **2009**, *465*, 99-103.
261. Glide, version 6.8. New York, NY: Schrödinger, LLC; **2015**.
262. Lohning, A.E.; Levonis, S.M.; Williams-Noonan, B. and Schweilker, S.S. "A practical guide to molecular docking and homology modelling for medicinal chemists," *Curr. Top Med. Chem.* **2017**, *17*, 2023-2040.
263. Çakır, B.; Dağ, Ö.; Yıldırım, E.; Erol, K. and Şahin, M.F. "Synthesis and anticonvulsant activity of some hydrazones of 2-[(3H)-oxobenzoxazolin-3-yl-aceto]hydrazide," *J. Fac. Pharm. Gazi.* **2001**, *18*, 99-106.
264. Morjan, R.Y.; Mkadmh, A.M.; Beadham, J.; Elmanama, A.A.; Mattar, M.R.; Raftery, J.; Pritchard, R.G.; Awadallah, A. and Gardiner, J.M. "Antibacterial activities of novel nicotinic acid hydrazides and their conversion into N-acetyl-1,3,4-oxadiazoles," *Bioorg. Med. Chem. Lett.* **2014**, *24*, 5796-5800.
265. Özdemir, A.; Turan-Zitouni, G.; Kaplancikli, Z.A. and Tunalı, Y. "Synthesis and biological activities of new hydrazide derivatives," *J. Enzyme Inhib. Med. Chem.* **2009**, *24*, 825-831.
266. Török, B.; Sood, A.; Bag, S.; Tulsan, R.; Ghosh, S.; Borkin, D.; Kennedy, A.; Melanson, M.; Madden, R.; Zhou, W.; LeVine III, H. and Török M. "Diaryl hydrazones as multifunctional inhibitors of amyloid self-assembly," *Biochemistry* **2013**, *52*, 1137-1148.
267. Greig, N.H. "Drug entry into the brain and its pharmacological manipulation," in Bradbury M.W.B. (Ed.) *Physiology and Pharmacology of the Blood-Brain Barrier*. Springer-Verlag, New York; **1992**, 487-524.

268. Bonina, F.P.; Arenare, L.; Palagiano, F.; Saija, A.; Nava, F.; Trombetta, D.; De Caprariis, P. Synthesis, stability and pharmacological evaluation of nipecotic acid prodrugs," *J. Pharm. Sci.* **1999**, *88*, 561–567.
269. Hellenbrand, T.; Höfner, G.; Wein, T.; Wanner, K.T. "Synthesis of 4-substituted nipecotic acid derivatives and their evaluation as potential GABA uptake inhibitors," *Bioorg. Med. Chem.* **2016**, *24*, 2072–2096.
270. Padmini, K.; Preethi, P.J.; Divya, M.; Rohini, P.; Lohita, M.; Swetha, K. and Kaladar, P. "A review on biological importance of hydrazones," *Int. J. Pharm. Res. Rev.* **2013**, *1*, 43–58.
271. Belskaya, N.P.; Dehaen, W. and Bakuleva, V.A. "Synthesis and properties of hydrazones bearing amide, thioamide and amidine functions," *Arkivoc* **2010**, *2010*, 275–332.
272. Lima, P.C.; Lima, L.M.; Silva, K.C.; Leda, P.H.; Miranda, A.L.P.; Fraga, C.A.M. and Barreiro, E.J. "Synthesis and analgesic activity of novel N-acylhydrazones and isosters, derived from natural saffrole," *Eur. J. Med. Chem.* **2000**, *35*, 187–203.
273. Mangialasche, F.; Solomon, A.; Winblad, B.; Mecocci, P. and Kivipelto, M. "Alzheimer's disease: Clinical trials and drug development," *Lancet Neurol.* **2010**, *9*, 702–716.
274. Kryger, G.; Silman, I. and Sussman, J.L. "Structure of acetylcholinesterase complexed with E2020 (Aricept): Implications for the design of new anti-Alzheimer drugs," *Structure* **1999**, *7*, 297–307.
275. Martorana, A.; Giacalone, V.; Bonsignore, R.; Pace, A.; Gentile, C.; Pibiri, I.; Buscemi, S.; Lauria, A. and Palumbo Piccionello, A. "Heterocyclic scaffolds for the treatment of Alzheimer's disease," *Curr. Pharm. Des.* **2016**, *22*, 3971–3995.
276. Silva, A.G.; Zapata-Sudo, G.; Kummerle, A.E.; Fraga, C.A.M.; Barreiro, E.J. and Sudo, R.T. "Synthesis and vasodilatory activity of new N-acylhydrazones derivatives, designed as LASSBio-294 analogues," *Bioorg. Med. Chem.* **2005**, *13*, 3431–3437.
277. Ismail, M.M.; Kamel, M.M.; Mohamed, L.W. and Faggal, S.I. "Synthesis of new indole derivatives structurally related to donepezil and their biological evaluation as acetylcholinesterase inhibitors," *Molecules* **2012**, *17*, 4811–4823.
278. Sanner, M.F. Python: A programming language for software integration and development. *J. Mol. Graph. Model.* **1999**, *17*, 57–61.



279. Dimmock, J.R.; Vashishtha, S.C. and Stables, J.P. "Anticonvulsant properties of various acetylhydrazones, oxamoylhydrazones and semicarbazones derived from aromatic and unsaturated carbonyl compounds," *Eur. J. Med. Chem.* **2000**, *35*, 241-248.
280. Ragavendran, J.; Sriram, D.; Patel, S.; Reddy, I.; Bharathwajan, N.; Stables, J. and Yogeeswari, P. "Design and synthesis of anticonvulsants from a combined phthalimide-GABA-anilide and hydrazone pharmacophore," *Eur. J. Med. Chem.* **2007**, *42*, 146-151.
281. Todeschini, A.R.; Miranda, A.L.; de Silva, K.C.; Parrini, S.C. and Barreiro, E.J. "Synthesis and evaluation of analgesic, antiinflammatory and antiplatelet properties of new 2pyridylarylhydrazone derivatives," *Eur. J. Med. Chem.* **1998**, *33*, 189-199.
282. Özkay, Y.; Tunah, Y.; Karaca, H. and Işıkdag, İ. "Antimicrobial activity and a SAR study of some novel benzimidazole derivatives bearing hydrazone moiety," *Eur. J. Med. Chem.* **2010**, *45*, 3293–3298.
283. Subhashini, N.J.P.; Janaki, P. and Bhadrachari, B. "Synthesis of hydrazone derivatives of benzofuran and their antibacterial and antifungal activity," *Russ. J. Gen. Chem.* **2017**, *87*, 2021-2026.
284. Mandewale, M.C.; Thorat, B.; Shelke, D. and Yamgar, R. "Synthesis and Biological Evaluation of New Hydrazone Derivatives of Quinoline and Their Cu(II) and Zn(II) Complexes against Mycobacterium tuberculosis," *Bioinorg. Chem. Appl.* **2015**, *2015*, doi: 10.1155/2015/153015.
285. Zhang, J.P.; Li, X.Y.; Dong, Y.W.; Qin, Y.G.; Li, X.L.; Song, B.A. and Yang, X.L. "Synthesis and biological evaluation of 4-methyl-1,2,3-thiadiazole-5-carboxaldehyde benzoyl hydrazone derivatives," *Chin. Chem. Lett.* **2017**, *28*, 1238-1242.
286. Walcourt, A.; Loyevsky, M.; Lovejoy, D.B.; Gordeuk, V.R. and Richardson, D.R. "Novel aroylhydrazone and thiosemicarbazone iron chelators with anti-malarial activity against chloroquine-resistant and -sensitive parasites," *Int. J. Biochem. Cell Biol.* **2004**, *36*, 401-407.
287. Paiva, S.A. and Russell, R.M. "Beta-carotene and other carotenoids as antioxidants," *J. Am. Coll. Nutr.* **1999**, *18*, 426–433.

288. Hegazy, W.H. "Synthesis and structural studies of some  $\beta$ -diketone Schiff bases phenylhydrazones and some of their metal complexes with Co (II), Ni (II) and Cu (II) ions," *Monatsh. Chem.* **2001**, *132*, 639-650.
289. Alov, P.; Tsakova, I. and Pajeva, I. "Computational studies of free radical-scavenging properties of phenolic compounds," *Curr. Top Med. Chem.* **2015**, *15*, 85–104.
290. Rodriguez, S.A. and Baumgartner, M.T. "Theoretical study of reaction mechanism of a series of 4-hydroxycoumarins against the DPPH radical," *Chem. Phys. Lett.* **2014**, *601*, 116-123.
291. Kareem, H.S.; Ariffin, A.; Nordin, N.; Heidelberg, T.; Abdul-Aziz, A.; Wong, K.W. and Yehye, W.A. "Correlation of antioxidant activities with theoretical studies for new hydrazone compounds bearing a 3, 4, 5-trimethoxy benzyl moiety," *Eur. J. Med. Chem.* **2015**, *103*, 497–505.
292. Rouaiguia-Bouakkaz, S. and Benayahoum, A. "The antioxidant activity of 4-hydroxycoumarin derivatives and some sulfured analogs," *J. Phys. Org. Chem.* **2015**, *28*, 714–722.
293. Manach, C.; Scalbert, A.; Morand, C.; Rémésy, C. and Jiménez, L. "Polyphenols: food sources and bioavailability," *Am. J. Clin. Nutr.* **2004**, *79*, 727-747.
294. Shahidi, F. and Ambigaipalan, P. "Phenolics and polyphenolics in foods, beverages and spices: antioxidant activity and health effects – a review," *J. Funct. Foods* **2015**, *18*, 820-897.
295. Klein, E.; Lukeš, V.; Cibulková, Z. and Polovková, J. "Study of N–H, O–H and S–H bond dissociation enthalpies and ionization potentials of substituted anilines, phenols and thiophenols," *J. Mol. Struct.* **2006**, *758*, 149-159.
296. Bordwell, F.G.; Zhang, X.M. and Cheng, J.P. "Bond dissociation energies of the nitrogen-hydrogen bonds in anilines and in the corresponding radical anions. Equilibrium acidities of aniline radical cations," *J. Org. Chem.* **1993**, *58*, 6410-6416.
297. Saqib, M.; Mahmood, A.; Akram, R.; Khalid, B.; Afzal, S. and Kamal, G.M. "Density functional theory for exploring the structural characteristics and their effects on the antioxidant properties," *J. Pharm. Appl. Chem.* **2015**, *1*, 65-71.
298. Leopoldini, M.; Russo, N. and Toscano, M. "The molecular basis of working mechanism of natural polyphenolic antioxidants," *Food Chem.* **2011**, *125*, 288-306.

299. Mazzone, G.; Malaj, N.; Russo, N. and Toscano, M. "Density functional study of the antioxidant activity of some recently synthesized resveratrol analogues," *Food Chem.* **2013**, *141*, 2017-2024.
300. Alaşalvar, C.; Soylu, M.S.; Güder, A.; Albayrak, Ç.; Apaydin, G. and Dilek, N. "Crystal structure, DFT and HF calculations and radical scavenging activities of (E)-4,6-dibromo-3-methoxy-2-[(3-methoxyphenylimino)methyl]phenol," *Spectrochim. Acta. A: Mol. Biomol. Spectr.* **2014**, *125*, 319-327.
301. Szeląg, M.; Mikulski, D. and Molski, M. "Quantum-chemical investigation of the structure and the antioxidant properties of  $\alpha$ -lipoic acid and its metabolites," *J. Mol. Model.* **2012**, *18*, 2907-2916.
302. Kirk, K.L. "Fluorine in medicinal chemistry: Recent therapeutic applications of fluorinated small molecules," *J. Fluorine Chem.* **2006**, *127*, 1013-1029.
303. Hagmann, W.K. "The many roles for fluorine in medicinal chemistry," *J. Med. Chem.* **2008**, *51*, 4359-4369.
304. Wang, J.; Sánchez-Roselló, M.; Aceña, J.L.; del Pozo, C.; Sorochinsky, A.E.; Fustero, S.; Soloshonok, V.A. and Liu, H. "Fluorine in pharmaceutical industry: fluorine-containing drugs introduced to the market in the last decade (2001–2011)," *Chem. Rev.* **2014**, *114*, 2432-2506.
305. Reid, D.G. and Murphy, P.S. "Fluorine magnetic resonance in vivo: A powerful tool in the study of drug distribution and metabolism," *Drug Discovery Today* **2008**, *13*, 473-480.
306. Jones, O.G. and Mezzenga, R. "Inhibiting, promoting and preserving stability of functional protein fibrils," *Soft Matter* **2012**, *8*, 876-895.
307. Tycko, R. and Wickner, R.B. "Molecular structures of amyloid and prion fibrils: consensus versus controversy," *Acc. Chem. Res.* **2013**, *46*, 1487-1496.
308. Frare, E.; de Laureto, P.P.; Zurdo, J.; Dobson, C.M. and Fontana, A. "A highly amyloidogenic region of hen lysozyme," *J Mol. Biol.* **2004**, *340*, 1153-1165.
309. Zou, Y.; Li, Y.; Hao, W.; Hu, X. and Ma, G. "Parallel  $\beta$ -sheet fibril and antiparallel  $\beta$ -sheet oligomer: New insights into Amyloid Formation of Hen Egg White Lysozyme under Heat and Acidic Condition from FTIR Spectroscopy," *J. Phys. Chem. B* **2013**, *117*, 4003-4013.

310. Holley, M.; Eginton, C.; Schaefer, D. and Brown, L.R. "Characterization of amyloidogenesis of hen egg lysozyme in concentrated ethanol solution," *Biochem. Biophys. Res. Commun.* **2008**, 373, 164-168.

## BIBLIOGRAPHY

<https://www.alz.org/facts/#personalFinancialImpact> (accessed on 03-19-2018).

<http://www.diabetes.org/diabetes-basics/statistics/> (accessed on 03-19-2018).

Siegel, R.L.; Miller, K.D. and Jemal, A. "Cancer Statistics, 2018," *CA: Cancer J. Clin.* **2018**, *68*, doi: 10.3322/caac.21442

Kandimalla, R.; Thirumala, V. and Reddy, P.H. "Is Alzheimer's disease a Type 3 Diabetes A critical appraisal," *Biochim. Biophys. Acta Mol. Basis Dis.* **2017**, *1863*, 1078-1089.

Larner, A.J. "Cholinesterase inhibitors: beyond Alzheimer's disease," *Expert Rev. Neurother.* **2010**, *10*, 1699-1705.

Francis, P.T.; Ramirez, M.J. and Lai, M.K. "Neurochemical basis for symptomatic treatment of Alzheimer's disease," *Neuropharmacol.* **2010**, *59*, 221-229.

Darvesh, H. Hopkins, D.A. and Geula, C. "Neurobiology of butyrylcholinesterase," *Nat. Rev. Neurosci.* **2003**, *4*, 131-138.

Riviere, C.; Delaunay, J.C.; Immel, F.O.; Cullin, C. and Monti, J.P. "The polyphenol piceid destabilizes preformed amyloid fibrils and oligomers in vitro: hypothesis on possible molecular mechanisms," *Neurochem. Res.* **2009**, *34*, 1120-1128.

Ono, K.; Hirohata, M. and Yamada, M. "Ferulic acid destabilizes preformed  $\beta$ amyloid fibrils in vitro," *Biochem. Biophys. Res. Commun.* **2005**, *336*, 444-449.

Matsunaga, S. Kishi, T. and Iwata, N. "Combination therapy with cholinesterase inhibitors and memantine for Alzheimer's disease: a systematic review and meta-analysis," *Int. J. Neuropsychopharmacol.* **2014**, *18*, doi: 10.1093/ijnp/pyu115.

Atri, A.; Shaughnessy, L.W.; Locascio, J.J. and Growdon, J.H. "Long-term course and effectiveness of combination therapy in Alzheimer disease," *Alzheimer Dis. Assoc. Disord.* **2008**, *22*, 209-221.

Schmitt, B.; Bernhardt, T.; Moeller, H.J.; Heuser, I. and Frölich, L. "Combination therapy in Alzheimer's disease: a review of current evidence," *CNS Drugs* **2004**, *18*, 827-844.

Vogelstein, B. and Kinzler, K.W. "Cancer genes and the pathways they control," *Nat. Med.* **2004**, *10*, 789-799.

Reya, T.; Morrison, S.J.; Clarke, M.F. and Weissman, I.L. "Stem cells, cancer and cancer stem cells," *Nature* **2001**, *414*, 105-111.

Hanahan, D. and Weinberg, R.A. "Hallmarks of cancer: the next generation," *Cell* **2011**, *144*, 646-674.

Wang, J.; Liu, Q.; Yuan, S.; Xie, W.; Liu, Y.; Xiang, Y.; Wu, N.; Wu, L.; Ma, X.; Cai, T.; Zhang, Y.; Sun, Z. and Li, Y. "Genetic predisposition to lung cancer: comprehensive literature integration, meta-analysis and multiple evidence assessment of candidate-gene association studies," *Sci. Rep.* **2017**, *7*, doi:10.1038/s41598-017-07737-0.

Ramsay, R.R.; Popovic-Nikolic, M.R.; Nikolic, K.; Uliassi, E. and Bolognesi, M.L. "A perspective on multi-target drug discovery and design for complex diseases," *Clin. Transl. Med.* **2018**, *7*, doi: 10.1186/s40169-017-0181-2.

Bag, S.; Ghosh, S.; Tulsan, R.; Sood, A.; Zhou, W.; Schifone, C. and Foster, M. "Design, Synthesis and Biological Activity of Multifunctional  $\alpha,\beta$ -Unsaturated Carbonyl Scaffolds for Alzheimer's Disease," *Bioorg. Med. Chem. Lett.* **2013**, *23*, 2614-2618.

Schüttelkopf, A.W. and van Aalten, D.M. "PRODRG: a tool for high-throughput crystallography of protein-ligand complexes," *Acta Crystallogr. D. Biol. Crystallogr.* **2004**, *60*, 1355-1363.

Kumar, P.; Kadyan, K.; Duhan, M.; Sindhu, J.; Singh, V. and Saharan, B.S. "Design, synthesis, conformational and molecular docking study of some novel acyl hydrazone based molecular hybrids as antimalarial and antimicrobial agents," *Chem. Cent. J.* **2017**, *11*, doi: 10.1186/s13065-017-0344-7.

Apak, R.; Özyürek, M.; Güçlü, K. and Çapanoğlu, E. "Antioxidant Activity/Capacity Measurement. 2. Hydrogen Atom Transfer (HAT)-Based, Mixed-Mode (Electron Transfer (ET)/HAT) and Lipid Peroxidation Assays.," *J. Agric. Food. Chem.* **2016**, *64*, 1028-1045.

Valko, M.; Leibfritz, D.; Moncol, J.; Cronin, M.T.D.; Mazur, M. and Telser, J. "Free radicals and antioxidants in normal physiological functions and human disease," *Int. J. Biochem. Cell. Biol.* **2007**, *39*, 44–84.

Forman, H.J.; Augusto, O.; Brigelius-Flohe, R.; Dennery, P.A.; Kalyanaraman, B.; Ischiropoulos, H.; Mann, G.E.; Radi, R.; Roberts, L.J. 2<sup>nd</sup>; Vina, J. and Davies, K.J. "Even free radicals should follow some rules: a guide to free radical research terminology and methodology," *Free. Radic. Biol. Med.* **2015**, *78*, 233–235.

- Peerannawar, S.; Horton, W.; Kokel, A.; Török, F.; Török, M and Török, B. "Theoretical and Experimental Analysis of the Antioxidant Features of Diarylhydrazones," *Struct. Chem.* **2017**, *28*, 391-402.
- Gorantla, V.; Gundla, R.; Jadav, S.S.; Anugu, S.R.; Chimakurthy, J.; Nidasanametlab, S.K. and Korupolu, R. "Molecular hybrid design, synthesis and biological evaluation of N-phenyl sulfonamide linked N-acyl hydrazone derivatives functioning as COX-2 inhibitors: new anti-inflammatory, anti-oxidant and anti-bacterial agents," *New J. Chem.* **2017**, *41*, 13516-13532.
- Domalaon, R.; Idowu, T.; Zhanel, G.G. and Schweizer, F. "Antibiotic hybrids: the next generation of agents and adjuvants against gram-negative pathogens?," *Clin. Microbiol. Rev.* **2018**, *31*, doi: 10.1128/CMR.00077-17.
- Ferchtat, L.L and Makhove, N.N. "Molecular hybridization tools in the development of furoxan-based NO-donor prodrugs," *ChemMedChem.* **2017**, *12*, doi: 10.1002/cmdc.201700113.
- Moaedzadeh, S.; Madadlou, A. and Khosrowshahi asl, A. "Formation mechanisms, handling and digestibility of food protein nanofibrils," *Trends Food Sci. Technol.* **2015**, *45*, 50-59.
- McAllister, C.; Karymov, M.; Kawano, Y.; Lushnikov, A.Y.; Mikheykin, A.; Uversky, V. and Lyubchenko, Y. "Protein Interactions and Misfolding Analyzed by AFM Force Spectroscopy," *J. Mol. Biol.* **2006**, *354*, 1028-1042.
- Murray, R.K.; Bender, D.A.; Botham, K.M.; Kennely, P.J. Rodwell, V.W. and Weil, P.A. "Free radicals and antioxidant nutrients," *Harper's Illustrated Biochemistry*. McGraw-Hill Companies, Inc; **2012**, p. 543–548.
- Pisoschi, A.M. and Pop, A. "The role of antioxidants in the chemistry of oxidative stress: a review," *Eur. J. Med. Chem.* **2015**, *97*, 55–74.
- Delanty, N. and Dichter, M.A. "Oxidative injury in the nervous system," *Acta. Neurol. Scand.* **1998**, *98*, 145-153.
- Foyer, C.H "Redox homeostasis and antioxidant signaling: a metabolic interface between stress perception and physiological responses," *Plant Cell* **2005**, *17*, 1866-1875.
- Rajendran, P.; Nandakumar, N.; Rengarajan, T.; Palaniswami, R.; Gnanadhas, E.N.; Lakshminarasiah, U.; Gopas, J. and Nishigaki, I. "Antioxidants and human diseases," *Clin. Chim. Acta.* **2014**, *436*, 332-347.

- Halliwell, B. and Gutteridge, J.M. "Role of free radicals and catalytic metal ions in human disease: an overview," *Methods Enzymol.* **1990**, *186*, 1-85.
- Lin, M. and Beal, M.F. "Mitochondrial dysfunction and oxidative stress in neurodegenerative diseases," *Nature* **2006**, *443*, 787-795.
- Ames, B.; Shigenaga, M. and Hagen, T. "Oxidants, antioxidants and the degenerative diseases of aging," *Proc. Natl. Acad. Sci. U.S.A.* **1993**, *90*, 7915-7922.
- Reuter, S.; Gupta, S.; Chaturvedi, M.M. and Aggarwal, B.B. "Oxidative stress, inflammation and cancer: how are they linked?" *Free Radic. Biol. Med.* **2010**, *49*, 1603-1616.
- Kelsey, N.A.; Wilkins, H.M. and Linseman, D.A. "Nutraceutical antioxidants as novel neuroprotective agents," *Molecules* **2010**, *15*, 7792-7814.
- Galkina, O.V. "The specific features of free-radical processes and the antioxidant defense in the adult brain," *Neurochem. J.* **2013**, *7*, 89-97.
- Dröge, W. "Free Radicals in the Physiological Control of Cell Function," *Physiol. Rev.* **2002**, *82*, 47-95.
- Knight, J.A. "Review: Free radicals, antioxidants and the immune system," *Ann. Clin. Lab Sci.* **2000**, *30*, 145-158.
- Hensley, K.; Robinson, K.A.; Gabbita, S.P.; Salsman, S. and Floyd, R.A. "Reactive oxygen species, cell signaling and cell injury." *Free Radic. Biol. Med.* **2000**, *28*, 1456-1462.
- Denu, J. M. and Tanner, K. G. "Specific and reversible inactivation of protein tyrosine phosphatases by hydrogen peroxide: evidence for a sulfenic acid intermediate and implications for redox regulation," *Biochemistry* **1998**, *37*, 5633–5642.
- Lee, S.R.; Kwon, K.S.; Kim, S.R. and Rhee, S.G. "Reversible inactivation of protein-tyrosine phosphatase 1B in A431 cells stimulated with epidermal growth factor," *J. Biol. Chem.* **1998**, *273*, 15366–15372.
- Sundaresan, M.; Yu, Z.X.; Ferrans, V.J.; Irani, K. and Finkel, T. "Requirement for generation of H<sub>2</sub>O<sub>2</sub> for platelet-derived growth factor signal transduction," *Science* **1995**, *270*, 296–299.
- Lawrence, T. "The nuclear factor NF-kappaB pathway in inflammation," *Cold Spring Harb. Perspect. Biol.* **2009**, *1*, doi: 10.1101/cshperspect.a001651.



- Robinson, K.; Stewart, C.A.; Pye, Q.N.; Nguyen, X.; Kenney, L.; Salsman, S.; Floyd, R. A. and Hensley, K. "Redox sensitive protein phosphatase activity regulates the phosphorylation state of p38 protein kinase in primary astrocyte culture," *J. Neurosci Res.* **1999**, *55*, 724-732.
- Pryor, W.A. "Biological effects of cigarettes smoke, wood smoke and the smoke from plastics – the use of electron spin resonance," *Free Radic. Biol. Med.* **1992**, *13*, 659–676.
- Riley, P.A. "Free radicals in biology – oxidative stress and the effects of ionizing radiation," *Int. J. Radiat. Biol.* **1994**, *65*, 27–33.
- Benedetti, M.; Giuliani, M.E. and Regoli, F. "Oxidative metabolism of chemical pollutants in marine organisms: molecular and biochemical biomarkers in environmental toxicology," *Ann. N.Y. Acad. Sci.* **2015**, *1340*, 8–19.
- Bodel, A.M.; Dong, Z. and Wang, H. "Cancer prevention and control: alarming challenges in China," *Natl. Sci. Rev.* **2016**, *3*, 117-127.
- Horton, W. and Török, M. "Natural and nature-inspired synthetic small molecule antioxidants in the context of green chemistry," in *Green chemistry: an inclusive approach* (Török, B., Dransfield eds.). **2018**, Chp 3.27, pp 963-979, Elsevier, Oxford.
- Bouayed, J. and Bohn, T. "Exogenous antioxidants--double-edged swords in cellular redox state: health beneficial effects at physiologic doses versus deleterious effects at high doses," *Oxid. Med. Cell Longev.* **2010**, *3*, 228-237.
- Panieri, E. and Santoro, M.M. "ROS homeostasis and metabolism: a dangerous liason in cancer cells," *Cell Death Dis.* **2016**, *7*, doi:10.1038/cddis.2016.105.
- Slimen, I.; Najjar, T. and Abderrabba, M. "Chemical and Antioxidant Properties of Betalains," *J. Agric. Food Chem.* **2017** *65*, 675-689.
- Halake, K.; Birajdar, M. and Lee, J. "Structural implications of polyphenolic antioxidants," *J. Ind. Eng. Chem. Res.* **2016**, *35*, 1-7.
- Poljšak, B. and Fink, R. "The protective role of antioxidants in the defence against ROS/RNS-mediated environmental pollution," *Oxid. Med. Cell Longev.* **2014**, doi: 10.1155/2014/671539.
- Neto, C.C. "Cranberry and blueberry: evidence for protective effects against cancer and vascular diseases," *Mol. Nutr. Food Res.* **2007**, *51*, 652-664.
- Neto, C.C. "Cranberries: ripe for more cancer research?," *J. Sci. Food Agric.* **2011**, *91*, 2303-2307.

Xia, E.; Deng, G.; Guo, Y. and Li, H. "Biological activities of polyphenols from grapes," *Int. J. Mol. Sci.* **2010**, *11*, 622-646.

Azeredo, H. "Betalains: properties, sources, applications and stability – a review," *Int. J. Food Sci. Nutr.* **2009**, *44*, 2365-2376.

Butera, D.; Tesoriere, L.; Gaudio, F.; Bongiorno, A.; Allegra, M.; Pintaudi, A.M.; Kohen, R. and Livrea, M.A. "Antioxidant activities of sicilian prickly pear (*Opuntia ficus indica*) fruit extracts and reducing properties of its betalains: betanin and indicaxanthin," *J. Agric. Food. Chem.* **2002**, *50*, 6895-6901.

Gengatharan, A.; Dykes, G. and Choo, W. "Betalains: Natural plant pigments with potential application in functional foods," *LWT-Food Sci. Technol.* **2015**, *64*, 645-649.  
Swieca, M.; Gawlik-Dziki, U.; Dziki, D. and Baraniak, B. "Wheat bread enriched with green coffee - In vitro bioaccessibility and bioavailability of phenolics and antioxidant activity," *Food Chem.* **2017**, *221*, 1451-1457.

Foti, M. and Amorati, R. "Non-phenolic radical-trapping antioxidants," *J. Pharm. Pharmacol.* **2009**, *61*, 1435-1448.

Shahidi, F. and Ambigaipalan, P. "Phenolics and polyphenolics in foods, beverages and spices: Antioxidant activity and health effects: A review," *J. Funct. Foods* **2015**, *18*, 820-897.

Sarmadi, B. and Ismail, A. "Antioxidative peptides from food proteins: a review," *Peptides* **2010**, *31*, 1949-1956.

Dai, J. and Mumper, R. "Plant phenolics: extraction, analysis and their antioxidant and anticancer properties," *Molecules* **2010**, *15*, 7313-7352.

Manach, C.; Scalbert, A.; Morand, C.; Rémésy, C. and Jiménez, L. "Polyphenols: food sources and bioavailability," *Am. J. Clin. Nutr.* **2004**, *79*, 727-747.

Forman, H.J.; Davies, K.J. and Ursini, F. "How do nutritional antioxidants really work: nucleophilic tone and para-hormesis versus free radical scavenging in vivo," *Free Radic. Biol. Med.* **2014**, *66*, 24-35.

Kanner, J.; Harel, S. and Granit, R. "Betalains - a new class of dietary cationized antioxidants," *J. Agric. Food. Chem.* **2001**, *49*, 5178-5185.

Manach, C.; Williamson, G.; Morand, C.; Scalbert, C. and Rémésy, C. "Bioavailability and bioefficacy of polyphenols in humans. I. Review of 97 bioavailability studies," *Am. J. Clin. Nutr.* **2005**, *81*(suppl), 230S-242S.

- Manach, C.; Williamson, G.; Morand, C.; Scalbert, C. and Rémésy, C. “Bioavailability and bioefficacy of polyphenols in humans. II. Review of 93 intervention studies,” *Am. J. Clin. Nutr.* **2005**, *81(suppl)*, 243S-255S.
- Hollman, P.C. “Unravelling of the health effects of polyphenols is a complex puzzle complicated by metabolism,” *Arch. Biochem. Biophys.* **2014**, *559*, 100-105.
- Crozier, A.; Jaganath, I.B. and Clifford, M.N. “Dietary phenolics: chemistry, bioavailability and effects on health,” *Nat. Prod. Rep.* **2009**, *26*, 1001-1043.
- Scalbert, A. and Williamson, G. “Dietary intake and bioavailability of polyphenols,” *J. Nutr.* **2000**, *130*, 2073S-2085S.
- Walle, T.; Hsieh, F.; DeLegge, M.; Oatis, J. and Walle, K. “High absorption but very low bioavailability of oral resveratrol in humans,” *Drug Metab. Dispos.* **2004**, *32*, 1377-1382.
- Albanes, D.; Heinonen, O.P.; Taylor, P.R.; Virtamo, J.; Edwards B.K.; Rautalahti, M.; Hartman, A.M.; Palmgren, J.; Freedman, L.S.; Haapakoski, J.; Barrett, M.J.; Pietinen, P.; Malila, N.; Tala, E.; Liippo, K.; Salomaa, E.R.; Tangrea, J.A.; Teppo, L.; Askin, F.B.; Taskinen, E.; Erozan, Y. Greenwald, P. and Huttunen, J.K. “Alpha-tocopherol and beta-carotene supplements and lung cancer incidence in the alpha-tocopherol, beta-carotene cancer prevention study: effects of base-line characteristics and study compliance,” *J. Natl. Cancer Inst.* **1996**, *88*, 1560–1570.
- Heinonen, O.P.; Albanes, D.; Virtamo, J.; Taylor, P.R.; Huttunen, J.K.; Hartman, A.M.; Haapakoski, J.; Malila, N.; Rautalahti, M.; Ripatti, S.; Mäenpää, H.; Teerenhovi, L.; Koss, L.; Virolainen, M. and Edwards, B.K. “Prostate cancer and supplementation with alpha-tocopherol and beta-carotene: incidence and mortality in a controlled trial,” *J. Natl. Cancer Inst.* **1998**, *90*, 440–446.
- Bolognesi, M.L. “Polypharmacology in a single drug: multitarget drugs,” *Curr. Med. Chem.* **2013**, *20*, 1639–1645.
- Bolognesi, M.L. and Cavalli, A. “Multitarget drug discovery and polypharmacology,” *ChemMedChem.* **2016**, *11*, 1190–1192.
- Talevi, A. “Multi-target pharmacology: possibilities and limitations of the “skeleton key approach” from a medicinal chemist perspective,” *Front Pharmacol.* **2015**, doi: 10.3389/fphar.2015.00205.
- Morphy, R.; Kay, C. and Rankovic, Z. “From magic bullets to designed multiple ligands,” *Drug Discov. Today* **2004**, *9*, 641–651.

Youdim, M.B.H. and Buccafusco, J.J. (2005) Multi-functional drugs for various CNS targets in the treatment of neurodegenerative disorders,” *Trends Pharm. Sci.* **2005**, *26*, 27–35.

Roth, B.L.; Sheffler, D.J. and Kroeze, W.K. “Magic shotguns versus magic bullets: selectively non-selective drugs for mood disorders and schizophrenia,” *Nat. Rev. Drug Discov.* **2004**, *3*, 353–359.

Lin, H.H.; Zhang, L.L.; Yan, R.; Lu, J.J. and Hu, Y.J. (2017) “Network analysis of drugtarget interactions: a study on FDA-approved new molecular entities between 2000 to 2015,” *Sci. Rep.* **2017**, *7*, doi: 10.1038/s41598-017-12061-8.

Zimmermann, G.R.; Lehár, J. and Keith, C.T. “Multi-target therapeutics: when the whole is greater than the sum of the parts,” *Drug Discov. Today* **2007**, *12*, 34-42.  
Xie, L. and Bourne, P.E. “Developing multi-target therapeutics to fine-tune the evolutionary dynamics of the cancer ecosystem,” *Front Pharmacol.* **2015**, *6*, doi: 10.3389/fphar.2015.00209.

Cavalli, A.; Bolognesi, M.L.; Minarini, A.; Rosini, M.; Tumiatti, V.; Recanatini, M. and Melchiorre, C. “Multi-target-directed ligands to combat neurodegenerative diseases,” *J. Med. Chem.* **2008**, *51*, 347–372.

Viayna, E.; Sola, I.; Di Pietro, O. and Munoz-Torrero, D. (2013) “Human disease and drug pharmacology, complex as real life,” *Curr. Med. Chem.* **2013**, *20*, 1623–1634.

Morphy, R. and Rankovic, Z. “Design of multitarget ligands,” in Lead generation approaches in drug discovery. (Morphy, R. and Rankovic, Z.). **2010**, Wiley, Hoboken, 141–164.

Morphy, R. and Rankovic, Z. “Designing multiple ligands—medicinal chemistry strategies and challenges,” *Curr. Pharm. Des.* **2009**, *15*, 587–600.

Felice, D.; Gardier, A.M.; Sanchez, C. and David, D.J. (2017) “Innovative solutions to the development of novel antidepressants,” *Frontiers Drug Disc.* **2017**, *2*, 1-40.

Bannwart, L.M.; Carter, D.S.; Cai, H.Y.; Choy, J.C.; Greenhouse, R.; Jaime-Figueroa, S.; Iyer, P.S.; Lin, C.J.; Lee, E.K.; Lucas, M.C.; Lynch, S.M.; Madera, A.M.; Moore, A.; Ozboya, K.; Raptova, L.; Roetz, R.; Schoenfeld, R.C.; Stein, K.A.; Steiner, S.; Villa, M.; Weikert, R.J. and Zhai, Y. “Novel 3,3-disubstituted pyrrolidines as selective triple serotonin/norepinephrine/dopamine reuptake inhibitors,” *Bioorg. Med. Chem. Lett.* **2008**, *18*, 6062–6066.

Morphy, R. and Rankovic, Z. “Designed multiple ligands. An emerging drug discovery paradigm,” *J. Med. Chem.* **2005**, *48*, 6523–6543.

Sliwoski, G.; Kothiwale, S.; Meiler, J. and Lowe, E.W. Jr. "Computational methods in drug discovery," *Pharmacol. Rev.* **2014**, *66*, 334–395.

Cherkasov, A.; Muratov, E.N.; Fourches, D.; Varnek, A.; Baskin I.I.; Cronin M.; Dearden, J.; Gramatica, P.; Martin, Y.C.; Todeschini, R.; Consonni, V.; Kuz'min, V.E.; Cramer, R.; Benigni, R.; Yang, C.; Rathman, J.; Terfloth, L.; Gasteiger, J.; Richard, A. and Tropsha, A. "QSAR modeling: where have you been? Where are you going to?," *J. Med. Chem.* **2014**, *57*, 4977–5010.

Danishuddin and Khan, A.U. "Descriptors and their selection methods in QSAR analysis: paradigm for drug design," *Drug Discov. Today.* **2016**, *21*, 1291–1302.  
Morris, G.M.; Huey, R.; Lindstrom, W.; Sanner, M.F.; Belew, R.K.; Goodsell, D.S. and Olson, A.J. "AutoDock4 and AutoDockTools4: automated docking with selective receptor flexibility," *J. Comput. Chem.* **2009**, *30*, 2785–2791.

Meng, X.Y.; Zhang, H.X.; Mezei, M. and Cui, M. "Molecular docking: a powerful approach for structure-based drug discovery," *Curr. Comput. Aided Drug Des.* **2011**, *7*, 146–157.

Hua, Q.X. and Weiss, M.A. "Mechanism of insulin fibrillation: the structure of insulin under amyloidogenic conditions resembles a protein-folding intermediate," *J. Biol. Chem.* **2004**, *179*, 21499-21460.

Hartl, F.U. "Protein misfolding diseases," *Annu. Rev. Biochem.* **2017**, *86*, 21-26.  
Chaudhuri, T.K. and Paul, S. "Protein-misfolding diseases and chaperone-based therapeutic approaches," *FEBS J.* **2006**, *273*, 1331-1349.

Horwich, A.L.; Neupert, W. and Hartl, F.U. "Protein-catalysed protein folding," *Trends in Biotech.* **1990**, *8*, 126-131.

Creighton, T.E. "Protein folding," *Biochem. J.* **1990**, *270*, 1-16.  
Privalov, P.L. "Stability of proteins: small globular proteins," *Adv. Protein Chem.* **1979**, *33*, 167-241.

Page, M.I. and Jencks, W.P. "Entropic Contributions to Rate Accelerations in Enzymic and Intramolecular Reactions and the Chelate Effect," *Proc. Natl. Acad. Sci. U.S.A.* **1971**, *68*, 1678-1683.

Smith, R.C.; Rosen, K.M.; Pola, R. and Magrané, J. "Stress proteins in Alzheimer's disease," *Int. J. Hyperthermia* **2005**, *21*, 421-431.

Kelley, B.J. and Petersen, R.C. "Alzheimer's disease and mild cognitive impairment," *Neur. Clin.* **2007**, *25*, 577-609.

- Ballard, C.; Gauthier, S.; Corbett, A.; Brayne, C.; Aarsland, D. and Jones, E. "Alzheimer's disease," *Lancet* **2011**, *377*, 1019-1031.
- Chen, X.; Tikhonova, I.G. and Decker, M. "Probing the mid-gorge of cholinesterases with spacer-modified bivalent quinazolinimines leads to highly potent and selective butyrylcholinesterase inhibitors," *Bioorg. Med. Chem.* **2011**, *19*, 1222-1235.
- Jakob-Roetne, R. and Jacobsen, H. "Alzheimer's disease: from pathology to therapeutic approaches," *Angew. Chem. Int. Ed.* **2009**, *121*, 3030-3059.
- Neugroschl, J. and Sano, M. "An update on treatment and prevention strategies for Alzheimer's disease," *Curr. Neurol. Neurosci. Rep.* **2009**, *5*, 368-376.
- Bolognesi, M.L.; Matera, R.; Minarini, A.; Rosini, M. and Melchiorre, C. "Alzheimer's disease: new approaches to drug discovery," *Curr. Opin. Chem. Biol.* **2009**, *13*, 303-308.
- Relkin, N.R. "Beyond symptomatic therapy: a re-examination of acetylcholinesterase inhibitors in Alzheimer's disease," *Expert. Rev. Neurother.* **2007**, *7*, 735-748.
- Bartus, R.T.; Dean III, R.L.; Beer, B. and Lippa, A.S. "The cholinergic hypothesis of geriatric memory dysfunction," *Science* **1982**, *217*, 408-414.
- Belinson, H.; Kariv-Inbal, Z.; Kaye, R.; Masliah, E. and Michaelson, D.M. "Following activation of the amyloid cascade, apolipoprotein E4 drives the in vivo oligomerization of amyloid- $\beta$  resulting in neurodegeneration," *J. Alz. Dis.* **2010**, *22*, 959-970.
- Selkoe, D.J. "The cell biology of beta-amyloid precursor protein and presenilin in Alzheimer's disease," *Trends Cell Biol.* **1998**, *8*, 447-453.
- Selkoe, D.J. "Alzheimer's disease genes, proteins and therapy," *Physiol. Rev.* **2001**, *81*, 741-766.
- Török, B.; Bag, S.; Sarkar, M.; Dasgupta, S. and Török, M. "Structural features of small molecule amyloid-beta self-assembly inhibitors," *Curr. Bioact. Comp.* **2013**, *9*, 37-63.
- Adamski-Werner, S.L.; Palaninathan, S.K.; Sacchetti, J.C. and Kelly, J.W. "Diflunisal analogues stabilize the native state of transthyretin. potenti of amyloidogenesis," *J. Med. Chem.* **2004**, *47*, 355-374.
- Byeon, S.R.; Lee, J.H.; Sohn, J.H.; Kim, D.C.; Shin, K.J.; Yoo, K.H.; Mook-Jung, I.; Lee, W.K. and Kim, D.J. "Bis-styrylpyridine and bis-styrylbenzene derivatives as inhibitors for A $\beta$  fibril formation," *Bioorg. Med. Chem. Lett.* **2007**, *17*, 1466-1470.

Török, M.; Abid, M.; Mhadgut, S.C. and Török, B. "Organofluorine inhibitors of amyloid fibrillogenesis," *Biochemistry* **2006**, *45*, 5377-5383.

Török, B.; Sood, A.; Bag, S.; Kulkarni, A.; Borkin, D.; Lawler, E.; Dasgupta, S.; Landge, S.M.; Abid, M.; Zhou, W.; Foster, M.; LeVine III, H. and Török, M. "Structure-activity relationship of organofluorine inhibitors of amyloid-beta self-assembly," *ChemMedChem* **2012**, *7*, 910-919.

Ono, K.; Yoshiike, Y.; Takashima, A.; Hasegawa, K.; Naiki, H. and Yamada, M. "Potent anti-amyloidogenic and fibril-destabilizing effects of polyphenols *in vitro*: implications for the prevention and therapeutics of Alzheimer's disease," *J. Neurochem.* **2003**, *87*, 172-81.

Porat, Y.; Abramowitz, A. and Gazit, E. "Inhibition of amyloid fibril formation by polyphenols: structural similarity and aromatic interactions as common Inhibition mechanism," *Chem. Biol. Drug. Des.* **2006**, *67*, 27-37.

Taniguchi, S.; Suzuki, N.; Masuda, M.; Hisanaga, S.; Iwatsubo, T.; Goedert, M. and Hasegawa, M. "Inhibition of heparin-induced tau filament formation by phenothiazines, polyphenols and porphyrins," *J. Biol. Chem.* **2005**, *280*, 7614-7623.  
Riviere, C.; Richard, T.; Vitrac, X.; Merillon, J.M.; Walls, J. and Monti, J.P. "New polyphenols active on  $\beta$ -amyloid aggregation," *Bioorg. Med. Chem. Lett.* **2008**, *18*, 828-831.

Ono, K.; Hasegawa, K.; Naiki, H. and Yamada, M. "Anti-amyloidogenic activity of tannic acid and its activity to destabilize Alzheimer's  $\beta$ -amyloid fibrils *in vitro*," *Biochim. Biophys. Acta* **2004**, *1690*, 193-202.

Hirohata, M.; Hasegawa, K.; Tsutsumi-Yasuhara, S.; Ohhashi, Y.; Ookoshi, T.; Ono, K.; Yamada, M. and Naiki, H. "The anti- amyloidogenic effect is exerted against Alzheimer's  $\beta$ -amyloid fibrils *in vitro* by preferential and reversible binding of flavonoids to the amyloid fibril structure," *Biochemistry* **2007**, *46*, 1888-1899.

Heo, H.J.; Kim, D.O.; Shin, S.C.; Kim, M.J.; Kim, B.G. and Shin, D.H. "Effect of antioxidant flavanone, naringenin, from citrus junos on neuroprotection," *J. Agric. Food Chem.* **2004**, *52*, 1520-25.

Cosentino, U.; Vari, M.R.; Saracino, A.A.G.; Pieta, D.; Moro, G. and Salmona, M. "Tetracycline and its analogues as inhibitors of amyloid fibrils: searching for a geometrical pharmacophore by theoretical investigation of their conformational behavior in aqueous solution," *J. Mol. Model.* **2005**, *11*, 17-25.

Lenhart, J.A.; Ling, X.; Gandhi, R.; Guo, T.L.; Gerk, P.M.; Brunzell, D.H. and Zhang, S. "Clicked" Bivalent ligands containing curcumin and cholesterol as multifunctional A $\beta$  oligomerization inhibitors: design, synthesis and biological characterization," *J. Med. Chem.* **2010**, *53*, 6198-209.

Ortega, A.; Rincón, A.; Jiménez-Aliaga, K.L.; Bermejo-Bescós, P.; Martín-Aragón, S.; Molina, M.T. and Csáky, A.G. "Synthesis and evaluation of arylquinones as BACE1 inhibitors,  $\beta$ -amyloid peptide aggregation inhibitors and destabilizers of preformed  $\beta$ -amyloid fibrils," *Bioorg. Med. Chem. Lett.* **2011**, *21*, 2183-2187.

Soto-Ortega, D.D.; Murphy, B.P.; Gonzalez-Velasquez, F.J.; Wilson, K.A.; Xie, F.; Wang, Q. and Moss, M.A. "Inhibition of amyloid- $\beta$  aggregation by coumarin Analogs can be manipulated by functionalization of the aromatic center," *Bioorg. Med. Chem.* **2011**, *19*, 2596-2602.

Hamley, I.W. "Peptide Fibrillization," *Angew. Chem. Int. Ed.* **2007**, *46*, 8128-8147.  
Broersen, K.; Rouaeeau, F. and Schymkowitz, J. "The culprit behind amyloid beta peptide related neurotoxicity in Alzheimer's disease: oligomer size or conformation?," *Alzheimers Res. Ther.* **2010**, *2*, doi: 10.1186/alzrt36.

Galzitskay, O.V.; Galushko, E.I. and Selivanova, O.M. "Studies of the process of amyloid formation by A $\beta$  peptide," *Biokhimiya* **2018**, *83 (suppl)*, S62-S80.

Kayed, R.; Canto, I.; Breydo, L.; Rasool, S.; Lukacsovich, T.; Wu, J.; Albay III, R.; Pensalfini, A.; Yeung, S.; Head, E.; Marsh, J.L. and Glabe, C. "Conformation dependent monoclonal antibodies distinguish different replicating strains or conformers of prefibrillar A $\beta$  oligomers," *Mol. Neurodegener.* **2010**, *5*, 57-67.

Shankar, G.M.; Leissring, M.A.; Adame, A.; Sun, X.; Spooner, E.; Masliah, E.; Selkoe, D.J.; Lemere, C.A. and Walsh, D.M. "Biochemical and immunohistochemical analysis of an Alzheimer's disease mouse model reveals the presence of multiple cerebral Abeta assembly forms throughout life," *Neurobiol. Dis.* **2009**, *36*, 293-302.

Zhao, W.Q.; Santini, F.; Breese, R.; Ross, D.; Zhang, X.D.; Stone, D.J.; Ferrer, M.; Townsend, M.; Wolfe, A.L.; Seager, M.A.; Kinney, G.G.; Shughrue, P.J. and Ray, W.J. "Inhibition of calcineurin-mediated endocytosis and alpha-amino-3-hydroxy-5-methyl-4-isoxazolepropionic acid (AMPA) receptors prevents amyloid beta oligomer-induced synaptic disruption," *J. Biol. Chem.* **2010**, *285*, 7619-7632.

Kayed, R.; Head, E.; Thompson, J.L.; McIntire T.M.; Milton, S.C.; Cotman, C.W. and Glabe, C.G. "Common structure of soluble amyloid oligomers implies common mechanism of pathogenesis," *Science* **2003**, *300*, 486-489.



Török, B.; Dasgupta, S. and Török, M. "Chemistry of small molecule inhibitors in self-assembly of Alzheimer's disease related amyloid-beta peptide," *Curr. Bioact. Comp.* **2008**, *4*, 159-174.

Verma, M.; Vats, A. and Taneja, V. "Toxic species in amyloid disorders: oligomers or mature fibrils," *Ann. Indian Acad. Neurol.* **2015**, *18*, 138-145.

DeKosky, S.T. and Scheff, S.W. "Synapse loss in frontal cortex biopsies in Alzheimer's disease: correlation with cognitive severity," *Ann. Neurol.* **1990**, *27*, 457-464.

Ferreira-Vieira, T.H.; Guimaraes, I.M.; Silva, F.R. and Ribeiro, F.M. "Alzheimer's disease: targeting the cholinergic system," *Curr. Neuropharmacol.* **2016**, *14*, 101-115.  
Butterfield, D.A. "A review, amyloid  $\beta$ -peptide (1-42)-induced oxidative stress and neurotoxicity implications for neurodegeneration in Alzheimer's disease brain," *Free Radic. Res.* **2002**, *36*, 1307-1313.

Barnham, K.J.; Masters, C.L. and Bush, A.I. "Neurodegenerative diseases and oxidative stress," *Nat. Rev.* **2004**, *3*, 205-214.

Huang, X.; Moir, R.D.; Tanzi, R.E.; Bush, A.I. and Rogers, J.T. "Redox-active metals, oxidative stress and Alzheimer's disease pathology," *Ann. N.Y. Acad. Sci.* **2004**, *1012*, 153-163.

Wollen, K.A. "Alzheimer's disease: the pros and cons of pharmaceutical, nutritional, botanical and stimulatory therapies, with a discussion of treatment strategies from the perspective of patients and practitioners," *Alt. Med. Rev.* **2010**, *15*, 223-244.

Bolognesi, M.L.; Simoni, E.; Rossini, M.; Minarini, A.; Tumiatti, V. and Melchiorre, C. "Multitarget-directed ligands: innovative chemical probes and therapeutic tools against Alzheimer's disease," *Curr. Top Med. Chem.* **2011**, *11*, 2797-2806.

Butterfield, D.A.; Di Domenico, F. and Barone, E. "Elevated risk of type 2 diabetes for development of Alzheimer disease a key role for oxidative stress in brain," *Biochim. Biophys. Acta* **2014**, *1842*, 1693-1706.

Guzior, N.; Więckowska, A.; Panek, D. and Malawska, B. "Recent development of multifunctional agents as potential drug candidates for the treatment of Alzheimer's disease," *Curr. Med. Chem.* **2015**, *22*, 373-404.

Ashcroft, F.M. and Rorsman, P. "Diabetes mellitus and the  $\beta$  cell: the last ten years," *Cell* **2012**, *6*, 1160-1171.

Guo, S. "Insulin signaling, resistance and the metabolic syndrome: insights from mouse models to disease mechanisms," *J. Endocrinol.* **2014**, *220*, T1-T23.

- Pozzilli, P.; Battelino, T.; Danne, T.; Hovorka, R.; Jarosz-Chobot, P. and Renard, E. "Continuous subcutaneous insulin infusion in diabetes: patient populations, safety, efficacy and pharmacoeconomics," *Diabetes Metab. Res. Rev.* **2016**, *32*, 21-39.
- Eckel, R.H.; Kahn, S.E.; Ferrannini, E.; Goldfine, A.B.; Nathan, D.M.; Schwartz, M.W.; Smith, R.J. and Smith, S.R. "Obesity and type 2 diabetes: what can be unified and what needs to be individualized?," *J. Clin. Endocrinol. Metab.* **2011**, *96*, 1654-1663.
- Pomytkin, I.A. "H<sub>2</sub>O<sub>2</sub> signalling pathway: a possible bridge between insulin receptor and mitochondria," *Curr. Neuropharmacol.* **2012**, *10*, 311-320.
- Kaur, R.; Dahiya, L. and Kumar, M. "Fructose-1,6-bisphosphatase inhibitors: A new valid approach for management of type 2 diabetes mellitus," *Eur. J. Med. Chem.* **2017**, *141*, 473-505.
- Bie, J.; Liu, S.; Zhou, J.; Xu, B. and Shen, Z. "Design, synthesis and biological evaluation of 7-nitro-1H-indole-2-carboxylic acid derivatives as allosteric inhibitors of fructose-1,6-bisphosphatase," *Bioorg. Med. Chem.* **2014**, *22*, 1850-1862.
- Bie, J.; Liu, S.; Li, Z.; Mu, Y.; Xu, B. and Shen, Z. "Discovery of novel indole derivatives as allosteric inhibitors of fructose-1, 6-bisphosphatase," *Eur. J. Med. Chem.* **2014**, *90*, 394-405.
- Dang, Q.; Kasibhatla, S.R.; Xiao, W.; Liu, Y.; DaRe, J.; Taplin, F.; Reddy, K.R.; Scarlato, G.R.; Gibson, T.; van Poelje, P.D.; Potter, S.C. and Erion, M.D. "Fructose-1,6-bisphosphatase inhibitors. 2. design, synthesis and structure-activity relationship of a series of phosphonic acid containing benzimidazoles that function as 5'-adenosinemonophosphate (AMP) mimics," *J. Med. Chem.* **2010**, *53*, 441-451.
- Rudnitskaya, A.; Borkin, D.A.; Huynh, K.; Török, B. and Stieglitz, K. "Rational design, synthesis and potency of N-substituted indoles, pyrroles and triarylpyrazoles as potential fructose 1,6-bisphosphatase inhibitors," *ChemMedChem* **2010**, *5*, 384-389.
- Kahn, S.E.; Cooper, M.E. and Del Prato, S. "Pathophysiology and treatment of type 2 diabetes: perspectives on the past, present and future," *Lancet* **2014**, *383*, 1068-1083.
- de la Monte, S.M. "Insulin resistance and Alzheimer's disease," *BMB Rep.* **2009**, *42*, 475-481.
- Zhao, W.Q. and Townsend, M. "Insulin resistance and amyloidogenesis as common molecular foundation for type 2 diabetes and Alzheimer's disease," *Biochim. Biophys. Acta* **2009**, *1792*, 482-496.

- Craft, S. "Insulin resistance syndrome and Alzheimer's disease: age- and obesity-related effects on memory, amyloid and inflammation," *Neurobiol. Aging* **2005**, *26*, 65–69.
- Schulingkamp, R.J.; Pagano, T.C.; Hung, D. and Raffa, R.B. "Insulin receptors and insulin action in the brain: review and clinical implications," *Neurosci. Biobehav. Rev.* **2000**, *24*, 855–872.
- Banks, W.A.; Jaspan, J.B. and Kastin, A.J. "Selective, physiological transport of insulin across the blood–brain barrier: novel demonstration by species-specific radioimmunoassays," *Peptides* **1997**, *18*, 1257–1262.
- Gray, S.M.; Meijer, R.I. and Barrett, E.J. "Insulin Regulates Brain Function, but How Does It Get There?," *Diabetes* **2014**, *63*, 3992–3997.
- Baskin, D.G.; Figlewicz, D.P.; Woods, S.C.; Porte Jr. D. and Dorsa, D.M. "Insulin in the brain," *Annu. Rev. Physiol.* **1987**, *49*, 335–347.
- Gasparini, L.; Gouras, G.K.; Wang, R.; Gross, R.S.; Beal, M.F.; Greengard, P. and Xu, H. "Stimulation of beta-amyloid precursor protein trafficking by insulin reduces intraneuronal beta-amyloid and requires mitogen-activated protein kinase signaling," *J. Neurosci.* **2001**, *21*, 2561–2570.
- Solano, D.C.; Sironi, M.; Bonfini, C.; Solerte, S.B.; Govoni, S. and Racchi, M. "Insulin regulates soluble amyloid precursor protein release via phosphatidyl inositol 3 kinase-dependent pathway," *FASEB J.* **2000**, *14*, 1015–1022.
- Malito, E.; Hulse, R.E. and Tang, W.J. "Amyloid beta-degrading cryptidases: insulin degrading enzyme, presequence peptidase and neprilysin," *Cell Mol. Life Sci.* **2008**, *65*, 2574–2585.
- Lesort, M. and Johnson, G.V. "Insulin-like growth factor-1 and insulin mediate transient site-selective increases in tau phosphorylation in primary cortical neurons," *Neurosci.* **2000**, *99*, 305–316.
- Lesort, M.; Jope, R.S. and Johnson, G.V. "Insulin transiently increases tau phosphorylation: involvement of glycogen synthase kinase-3beta and Fyn tyrosine kinase," *J. Neurochem.* **1999**, *72*, 576–584.
- Pani, G.; Giannoni, E.; Galeotti, T. and Chiarugi, P. "Redox-based escape mechanism from death: the cancer lesson," *Antioxid. Redox Signal.* **2009**, *11*, 2791–2806.

Menendez, J.A.; Joven, J.; Cufí S.; Corominas-Faja, B.; Oliveras-Ferraros, C.; Cuyàs, E.; Martín-Castillo, B.; López-Bonet, E.; Alarcón, T. and Vazquez-Martin, A. “The warburg effect version 2.0: metabolic reprogramming of cancer stem cells,” *Cell Cycle* **2013**, *12*, 1166–1179.

Pacini, N. and Borziani, F. “Cancer stem cell theory and the warburg effect, two sides of the same coin?,” *Int. J. Mol. Sci.* **2014**, *15*, 8893-8930.

Warburg, O. “On the origin of cancer cells,” *Science* **1956**, *123*, 309–314.

Liou, G.Y. and Storz, P. “Reactive oxygen species in cancer,” *Free Radic. Res.* **2010**, *44*, 1-31.

Afanas’ev, I. “Reactive oxygen species signaling in cancer,” *Aging Dis.* **2011**, *2*, 219-230.

Peng, X. and Gandhi, V. “ROS-activated anticancer prodrugs: a new strategy for tumor-specific damage,” *Ther. Deliv.* **2012**, *3*, 823-833.

Ding, S.; Li, C.; Cheng, N.; Cui, X.; Xu, X. and Zhou, G. “Redox regulation in cancer stem cells,” *Oxid. Med. Cell Longev.* **2015**, *2015*, doi: 10.1155/2015/750798.

Qanungo, S.; Das, M.; Haldar, S. and Basu, A. “Epigallocatechin-3-gallate induces mitochondrial membrane depolarization and caspase-dependent apoptosis in pancreatic cancer cells,” *Carcinogenesis* **2005**, *26*, 958–967.

Zhang, R.; Humphreys, I.; Shau, R.P.; Shi, Y. and Srivastava, S.K. “In vitro and in vivo induction of apoptosis by capsaicin in pancreatic cancer cells is mediated through ROS generation and mitochondrial death pathway,” *Apoptosis* **2008**, *13*, 1465–1478.

Donadelli, M.; Costanzo, C.; Beghelli, S.; Scupoli, M.T.; Dandrea, M.; Bonora, A.; Piacentini, P.; Budillon, A.; Caraglia, M.; Scarpa, A. and Palmieri, M. “Synergistic inhibition of pancreatic adenocarcinoma cell growth by trichostatin A and gemcitabine,” *Biochim. Biophys. Acta* **2007**, *1773*, 1095–1106.

Sahu, R.P.; Zhang, R.; Batra, S.; Shi, Y. and Srivastava, S.K. “Benzyl isothiocyanate mediated generation of reactive oxygen species causes cell cycle arrest and induces apoptosis via activation of MAPK in human pancreatic cancer cells,” *Carcinogenesis* **2009**, *30*, 1744-1753.

Carew, J.S.; Zhou, Y.; Albitar, M.; Carew, J.D.; Keating, M.J. and Huang, P. “Mitochondrial DNA mutations in primary leukemia cells after chemotherapy: clinical significance and therapeutic implications,” *Leukemia* **2003**, *17*, 1437–1447.

- Ampofo, E.; Rudzitis-Auth, J.; Dahmke, I.N.; Rössler, O.G.; Thiel, G.; Montenarh, M.; Menger, M.D. and Laschke, M.W. "Inhibition of protein kinase CK2 suppresses tumor necrosis factor (TNF)- $\alpha$ -induced leukocyte-endothelial cell interaction," *Biochim. Biophys. Acta.* **2015**, 1852, 2123-2136.
- Janeczko, M.; Orzesko, A.; Kazimierczuk, Z.; Szyszka, R. and Baier, A. "CK2 $\alpha$  and CK2 $\alpha'$  subunits differ in their sensitivity to 4, 5,6,7-tetrabromo- and 4,5,6,7 tetraiodo-1H-benzimidazole derivatives," *Eur. J. Med. Chem.* **2012**, 47, 345-350.
- Najda-Bernatowicz, A.; Lebska, M.; Orzesko, A.; Kopańska, K.; Krywińska, E.; Muszyńska, G. and Bretner, M. "Synthesis of new analogs of benzotriazole, benzimidazole and phthalimide—potential inhibitors of human protein kinase CK2," *Bioorg. Med. Chem.* **2009**, 17, 1573-1578.
- Ryu, S.Y. and Kim, S. "Evaluation of CK2 inhibitor (E)-3-(2, 3,4,5-tetrabromophenyl) acrylic acid (TBCA) in regulation of platelet function," *Eur. J. Pharmacol.* **2013**, 720, 391-400.
- Guerra, B. and Issinger, O.G. "Protein kinase CK2 and its role in cellular proliferation, development and pathology," *Electrophoresis* **1999**, 20, 391-408.
- Ahmed, K.; Gerber, D.A. and Cochet, C. "Joining the cell survival squad: an emerging role for protein kinase CK2," *Trends Cell Biol.* **2002**, 12, 226-230.
- Litchfield, D.W. "Protein kinase CK2: structure, regulation and role in cellular decisions of life and death," *Biochem. J.* **2003**, 369, 1-15.
- Pinna, L.A. "Protein kinase CK2: a challenge to canons," *J. Cell. Sci.* **2002**, 115, 3873-3878.
- Seldin, D. C. and Leder, P. "Casein kinase 2 alpha-induced murine lymphoma: relation to Teilleriosis in cattle," *Science* **1995**, 267, 894-897.
- Orlandini, M.; Semplici, F.; Ferruzzi, R.; Meggio, F.; Pinna, L.A. and Oliviero, S. "Protein kinase CK2 $\alpha'$  is induced by serum as a delayed early gene and cooperates with Ha-ras in fibroblast transformation," *J. Biol. Chem.* **1998**, 273, 21291-21297.
- Lebrin, F.; Chambaz, E.M. and Bianchini, L. "A role for protein kinase CK2 in cell proliferation: evidence using a kinaseinactive mutant of CK2 catalytic subunit R," *Oncogene* **2001**, 20, 2010-2022.
- Meggio, F. and Pinna, L.A. "One-thousand-and-one substrates of protein kinase CK2?," *FASEB J.* **2003**, 17, 349-368.

Wang, S. and Jones, K.A. "CK2 controls the recruitment of Wnt regulators to target genes in vivo," *Curr. Biol.* **2006**, *16*, 2239-2244.

Lin, C.Y.; Navarro, S.; Reddy, S. and Comai, L. "CK2-mediated stimulation of Pol I transcription by stabilization of UBF-SL1 interaction," *Nucleic Acids Res.* **2006**, *34*, 4752-4766.

Duncan, J.S.; Gyenis, L.; Lenehan, J.; Bretner, M.; Graves, L.M.; Haystead, T.A. and Litchfield, D.W. "An unbiased evaluation of CK2 inhibitors by chemoproteomics: characterization of inhibitor effects on CK2 and identification of novel inhibitor targets," *Mol. Cell. Proteom.* **2008**, *7*, 1077-1088.

Schaefer, S.; Svenstrup, T.H.; Fischer, M. and Guerra, B. "D11-Mediated Inhibition of Protein Kinase CK2 Impairs HIF-1 $\alpha$ -Mediated Signaling in Human Glioblastoma Cells," *Pharmaceuticals (Basel)* **2017**, *10*, doi: 10.3390/ph10010005.

Trembley, J.H.; Wang, G.; Unger, G.; Slaton, J. and Ahmed, K. "Protein kinase CK2 in health and disease: CK2: A key player in cancer biology," *Cell. Mol. Life Sci.* **2009**, *66*, 1858–1867.

Guerra, B.; Issinger, O.-G. "Protein kinase CK2 in human diseases," *Curr. Med. Chem.* **2008**, *15*, 1870–1886.

Lolli, G.; Cozza, G.; Mazzorana, M.; Tibaldi, E.; Cesaro, L.; Donella-Deana, A.; Meggio, F.; Venerando, A.; Franchin, C.; Sarno, S.; Battistutta, R. and Pinna, L.A. "Inhibition of Protein Kinase CK2 by Flavonoids and Tyrphostins. A Structural Insight," *Biochemistry* **2012**, *51*, 6097-6107.

Sarno, S.; de Moliner, E.; Ruzzene, M.; Pagano, M.A.; Battistutta, R.; Bain, J.; Fabbro, D.; Schoepfer, J.; Elliott, M.; Furet, P.; Meggio, F.; Zanotti, G. and Pinna, L.A. "Biochemical and three-dimensional-structural study of the specific inhibition of protein kinase CK2 by [5-oxo-5, 6-dihydroindolo-(1,2-a)quinazolin-7-yl]acetic acid (IQA)," *Biochem. J.* **2003**, *374*, 639-646.

Critchfield, J.W.; Coligan, J.E.; Folks, T.M. and Butera, S.T. "Casein kinase II as a selective target of HIV-1 transcriptional inhibitors," *Proc. Natl. Acad. Sci. U.S.A.* **1997**, *94*, 6110–6115.

Yim, H.; Lee, Y.H.; Lee, C.H. and Lee, S.K. "Emodin, an anthraquinone derivative isolated from the rhizomes of *Rheum palmatum*, selectively inhibits the activity of casein kinase II as a competitive inhibitor," *Planta Med.* **1999**, *65*, 9–13.

Janeczko, M.; Maslyk, M.; Kubiński, K. and Golczyk, H. "Emodin, a natural inhibitor of protein kinase CK2, suppresses growth, hyphal development and biofilm formation of *Candida albicans*," *Yeast* **2017**, *34*, 253-265.

- Sarno, S.; Reddy, H.; Meggio, F.; Ruzzene, M.; Davies, S.P.; Donella-Deana, A.; Shugar, D. and Pinna, L.A. "Selectivity of 4,5,6,7-tetrabromobenzotriazole, an ATP site-directed inhibitor of protein kinase CK2 ('casein kinase-2')," *FEBS Lett.* **2001**, *496*, 44-48.
- Pagano, M.A.; Andrzejewska, M.; Ruzzene, M.; Sarno, S.; Cesaro, L.; Bain, J.; Elliott, M.; Meggio, F.; Kazimierczuk, Z. and Pinna, L. A. "Optimization of protein kinase CK2 inhibitors derived from 4,5,6,7-tetrabromobenzimidazole," *J. Med. Chem.* **2004**, *47*, 6239-6247.
- Meggio, F.; Pagano, M.A.; Moro, S.; Zagotto, G.; Ruzzene, M.; Sarno, S.; Cozza, G.; Bain, J.; Elliott, M.; Deana, A.D.; Brunati, A.M. and Pinna, L.A. "Inhibition of protein kinase CK2 by condensed polyphenolic derivatives. An in vitro and in vivo study," *Biochemistry* **2004**, *43*, 12931-12936.
- Ellman, G.L.; Courtney, K.D.; Andres, B.J. and Featherstone, R.M. "A new and rapid colorimetric determination of acetylcholinesterase activity," *Biochem. Pharmacol.* **1961**, *7*, 88-95.
- Komersova, A.; Komersa, K. and Cegan, A. "New findings about Ellman's method to determine cholinesterase activity," *Z Naturforsch C.* **2007**, *62*, 150-154.
- Walmsley, T.A.; Abernethy, M.H. and Fitzgerald, H.P. "Effect of daylight on the reaction of thiols with Ellman's reagent, 5,5'-dithiobis(2-nitrobenzoic acid)," *Clin. Chem.* **1987**, *33*, 1928-1931.
- Apak, R.; Özyürek, M.; Güçlü, K. and Çapanoğlu, E. "Antioxidant Activity/Capacity Measurement. 1. Classification, Principles, Mechanisms and Electron Transfer (ET)-Based Assays," *J. Agric. Food. Chem.* **2016**, *64*, 997-1027.
- Mayer, J.M.; Hrovat, D.A.; Thomas, J.L. and Borden, W.T. "Proton-coupled electron transfer versus hydrogen atom transfer in benzyl/toluene, methoxyl/methanol and phenoxy/ phenol self-exchange reactions," *J. Am. Chem. Soc.* **2002**, *124*, 11142-11147.
- Lu, J.M.; Lin, P.; Yao, Q. and Chen, C. "Chemical and molecular mechanisms of antioxidants: experimental approaches and model systems," *J. Cell. Mol. Med.* **2010**, *14*, 840-860.
- Ou, B.; Huang, D.; Hampsch-Woodill, M.; Flanagan, J.A. and Deemer, E.K. "Analysis of antioxidant activities of common vegetables employing oxygen radical absorbance capacity (ORAC) and ferric reducing antioxidant power (FRAP) assays: a comparative study," *J. Agric. Food Chem.* **2002**, *50*, 3122-3128.

- Glazer, A. N. "Phycocerythrin fluorescence-based assay for reactive oxygen species," *Methods Enzymol.* **1990**, *186*, 161–168.
- Cao, G.; Alessio, H.M. and Cutler, R.G. "Oxygen-radical absorbance capacity assay for antioxidants," *Free Radic. Biol. Med.* **1993**, *14*, 303– 311.
- Huang, D.; Ou, B.; Hampsch-Woodill, M.; Flanagan, J.A. and Prior, R.L. "High-Throughput Assay of Oxygen Radical Absorbance Capacity (ORAC) Using a Multichannel Liquid Handling System Coupled with a Microplate Fluorescence Reader in 96-Well Format," *J. Agric. Food Chem.* **2002**, *50*, 4437-4444.
- Schmittschmitt, J.P. and Scholtz, J.M. "The role of protein stability, solubility and net charge in amyloid fibril formation," *J. Mol. Biol.* **1996**, *256*, 870–877.
- Hortschansky, P.; Schroeckh, V.; Christopeit, T.; Zandomenighi, G. and Fandrich, M. "The aggregation kinetics of Alzheimer's  $\beta$ -Amyloid peptide is controlled by stochastic nucleation," *Prot. Sci.* **2005**, *14*, 1753-1759.
- Lomakin, A.; Teplow, D.B.; Kirschner, D.A. and Benedek, G.B. "Kinetic theory of fibrillogenesis of amyloid  $\beta$ -protein," *Proc. Natl. Acad. Sci. USA* **1997**, *94*, 7942-7947.
- Iannuzzi, C.; Borriello, M.; Portaccio, M. Irace, G. and Sirangelo, I. "Insights into insulin fibril assembly at physiological and acidic pH and related amyloid intrinsic fluorescence," *Int. J. Mol. Sci.* **2017**, *18*, doi: 10.3390/ijms18122551.
- Bolder, S.G.; Sagis, L.M.; Venema, P. and van der Linden, E. "Thioflavin T and birefringence assays to determine the conversion of proteins into fibrils," *Langmuir* **2007**, *23*, 4144–4147.
- Hawe, A.; Sutter, M. and Jiskoot, W. "Extrinsic fluorescent dyes as tools for protein characterization," *Pharm. Res.* **2008**, *25*, 1487–1499.
- LeVine III, H. "Thioflavine T interactions with amyloid  $\beta$ -sheet structures," *Amyloid* **1995**, *2*, 1–6.
- Krebs, M.R.H.; Bromley, E.H.C. and Donald, A.M. "The binding of thioflavin-T to amyloid fibrils: localization and implications," *J. Struct. Biol.* **2005**, *149*, 30-37.
- Hudson, S.A.; Ecroyd, H.; Kee, T.W. and Carver, J.A. "The Thioflavin-T fluorescence assay for amyloid fibril detection can be biased by the presence of exogenous compounds," *FEBS J.* **2009**, *276*, 5960-5972.



Eisert, R.; Felau, L. and Brown, L. "Methods for enhancing the accuracy and reproducibility of Congo red and thioflavin-T assays," *Anal. Biochem.* **2006**, *353*, 144-146.

Morton, K.C. and Baker, L.A. "Atomic force microscopy-based bioanalysis for the study of disease," *Anal. Methods* **2014**, *6*, 4932–4955.

Eaton, P. and West P. "Atomic Force Microscopy," in *Atomic Force Microscopy* (Eaton, P. and West P.). **2010**, Oxford University Press.

Stine, W.B.; Snyder, S.W.; Ladrer, U.S.; Wade, W.S.; Miller, M.F.; Perun, T.J.; Holzman, T.F. and Kraftt, G.A. "The nanometer-scale structure of amyloid-beta visualized by atomic force microscopy," *J. Protein Chem.* **1996**, *15*, 193-203.

Iannuzzi, C.; Borriello, M.; Irace, G.; Cammarota, M. and Sirangelo, I. "Vanillin affects amyloid aggregation and non-enzymatic glycation in human insulin," *Sci. Rep.* **2017**, *7*, doi: 10.1038/s41598-017-15503-5.

Yoshihara, H.; Saito, J.; Tanabe, A.; Amada, T.; Kitagawa, K. and Asada, S. "Characterization of novel insulin fibrils that show strong cytotoxicity under physiological pH," *J. Pharm. Sci.* **2016**, *105*, 1419-1426.

<http://rsbweb.nih.gov/ij/download.html> (accessed on 03-19-2018).

<https://imagej.nih.gov/ij/docs/guide/user-guide.pdf> (accessed on 03-19-2018).

Mierts, S.; Scrocco, E. and Tomasi, J. "Electrostatic interaction of a solute with a continuum. A direct utilization of AB initio molecular potentials for the prevision of solvent effects," *Chem. Phys.* **1981**, *55*, 117–129.

Wolinski, K.; Hilton, J.F. and Pulay, P. "Efficient implementation of the gauge-independent atomic orbital method for NMR chemical shift calculations," *J. Am. Chem. Soc.* **1990**, *112*, 8251–8260.

Hansch, C.; Leo, A. and Taft, W. "A survey of Hammett substituent constants and resonance and field parameters," *Chem. Rev.* **1991**, *91*, 165-195.

Becke, A.D. "Density-functional exchange-energy approximation with correct asymptotic behavior," *Phys. Rev. A.* **1988**, *38*, 3098-3100.

Lee, C.; Yang, W. and Parr, R.G. "Development of the Colle-Salvetti correlation-energy formula into a functional of the electron density," *Phys. Rev. A.* **1988**, *37*, 785-789.

Gaussian 16, Revision B.01, Frisch, M. J.; Trucks, G. W.; Schlegel, H. B.; Scuseria, G. E.; Robb, M. A.; Cheeseman, J. R.; Scalmani, G.; Barone, V.; Petersson, G. A.; Nakatsuji, H.; Li, X.; Caricato, M.; Marenich, A. V.; Bloino, J.; Janesko, B. G.; Gomperts, R.; Mennucci, B.; Hratchian, H. P.; Ortiz, J. V.; Izmaylov, A. F.; Sonnenberg, J. L.; Williams-Young, D.; Ding, F.; Lipparini, F.; Egidi, F.; Goings, J.; Peng, B.; Petrone, A.; Henderson, T.; Ranasinghe, D.; Zakrzewski, V. G.; Gao, J.; Rega, N.; Zheng, G.; Liang, W.; Hada, M.; Ehara, M.; Toyota, K.; Fukuda, R.; Hasegawa, J.; Ishida, M.; Nakajima, T.; Honda, Y.; Kitao, O.; Nakai, H.; Vreven, T.; Throssell, K.; Montgomery, J. A., Jr.; Peralta, J. E.; Ogliaro, F.; Bearpark, M. J.; Heyd, J. J.; Brothers, E. N.; Kudin, K. N.; Staroverov, V. N.; Keith, T. A.; Kobayashi, R.; Normand, J.; Raghavachari, K.; Rendell, A. P.; Burant, J. C.; Iyengar, S. S.; Tomasi, J.; Cossi, M.; Millam, J. M.; Klene, M.; Adamo, C.; Cammi, R.; Ochterski, J. W.; Martin, R. L.; Morokuma, K.; Farkas, O.; Foresman, J. B.; Fox, D. J. Gaussian, Inc., Wallingford CT, **2016**.

Ishida, J.; Wang, H.K.; Bastow, K.F.; Hu, C.Q. and Lee, K.H. "Antitumor agents 201. Cytotoxicity of harmine and beta-carboline analogs," *Bioorg. Med. Chem. Lett.* **1999**, *9*, 3319-3324.

Chen, H.; Gao, P.; Zhang, M.; Liao, W. and Zhang, J. "Synthesis and biological evaluation of a novel class of  $\beta$ -carboline derivatives," *New J. Chem.* **2014**, *38*, 4155-4166.

Chen, Y.F.; Lin, Y.C.; Chen, J.P.; Chan, H.C.; Hsu, M.H.; Lin, H.Y.; Kuo, S.C. and Huang, L.J. "Synthesis and biological evaluation of novel 3,9-substituted  $\beta$ -carboline derivatives as anticancer agents," *Bioorg. Med. Chem. Lett.* **2015**, *25*, 3873-3877.

Gohil, V.M.; Brahmabhatt, K.G.; Loiseau, P.M. and Bhutani, K.K. "Synthesis and anti-leishmanial activity of 1-aryl- $\beta$ -carboline derivatives against *Leishmania donovani*," *Bioorg. Med. Chem. Lett.* **2012**, *22*, 3905-3907.

Gellis, A.; Dumètre, A.; Lanzada, G.; Hutter, S.; Ollivier, E.; Vanelle, P. and Azas, N. "Preparation and antiprotozoal evaluation of promising  $\beta$ -carboline alkaloids," *Biomed. Pharmacother.* **2012**, *66*, 339-347.

Espinoza-Moraga, M.; Caballero, J.; Gaube, F.; Winckler, T. and Santos, L.S. "1-Benzyl-1,2,3,4-Tetrahydro- $\beta$ -Carboline as Channel Blocker of N-Methyl-d-Aspartate Receptors," *Chem. Biol. Drug Des.* **2012**, *79*, 594-599.

May, A.C.; Fleischer, W.; Kletke, O.; Haas, H.L. and Sergeeva, O.A. "Benzodiazepine-site pharmacology on GABAA receptors in histaminergic neurons," *Br. J. Pharmacol.* **2013**, *170*, 222-232.

Francik, R.; Kazek, G.; Cegla, M. and Stepniewski, M. "Antioxidant activity of beta-carboline derivatives," *Acta Pol. Pharm.* **2011**, *68*, 185-189.

Kulkarni, A.; Abid, M.; Török, B. and Huang, X. "A direct synthesis of [beta]-carbolines via a three-step one-pot domino approach with a bifunctional Pd/C/K-10 catalyst," *Tetrahedron Lett.* **2009**, *50*, 1791-1794.

LeVine III, H. "Biotin-avidin interaction-based screening assay for Alzheimer's beta-peptide oligomer inhibitors," *Anal. Biochem.* **2006**, *356*, 265-272.

LeVine III, H. Ding, Q. Walker, J.A. Voss, R.S. and Augelli-Szafran, C.E. "Clioquinol and other hydroxyquinoline derivatives inhibit A beta(1-42) oligomer assembly," *Neurosci Lett.* **2009**, *465*, 99-103.

Glide, version 6.8. New York, NY: Schrödinger, LLC; **2015**.

Lohning, A.E.; Levonis, S.M.; Williams-Noonan, B. and Schweilker, S.S. "A practical guide to molecular docking and homology modelling for medicinal chemists," *Curr. Top Med. Chem.* **2017**, *17*, 2023-2040.

Çakır, B.; Dağ, Ö.; Yıldırım, E.; Erol, K. and Şahin, M.F. "Synthesis and anticonvulsant activity of some hydrazones of 2-[(3H)-oxobenzoxazolin-3-yl-aceto]hydrazide," *J. Fac. Pharm. Gazi.* **2001**, *18*, 99-106.

Morjan, R.Y.; Mkadmh, A.M.; Beadham, J.; Elmanama, A.A.; Mattar, M.R.; Raftery, J.; Pritchard, R.G.; Awadallah, A. and Gardiner, J.M. "Antibacterial activities of novel nicotinic acid hydrazides and their conversion into N-acetyl-1,3,4-oxadiazoles," *Bioorg. Med. Chem. Lett.* **2014**, *24*, 5796-5800.

Özdemir, A.; Turan-Zitouni, G.; Kaplancikli, Z.A. and Tunali, Y. "Synthesis and biological activities of new hydrazide derivatives," *J. Enzyme Inhib. Med. Chem.* **2009**, *24*, 825-831.

Török, B.; Sood, A.; Bag, S.; Tulsan, R.; Ghosh, S.; Borkin, D.; Kennedy, A.; Melanson, M.; Madden, R.; Zhou, W.; LeVine III, H. and Török M. "Diaryl hydrazones as multifunctional inhibitors of amyloid self-assembly," *Biochemistry* **2013**, *52*, 1137-1148.

Greig, N.H. "Drug entry into the brain and its pharmacological manipulation," in Bradbury M.W.B. (Ed.) *Physiology and Pharmacology of the Blood-Brain Barrier*. Springer-Verlag, New York; **1992**, 487-524.

Bonina, F.P.; Arenare, L.; Palagiano, F.; Saija, A.; Nava, F.; Trombetta, D.; De Caprariis, P. Synthesis, stability and pharmacological evaluation of nipecotic acid prodrugs," *J. Pharm. Sci.* **1999**, *88*, 561-567.

- Hellenbrand, T.; Höfner, G.; Wein, T.; Wanner, K.T. "Synthesis of 4-substituted nipecotic acid derivatives and their evaluation as potential GABA uptake inhibitors," *Bioorg. Med. Chem.* **2016**, *24*, 2072–2096.
- Padmini, K.; Preethi, P.J.; Divya, M.; Rohini, P.; Lohita, M.; Swetha, K. and Kaladar, P. "A review on biological importance of hydrazones," *Int. J. Pharm. Res. Rev.* **2013**, *1*, 43–58.
- Belskaya, N.P.; Dehaen, W. and Bakuleva, V.A. "Synthesis and properties of hydrazones bearing amide, thioamide and amidine functions," *Arkivoc* **2010**, *2010*, 275–332.
- Lima, P.C.; Lima, L.M.; Silva, K.C.; Leda, P.H.; Miranda, A.L.P.; Fraga, C.A.M. and Barreiro, E.J. "Synthesis and analgesic activity of novel N-acylhydrazones and isosters, derived from natural safrole," *Eur. J. Med. Chem.* **2000**, *35*, 187-203.
- Mangialasche, F.; Solomon, A.; Winblad, B.; Mecocci, P. and Kivipelto, M. "Alzheimer's disease: Clinical trials and drug development," *Lancet Neurol.* **2010**, *9*, 702–716.
- Kryger, G.; Silman, I. and Sussman, J.L. "Structure of acetylcholinesterase complexed with E2020 (Aricept): Implications for the design of new anti-Alzheimer drugs," *Structure* **1999**, *7*, 297–307.
- Martorana, A.; Giacalone, V.; Bonsignore, R.; Pace, A.; Gentile, C.; Pibiri, I.; Buscemi, S.; Lauria, A. and Palumbo Piccionello, A. "Heterocyclic scaffolds for the treatment of Alzheimer's disease," *Curr. Pharm. Des.* **2016**, *22*, 3971–3995.
- Silva, A.G.; Zapata-Sudo, G.; Kummerle, A.E.; Fraga, C.A.M.; Barreiro, E.J. and Sudo, R.T. "Synthesis and vasodilatory activity of new N-acylhydrazones derivatives, designed as LASSBio-294 analogues," *Bioorg. Med. Chem.* **2005**, *13*, 3431–3437.
- Ismail, M.M.; Kamel, M.M.; Mohamed, L.W. and Faggal, S.I. "Synthesis of new indole derivatives structurally related to donepezil and their biological evaluation as acetylcholinesterase inhibitors," *Molecules* **2012**, *17*, 4811–4823.
- Sanner, M.F. Python: A programming language for software integration and development. *J. Mol. Graph. Model.* **1999**, *17*, 57–61.
- Dimmock, J.R.; Vashishtha, S.C. and Stables, J.P. "Anticonvulsant properties of various acetylhydrazones, oxamoylhydrazones and semicarbazones derived from aromatic and unsaturated carbonyl compounds," *Eur. J. Med. Chem.* **2000**, *35*, 241-248.

- Ragavendran, J.; Sriram, D.; Patel, S.; Reddy, I.; Bharathwajan, N.; Stables, J. and Yogeewari, P. "Design and synthesis of anticonvulsants from a combined phthalimide-GABA-anilide and hydrazone pharmacophore," *Eur. J. Med. Chem.* **2007**, *42*, 146-151.
- Todeschini, A.R.; Miranda, A.L.; de Silva, K.C.; Parrini, S.C. and Barreiro, E.J. "Synthesis and evaluation of analgesic, antiinflammatory and antiplatelet properties of new 2pyridylarylhydrazone derivatives," *Eur. J. Med. Chem.* **1998**, *33*, 189-199.
- Özkay, Y.; Tunah, Y.; Karaca, H. and Işıkdag, İ. "Antimicrobial activity and a SAR study of some novel benzimidazole derivatives bearing hydrazone moiety," *Eur. J. Med. Chem.* **2010**, *45*, 3293–3298.
- Subhashini, N.J.P.; Janaki, P. and Bhadraiah, B. "Synthesis of hydrazone derivatives of benzofuran and their antibacterial and antifungal activity," *Russ. J. Gen. Chem.* **2017**, *87*, 2021-2026.
- Mandewale, M.C.; Thorat, B.; Shelke, D. and Yamgar, R. "Synthesis and Biological Evaluation of New Hydrazone Derivatives of Quinoline and Their Cu(II) and Zn(II) Complexes against Mycobacterium tuberculosis," *Bioinorg. Chem. Appl.* **2015**, *2015*, doi: 10.1155/2015/153015.
- Zhang, J.P.; Li, X.Y.; Dong, Y.W.; Qin, Y.G.; Li, X.L.; Song, B.A. and Yang, X.L. "Synthesis and biological evaluation of 4-methyl-1,2,3-thiadiazole-5-carboxaldehyde benzoyl hydrazone derivatives," *Chin. Chem. Lett.* **2017**, *28*, 1238-1242.
- Walcourt, A.; Loyevsky, M.; Lovejoy, D.B.; Gordeuk, V.R. and Richardson, D.R. "Novel aroylhydrazone and thiosemicarbazone iron chelators with anti-malarial activity against chloroquine-resistant and -sensitive parasites," *Int. J. Biochem. Cell Biol.* **2004**, *36*, 401-407.
- Paiva, S.A. and Russell, R.M. "Beta-carotene and other carotenoids as antioxidants," *J. Am. Coll. Nutr.* **1999**, *18*, 426–433.
- Hegazy, W.H. "Synthesis and structural studies of some  $\beta$ -diketone Schiff bases phenylhydrazones and some of their metal complexes with Co (II), Ni (II) and Cu (II) ions," *Monatsh. Chem.* **2001**, *132*, 639-650.
- Alov, P.; Tsakova, I. and Pajeva, I. "Computational studies of free radical-scavenging properties of phenolic compounds," *Curr. Top Med. Chem.* **2015**, *15*, 85–104.
- Rodriguez, S.A. and Baumgartner, M.T. "Theoretical study of reaction mechanism of a series of 4-hydroxycoumarins against the DPPH radical," *Chem. Phys. Lett.* **2014**, *601*, 116-123.

Kareem, H.S.; Ariffin, A.; Nordin, N.; Heidelberg, T.; Abdul-Aziz, A.; Wong, K.W. and Yehye, W.A. "Correlation of antioxidant activities with theoretical studies for new hydrazone compounds bearing a 3, 4, 5-trimethoxy benzyl moiety," *Eur. J. Med. Chem.* **2015**, *103*, 497–505.

Rouaiguia-Bouakkaz, S. and Benayahoum, A. "The antioxidant activity of 4-hydroxycoumarin derivatives and some sulfured analogs," *J. Phys. Org. Chem.* **2015**, *28*, 714–722.

Manach, C.; Scalbert, A.; Morand, C.; Rémésy, C. and Jiménez, L. "Polyphenols: food sources and bioavailability," *Am. J. Clin. Nutr.* **2004**, *79*, 727-747.

Shahidi, F. and Ambigaipalan, P. "Phenolics and polyphenolics in foods, beverages and spices: antioxidant activity and health effects – a review," *J. Funct. Foods* **2015**, *18*, 820-897.

Klein, E.; Lukeš, V.; Cibulková, Z. and Polovková, J. "Study of N–H, O–H and S–H bond dissociation enthalpies and ionization potentials of substituted anilines, phenols and thiophenols," *J. Mol. Struct.* **2006**, *758*, 149-159.

Bordwell, F.G.; Zhang, X.M. and Cheng, J.P. "Bond dissociation energies of the nitrogen-hydrogen bonds in anilines and in the corresponding radical anions. Equilibrium acidities of aniline radical cations," *J. Org. Chem.* **1993**, *58*, 6410-6416.

Saqib, M.; Mahmood, A.; Akram, R.; Khalid, B.; Afzal, S. and Kamal, G.M. "Density functional theory for exploring the structural characteristics and their effects on the antioxidant properties," *J. Pharm. Appl. Chem.* **2015**, *1*, 65-71.

Leopoldini, M.; Russo, N. and Toscano, M. "The molecular basis of working mechanism of natural polyphenolic antioxidants," *Food Chem.* **2011**, *125*, 288-306.

Mazzone, G.; Malaj, N.; Russo, N. and Toscano, M. "Density functional study of the antioxidant activity of some recently synthesized resveratrol analogues," *Food Chem.* **2013**, *141*, 2017-2024.

Alaşalvar, C.; Soyulu, M.S.; Güder, A.; Albayrak, Ç.; Apaydin, G. and Dilek, N. "Crystal structure, DFT and HF calculations and radical scavenging activities of (E)-4,6-dibromo-3-methoxy-2-[(3-methoxyphenylimino)methyl]phenol," *Acta. A: Mol. Biomol. Spectr.* **2014**, *125*, 319-327.

Szeląg, M.; Mikulski, D. and Molski, M. "Quantum-chemical investigation of the structure and the antioxidant properties of  $\alpha$ -lipoic acid and its metabolites," *J. Mol. Model.* **2012**, *18*, 2907-2916.

Kirk, K.L. "Fluorine in medicinal chemistry: Recent therapeutic applications of fluorinated small molecules," *J. Fluorine Chem.* **2006**, *127*, 1013-1029.

Hagmann, W.K. "The many roles for fluorine in medicinal chemistry," *J. Med. Chem.* **2008**, *51*, 4359-4369.

Wang, J.; Sánchez-Roselló, M.; Aceña, J.L.; del Pozo, C.; Sorochinsky, A.E.; Fustero, S.; Soloshonok, V.A. and Liu, H. "Fluorine in pharmaceutical industry: fluorine-containing drugs introduced to the market in the last decade (2001–2011)," *Chem. Rev.* **2014**, *114*, 2432-2506.

Reid, D.G. and Murphy, P.S. "Fluorine magnetic resonance in vivo: A powerful tool in the study of drug distribution and metabolism," *Drug Discovery Today* **2008**, *13*, 473-480.

Jones, O.G. and Mezzenga, R. "Inhibiting, promoting and preserving stability of functional protein fibrils," *Soft Matter* **2012**, *8*, 876-895.

Tycko, R. and Wickner, R.B. "Molecular structures of amyloid and prion fibrils: consensus versus controversy," *Acc. Chem. Res.* **2013**, *46*, 1487-1496.

Frare, E.; de Laureto, P.P.; Zurdo, J.; Dobson, C.M. and Fontana, A. "A highly amyloidogenic region of hen lysozyme," *J Mol. Biol.* **2004**, *340*, 1153-1165.

Zou, Y.; Li, Y.; Hao, W.; Hu, X. and Ma, G. "Parallel  $\beta$ -sheet fibril and antiparallel  $\beta$ -sheet oligomer: New insights into Amyloid Formation of Hen Egg White Lysozyme under Heat and Acidic Condition from FTIR Spectroscopy," *J. Phys. Chem. B* **2013**, *117*, 4003-4013.

Holley, M.; Eginton, C.; Schaefer, D. and Brown, L.R. "Characterization of amyloidogenesis of hen egg lysozyme in concentrated ethanol solution," *Biochem. Biophys. Res. Commun.* **2008**, *373*, 164-168.